STRATIGRAPHY AND MINERALIZATION OF THE BONGARA MVT ZINC-LEAD DISTRICT, NORTHERN PERU

by

Christopher Justin Reid

A thesis submitted in conformity with the requirements

for the degree of Master of Science

Graduate Department of Geology

University of Toronto

STRATIGRAPHY AND MINERALIZATION OF THE BONGARA MVT ZINC-LEAD DISTRICT, NORTHERN PERU

by
Christopher Justin Reid
A thesis submitted in conformity with the requirements
for the degree of Master of Science
Graduate Department of Geology
University of Toronto

THESIS ABSTRACT

The Bongara MVT zinc-lead district is located in the sub-Andean fold-and-thrust belt of the northern Peruvian Eastern Foreland Basin. Lower Mesozoic Pucara Group carbonates form a craton-margin platform that represents the first marine transgression of the Andean Cycle. The northern Pucara Group developed discordantly over piano-key shaped horst-and-graben terrestrial sequences formed under extensional tectonic conditions. Lithofacies differences within the Pucara Group are a result of deposition along paleogeographic basement highs through the Utcubamba Valley. MVT-style zinc-lead mineralization is hosted within Pucara carbonates associated with pervasive dolomitization, pseudobrecciation, and structural zones of carbonate dissolution. Mineralization is predominantly sphalerite, galena, and pyrite observed as replacive and open-space filling textures. The paragenetic sequence includes early burial and compaction-related carbonate cements, and later diagenetic/epigenetic zoned sparry dolomite and calcite. Petrographic and isotopic analysis suggests that early and late diagenetic alteration associated with mineralization occurred through an interconnected, district-wide, structurally controlled plumbing system.

CONTENTS

LIST OF PLATES

LIST OF FIGURES

LIST OF APPENDICIES

THESIS INTRODUCTION

Over the course of 6 months between 1999 and 2001 the author conducted a geological study of the northern Pucara Group, within the Utcubamba Valley of northern Peru. Geological interest in the area arose from mining companies after the discovery of significant MVT-style mineralization in the Florida Canyon area towards the northwest edge of the valley in 1996.

The high-energy lithofacies of the middle Chambara Formation (lower Pucara Group) is the most significant host of zinc-lead mineralization in the district. The main objective of this study was to examine the distribution of Pucara Group carbonates across the area, and identify depositional, tectonic, and internal basinal variations responsible for focusing zinc-lead sulphide mineralization. The northern Pucara Basin specific to the Utcubamba Valley and Bongara district has undergone very little scientific study as a result of poor rock exposure, high elevations, and arduous travel. Mineralization, alteration, and ground preparation is observed extensively throughout the area. An attempt was made to identify various diagenetic stages associated with early burial and late mineralizing alteration systems. Various alteration and diagenetic stages specific to mineralized and barren areas have been studied in an attempt to identify if certain carbonate or alteration phases are specific to mineralized horizons when compared with those from barren areas.

This work is presented in two separate papers. The first paper discusses the geology, stratigraphy and mineralization of the Bongara area. To define the primary basinal controls on deposition of the Pucara Group various methods of geological investigation were attempted, including stratigraphic analysis, mapping, core study, and petrographic analysis. A comparison is made with global MVT districts in an attempt to compare and contrast geological features with those from proven economic areas.

The second paper discusses diagenetic and epigenetic alteration phases identified through field study, petrographic, and cathodoluminescent analysis. A detailed study of paragenetic sequences from both mineralized and barren areas is made in an attempt to identify if characteristics unique to mineralized horizons can be identified and to determine if the main areas of study are genetically linked by an interconnected hydrothermal system. Stable carbonate isotopic analysis was conducted in an attempt to expand petrographic observations and provide geochemical correlation to basinal alteration patterns.

This work provides the first produced academic study discussing MVT-style mineralization in the Bongara region. The northern Pucara Group shows unique basinal stratigraphic relationships when compared with similar studies from the San Vicente and Central Zinc Belt of central Peru. Further academic study is required in the area. This work presents a summary of observations collected through a very large area over a short period of time. Observations regarding the depositional and structural controls on carbonate sedimentation and emplacement of zinc-lead mineralization in the area can provide industry with guidelines for site specific exploration.

PAPER 1.
STRATIGRAPHIC, BASINAL, AND TECTONIC DEVELOPMENT OF THE BONGARA MVT ZINC-LEAD DISTRICT, NORTHERN PERU

1.1 Abstract

The Bongara zinc-lead district is located within the sub-Andean fold-and-thrust belt of the northern Peruvian Eastern Foreland Basin. Lower Mesozoic Pucara Group carbonates, host to MVT-style mineralization, form a craton-margin carbonate platform that represents the first marine transgression of the Andean Cycle. The northern Pucara Group developed discordantly over piano-key shaped horst-and-graben terrestrial sequences formed under extensional tectonic conditions. Marked lithofacies differences within the Pucara Group are observed as a result of deposition along paleogeographic basement highs through the Utcubamba Valley. MVT-style zinc-lead mineralization is hosted within Pucara carbonates with the most significant being associated with pervasive dolomitization, pseudobrecciation, and carbonate dissolution in the Florida Canyon area. Mineralization is predominantly sphalerite, galena, and pyrite with various replacive and open-space filling textures. Comparison with global MVT districts suggests that the Bongara area represents an emerging under explored carbonate-hosted zinc district.

1.2 Introduction

The Bongara zinc-lead district is located within the sub-Andean fold-and-thrust belt of the Peruvian Eastern Foreland Basin in northern Peru. The Pucara Basin is a craton-margin carbonate platform that represents the first marine transgression of the Andean Cycle over continental clastic sediments, volcanic and volcaniclastic rocks of the Permian-Triassic Mitu Group and other Paleozoic rocks. The wide carbonate platform of the Pucara Group developed discordantly over piano-key shaped horst and graben terrestrial sequences formed under extensional tectonic conditions, on the western margin of the Brazilian Shield in northern and central Peru.

The Pucara Group of the northern Pucara Basin can be divided stratigraphically into the Chambara, Aramachay and Condorsinga Formations. Marked lithofacies differences, especially in the Chambara Formation have allowed informal subdivisions to be applied locally. These lithofacies differences likely reflect development in a differentiated extensional basin controlled by localized paleogeographic highs exhibiting substantial vertical and spatial variation over kilometer-scale distances. Syndepositional tectonic, and structural modification of this original paleo-relief may have affected the stratigraphic character and distribution of the Pucara carbonates throughout the study area.

The northern Pucara Group is indicative of a large evolving isolated carbonate platform initiated on fault-generated topography likely representing a series of isolated basally-connected smaller platforms each developed upon fault generated topographic highs having a limited spatial distribution. This accounts for the lack of stratigraphic continuity between studied areas, explains the lack of high-energy carbonates across the central platform and the extent of fore-reef carbonates associated with paleo-lows and deeper platformal environments.

Mississippi Valley type (MVT) lead-zinc (Pb-Zn) mineralization occurring in a variety of types, textures and concentrations attracted the interest of exploration companies to the Bongara area. Mineralization is predominantly, though not exclusively, confined to the Chambara Formation of the Pucara Group, with the most significant mineralization discovered in the Florida Canyon area. The best mineralization in the Bongara region is generally associated with strong ground preparation observed as pervasive dolomitization, pseudobrecciation, and structurally confined carbonate dissolution. Three textures of mineralization have been identified and defined as: i) bedding and/or small cavity replacement, ii) collapse breccia hosted and iii) minor zinc in vein, crackle and mosaic breccias in the upper Chambara Formation (Chambara 3). Zinc mineralization consists of dark red to brown sphalerite with lesser dull yellow beige sphalerite being identified locally. Sphalerite is observed as coarse euhedral to fine-grained (mm to cm scale) aggregates with locally colloformal zoned varieties. Lead mineralization is exclusively observed as galena, though oxide varieties of both zinc and lead mineralization have been observed in the district. Most commonly zinc and lead sulphides are observed together as an intermeshed mosaic of sulphides, though galena veining has also been identified crosscutting early sphalerite phases. Pyrite is observed throughout the mineralizing sequence ranging from fine mm-scale disseminations to cm-scale massive replacement of the host. Later silicification and calcification is observed towards the waning stages of the mineralizing system. Other examples of zinc-lead

mineralization have been documented throughout the property, but the above best describes the typical sulphide morphology.

The Bongara district when compared with geological characteristics from other global MVT districts represents an emerging, under-explored, belt having significant potential for future discoveries of economic zinc-lead mineralization.

1.2.1 Location

The Bongara study area is situated between 5°20' to 6°50' south and 78° to 77°30' west, within the Eastern Cordillera of the northern Peruvian Andes (Fig.1.1). The study area is confined to an elongate northeast corridor extending from the southern Maino region, northeast through the Utcubamba Valley totaling approximately 90 kilometers in length and 12-20 kilometers in width. The Utcubamba Valley continues to the southeast for an additional 40 kilometers through the Leimebamba area. The study area is located in the Bongara territory of the Amazonas Department.

Access to the area is by paved highway from the city of Chiclayo via the town of Bagua Grande to the village of Pedro Ruiz. Pedro Ruiz acted as the central logistic base for study and exploration work carried out in the region. The paved highway continues east of Pedro Ruiz to the jungle towns of Rioja and Tarapoto. There are daily commercial flights from Lima to both Chiclayo and Tarapoto. Driving time from both cites to Pedro Ruiz is approximately 6 hours. An unpaved road connects Pedro Ruiz with Chachapoyas, the capital of the Department of Amazonas, and continues south to Cajamarca. Access to the area is relatively easy by road; however, travel within the property is arduous due to high elevations and jungle cover requiring helicopter support or local guides with knowledge of the jungle areas and passes.

1.3 Geological Setting

1.3.1 Tectonic Development of the Peruvian Andes (The Andean Cycle)

This section describes the geochronological development of the Andean Cycle (Megard, 1987). The description here is a summary of geological work emphasizing the tectonic development and morphological division of the Peruvian Andes. The work of the author is confined to a very well-

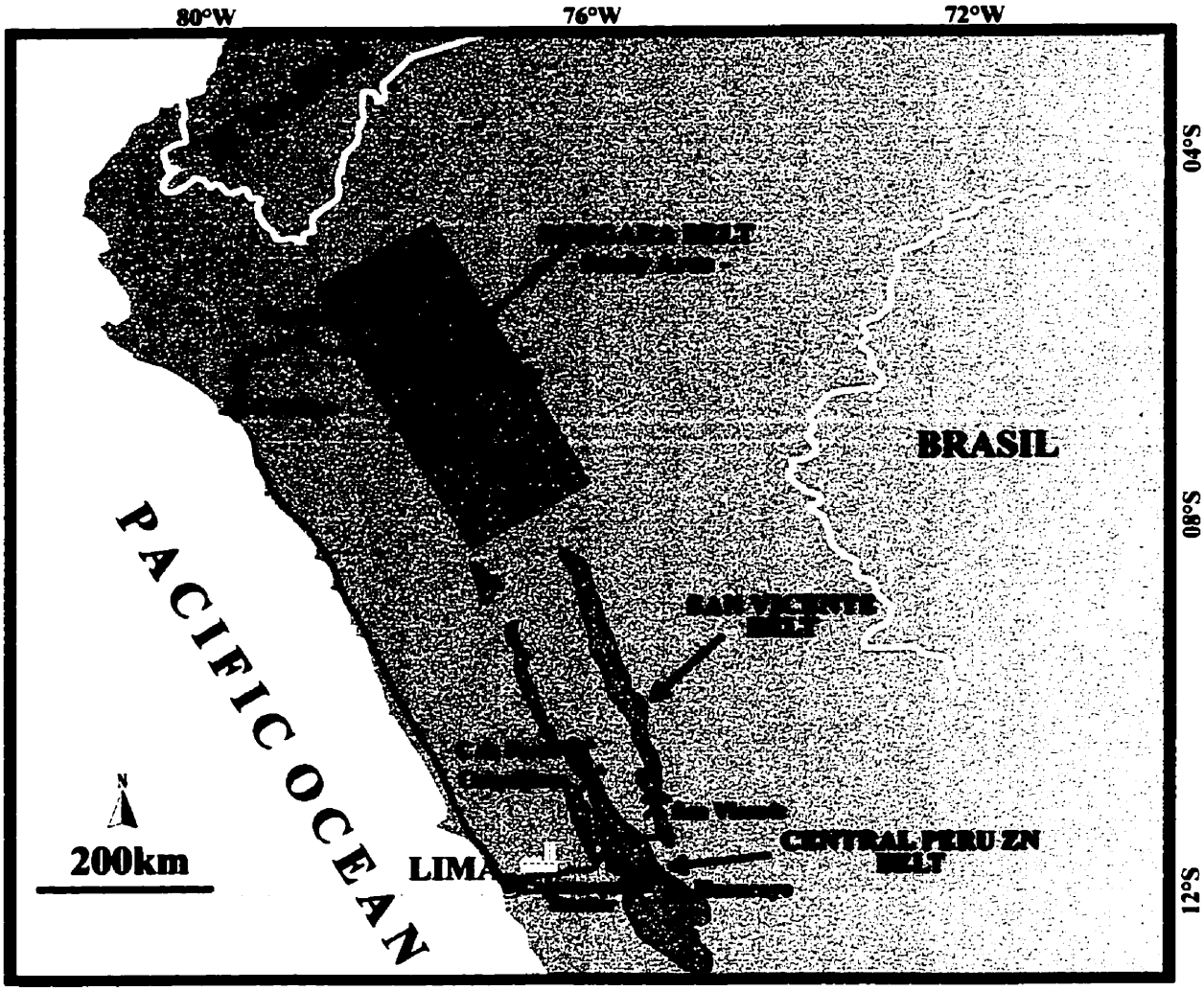

Figure 1.1 - Location of the Bongara, San Vicente, and Central Peru CRD zinc districts.

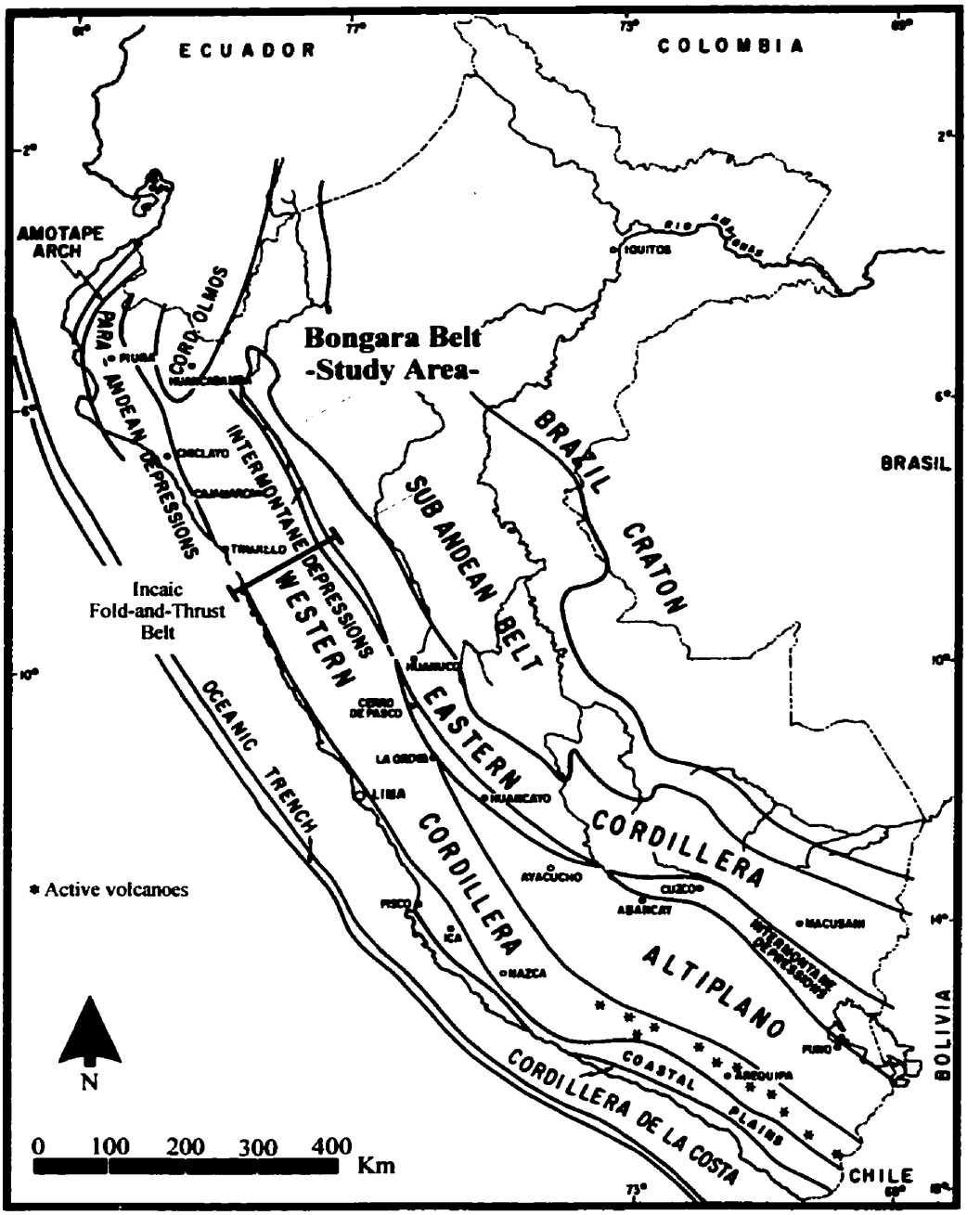

Figure 1.2 Main morphostructural units of Peru. Modified from Benavides-Caceres, 1999.

defined segment of the Eastern Foreland Basin located in the northern portion of the Sub-Andean zone (Fig.1.2).

The Andean Cordillera, a major mountain range located between the Peru-Chile oceanic trench in the west and the Brazilian shield in the east, forms the western-central part of Peru. The formation of the Andes is a result of the Mariana-type subduction of the Nazca Plate beneath the ensialic South American Plate. Along the western margin of the plate the development of over 70 km. of crustal thickening has led to cordilleran uplift of approximately 4000 meters from the Late Triassic to Present (Megard, 1987; Benavides-Caceres, 1999).

The Andean Cordillera is a result of three geodynamic pulses (Benavides-Caceres, 1999): Precambrian; Paleozoic to Early Triassic; and Late Triassic to Present. The Cordillera can be divided into two dominant ranges: the Western Cordillera, resulting from the formation of a magmatic arc, and the Eastern Cordillera, representing the zone of uplift. Between these ranges is the Altiplano, a zone between the Pacific margin of the magmatic arc and the oceanic trench.

Prominent features of the Andes include the Cretaceous-Paleocene Coastal Batholith, which is bounded to the east by the Incaic fold-and-thrust belt, the site of a series of compressive events. East of the eastern Cordillera horst is the Sub-Andean fold-and-thrust belt formed during the Late Miocene. The Eastern Foreland Basin marks the eastern edge of the Andean Cordillera with a thinning sedimentary package unconformably overlying the Brazilian Shield.

By the end of the Paleozoic, the Andean region was part of the western Pangean margin. During Middle Triassic time intense intracontinental rifting formed a large horst-and graben-system occupying the present Andean trend. The most dramatic of these systems was the Mitu Graben, which received over 3000 meters of continental red beds, volcaniclastics, and alkaline volcanic rocks (Megard, 1987; Benavides-Caceres, 1999) (Fig.1.3). Large master faults along the axial parts of this system became the sites of mantle-derived continental volcanism and intrusions that dominated the Eastern Cordillera. The focus of this review will be on the Andean Cycle (Megard, 1987) encompassing those tectonic processes occurring from the Late Triassic to Present. It is within this tectonic system that the mechanisms and processes inherently important to this paper are studied.

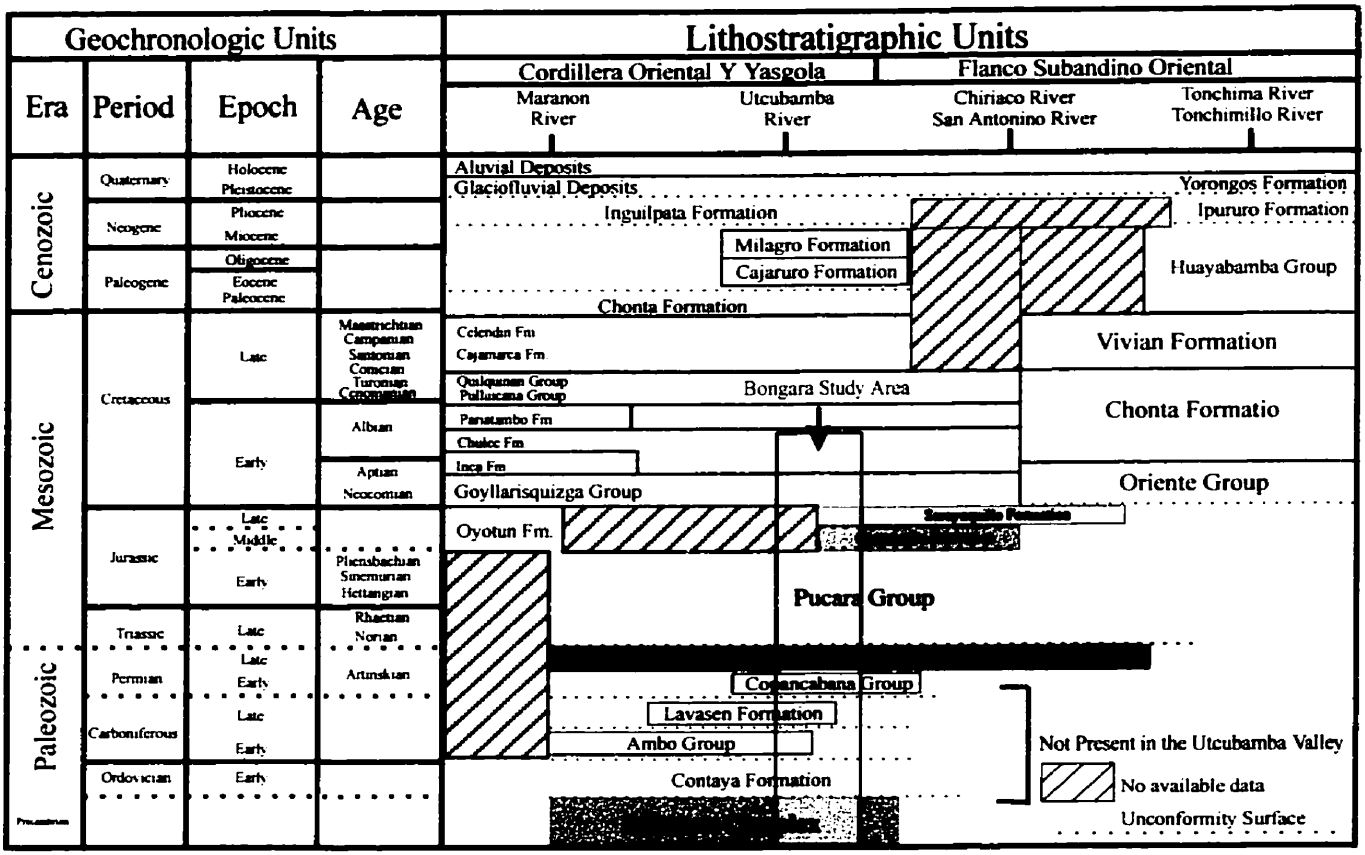

Figure 1.3 Time-space stratigraphic tabulation for the Maranon, Utcubamba, Chiriaco, San Antonio, Tonchima and Tonchimillo River Valleys of Northern Peru. Modified from Ingemmet Boletin No.56, 1995.

1.3.1.1 The Andean Cycle - Late Triassic to Present

The Andean Cycle defined by Megard (1987) encompasses all processes that led to the formation of the present Andes from the initial opening of the Atlantic Ocean in the Triassic. The Andean Cycle is defined by two major periods of formation. The first period was primarily an extensional phase that lasted from the Late Triassic to the Late Cretaceous, during which time the Andean region underwent crustal attenuation and marine sedimentation (Megard, 1987; Benavides-Caceres, 1999). The second phase showed an absence of marine sedimentation along the cordilleran margin, reccurring compressive episodes, intense continental volcanism and plutonism, extreme crustal thickening and massive uplift. These characteristics form the basis of Andean-type subduction (Benavides-Cáceres, 1999).

1.3.1.2 The Andean Cycle - Extensional Tectonics

Late Triassic through Senonian time was characterized by widespread extensional tectonics. Through most of the Mesozoic, the back arc region between the subduction complex and the Brazilian Shield saw the formation of belts with differential subsidence bounded by major separating longitudial crustal faults, which were likely reactivated Paleozoic basement lineaments. The major longitudinal feature prominent through Mesozoic time was the Maranon Arch (Fig. 1.4) that resulted in the formation of the Eastern Cordillera. Transverse or Andean-normal features include the Huancabamba and Ababcay deflections and the Bolivian Elbow. These structures trend almost east-west, normal to the main direction of Andean tectonics.

Late Triassic to Early Jurassic development of the Andes led to the development of definable geotectonic regions. The eastern margin is defined by the Brazilian Craton, bordered to the west by the Eastern Basin. The Eastern Basin includes areas presently occupied by the Sub-Andean fold-and- thrust belt and the Eastern Foreland Plains, site of epicontinental evaporite and carbonate sedimentation of the Pucara Group (Fig.1.4). The Eastern Basin is bounded to the west by the Maranon Arch geanticline, a zone of lesser subsidence, and site of the current Eastern Cordillera. The Maranon Arch started to develop as a horst in the Mitu Graben and provided the base for shallow water carbonate platformal sedimentation of the Pucara Group (Benavides-Caceres, 1999; Megard, 1987; Rosas, 1994). The Maranon Arch is bordered by the Western Platform consisting of shallow marine carbonate sedimentation of the Pucara Group. The Pucara

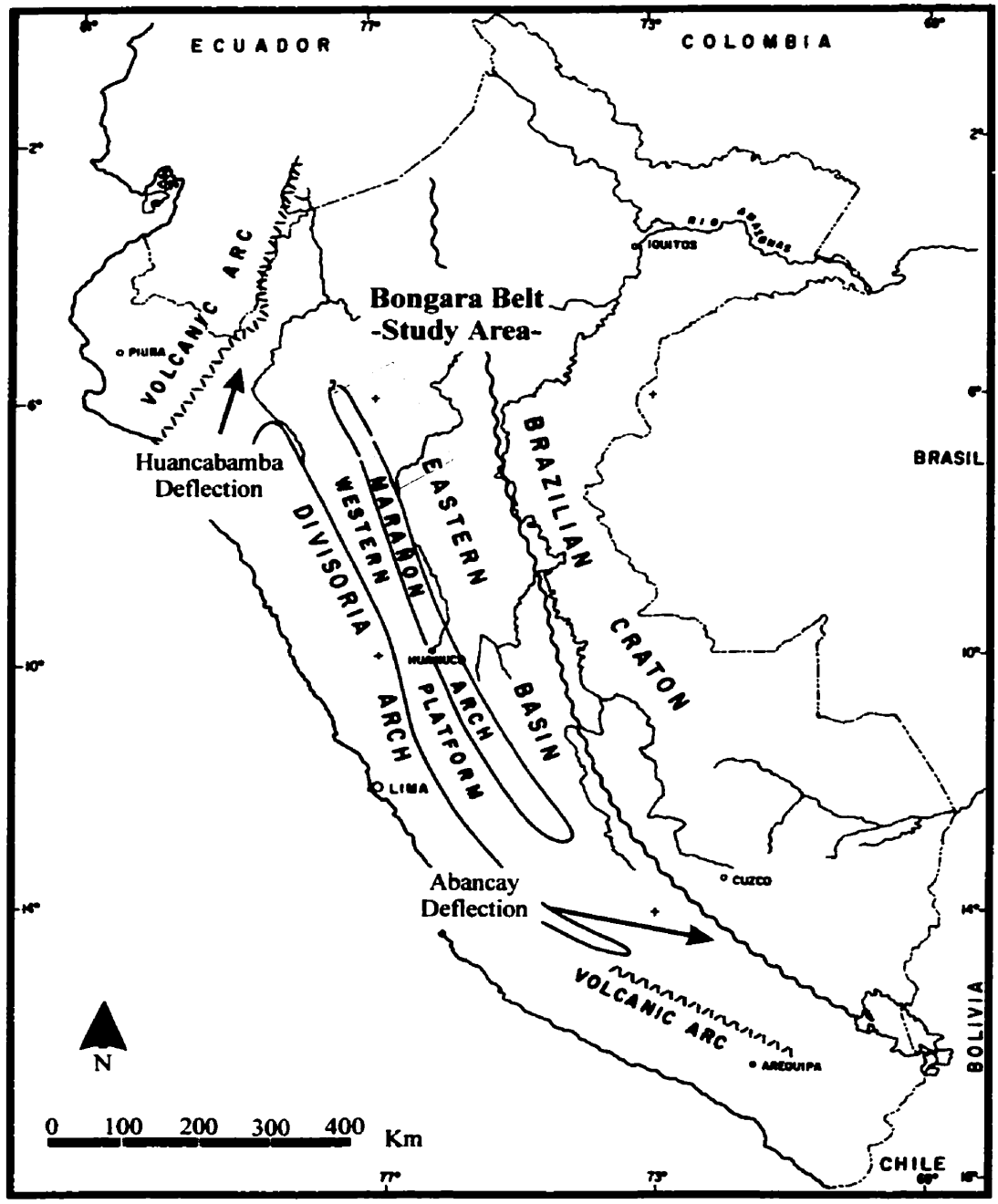

Figure 1.4 Main tectonic units of Peru during Late Triassic-Middle Jurassic time. Modified from Benavides-Caceres, 1999.

transgression began in the Middle Norian in northern Peru, reached central Peru by Upper Norian time and the south by Sinemurian time. The Western Platform is bordered by the Divisoria Arch, which, like the Maranon Arch, is a zone of lesser subsidence and bordered by subduction-related volcanics to the west.

The Early to Middle Jurassic Vicusian Orogeny of South-Central Ecuador and Northern Peru truncated the Peruvian Andean elements at the Huancabamba Deflection. The Vicusian Orogeny was characterized by a major regressive marine event, cessation of Pucara Group carbonate sedimentation, and the development of the northeast-trending Vicus fold belt. Regional emergence and subsequent unconformity development marked the shift from carbonate to siliciclastic sedimentation. There was a tectonic shift from an island arc volcanic setting to a continental volcanic arc environment. Major batholithic intrusions developed an inner foreland trough along the present Sub-Andean region that extended southward to the Abancay Deflection. The Vicusian Orogeny resulted in up to 3 km. of material being removed from the Maranon Arch and redeposited along the western margin of the foreland trough (Benavides-Cacereces, 1999; Laubacher and Naeser, 1994).

Following the Vicusian Orogen a new extensional tectonic period commenced (Callovian-Tithonian time) that saw the emergence of the regions containing the Eastern Basin, Maranon Arch, and the Huancabamba Deflection. During this time subsidence remained confined to areas of the Western Basin. Sedimentation was predominantly siliciclastic paralic and deltaic in origin. During the Lower Cretaceous (Valanginian), a major siliciclastic sequence (The Chimu Group) was deposited regionally over the Peruvian territories.

Mid Cretaceous (Middle Albian) extension led to formation of a major rift trough, known as the Huarmey-Canete Trough, located along the western margin of the back arc basin.
During the Aptian to Albian east of the marginal trough the Goyllarisquizga Formation was deposited, initially as a basal quartzose sedimentary wedge, succeeded by a transgressive molasse and carbonate sequence in northern and central Peru (Yates et al., 1951; Paredes, 1980; and Soler, 1989,1991).

During the Early-Middle Albian (100-95 Ma) the compressive Mochica Orogeny developed (Myers, 1974; Cobbing et al, 1981; Megard, 1984; Benavides-Caceres, 1999). This caused regional emergence and the subsequent formation of a significant regional unconformity through

the Peruvian territories. Through the Late Albian to Campanian the tectonic regime returned to extension and a new sedimentary cycle was initiated, paralleling the orientation of the earlier extensional phases (Myers, 1974, 1980; Benavides-Caceres, 1999).

The final major event ending the primarily early extensional formation of the Andes was the emplacement of the coastal batholith during the Middle Albian (100-55 Ma) (Atherton, 1990). This continental scale feature was located along the Pacific flank of the Cordillera. As described by Benavides-Caceres (1999) based upon the work of Atherton (1990), magmatism changed from early tholeiitic dike and gabbroic plutonism to emplacement of the large calc-alkaline dioritic and tonalitic plutons.

1.3.1.3 The Andean Cycle – Compressive Tectonics

In the Early Senonian, a geodynamic change heralded Andean-type subduction, marine withdrawal, and Cordilleran emergence. This shift was characterized by recurring eastward-developing compressive pulses and the presence of a magmatic arc along the continental margin. A series of 9 compressive events - Peruvian (84-79 Ma), Incaic I (59-55 Ma), Incaic II (43-42 Ma), Incaic III (30-27 Ma), Incaic IV (22 Ma), Quechua I (17 Ma), Quechua II (8-7 Ma), Quechua III (5-4 Ma) and Quechua IV (Early Pleistocene) - formed three major fold-and-thrust belts: the Peruvian (Campanian), Incaic (Paleocene-Eocene) and sub-Andean (Neogene). These resulted in crustal thickening and uplift, which was followed by erosion and formation of major unconformity surfaces. The compressive pulses interrupted longer periods of extension during which the magmatic arc was particularly active, and which were also characterized by the development of fore-arc basins, intermontane grabens, and the great Eastern Foreland Basin (Benavides-Caceres, 1999). This period of Andean-type subduction was characterized by a change from a marine volcanic arc into a continental volcanic arc, formation of a fore-arc, intermontane and foreland basins during the extensional intervals, great crustal shortening and thickening with attendant continental emergence and uplift. This resulted in the development of several significant regional erosional surfaces indicative of periods of relative stability following the compressive pulses (Benavides-Caceres, 1999).

The Peruvian fold-and-thrust belt developed between the Early to Middle-Campanian (84-79Ma) and the Incaic I compressional pulse (59-55Ma). The Peruvian fold-and-thrust belt formed as a result of compression between the Amotape and Olmos Massifs in northern Peru and

compression west of the coastal batholith along the remainder of the country. During the formation of this belt the tectonic framework from east to west included the Brazilian Craton, the Eastern Foreland Basin (sight of major non-marine red-bed deposition), the Maranon Arch, intermontane basin, the continental arc, and the beginning of a fore-arc basin to the west, against the Pacific realm (Benavides-Caceres, 1999).

The Incaic fold-and-thrust belt formed as a result of at least four compressive events between the coastal block and the Maranon Arch. The Incaic I and II (59-55 Ma and 42-42 Ma respectively) are considered to have been the most tectonically dynamic of the pulses (Steinmann, 1929; Noble et al., 1979, 1985, 1990). The belt developed east of the Incaic megafault that is now marked by the Cordillera Blanca fault zone (Benavides-Caceres, 1999). West of this lineament compression was active but did not result in any major deformation. Both the Incaic I and II compressional pulses were followed by a period of dramatic uplift and erosion forming the Incaic I and II unconformities (Megard, 1987). Structures indicate compression in a southwest-northeast direction. Surface geology shows major shortening, accommodated by the folding and thrusting east of the Incaic megafault (Megard, 1987; Benavides-Caceres, 1999).

The eastern margin of the Maranon Arch is formed by the Sub-Andean fault system (Ham and Herrera, 1963). This system acted as a hinge line west of which was the highest part of the Pucara carbonate platform, and to the east, a subsiding area where Norian shallow-water and evaporitic sediments gave way to pelitic carbonates. During the Senonian, as the Cretaceous seas withdrew from the cordillera interior, the Eastern Basin east of the sub-Andean fault system evolved into an asymmetric, increasingly subsiding foreland basin filled by upward coarsening siliciclastic mollasse deposits derived from the Andean hinterland (Benavides-Caceres, 1999). Movement along the Sub-Andean fault system has been uneven, with greatest displacement in northern Peru. Precambrian rocks are exposed along the upthrown side of the Maranon Arch, and within the Eastern Foreland Basin the greatest subsidence is reached with over 10,000 meters of Tertiary-Quaternary sediments accumulating, representing a combined throw of approximately 12,000 meters. During the Quechua II orogenic pulse (8-7 Ma) the Sub-Andean megafault played a major role in the formation of the Sub-Andean fold-and-thrust belt (Megard, 1984; Benavides-Caceres, 1999).

Along the western margin of the Eastern Foreland Basin, late Miocene (10-8 Ma) compression deformed the sedimentary pile into the sub-Andean fold-and-thrust belt (Megard, 1984, 1987;

Benavides-Caceres, 1999). The Sub-Andean zone is located between the Maranon Arch and the Brazilian shield. East of this belt is the undeformed, west-dipping monocline of the foreland area, where eastward-thinning sedimentary units lie over the Brazilian shield. The Sub-Andean fold-and-thrust belt is primarily the expression of thin-skinned tectonics and crustal shortening. It also includes some important basement involved features, as well as the belt of crustal shortening (Megard, 1987; Roeder and Chamberlain, 1995; Benavides-Caceres, 1999). Sedimentary deformation occurs across the expanse of the fold-and-thrust belt, particularly at its eastern margins. Crustal shortening takes place at the Sub-Andean fault zone, which is seen as the root of the fold-and-thrust belt and as the locus of absorption of the shortening caused during its formation (Fukao and Yamamoto, 1989; Dorbath et al, 1993; Suarez et al 1983, 1990).

1.3.1.4 Summary

The third geodynamic cycle in the formation of the Andes (Andean Cycle) commenced with the opening of the Atlantic in the Triassic, including an extensional phase (Late Triassic to early Senonian) of Mariana-type subduction which was basically extensional and of crustal attenuation (Megard, 1984, 1987; Benavides-Caceres, 1999). During this time the cordilleran belt was the site of major shelf sedimentation, bordered on the west by island arc volcanism or a marginal volcanic rift. In the Early Senonian, a geodynamic change evoked Andean-type subduction, marine withdrawal, and cordilleran emergence. This shift was characterized by reoccurring compressive pulses and the presence of a magmatic arc along the continental margin. A series of 9 compressive events formed three major fold-and-thrust belts: the Peruvian (Campanian); Incaic (Paleocene-Eocene); and Sub-Andean (Neogene). These resulted in crustal thickening and uplift, which was followed by erosion and formation of major unconformity surfaces. The compressive pulses interrupted longer periods of extension during which the magmatic arc was particularly active, and which were also characterized by the development of fore-arc basins, intermontane grabens, and the Great Eastern Foreland Basin. Throughout this Andean development the presence of a magamatic arc, the Maranon Arch, and Eastern Foreland Basin remained persistent (Benavides-Caceres, 1999).

1.3.2 Regional Geological Setting of the Pucara Basin

The Pucara Basin is a craton-margin carbonate platform that represents the first marine transgression of the Andean Cycle over continental clastic sediments, volcanic and volcaniclastic rocks of the Permian-Triassic Mitu Group and other Paleozoic rocks (Fig.1.5). The wide carbonate platform of the Pucara Group developed discordantly over piano-key shaped horst and graben terrestrial sequences formed under extensional tectonic conditions, on the western margin of the Brazilian Shield in Northern and Central Peru (Fontbote, 1990; Megard, 1987).

The Pucara Basin has been best studied in the Altiplano region of central and south central Peru where it has been subdivided into three formations: Chambara, Aramachay, and Condorsinga. In the Altiplano region of Peru the Chambara Formation consists primarily of shaley and bituminous limestones up to 1500 meters in thickness. The Aramachay Formation consists of bituminous shale, sandstone, chert and phosphatic rocks up to 600 meters thick, and the Condorsinga Formation comprises mainly bioclastic and cherty limestones and shales up to 2900 meters in thickness (Fontbote, 1990; Rosas, 1994).

This study is confined to a detailed area of the Utcubamba Valley in Northern Peru. Other investigations of the Pucara Group in northern Peru include that of Wilson and Reyes (1964) and Prinz (1985). Other studies of Pucara Group stratigraphy in the Sub-Andean region of central Peru include those of Levin (1974) and Palcios (1980). Generally the age range of sediments in the Eastern Pucara belt is comparable with those of the central Pucara. Fontbote (1990) notes important difference in the depositional environments between the eastern and central Pucara. The Eastern Pucara is characterized by the presence of several thick peritidal dolomitic units with abundant algal lamination and sulfate molds deposited in sabkha-like environments whereas the Central Pucara consists of predominantly stable shallow water calcareous carbonates. The eastern Pucara represents the basin margin as it interfingers with the clastic-evaporitic sediments of the lower Sarayaquillo Formation (Megard, 1978) along the western margin of the Brazilian Shield.

Many models have been proposed concerning the development of the Pucara Basin. Loughman and Hallam (1982) proposed an unrestricted open shelf to the Paleo-Pacific in the west. Szekely and Grose (1972) and Megard (1978) proposed the existence of a structural high with emergent areas between the Pucara Basin and the Paleo-Pacific. Fontbote (1990) suggests that the

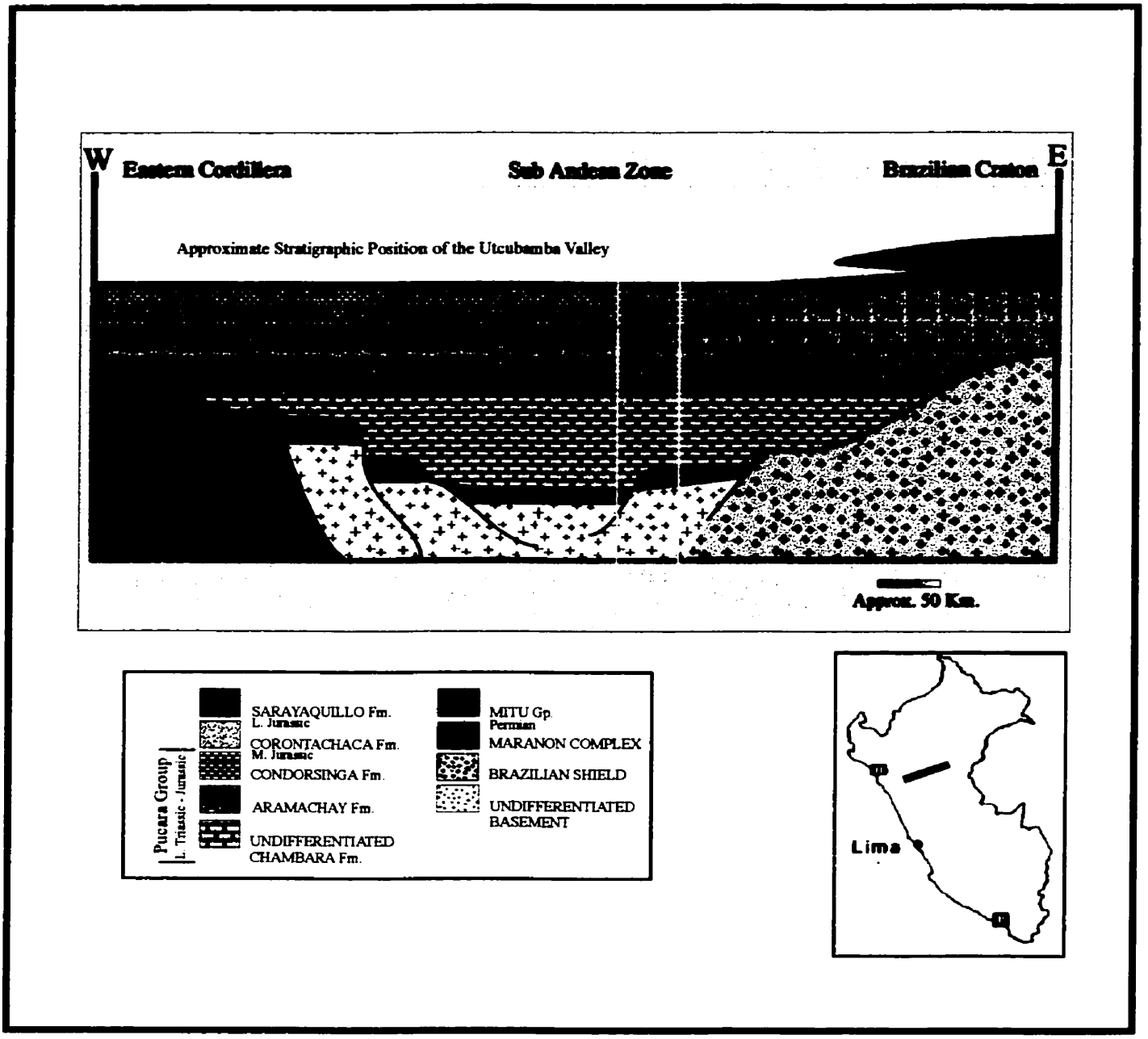

Figure 1.5 Schematic W-E profile of the Pucara encompassing the Utcubamba Study area. Modified from Fontbote, 1990. Based upon data from Ingemmet Boletin No.60, 1995 and stratigraphic data collected by the author.

evolution of Triassic-Liassic Pucara basin has more similarities to basins in the Triassic of the Alpino-type lithofacies than to the Andean basins related to paired magmatic arc-back-arc. These similarities include high subsidence rates, predominant carbonate sedimentation, and the paleogeographic situation at the margin of an emerged continent.

This study will focus on the stratigraphy and stratigraphic distribution of the Pucara Group, in a discrete (90 x 20 km) area of northern Peru, within the Utcubamba valley (Fig.1.6).

1.3.3 Geological Setting of the Northern Pucara Basin

The Pucara Group of the Northern Pucara Basin can be divided stratigraphically into the Chambara, Aramachay and Condorsinga Formations, as described from studies of the Pucara group from the central Altiplano region of Peru. However, marked lithofacies differences, especially in the Chambara Formation have allowed informal subdivisions to be applied locally. These lithofacies differences (discussed below) likely resulted from a differentiated extensional basin controlled by localized paleogeographic highs exhibiting substantial vertical and spatial variation over kilometer-scale distances. As well, syndepositional tectonic, structural modification of this original paleo-relief may have affected the stratigraphic character and distribution of the Pucara carbonates throughout the study area.

The study area (Fig.1.6) is confined to an elongate northeast corridor that extends from the southern Maino region northeast through the Utcubamba valley and terminates north of Florida Canyon in the Naranjitos area, approximately 90 kilometers in length and 12-20 kilometers in width. The Utcubamba Valley continues to the southeast for an additional 40 kilometers through the Leimebamba area. Six partial stratigraphic sections, accompanied by local geological mapping were measured within the study area. Sections were confined to carbonate rocks of the Pucara Group. Section selection was a function of accessibility, exposure, infrastructure, and ultimately time and budget constraints. At the time of the study exploration was being carried out by Cominco Ltd. and later through a joint venture between Cominco Ltd. and Pasminco Ltd. Due to very poor exposure, heavy vegetation, extreme topography, and intensive post-depositional structural modification it was difficult to measure complete stratigraphic sections through the entire Pucara Group in any one locale.

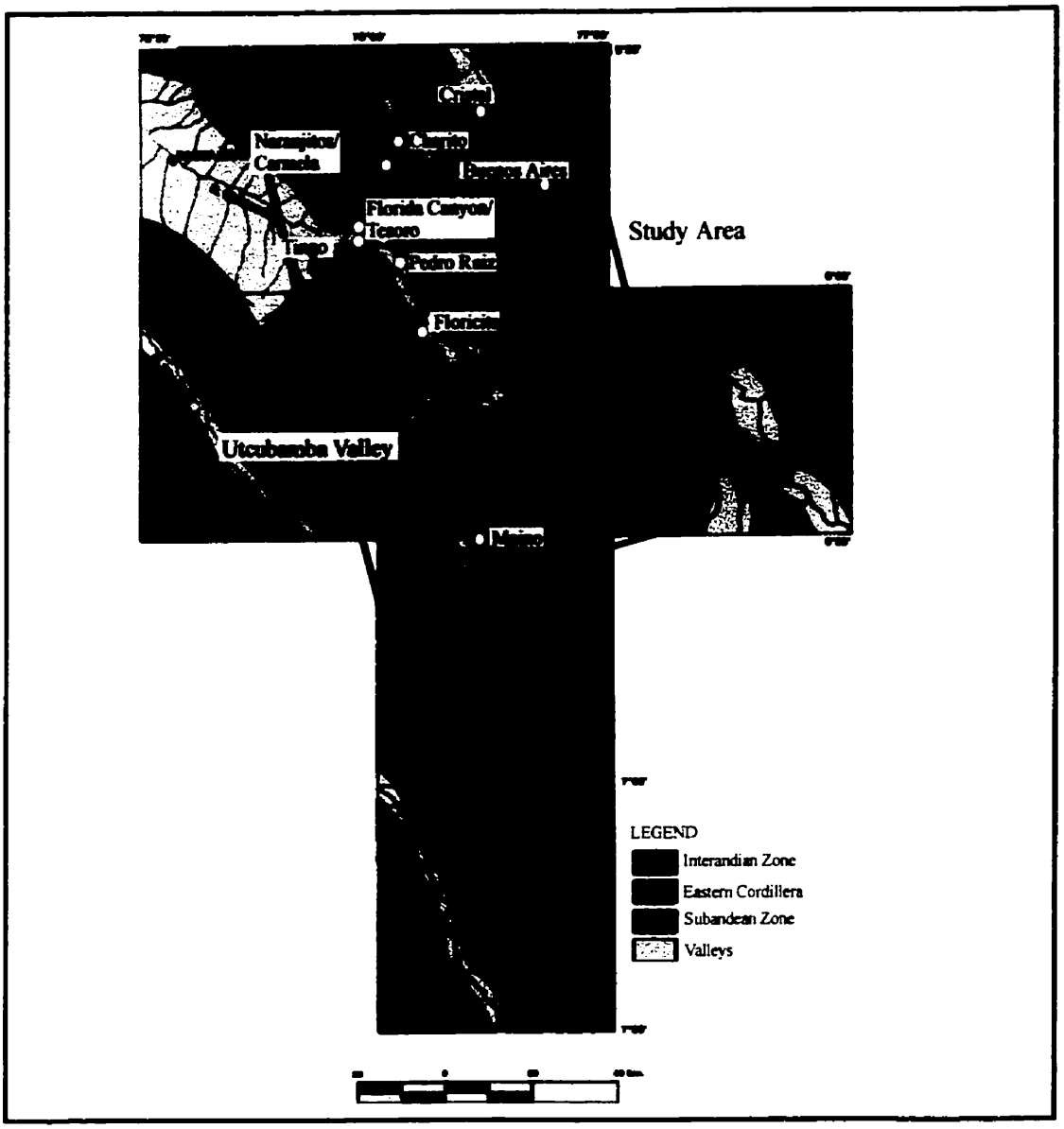

Figure 1.6 Bongara Location Map. Locations of major villages, zinc occurences, and measured stratigraphic sections with relation to the major geographic subdivisions of the region. Modified from Fig. 2.1 of Ingemmet Boletin No.56, 1995.

Stratigraphic sections were measured in the following locations: Florida Canyon, Tesoro Canyon, Tingo, Floricita, Maino, Buenos Aires, and Naranjitos, as indicated on figure 1.6. A significant drill core database exists for Florida Canyon (70+ ddh's), Tesoro, and Floricita. During stratigraphic work, over 700 samples were collected by the author (Appendix 1; Reid, 2001).

1.3.4 Stratigraphy of the Utcubamba Corridor

Unlike most global MVT districts, the Bongara area is located centrally within a moderately stable carbonate platform rather than along the basin margins. Within the study area the formal stratigraphic division of the Pucara Group (Gp.) as suggested by Harrison (1943), and Megard (1968) can be identified, though regional lithofacies correlation is difficult due to depositional controls, structural modification and lack of exposure. The Pucara sequences of this area provide a unique stratigraphic study due to the fact that tectonism and structural movements were active during and after Pucara Gp. deposition. This structural movement was both local and regional and variable in intensity. The end result is a northwest-southeast corridor of structural highs and lows preserved in an elongate structural belt corresponding grossly with the horst and graben structures of the underlying Mitu graben and elongate perpendicular to the later Andean thrust movement. These variable basement structures provided antecedent surface on which carbonate deposition was initiated, and appear confined within the Utcubamba Valley, an area of significant basement uplift. The distribution of carbonate facies observed in the area is a function of original Mitu basement topography, depth of water during carbonate production and distribution of structural reactivation of basement structures through the sediment pile during active deposition. The end result is a structurally controlled depositional pattern that closely conforms to the distribution of paleo-highs formed as a result of extensional tectonics and the associated structural reactivation along these topographic margins.

The best applicable depositional model is one of a series of stepped, piano-keyed, isolated, carbonate platforms distributed within a much larger platform that extends the length of the study area. The following section will discuss the general stratigraphy for the study area, encompassing local variations within the corridor as per observation from measured sections and regional mapping, as well as from detailed area studies conducted by the author and other Cominco Ltd. personnel involved in exploration of the area.

1.3.4.1 Basement

The oldest rocks in the study area are Precambrian gneisses of the Maranon complex, exposed in elongate, northwest trending, fault-bounded blocks which outcrop to the north of the study area and form the topographically highest blocks to the north of the study area (Fig.1.3).

The Permian Mitu red beds unconformably overlie the Maranon Complex and are well exposed throughout the study area, predominantly on the main road between the towns of Bagua Grande in the west to Pedro Ruiz in the east. In the study area the Mitu Formation consists of coarse-grained ferruginous sandstones and both oligomictic and polymictic conglomerates and/or local debris flows (Plates 1.1 and 1.2). These rocks are associated with horst and graben structures related to an failed ensialic rift (Noble et al; 1978; Kontak et al; 1985). Stratabound copper deposits and occurrences have been reported in the Mitu within central Peru (Amstutz, 1956; Kobe, 1960, 1990). The rift-related horst-and-graben structures of the Mitu provide the differentiated piano-key shaped basin surface, or paleorelief in which the carbonates of the Pucara Group were deposited.

1.3.4.2 Local Pucara Group

Through the studied area, the Pucara Group can be observed from the basal Chambara Formation unconformably overlying the Mitu redbeds through to the Aramachay Formation and in places, where preserved, the Condorsinga Formation (Fig.1.3)

1.3.4.2.1 Chambara Formation

Weaver (1942) applied different names to various intervals of the Chambara Formation, including the Utcubamba Fm. within this study area. The Upper Triassic limestones were named the Chambara Formation by Grose (1961) based upon outcrops near the Chambara village, about 20 km. northwest of the town of Huancayo. Stratigraphic correlations made between central and northern Peru have ensured the acceptance of the Grose (1961) nomenclature for the Chambara Fm. and has become the scientific standard. Though persistent through the study area, the Chambara exhibits laterally variable lithofacies, depending on the depth and location of the carbonate depositional environment in relation to basement paleo highs. For the purpose of this discussion the "reference" section for the Chambara Fm. will be that at Florida Canyon (Fig.1.6)

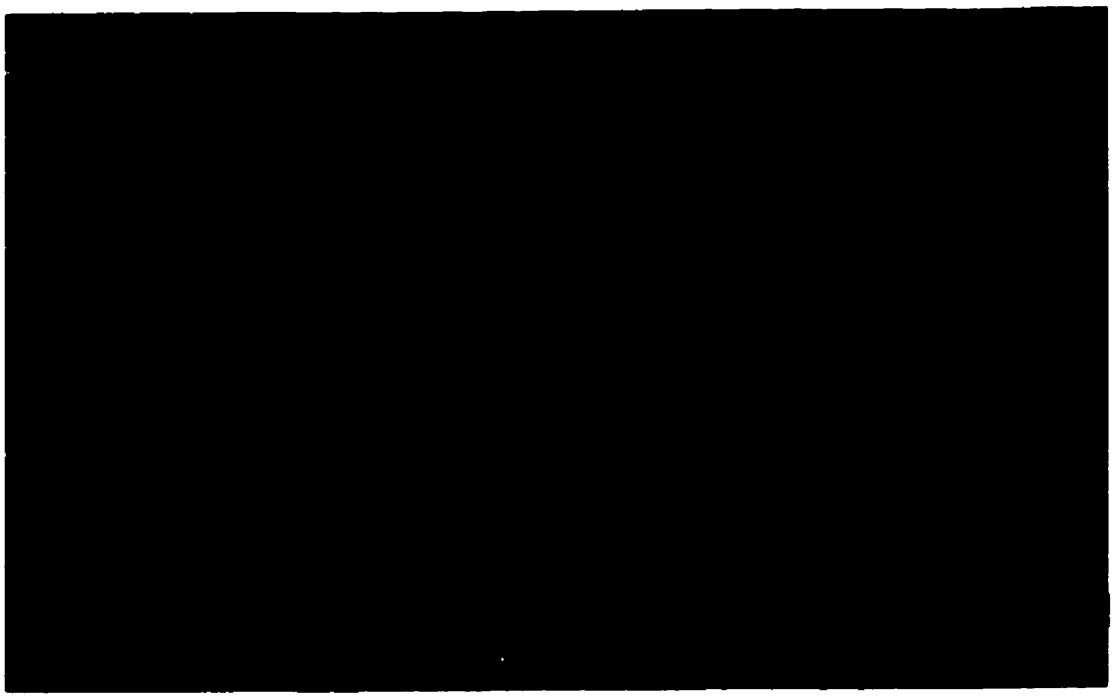

Plate 1.1 - Mitu Conglomerate; fragments of Proterozoic Maranon Complex gneisses supported within coarse-grained, well-sorted, consolidated ferriginous sand.

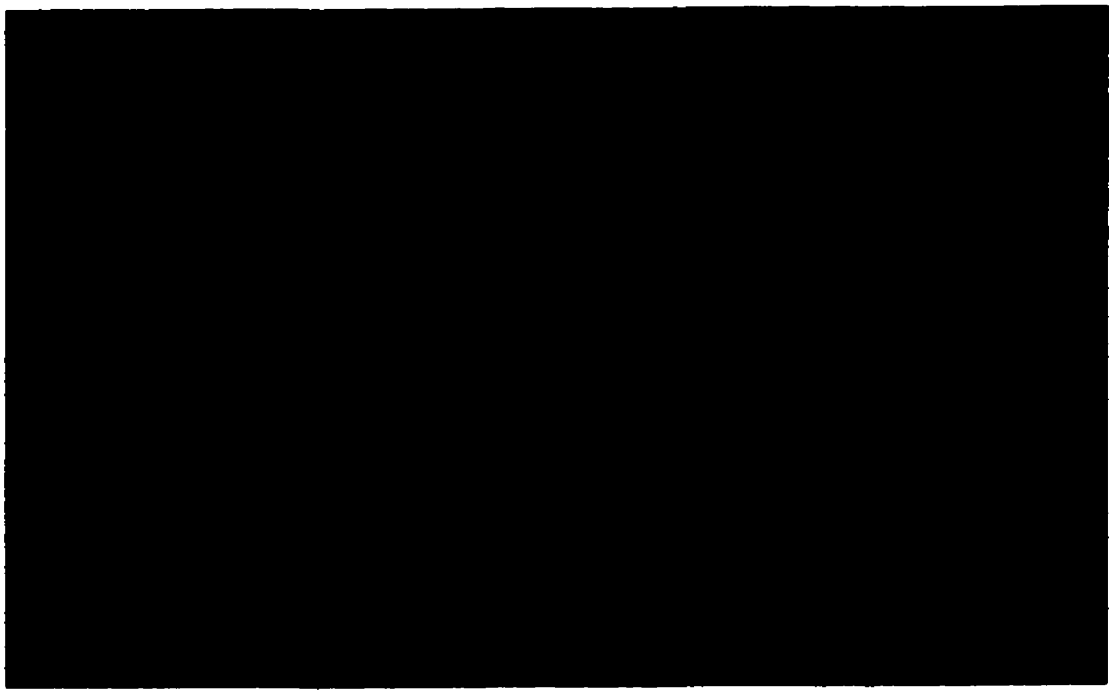

Plate 1.2 - Mitu Sandstones; laminated and cross-bedded,composed of well-sorted, consolidated, ferruginous sand.

being the best exposed of the seven measured and also having the most associated diamond drill core information. As a consequence, the Chambara has been informally divided into three sub-members designated Chambara 1,2, and 3, as described below. It should be noted at this point that throughout the Bongara region, carbonate stratigraphy has been overprinted by local and regional multiphase dolomitization. Based on stratigraphic, petrographic and isotopic work by the author (Reid, 2001) no early syn-depositional dolomite is present. All identified dolomite is late diagenetic to epigenetic, associated exclusively with the early ground preparation and post-metal precipitating phases of the MVT-style mineralization.

The Chambara 1 lies unconformably on Mitu Gp. red beds and where identified is comprised predominantly of algal limestones and lime mudstones, deposited in a very shallow, hypersaline sea with algal mats being common and evaporitic conditions being sufficient to precipitate anhydrite nodules within the lime muds. Substantial facies variations exist ranging from algal lime mudstones to local wackestones and storm deposits.

The Chambara 2 is composed of carbonate rocks from predominantly high-energy depositional carbonate environments. Lithologies range from nodular, bituminous lime mudstones through skeletal wackestones and packstones, fossiliferous floatstones and rudstones. Where exposed, the Chambara 2 –type lithologies remain relatively consistent and locally correlatable based upon a series of markers identified within the Florida Canyon, Tingo and Tesoro areas. These markers include the first appearance of a Sponge rudstone separating the Chambara 1 from the Chambara 2, a star crinoid marker, a well-developed and locally consistent coquina marker, and an intact bivalve marker. Centimetric to decimetric chert nodules are commonly observed within the Chamabara 2, but, due to lack of regional continuity, are useless for stratigraphic correlation.

The Chambara 3 is predominantly deep basinal lime mudstones and bituminous lime mudstones with minor shale interbeds, turbidities, and debris flows. Local work by exploration companies within the central part of the study area has defined a five-fold subdivision for the Chambara 3. The Chambara 3A is observed as a nodular textured lime mudstone. The Chambara 3B is a deep basinal turbiditic unit, while the Chambara 3C is predominantly a lime mudstone, with lesser shales, common bivalve debris, and is observed locally interbedded with 3B equivalents. Chambara 3D is dominantly silt laminated lime mudstones, turbiditic mudstones with minor interbedded shales. The 3E is very similar to 3D with the exception of the predominance of

variable sized concretions developed within the strata. The observation of concretions within the Chambara 3 marks the transitional contact into the Aramachay Formation.

1.3.4.2.2 Aramachay Formation

Megard (1968) named the Aramachay Formation based upon exposed shaley strata at the site of the Ichpachi mine, 2 km, southwest of the village of Aramachay about 30 km. northwest of the town of Hyancayo. Within the Bongara region the Aramachay is observed with various stratigraphic thicknesses throughout the district and is composed predominantly of deep basinal lime mudstones, calcareous shales and variable turbidites. The contact between the Aramachay and the upper Chambara Fm. is gradational over tens of meters and at times difficult to pick. The contact with the overlying Condorsinga where exposed is sharp and well defined.

1.3.4.2.3 Condorsinga Formation

Megard (1968) named the upper limestone unit of the Pucara Group the Condorsinga Formation. Within the Bongara area there is a marked difference in stratigraphic thickness regionally. Measured sections range from approximately 100 meters in the Floricita area (discussed below) to greater than 180 meters in the distal northeastern Buenos Aires section. Rhodes (1998) discusses the regional variations observed within the Condorsinga Formation with regards to both facies distribution and thickness. At Minas Grande, Rhodes (1998) observed coarsely pelletal lime mudstones, which overlie chicken wire-textured gypsum (after anhydrite). In the Floricita area the Condorsinga is predominantly medium-to-thin bedded limestones and dolomitized (mineralization-related) equivalents. In the Buenos Aires section the thickest exposures of Condorsinga were examined at over 200 meters thickness. Here the Condorsinga is predominantly a thin to fine bedded, bituminous, black to dark grey, fine-grained nodular lime mudstone. The Minas Grande area (Rhodes, 1998), and the Floricita area appear to represent a very shallow water depositional environments characteristic of a shallow hypersaline and restricted environment. On the other hand, the northeastern and eastern equivalents mark a much deeper basinal environment. This is a function of proximity to the general corridor of uplift within the Utcubamba Valley. The contact between the deeper basinal Aramachay and the Condorsinga in the central corridor of the area is much sharper than the eastern equivalents which appear to be a more inter-tonguing, transitional depositional center.

1.3.4.2.4 Post Pucara Group Units

To the east of the Utcubamba Valley the Corontochaca and Sarayaquillo formations are variably observed and pinch-out against a narrow high(s) formed by the uplifted Pucara Group and rapidly thicken away from it. Both units indicate a substantial degree of uplift, subaerial exposure and erosion of the Pucara group (Rhodes, 1998; Pardo and Sanz, 1979; Prinz, 1985; Rosas, 1994). The Corontochaca varies from very coarse scarp-derived boulder conglomerates to more sorted conglomerates, sandstones and silts of fluvial/deltaic character. The Sarayaquillo Formation is predominantly redbed shales, sandstones and marls with some gypsum beds. The contact with underlying stratigraphy in the Bongara region is unique and locally a strong angular unconformity is observed between the Pucara Group and the Corontochaca and Sarayaquillo Formations. This suggests a substantial degree of uplift and deformation, subaerial exposure and erosion of the Pucara Group rocks during the mid-Jurassic, confined within the Utcubamba Corridor.

The Lower Cretaceous clastic Goyllarizquisga Formation unconformably overlies the Pucara Group within the study area and the Sarayaquillo formation locally. The Goyllarizquisga Formation consists mainly of delta and shallow-marine clastic sediments (Wilson, 1963; Rosas, 1986). These continental siliciclastics are interpreted as synorogenic products of the Nevadian Orogeny and overlie a regional stratigraphic unconformity. Elsewhere within the study area, the unconformity surface cuts variably through different stratigraphic levels of the Pucara Group, and in places near Maino, rests upon the Mitu, suggesting complete erosion of the Pucara.

1.3.5 Description of Studied Sections

Throughout the study area, seven measured sections were completed, accompanied by geological mapping, sampling and drill core analysis when available. Investigations include petrographic and stratigraphic analysis as well as cathodoluminescence and stable carbonate isotope analysis. The six measured sections include the Florida Canyon, Tesoro, Tingo, Naranjitos, Floricita, Buenos Aires, and Maino areas. The following will discuss the stratigraphy of each area individually. An attempt to synthesize and interpret the data on a basinal and depositional scale will be made later along with a structural synthesis.

1.3.5.1 Florida Canyon

The Florida Canyon area is located approximately 13 km. northwest of the village of Pedro Ruiz (Fig1.6). This area has been the focus of study since the most significant amount of mineralization discovered thus far has been confined to this area. There is good access and exposure within the area. To date approximately seventy drill holes and significant detailed mapping have provided the author with a very good, detailed geological database from which to draw additional information.

The Florida Canyon area is located within a fold-and-thrust belt that resulted from continuous compressive orogenic events associated with the formation of the present Andes. The belt trends NNW-SSE and includes folds that are predominantly parallel to the belt and are characterized by relatively long wavelengths and small amplitudes (Szybinski, 1998). Florida Canyon cuts across the southwestern limb of a broad dome overlying exposed Chambara formation rocks. Rocks are generally flat lying, with minor gentle folds. Detailed mapping by Cominco staff shows that the Florida Canyon area is typified by a well-developed dome-and-basin pattern. Stratigraphic logging of all the holes confirms a domal stratigraphic pattern confined to the main area of interest (Fig.1.7 and Fig.1.8).

A major fault zone, the Sam Fault cuts the stratigraphy on the west side of Florida Creek and down drops Chambara 3 in the western block against Chambara 2 rocks in the eastern block. Movement of the Sam Fault is complex and has a scissor component with offset greater in the north (approx. 125 meters) than in the south (approx. 50 meters) (Szybinski, 1998; Wodzicki, 1998). The Sam Fault also has a right lateral strike slip component and some splays off the main fault in the northern part of the Canyon are in fact positive flower structures (Szybinski, 1998). Numerous northeast trending fractures cut rocks in the eastern block; however, the planar bedding does not appear to be displaced by faulting (Fig 1.9).

In the Florida Canyon section, only the Chambara and Aramachay Formations of the Pucara Gp. are exposed. As noted previously, the Chambara has been informally divided into 3 subunits, described below.

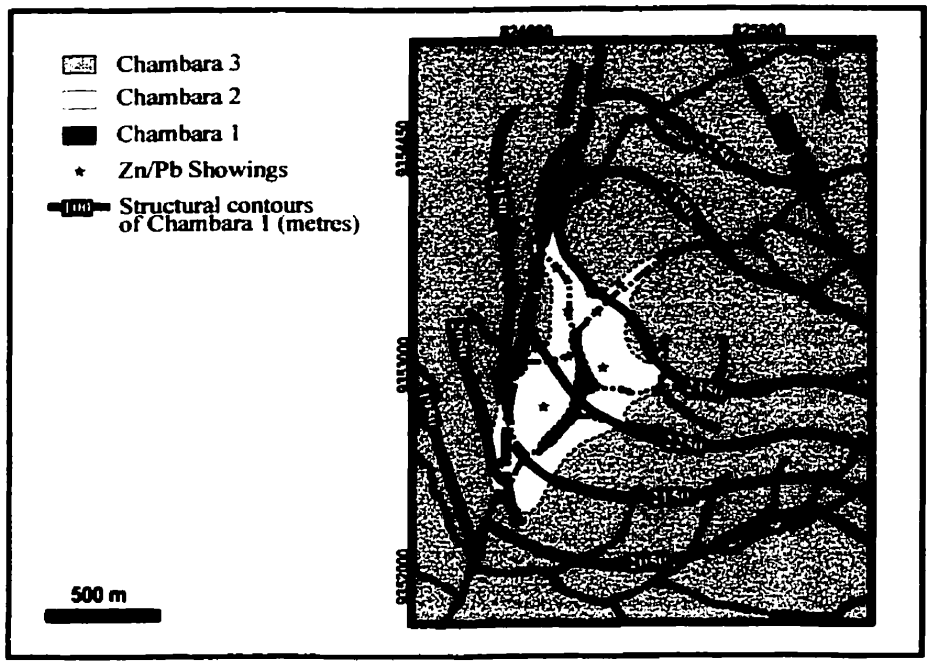

Figure 1.7 Structural contour map on the top of the Chambara 1, Florida Canyon.

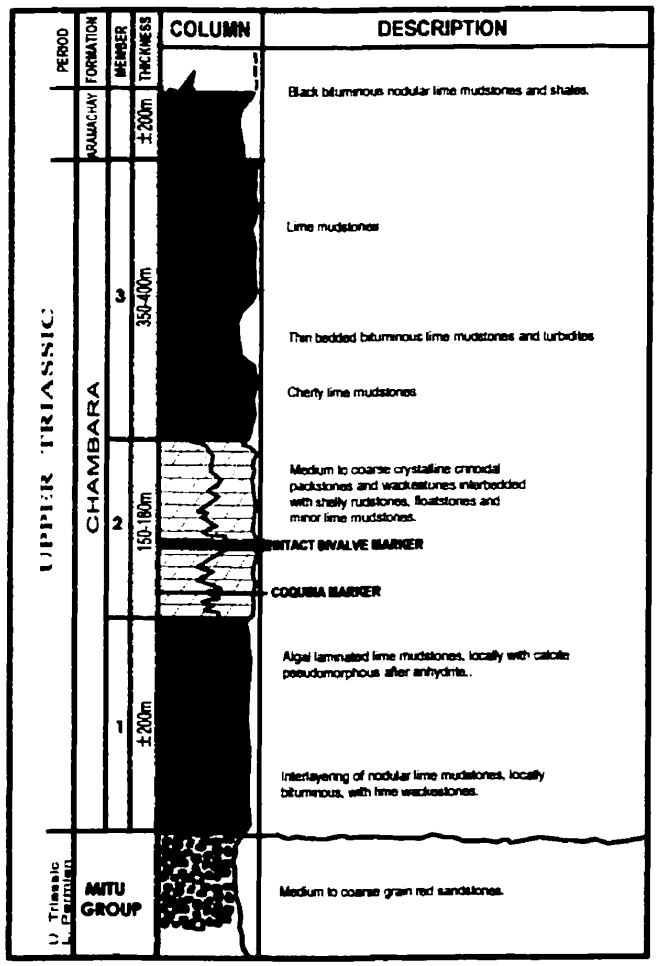

Figure 1.8 Stratigraphy of the Florida Canyon and Tesoro Canyon areas.

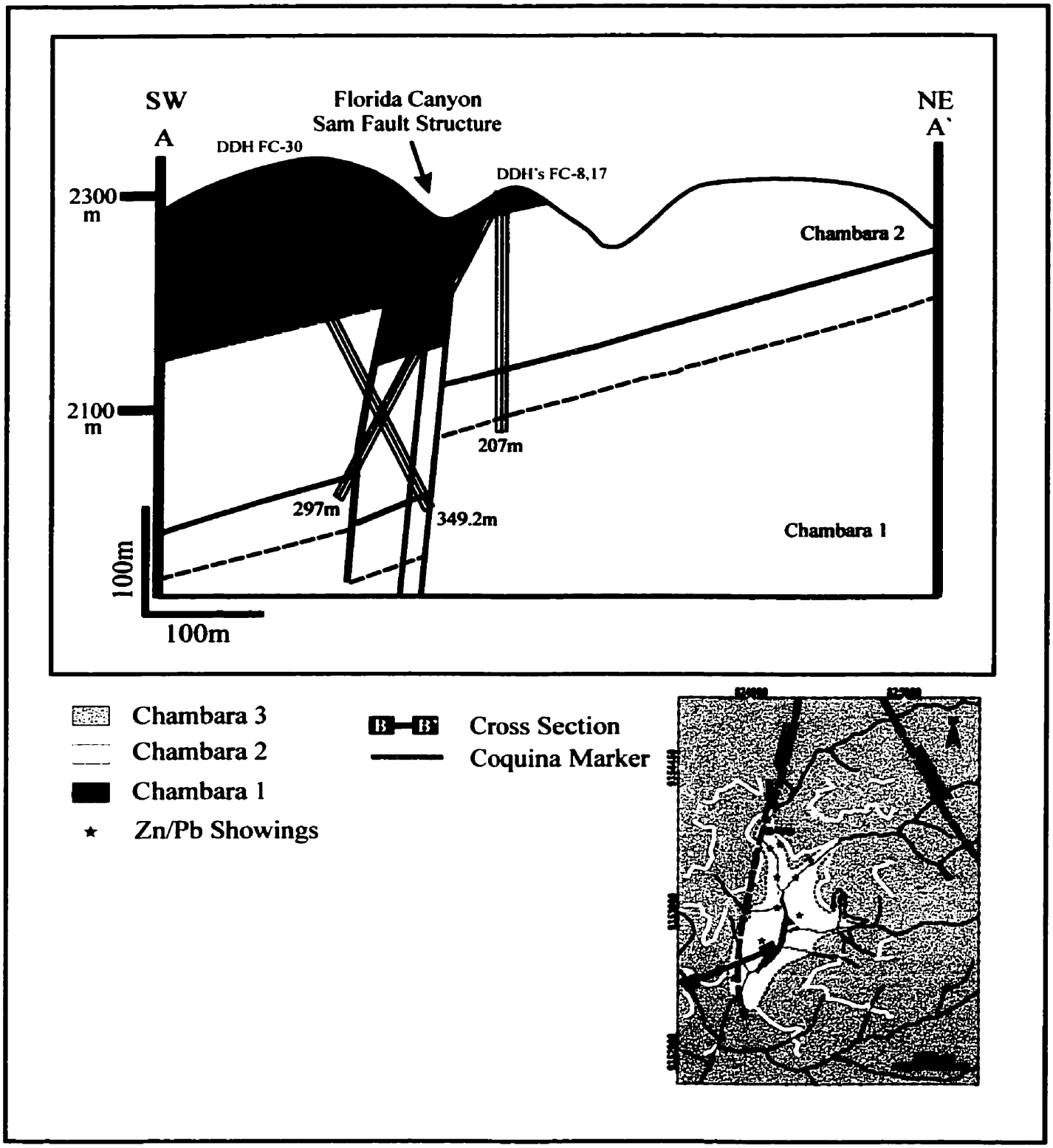

Figure 1.9 Structural cross section A-A', looking northwest, of the southern Sam Fault system in Florida Canyon.

The Chambara 1 Formation has been intersected by exploration drilling in the area and is well exposed within the lower Florida Canyon. It unconformably overlies an erosional surface on the underlying Mitu Gp. sediments and is observed with a general thickness of approximately 200 meters representative of a restrictive tidal flat depositional environment. The rocks consist of light to cream to medium brown, finely crystalline, lime mudstones with textures that vary from relatively massive, to fine and subtly laminated, with 0.1 to 4 mm dark brown to black, clay and/or organic rich layers (Rhodes, 1998.) Occasional small intraclast breccias are observed and likely resultant from periodic storm rip-up events. Evidence to the restrictive and evaporative nature of the environment is provided by the presence of 2 to 20 mm. irregularly bounded ovoid calcite spar forms that are typical of psuedomorphs after anhydrite nodules. Rhodes (1998) observed small-scale faults that cut some laminations but are capped by further undisplaced laminations as evidence for small tectonic disruptions of the algal flats. It seems likely that in many places within the study area active fault movement and reactivation persisted through sedimentation. In this study, only local sections of the Chambara 1 were observed in drill hole as most exploration holes were shut down when this unit was intersected.

Regionally, this tidal flat unit of algal laminations has only been identified in the Florida Area and in a slightly modified form in the southernmost Maino area. This initially suggests a localized, restricted depositional environment, likely on top of a paleo high, when compared with deeper basinal and platformal carbonate sedimentation observed elsewhere. The characteristics of these rocks indicate they were deposited in a very shallow (sub to intertidal), hypersaline sea with algal mats being common and evaporitic conditions being sufficient to precipitate anhydrite nodules within the lime mudstones (Plates 1.3 and 1.4) (Shinn, 1983).

The Chambara 2 formation is indicative of a shoal to biostrome unit deposited within a high-to very-high energy depositional environment. This is the major host to the bulk of mineralization observed within the Florida Canyon area. The contact with the lower Chambara 1 algally laminated lithofacie is sharp and easily correlatable. The section varies from 150 to 180 meters true thickness depending on proximity to the faults and location on the local platform. Rhodes (1998) identified five prominent lithofacies within this middle division (Chambara 2) of the formation. All of these lithofacies can be identified in the drill holes, in local mapping, and in measured sections from proximal areas. Throughout the Florida Canyon area this unit is observed pervasively dolomitized. Drill hole analysis and lithofacie distribution show that all

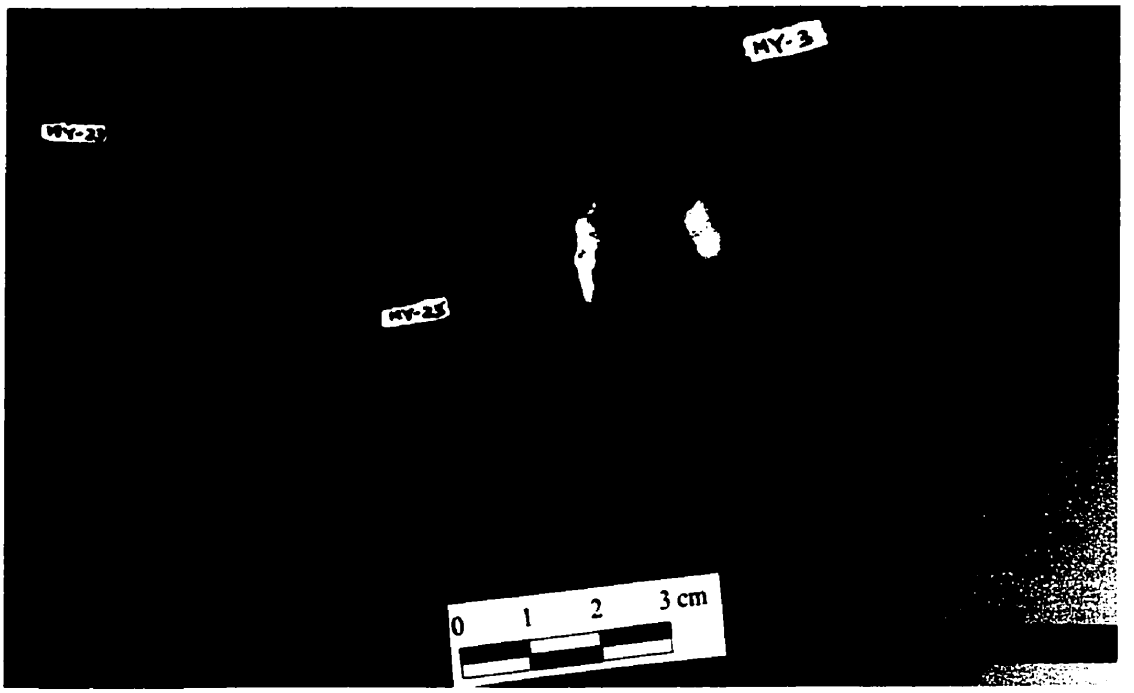

Plate 1.3 - Chambara 1 equivalent dolomitic limestones from the basal Maino section. Samples show open space infill and partial psuedobrecciation by late white dolospar.

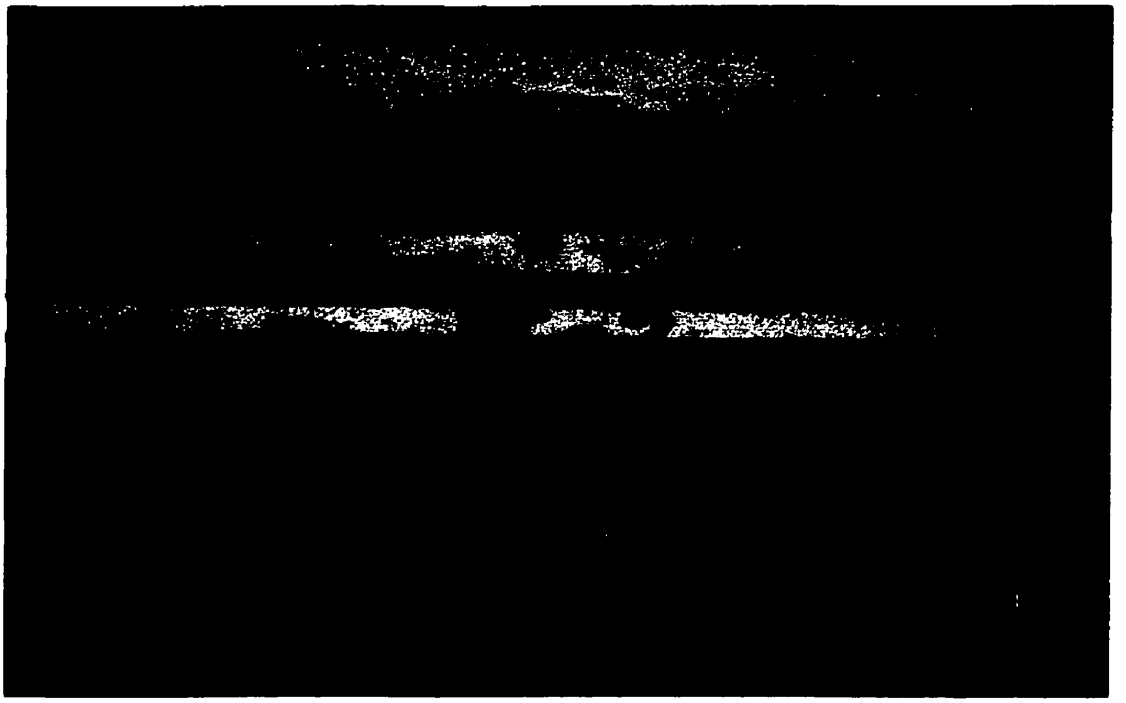

Plate 1.4 - Chambara 1 algal laminated lime mudstones and cream lime mudstones with calcite psuedomorphs after anhydrite nodules.

Chambara rocks in the Florida Canyon area were original limestones and any dolomitization is a result of evolving basinal fluids associated with mineralization and/or late diagenetic alteration.

The five lithofacies identified are: 1. Wispy, argillaceous, usually nodular, moderately dark to medium grey, fine grained bituminous lime mudstone (Plate 1.5). 2. Wackestones in which 10% or more fine skeletal debris generally crinoidal and/or fragmented bivalve shells, occurs in and is supported by a lime mud matrix (Plate 1.6). 3. Packstones comprised of abundant skeletal debris generally clast-supported with a fine lime mud matrix. Two types seem to be exclusively composed of intact to abraded crinoid ossicles and those that combine crinoid ossicles with some shelly debris represent the packstones. The former were deposited in a more strongly wave/current dominated environment than the latter. 4. Fossiliferous floatstones consist of greater than 10% fossil debris coarser than 2mm but in a mud and fine fossil matrix. The fossils are most commonly fragmental bivalves (pelecypod, brachiopod) but may include thicker celled or chambered forms that are probably corals, calcisponges and in some instances gastropods (Plate 1.7 and 1.8). 5. Fossil rudstones composed of abundant coarse fossil debris that is clast-supported with fine fossil and some lime mud matrix. The fossils are the same as those found in the floatstones.

The Chambara formation in the Florida Canyon area, especially the shoal/biostrome Chambara 2 middle division, shows a very high degree of stratigraphic control and planar stratigraphic correlation. In general the most useful units for stratigraphic correlation have proven to be the coarsely fossiliferous floatstones and rudstones. There are four such units that show the consistency of characteristics to act as reliable markers within the area. A distinctive black matrix, star crinoid-rich wackestone, also serves as a good stratigraphic marker. Most of the fossil units higher in the Chambara 2 show a degree of thickening and thinning, occasional absence and a lack of distinctiveness from each other.

The depositional environments of these rocks is predominantly one of high energy, wave and/or current conditions with relatively shallow water depths. Light and oxygen were sufficient to encourage abundant marine organism to thrive but at the same time to be broken up and winnowed to some degree so that concentrations of broken crinoid ossicles and shell debris accumulate. The depositional environment of the Chambara 2 in Florida Canyon is indicative of a common bank margin or wave-side reefal environment as defined by identified lithofacies assemblages (Fig.1.10) (James, 1983; Halley, et al., 1983). The coarser fossil lithologies represent

Plate 1.5 - Chambara Formation in the lower Florida Canyon near Tingo. Marked area represents, a sequence of fine-grained bituminous mudstones of the lower Chambara 2.

Plate 1.6 - Chambara 2 - Wackestone of which 10% +/- is comprised of fine skeletal debris gennerally of crinoidal and/or fragmental bivalve shells supported in a lime mud supported matrix.

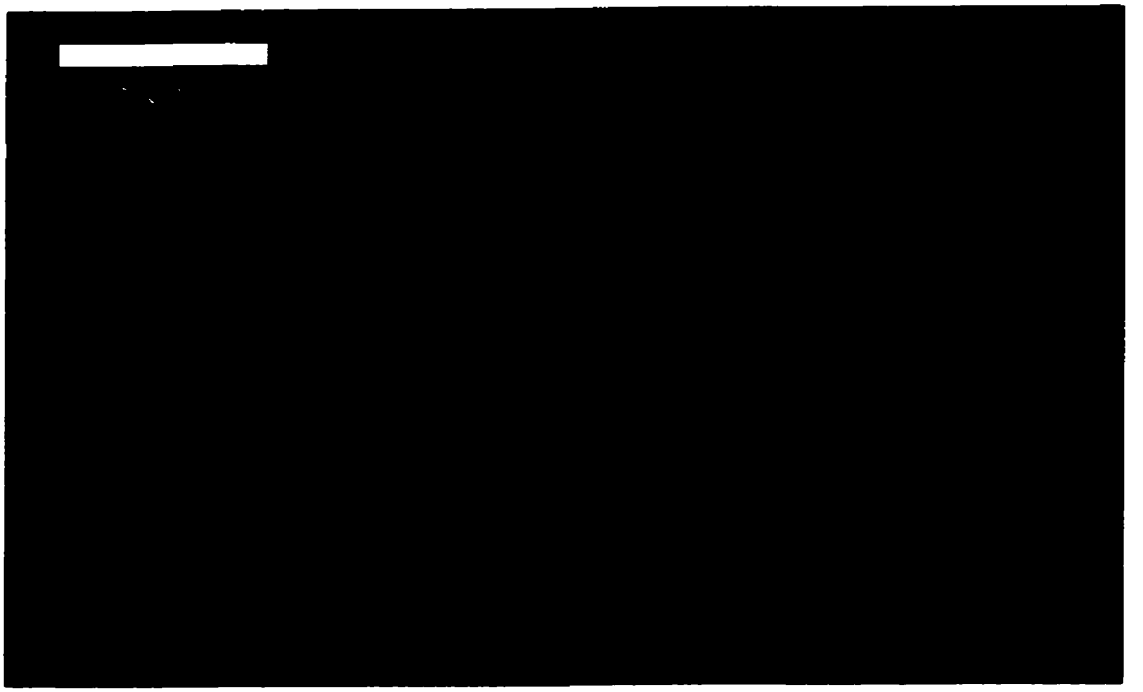

Plate 1.7 - Fossiliferous packstone composed of clast-supported skeletal debris with a fine lime mud matrix. Here the crinoidal packstone is partially psuedobrecciated.

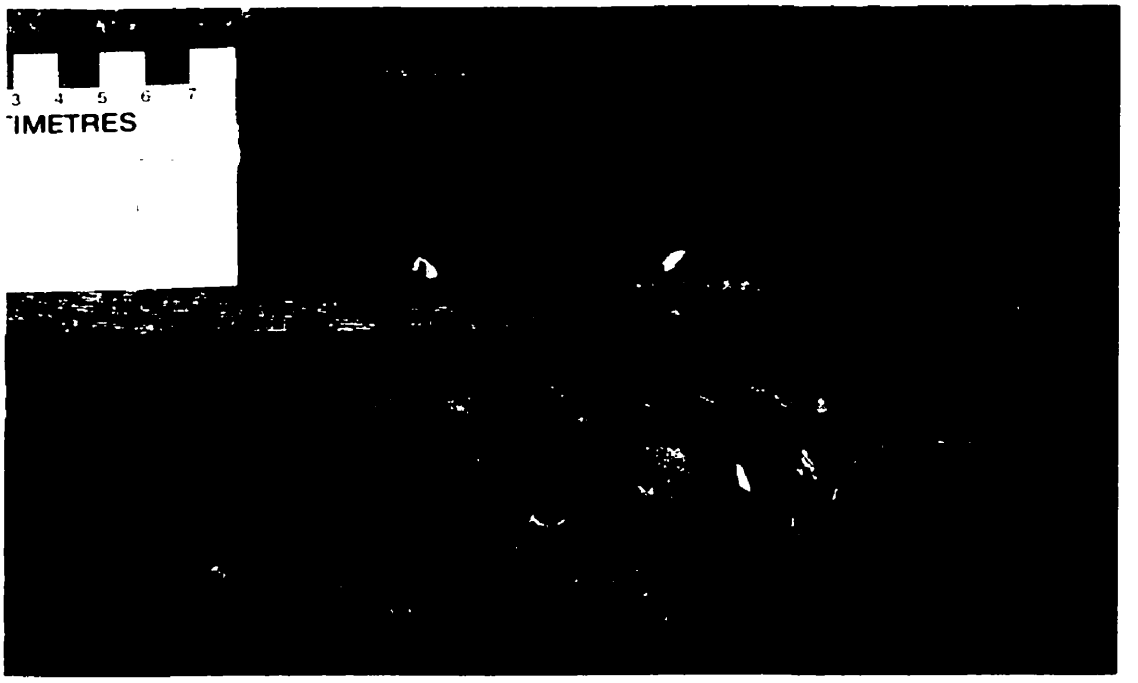

Plate 1.8 - Fossiliferous Floatstone consists of greater than 10% fossil debris coarser that 2 mm. But in a mud and fine fossil matrix.

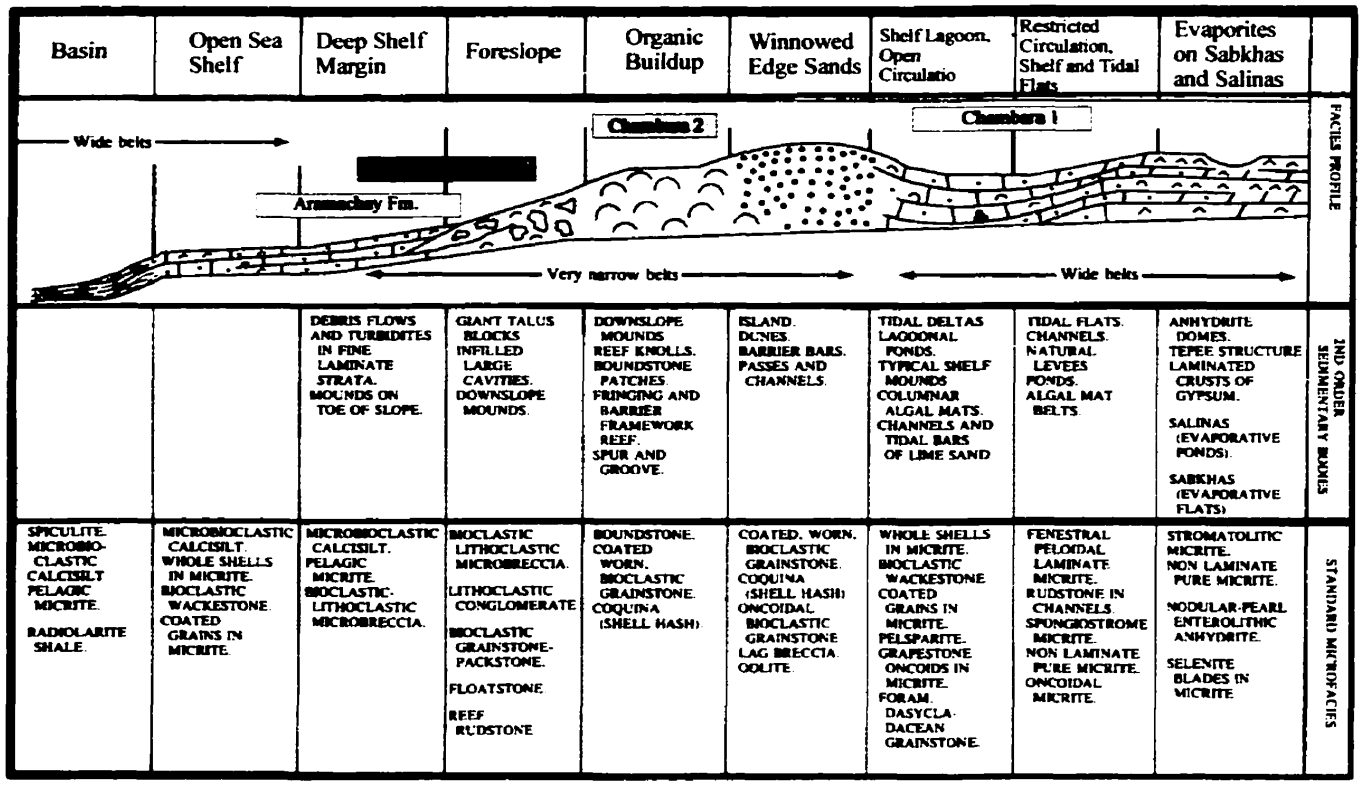

Figure 1.10 Standard facies belts on an idealized shallow-water carbonate platform. The pattern results from a combination on the effects of slope, geological age, water movement, and climate. Modified from Wilson, 1975.

lower energy and/or optimum conditions for larger fossil organisms and approach reefal conditions. The oscillation of the different lithofacies evident in the stratigraphy of the Chambara 2 represent slight and partially cyclic variations in the conditions of the environment.

The Chambara 3 is comprised predominantly of deep basinal lime mudstones and bituminous lime mudstones with minor shale, turbidite and local debris flow units identified. A gross informal subdivision can be applied to the Chambara 3. The Chambara 3A is observed as a nodular textured lime mudstone. The Chambara 3B is a deep basinal turbiditic unit. Chambara 3C is predominantly a lime mudstone with lesser shales and common bivalve debris, and is observed locally interbedded with 3B equivalents. Chambara 3D is predominantly silt laminated lime mudstones and turbiditic mudstones with minor interbedded shales. The 3E is very similar to D with the exception of the predominance of variable-sized concretions developed within the strata. The observation of concretions within the TCh3 mark the transitional contact into the Aramachay Formation (Plate 1.9).

The depositional environment of the Chambara 3 can be considered one of a typical fore-reef slope grading towards a slightly deeper basinal environment when shales are deposited (Fig.1.10) (Enos, 1983). The presence of local turbidites is indicative of some nearby basinal relief while the mudstone suggests fairly deep basinal conditions, or a fore-reef to basinal margin depository for carbonate sediments spilling off a shelf-edge environment. The Chambara 3 division has not been completely measured in the Florida canyon area due to extreme topography. However, in the proximal Tesoro area, a complete section has been documented. In general the Chambara 3 section in the Florida Canyon is at least 200 meters thick and conforms to the variations above.

The Chambara section at Florida Canyon is considered the type section for base metal work in the area as a result of the significant geological database, and drill hole information collected. Interestingly the consistency and definability of the stratigraphy in the area is unique and does not easily extrapolate regionally for more than 8 to 10 kilometers peripheral to the center of known mineralization.

1.3.5.2 Tingo

The Tingo Section is located at the southernmost end of Florida Canyon, approximately 5 kilometers south of the main exploration area (Fig.1.6). Though the section is well exposed and

Plate 1.9 - Transition between the upper Chambara 3 and the Aramachay Formations. In most areas this gradational contact ranges from 10 to 25 meters.

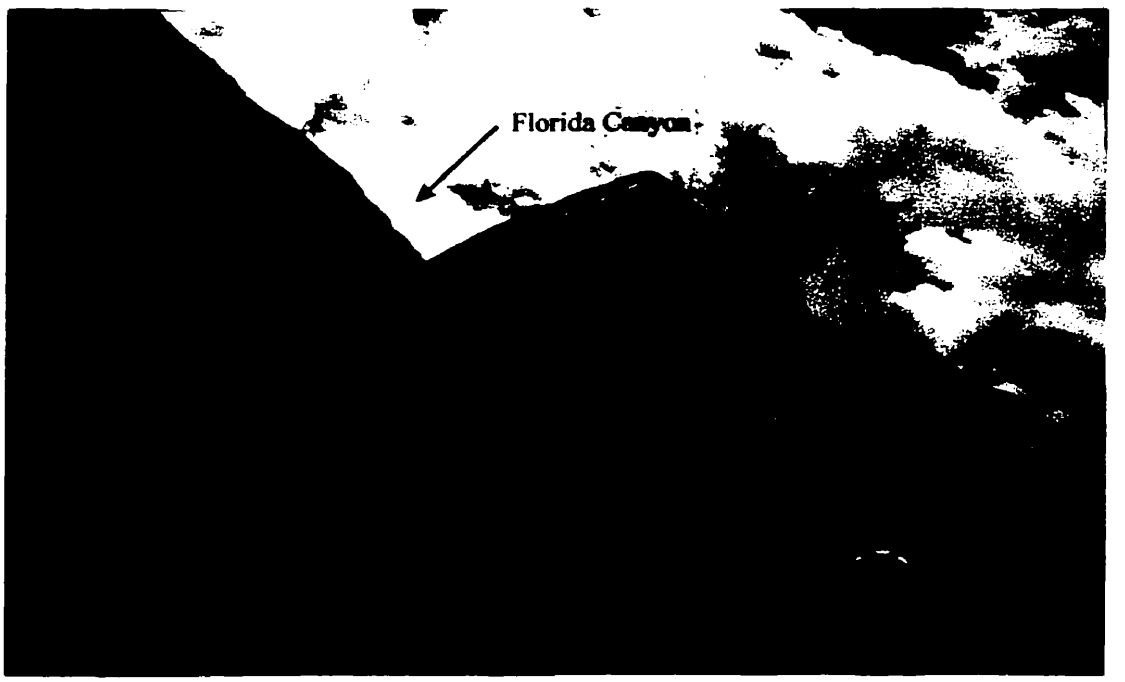

Plate 1.10 - Structurally-controlled valley near the village of Tingo. Slopes are assumed to have resulted from reactivated structures within the Mitu horst-and-graben system, likely representing platformal margins for Pucara Gp. carbonate sedimentation.

easily measurable along a trail that climbs from the village of Tingo into the rain forest, the section represents the southern most extrapolation of the northern trending Sam structure discussed above. A significant degree of structural reworking, late dolomitic overprinting and structural brecciation obscures the original lithofacie and makes identification difficult. A preserved section resting on the Mitu sandstones extending upward through the Chambara was obtained and is grossly correlative with the Florida Canyon section. The total section measured 335 meters, starting in the lower Chambara 1 tidal flat unit and extending through to the Chambara 3 of Florida Canyon.

Chambara 1 equivalent lithologies were observed over a thickness of approximately 160 meters. Distinct lithofacies comparable in part with Florida Canyon include algal laminated mudstones and argillaceous thin mudstones. Interestingly, lithofacies consisting of bioclastic wackestones and packstones, comprised of skeletal debris, indicative of higher energy depositional environments, were encountered interbedded throughout the lower Chambara section. At Tingo, these sequences were slightly thicker-bedded on the scale of 2-15 cm., were dark grey and conformed very closely to those described within the central stratigraphy of Florida Canyon (Refer to Appendix 2 of Reid, 2001 for detailed sections and lithologs). These units were consistently overlain by thin lime mudstone lithofacies.

The Chambara 2 equivalent lithofacies were observed over a thickness of 210 meters, which correlates very well with Florida Canyon. Lithofacies consisted of high-energy wackestones, packstones with rare floatstones, and rudstones. Markers observed in Florida Canyon were not encountered in the Tingo section likely due to the very strong overprinting of original sedimentary features by various coarse dolospar phases (discussed later). The contact between the lower tidal flat unit and the high-energy biostromal unit was based upon the first appearance of a thick packstone unit. Though pervasively dolomitized, they are identifiable by the nature of preserved bedding, relict textures and outcrop weathering.

Forty-five meters of Chambara 3 equivalent lithofacies was studied until exposure was lost to overburden. The lithologies seen were consistently fine-grained, thin-bedded, slightly bituminous lime mudstones with small chert nodules in the lower depths, grading upward into slightly more thinly bedded bituminous lime mudstones.

In general, though obscured by structural disruption and fluid alteration, the Tingo section remains relatively consistent with lithologies seen at Florida Canyon. The correlatability is unique when compared regionally and it can be concluded that both areas are located within a single isolated platform environment. Though not observed in great thicknesses, the presence of fossiliferous packstones and wackestone suggests that towards the southern end of this isolated platform the influence of a slightly higher-energy depositional environment than that of merely a tidal flat, as observed 5 kilometers to the north, suggests that this isolated platform may be nearing its southern extent in the Tingo area. This marks the edge or margin of the paleo high on which the carbonates where deposited. This is further verified by mapping south of Tingo, which shows predominantly deeper-water Chambara Fm. lithologies with no high-energy carbonates identified. The village of Tingo is located along a western trending valley that has huge structurally-controlled topographic relief. This could very well represent the edge of a paleotopographic block (Plate 1.10).

1.3.5.3 Tesoro Canyon

The Tesoro Canyon section is located 6 km, ENE of the main Florida Canyon area on the east side of the Tesoro-Florida anticline (Fig.1.11). Tesoro has the most extreme relief of the entire study area with cliff walls up to 200 meters high. Though a complete section can be mapped out extending from the basal Mitu red beds through to the Aramachay Formation, topographic limitations allowed for only the detailed study of the Chambara 3- type lithologies including the transition into the Aramachay Formation.

Regional mapping of the lower Canyon identified a thick sequence of fossiliferous packstones, and wackestones analogous to the higher energy carbonates of the Chambara 2 division in Florida Canyon. Drill testing of mineralized targets in the Canyon confirms a local stratigraphic correlation of lithofacies and depositional environments between Florida and Tesoro Canyon including identification of the Coquina marker in the lower Chambara.

The Tesoro section is important as it provides some of the best-preserved sequences of the upper Chambara and the transition into the Aramachay. The section measured just over 600 meters (Appendix 2). Of importance in the section was the visible and documented correlation between the sub members of the Chambara 3-type lithologies identified from Florida Canyon. Over 475 meters of measured section and all five divisions of the upper Chambara discussed above were

identified. The section was composed of predominantly of fine-grained, thin-bedded, planar lime mudstones interbedded with shales, rare thin turbidites, and higher-energy deposited packstones (Plates 1.11 and 1.12). The Chambara 3 in the section shows a very gradational contact with the Aramachay Formation marked by an increase in the overall organic contact of the lime mudstones with the presence of interbedded concretions ranging in size from 10 cm to 0.5 meters. The gradational contact with the Aramachay occurs over a thickness of 25 meters.
The author picked the base of the Aramachay at the predominance of black organic, non-calcareous mudstones and shales and the first appearance of ammonites along bedding planes.

The fore-reef depositional environment of the Chambara 3 in the Tesoro Canyon suggests that correlatable lithofacies across the platform are indicative of relatively stable basinal conditions during the transition into the Aramachay time. The presence of thin turbiditic units in the Chambara 3D equivalent lithologies suggests that there was significant basinal relief and instability at the time of deposition. For detailed log and sample descriptions from the section refer to Reid (2001) Appendix 2.

1.3.5.4 Floricita

The Floricita section is located at the main exploration target 16 kilometers SSE of the town of Pedro Ruiz, along the Utcubamba River, measured up a steep slope on the west side of the Utcubamba Valley. The section measured totaled 250 meters and was based in the upper Chambara, extending through the Aramachay and into the Condorsinga. The Section terminated at the Cretaceous unconformity and the overlying Goyllarisquizga sandstones (Plates 1.13)(Appendix 2).

Though incomplete the Chambara section consisted principally of deep basinal, bituminous lime mudstones, interbedded with mud dominated, pelletal wackestones and rare thin packstones. The measured section of upper Chambara totaled 150 meters. Most importantly, the distinct lithofacies identified at Tesoro and Florida Canyon within the upper Chambara (Chambara3-type) were absent. Though the rocks were accumulated in deeper basinal fore-reef slope conditions there was no indication of turbiditic units, concretions or chert nodules.
The transition into the Aramachay Formation was fairly sharp when compared with the other areas studied. The Aramachay in the Floricita area had a thickness of 70 meters total. The rocks

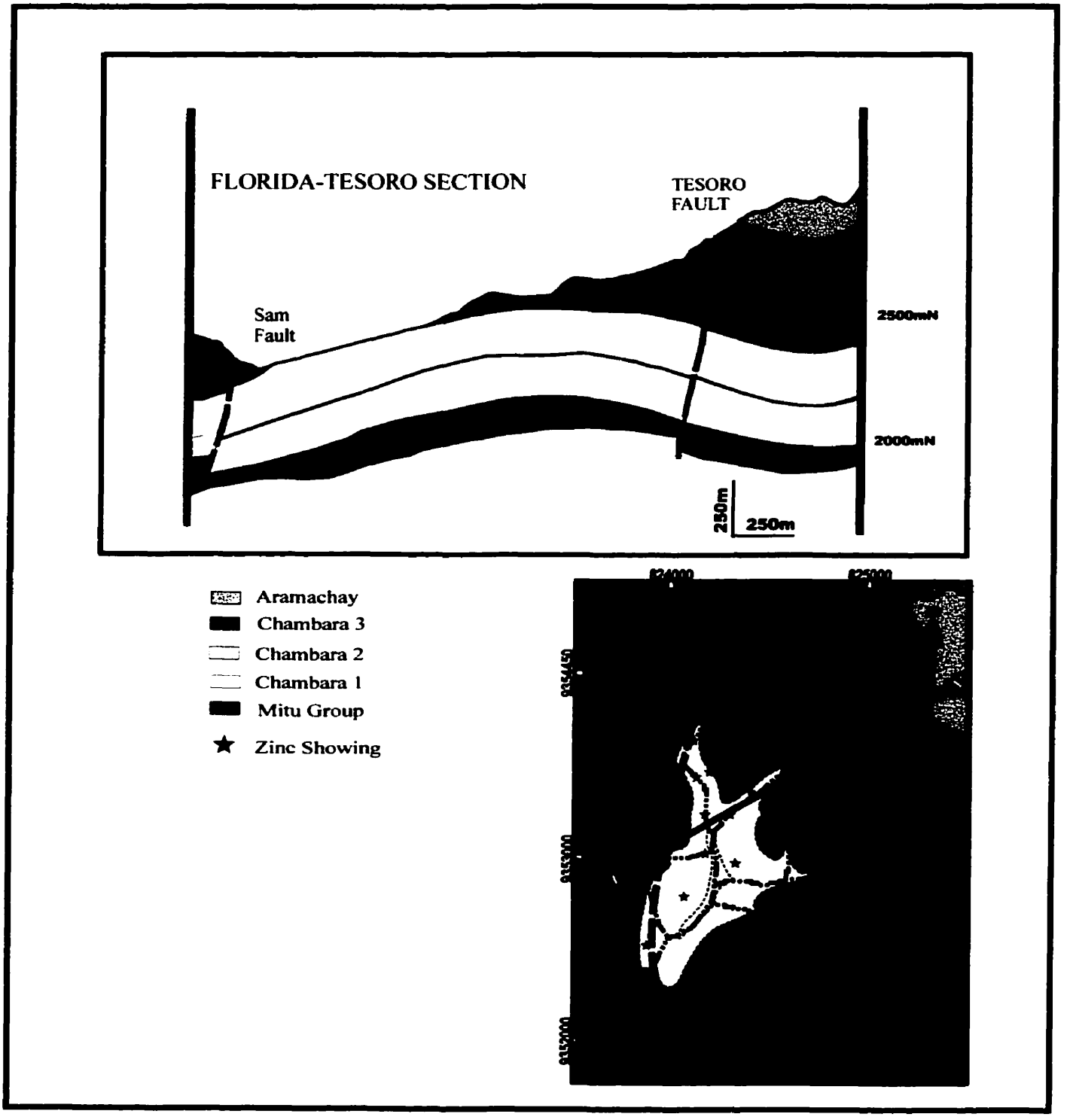

Figure 1.11 Cross section A-A'showing the stratigraphic relationships between the Florida and Tesoro Canyon areas.

Plate 1.11 - Thin-bedded turbidites in the Chambara 3 of Tesoro Canyon.

Plate 1.12- Nodular concretions within fine-grained, bituminous limestones of the upper Chambara 3 in Tesoro Canyon.

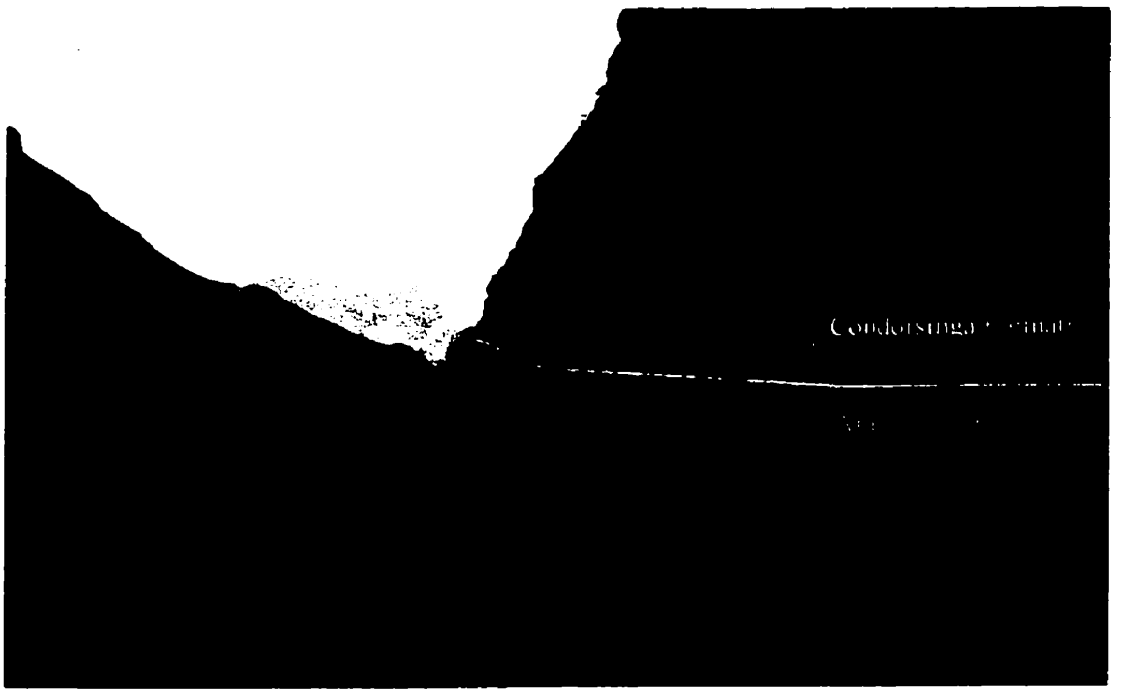

Plate 1.13 - Panoramic of the Utcubamba Valley at the Floricita section. The contact between the Aramachay and Condorsinga Formations have both a topographic and vegetative distinction.

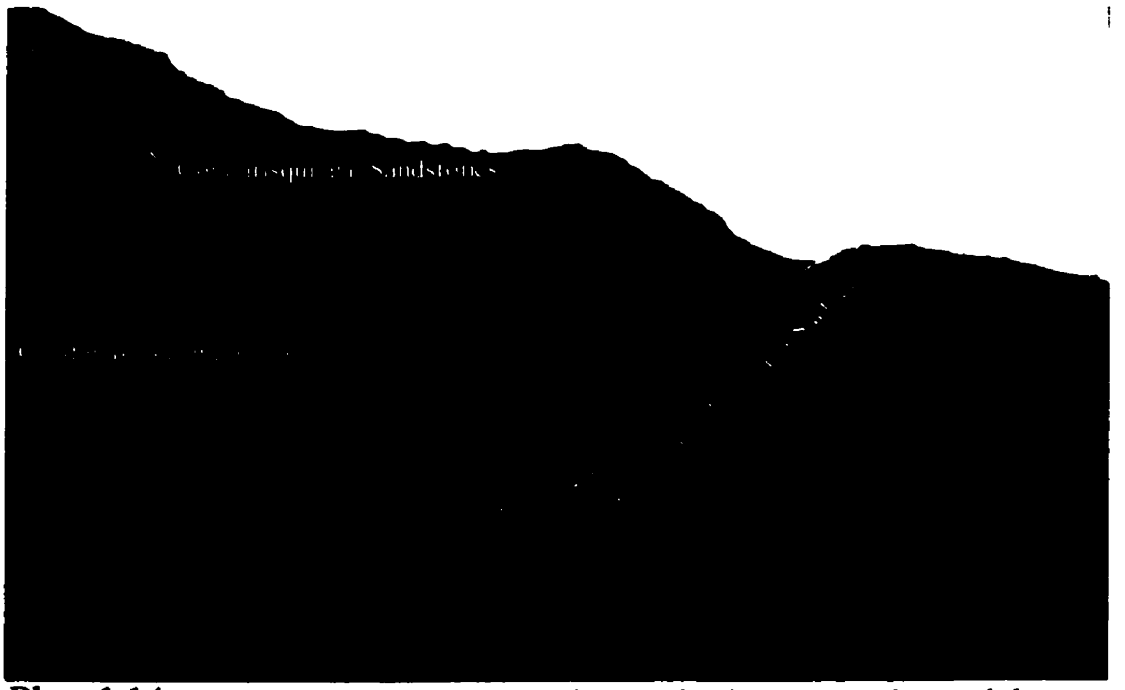

Plate 1.14 - Erosional contact between the Condorsinga Formation and the Goyllarisquizga sandstones.

are very fine-grained, thin-bedded, planar black mudstones with thin brown shale partings. The Aramachay in the Floricita area remains very consistent and easily definable. The transition into the Condorsinga formation is observed over approximately 10 meters thickness as a significant increase in the calcareous component of the rock, with a thickening of bedding and an increase in grain size to an eventual light brown to brown, thin to medium bedded calcareous mudstone and wackestone. Original sedimentary structures within the Condorsinga are obscured due to pervasive local dolomitization associated with mineralization. However, the general appearance suggests a more restricted environment, as possible algal laminations and wispy argillaceous bedding are locally observed. At the section the Condorsinga thins from 100 meters to 50 meters laterally, over approximately 300 meters from south to north as a result of a sloping erosional surface or pre-Cretaceous faulting (Plate 1.14).

The Floricita section is very important as a dramatic thinning is observed in the Aramachay formation when compared with the other sections and regional studies. The Aramachay Formation in the Floricita area is only 70 meters thick, whereas in the Florida and Tesoro Canyon areas it is a minimum of 200 meters thick. This strongly suggests that the Central Utcubamba Valley underwent significant structural uplift forming a paleo high during Aramachay deposition, or was already a location of elevated topography.

1.3.5.5 Naranjitos/Carmela

The Naranjitos/Carmela area is located approximately 27 kilometers northwest of the town of Pedro Ruiz. This area is underlain by Pucara Group rocks comprising the Chambara and Aramachay Formations, though no true stratigraphic marker or formational contact was identified that would enable a correctable stratigraphic interpretation to be made. The section did provide evidence as to the depositional setting of the upper Chambara formation to the north of Florida Canyon, an idea as to the location of the basin at time of deposition, and the morphology of the carbonate platform in that area.

The studied section was within upper Chambara and transitional Aramachay lithologies (Appendix 2). The lowermost 90 meters consisted primarily of grey lime mudstones, with black planar to finely bedded bioturbated nodular lime mudstones. Above this is a relatively thick interbedded sequence of 125 meters of calcareous lime mudstones, thin interbedded shaley horizons and local cm.-scale turbiditic horizons. The overall section is composed of principally

of deep basinal lime mudstones, shales and small thin turbiditic intervals. Of primary interest to this area is the presence of three identifiable debris flows within the stratigraphy. These range in thickness between 5 and 25 meters and contain fragments of various other lithologies. Clasts within this unit include packstones possibly of middle Chambara origin, as well as quartzites from the Maranon complex. A definite grading to the debris flows is identifiable, with larger clasts and fragments being deposited at the base and a fining upward texture observed. Local geological mapping has not identified any true high-energy biostromal or reefal carbonate units; however, they may exist at depth. A gross stratigraphic correlation is possible between the carbonates of the Naranjitos area and those of the Florida and Tesoro Canyon areas. The presence of middle Chambara lithofacies within the debris flows suggests that basinal instability existed during time of deposition and a paleo-high to the south likely existed, whereby rip-up fragments of the platform could be transported deeper in the basin. For a complete description of the section and samples the reader is forwarded to Reid (2001) Appendix 2.

1.3.5.6 Buenos Aires

The Buenos Aires section is located approximately 20 kilometers to the northeast of the town of Pedro Ruiz along the paved road to the village of Buenos Aires. The section is well exposed, though heavily faulted, and provided a good opportunity to look at the contact of the upper Chambara with Aramachay, and Aramachay with the Condorsinga Formations. The Buenos Aires section represents the northernmost studied section. It lies outside of the Utcubamba Valley and may reflect more of the original basinal characteristics away from the zone of structural influence.

The Chambara Formation observed totaled approximately 400 m. (Appendix 2). Unlike the Florida and Tesoro Canyon areas, very little high-energy carbonates were identified and the general lithologies noted were deeper basinal lime mudstones, and wackestones associated with a fore-reef slope depositional environment. Variations existed in the wackestones as some had a very fine pelletal component not identified in the core study area. The lithofacies remained very consistent except for variable bedding thickness.

The transition to Aramachay is relatively gradational compared to Florida Canyon, and is identified over a thickness of 20 meters. The transition shows a sharp decrease in calcareous content of the carbonates, and an increase in overall organic character as well as, a thinning of

bedding to a cm-mm scale and the introduction of very fine shale partings and interbeds. Overall, the Aramachay is approximately 300 meters in thickness, though a large normal fault offsets the section and the author was forced to extrapolate measurements. Throughout the Aramachay section in this area, large ammonites are preserved along thin bedding planes.

The contact between the upper Aramachay and the Condorsinga is very sharp, identified by an overall lighter colour, an increase in bed thickness, and an increase in calcareous content back to true limestones, lime mudstones and predominantly wackestones with rare pelletal packstones. There are also no ammonites. In general, the overall lithofacies remain confined to deeper water facies.

The section was stopped within the Condorsinga due to overburden and lack of exposure. The depositional environment of this section was almost exclusively confined to fairly deep basinal conditions. The lack of turbidites or debris flows in the upper Chambara or Aramachay suggests stability during sedimentation. The lack of any higher energy lithofacies as observed within the central study area also suggests that overall water depth was deeper and below wave base.

1.3.5.7 Maino

The Maino area is located 40 kilometers south of the town of Pedro Ruiz and represents the southern-most portion of the study area along the Utcubamba valley. The oldest rocks outcropping in the area are the Mitu redbeds overlain by Chambara formation carbonates, succeeded unconformably by Cretaceous Goyllarizquisga Group sandstones that have cut through the entire upper Pucara sequence. The Aramachay and Condorsinga are missing, presumably eroded. The area was of immediate interest because it contains the best dolomitization and ground preparation for MVT-style mineralization observed in the district, without any known associated mineralization. A well preserved, though extensively dolomitized section resting on the Mitu red beds and extending through lower to middle Chambara, was provided along a slope northeast of the village of Maino, along a farmers trail in the Shiguar Valley.

The section was commenced just above the Chambara contact with the Mitu redbeds (Appendix 2) and totaled 365 meters of totally exposed stratigraphy. The Maino section may provide the best exposure of continuous Chambara lithologies in the area. Of significance is the different nature of lower Chambara lithofacies in the Maino area when compared to those of the central

Florida core. The lower Chambara Formation in this area is approximately 85 to 100 meters in thickness and is dominated by algal laminated, fine grained, lime and dolomitic mudstones. All dolomite discussed in this section is secondary in nature, the significance of which will be discussed later. Within the lower 100 meters of Chambara formation a series of meter-scale wacke and packstones horizons are observed. These for the most part are pelletal and oolitic in composition and interbedded black with light grey to light brown mudstones and wackestones, devoid of pelletal content. The upper 20 meters of this lower division show a marked increase in bed thickness and an increase in fossiliferous and pelletal content.

The middle measured section is indicative of high-energy carbonates, dominated by grain-supported packstones and fossiliferous packstones, interbedded with wackestones. Within this section there appears to be a very distinct cyclical nature to the carbonate sedimentation ranging from a basal, thin, lime mudstone transitional into a wackestone and then into a thick packstone to grainstone or rudstone over metric intervals, again capped by a thin mud interval. This cyclicity is repeated at least four times through the 180 m. thickness of the middle Chambara unit. Though the lithofacies identified in the Florida Canyon area are not seen here, the general thickness of the middle Chambara is similar.

The upper Chambara Formation in the Maino area was observed for 80 meters before a large normal fault was intersected. The strata was down dropped back to the middle Chambara and the erosive contact with the Goyllarizquisga Formation was encountered. The upper Chambara lithologies in this section are composed of monotonous fine-grained lime mudstones, finely to very finely bedded with thin silt horizons observed rarely. No turbidites or debris flows were recognized, suggestive of stable depositional conditions. The identification of Chambara Formation with lithofacies transitions from a shallow tidal flat setting through a lagoonal to higher energy bank facies and then into deeper basinal conditions, suggests that either the Maino area is representative of a paleo-high within an evolving single carbonate platform, or is an isolated carbonate platform separate from those of the north.

1.4 Sequence Stratigraphic Analysis

A sequence stratigraphic analysis has been attempted within the northern Pucara section of the study area. As a result of incomplete section measurement, lack of continuous exposure , and variability in the data collected, the author has made certain assumptions. Of great importance to

the stratigraphic distribution of the Pucara and specifically the Chambara Formation in this area is the role of structural and tectonic controls on sedimentation. Eustatic sea-level changes alone could not account for the large stratigraphic variations observed over such a very short geological distance. It is the author's judgement that within the study area both the thicknesses of sediments and the depositional stratal patterns are controlled by tectonic subsidence and evolving basement architecture. Rosas (1994) suggests that stratal patterns and lithofacies distribution in the Pucara of central Peru are controlled by the rate of relative changes in sea-level.

The Pucara Group of the study area shows a fairly classical sequence stratigraphic profile associated with a developing or isolated carbonate platform (Emery and Meyers, 1996; Tucker, 1988)(Fig.1.12). Initial carbonate production marked the beginning of a transgressive systems tract, whereby sea floods an antecedent high, and carbonate production is initiated. For the case of the Pucara Group in the study area, this antecedent high is represented by the underlying Mitu red beds that form a series of piano-key shaped horst-and-graben structures along the length of the Utcubamba Corridor, following the structural rift alignment. The paleo-elevation of these surfaces relative to the sea level at the time of carbonate start-up determined the lithofacies observed. In the Florida and Tesoro Canyon areas, Tingo, and Maino very shallow intertidal lithologies have been recorded. With rising sea-level or slight basement subsidence, carbonate sedimentation tracked the rising relative sea level and built an aggradational margin. This is identified in the Florida, Tesoro, Tingo, and Maino areas by the well-defined accumulation of higher energy carbonates (Chambara 2) derived from within an tidal environment and deposited slightly down slope on the carbonate platform in relatively shallow water.

Once a maximum flooding surface was reached, carbonate production exceeded the rate of creation of accommodation space. Most of the carbonate was shed off the platform to the slope and basin. This marks the start of the highstand systems tract and represents the mechanism by which most of the higher energy middle Chambara 2 carbonates were deposited. A sequence boundary is inferred between middle Chambara 2 and upper Chambara 3. During this period there is the possibility of subaerial exposure of the middle Chambara Formation (Fig.1.12). If this did occur, in situ carbonate production was largely terminated apart from minor fringing reefs, and the top of the platform was possibly karstified. This may have occurred in the Florida, Tesoro, and Maino areas.

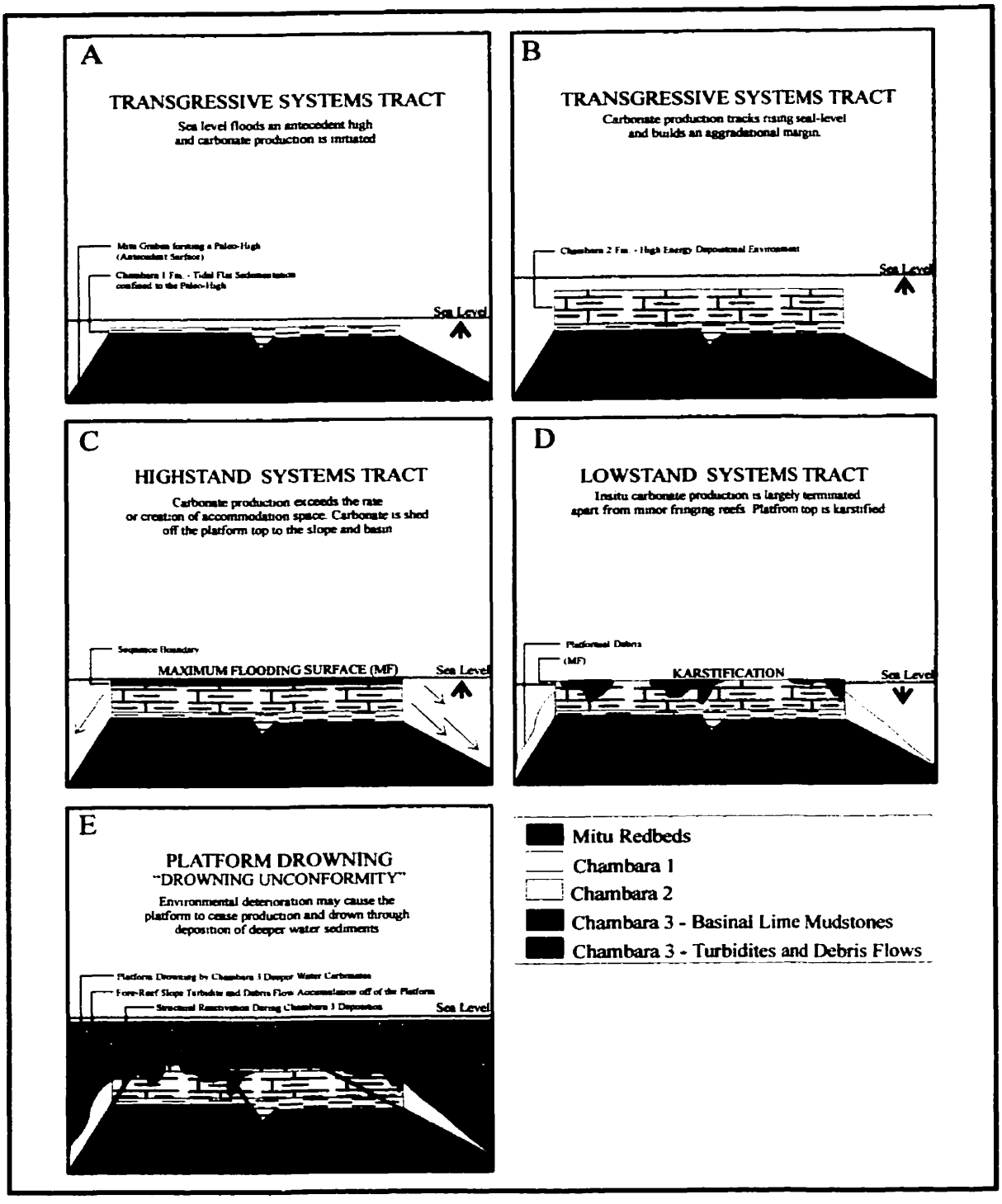

Figure 1.12 Sequence stratigraphic interpretation of the Chambara Fm.for the Bongara study area. The model infers carbonate deposition confined to an isolated platform(s) across the length of the Utcubamba Valley. Diagram modified from Tucker (1991).

The platform then drowned as a result of sudden sea-level rise or basement subsidence along reactivated fault structures through the Mitu graben. Deeper sedimentation occurred, derived from still elevated parts of the platform, or through deeper water carbonate sedimentation. This process would include the upper Chambara Formation and continue through the deep basinal Aramachay setting and a regressive systems tract. This interpretation holds well with those of Rosas (1994) and Hillebrandt (1973, 1986) from Pucara Group studies of south and central Peru. Rosas (1994) infers a more eustatic control to sequence distribution throughout the Pucara. The author prefers a structural controlled model for carbonate deposition in the area as tectonic evidence exists suggesting multiple periods of structural reactivation during sedimentation. Carbonate rocks inferred to represent deeper basinal environments distal to the Utcubamba Corridor can be correlated with those of shallower water as fills within extensional half-graben structures. The continuity of the upper Chambara 3 sediment within the main platform suggests that the central basin remained relatively stable through upper Chambara and Aramachay times, though debris flows to the north suggest basinal instability to the northwest off the main platform.

1.5 Basinal Interpretation

Two possible models are proposed to account for the stratigraphic distribution of the Pucara Group across the Utcubamba Corridor. Due to the lack of exposure, heavy vegetation cover and extreme topography, as well as late faulting, it is currently not possible to determine which is correct.

The northern Pucara Group within the study area confined within the Utcubamba Valley is indicative of an evolving isolated carbonate platform initiated on a fault-generated topography. Two possibilities exist. First, the entire length of the study area extending from just north of Florida Canyon through Maino could be regarded as a single large isolated carbonate platform within the Pucara basin with internal localized basement highs responsible for the distribution of the higher energy facies observed locally within the middle Chambara Formation. Secondly, there could be a series of isolated unconnected smaller platforms each developed upon fault-generated topographic highs, with a very limited spatial distribution (Fig.1.13a and 1.13b).

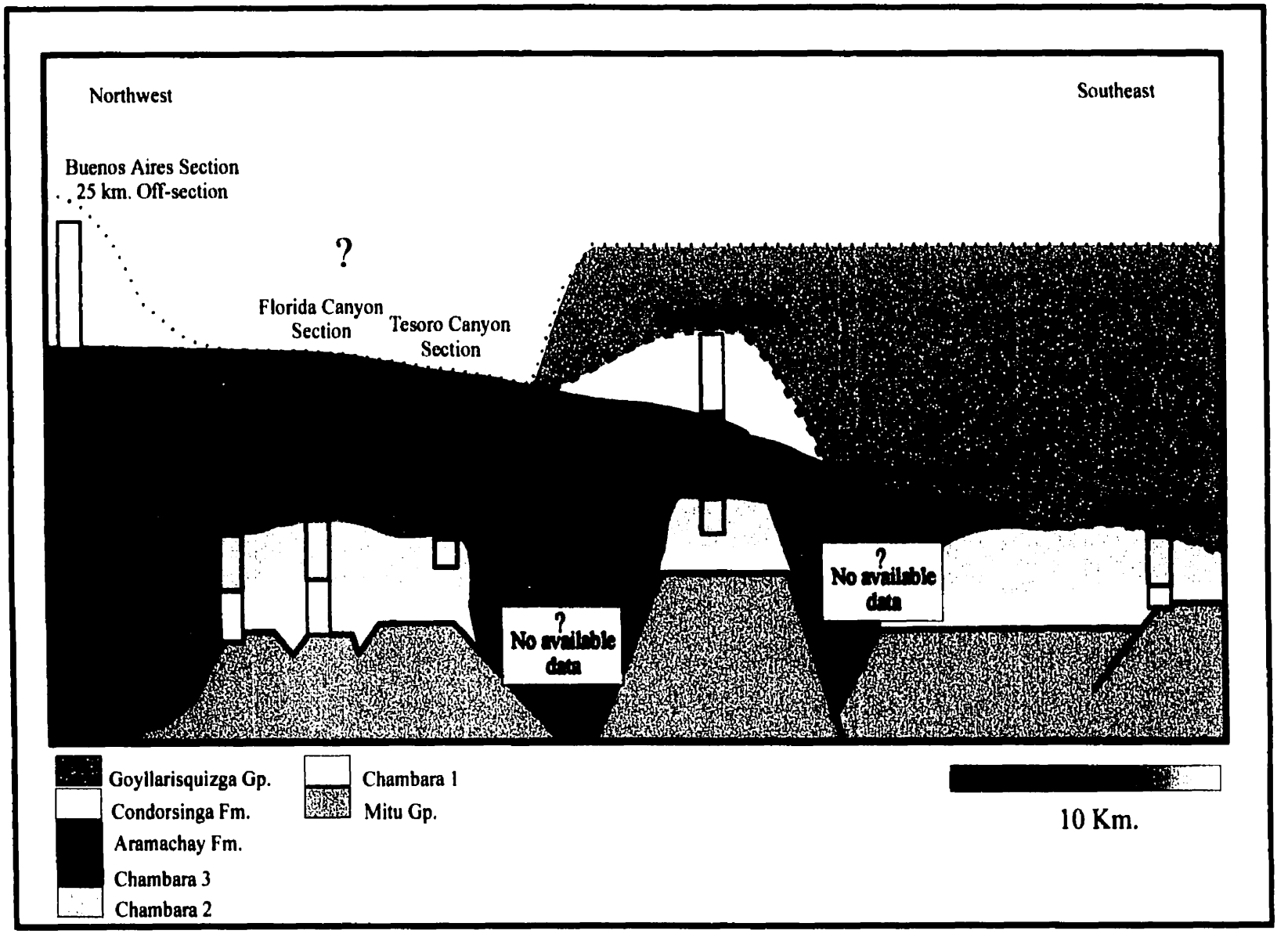

Figure 1.13a Schematic section, looking northeast across the Utcubamba Valley. This figure attempts to put all measured sections into a basinal and depositional framework. Correlation proves difficult due to the lack of identifiable surfaces resulting from poor regional stratigraphic exposure. Not to scale. The reader is referred to Appendix 2 for detailed sections and logs.

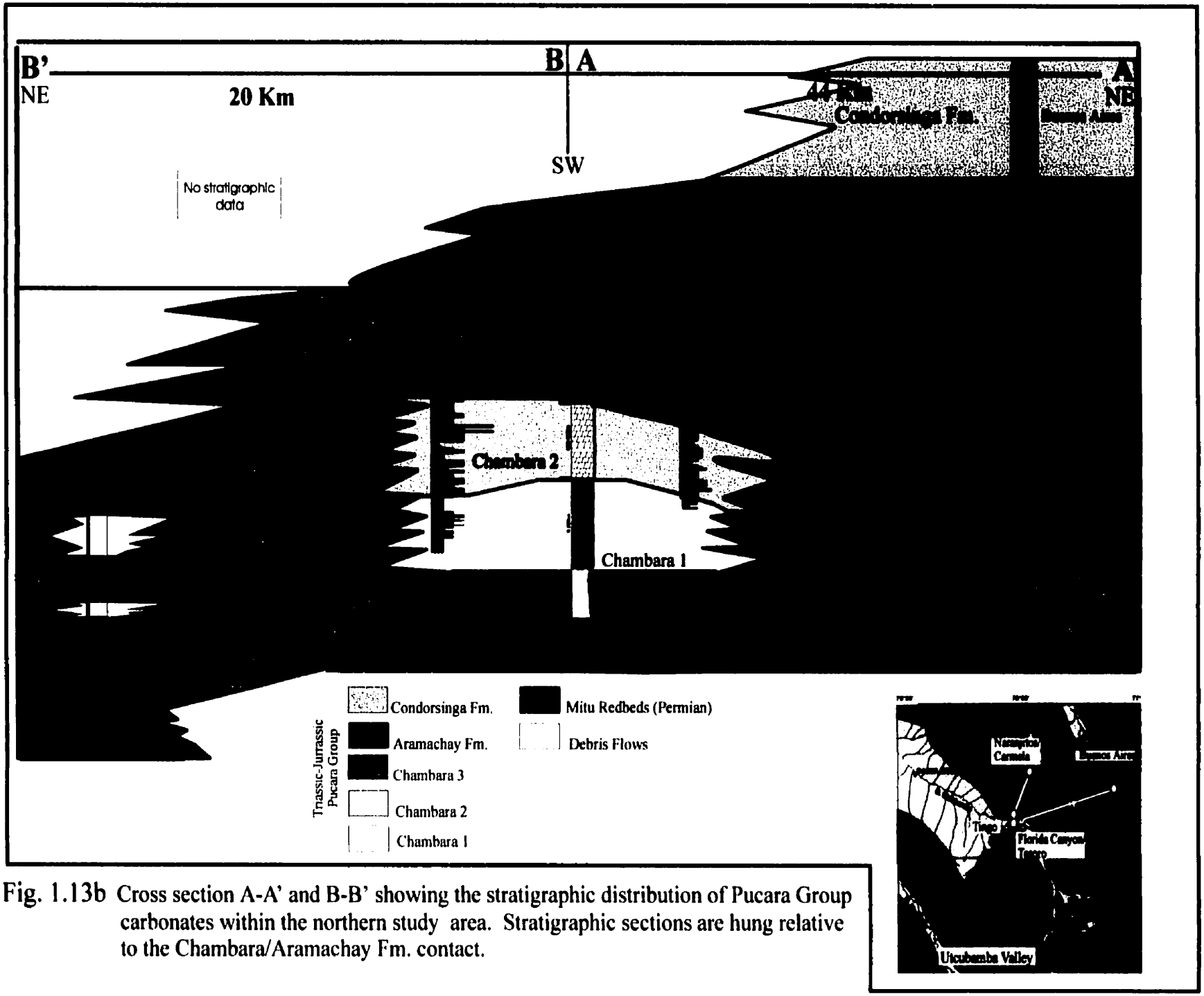

Fig. 1.13b Cross section A-A' and B-B' showing the stratigraphic distribution of Pucara Group carbonates within the northern study area. Stratigraphic sections are hung relative to the Chambara/Aramachay Fm. contact.

The author favors a depositional environment embracing a large single carbonate platform as envisaged in the first scenario. On this platform, confined to the uplifted Utcubamba valley, are a series of elevated basement highs situated along horst and graben structures of the Mitu rift. These elevated terrains act as isolated platforms within an evolving larger platform. This accounts for the lack of continuity between the Florida Canyon and Maino areas and explains the lack of high energy carbonates across the central portion of the study area and the extent of fore-reef carbonates associated with paleo lows and deeper platformal environments. The margins of this platform are difficult to determine; however, the identification of thick debris flows to the north of Florida Canyon in the Naranjitos area, suggests that significant relief existed off a paleo high to the northwest which could represent the platformal margin. To the northeast, the Buenos Aires section is an almost completely deep-water facies of the Pucara Group. Regional geological mapping has not identified any shallow water facies suggesting that between Buenos Aires and Florida Canyon an eastern platformal margin exists. Very little information exists to the west of the Utcubamba Corridor and a western margin cannot be inferred. Of importance is that shallow water facies have only been identified within what the author calls the Utcubamba Corridor a 12 km-wide strip through Florida Canyon, south 90 km to Maino. All significant shallow water facies observed in the study area have been confined to this internal area. It is the author's interpretation that the Utcubamba Corridor represents an isolated area of uplift or paleo-relief on which shallow water carbonate sedimentation was confined. This interpretation has important implications with respect to the localization of mineralization discussed in the next section.

1.6 Mineralization and Associated Features

Mississippi Valley Type (MVT) lead-zinc (Pb-Zn) mineralization, occurring in a variety of types, textures and concentrations has attracted the interest of exploration companies to the Bongara area. Mineralization is predominantly, though not exclusively, confined to the Chambara formation of the Pucara Group and the most significant mineralization discovered to date is around Florida Canyon. Other significant mineralized occurrences have been identified in the Floricita, Naranjitos and Cristal exploration areas. Significant dolomitization thought to be associated with, or genetically related to, zinc mineralization is observed throughout the study area in various forms, and may have implications with regard to the presence of mineralization in areas distal from the Florida Canyon core.

The following section will discuss the MVT-style carbonate-hosted Pb-Zn mineralization observed in the study area, and regional variations therein. The most abundant information collected thus far has been from Florida Canyon, where the greater part of this discussion will focus. Mineralization from other areas will be touched on and compared with that at Florida Canyon. For the purpose of this investigation dolomitization, dissolution/ground preparation, and mineralization will be discussed separately, followed by a paragenetic sequence, and a proposed mineralization model.

1.6.1 Dolomitization

All carbonates in the Bongara area were originally calcareous limestones. This can be demonstrated at Florida Canyon by drilling and local stratigraphic correlations, isopach studies of dolomite thickness in relation to structures, and through cathodoluminescent and stable isotope work carried out by the author. Rhodes (1998) observed three modes of dolomite emplacement as finely crystalline, medium crystalline, and medium coarsely crystalline dolomites that show a significant sparry white dolomite component referred to as a pseudo-breccia. Throughout this work, only two types of dolomite have been subdivided based upon paragenetic sequencing. Significant textural differences exist that allow for a larger classification to be developed, but genetically only two phases are evident. All phases of dolomitization are spatially associated and in places develop a complicated overprinting that at times proves difficult to interpret when attempting to ascertain the paragenetic placement of various phases.

The two stages of dolomitization identified are referred to as dolomite Stage 1 and Stage 2, respectively. Stage 1 corresponds to the finely crystalline and medium to coarsely crystalline dolomite phases identified by Rhodes (1998). The Stage 1 dolomite at Florida Canyon is thought to result from the predominant fluid phase responsible for the early ground preparation, and the premineralizing fluid dissolution event in the area. Commonly this is a fine to medium grained, euhedral dolomite that overprints both the lower Chambara 1 lithologies deposited within a tidal flat environment and extensively through the middle Chambara 2 high-energy carbonates. The dolomite is observed both replacing original intact limestones and as fracture and open space infillings, in the latter case enhancing and exploiting available porosity and open space (Plate 1.15). In the Florida Canyon area the largest concentration of Stage 1 dolomite is directly associated with the western Sam fault and centrally within the Florida-Tesoro structure. Replacement by this dolomite phase involves an in situ substitution of original rock fabric with

grain size ranging from less than 0.2 mm to 5 mm depending on the original sedimentary texture. According to Rhodes (1998), it produces a rock whose primary constituents and textures are still recognizable but which is slightly darker and tends to have a variable degree of fine pinpoint (<0.1-1mm) and occasionally finely vuggy (1-5mm) porosity. The darker colour of this dolomite phase is a result of introduction of organic matter during the replacement process. Standard petrographic and cathodoluminescent analysis of this phase suggests that both finely crystalline dolomites of the lower Chambara Formation (Chambara1) and early dark grey fine-to-medium crystalline dolomites observed in the Chambara 2 host are correlatable and genetically linked to a related similar dolomitizing fluid. Replacement textures are a function of original carbonate texture.

In Florida Canyon, Stage 2 dolomites are defined as rocks with greater than 5 percent coarsely crystalline white dolomite spar observed mottling the original dolomite in an in situ replacive pattern (Rhodes, 1998). This texture has been called pseudobrecciation and is a term commonly used to describe this coarse replacement and vuggy porosity-generating event within MVT literature (Plate 1.16). These rocks have been arbitrarily divided by those working on the exploration of the district into weak pseudobreccias for those with 5% to 15% dolomite spar and strong pseudobreccias for those with >15% spar. In some instances of altered fossiliferous floatstones and rudestones, the secondary dolomite is largely present as a replacement of the fossil skeletons which produces a spar-mottled rock that is termed pseudobreccia. This is not typical of the more irregularly mottled rock where spar replaces other fabrics such as burrows and stylolites. Occasionally the dolomite spar appears to invade along inclined fractures and spread out in a replacive network from them. In other cases only primary porosity seems to control dolomite spar distribution. Moderately to strong dissolved lithologies (discussed below) commonly have spar filling in open space or aggressively replacing fine rock detritus of dissolution features. These textures are not commonly referred to as pseudobreccias but it is sometimes difficult to separate them from the simple dolomite spar replacement beds and it is probable that one may grade laterally into the other.

The pseudobreccias mark the pathways of the most aggressive and replacive dolomitization either in the same process as dolomitization Stage 1 or marking a later dolomitizing fluid. Pseudobreccias commonly show an association with the more preferentially mineralized horizons as well as the areas of maximum dissolution and dolomitization.

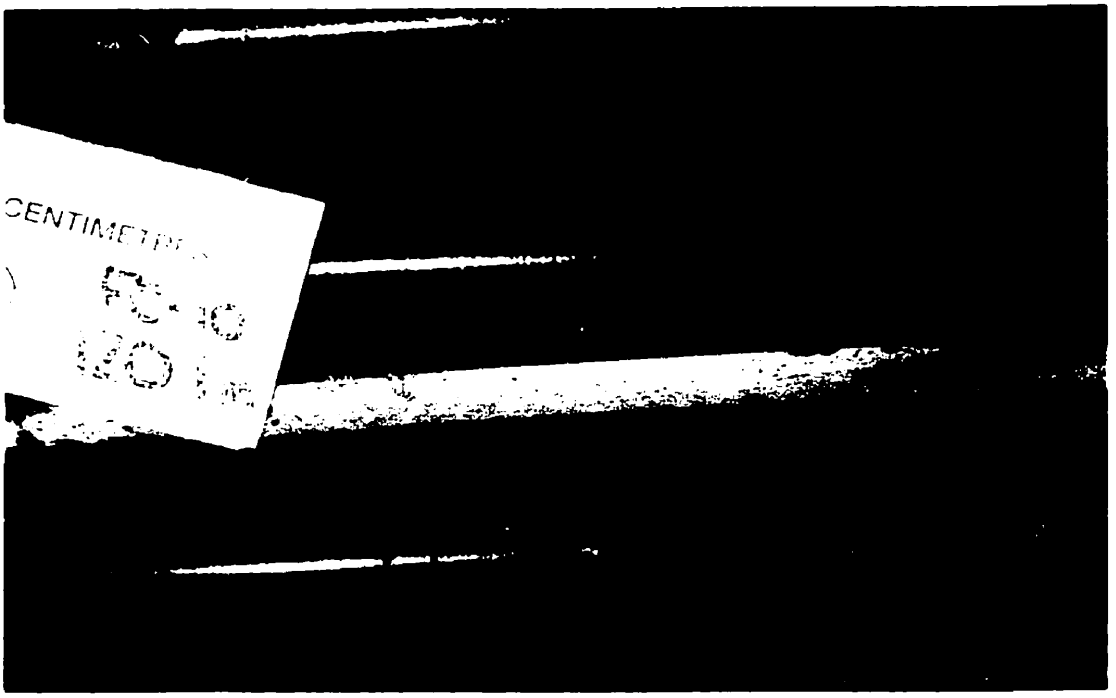

Plate 1.15 - Stage 1 dolomite observed exploiting available open space and porosity in a solution collapse breccia of the Chambara 2 at Florida Canyon.

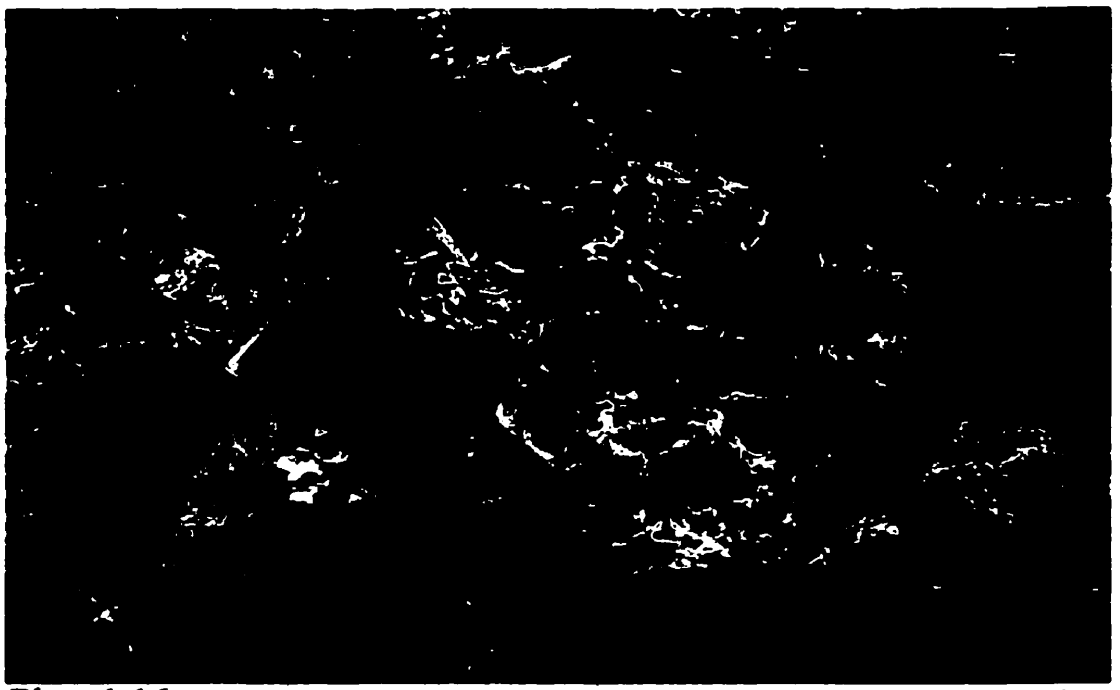

Plate 1.16 - Stage 2 dolomite forming a psuedobreccia texture within Chambara 2 lithofacies in the Maino area. Most of the original sedimentary features have been completely obliterated.

Other locations in the Bongara area that have significant dolomitization, studied by the author, include Floricita, Maino, Tesoro Canyon and to a lesser extent Naranjitos/Carmela. Areas not visited by the author but which have various stages of dolomitization identified include Helen/Sonche, Cristal, Charito and Florida south. Both the Maino and Floricita areas have a truly significant concentration of both dolomite stages. The Floricita mineralization though hosted in the Condorsinga Formation at the contact with the Cretaceous unconformity, shows some of the coarsest white dolomite spar and pseudobrecciation evident in the region. Both Stage 1 and 2 dolomites as described from the Florida Canyon area are present and closely associated with zinc-lead mineralization. Stage 1 is observed exclusively as fine to medium grained euhedral replacement and vein infillings vertically through the stratigraphy moving to the depocenter of both mineralization and concentration of Stage 2 dolomite spar. Petrographically Stage 1 dolomite can be identified from the main showing area; however, this is generally strongly overprinted by late Stage 2 dolospar. Stage 1 dolomite replaces micritic beds of the Condorsinga Formation at Floricita. Whether this early dolomite stage is correlatable with Stage 1 dolomites of Floricita Canyon is in question. Cathodoluminescent petrography helps to distinguish between the two phases and makes the relationship between the two quite identifiable (Reid, 2001, Paper 2).

The Maino area has the most pervasive dolomitization identified in the region. The studied section shows both dolomite phases clearly distinguished by cathodoluminescence. The lower Chambara formation, possibly correlateable with the Florida Canyon area, shows very fine grained, pale pink to brown and grey dolomite locally grading to medium grained euhedral rhombs proximal to small scale faults and fractures through the stratigraphy. Coarse Stage 1 dolomites are observed throughout the section; however, these become obscured and overprinted by thick intervals of very coarse euhedral dolomite spar and various stages of pseudobrecciation and replacement of later Stage 2 dolomites. The thickness and concentration of dolomites in the Maino area appear to be both structurally and stratigraphically controlled the thickest sequences are identified in higher energy carbonate lithologies of the middle Chambara 2 Fm located proximal to major lineaments and structures.

Volumes of dedolomitized rocks have been observed throughout the district associated with both barren and mineralized areas. These rocks have a crystallinity typical of dolomitized carbonates but the magnesium component has been partially or totally replaced by calcium. The resultant rocks have a slight fuzzy outline to crystals and a partially bleached aspect. It is common for

these dedolomitized rocks to show strong differential solution and crumbling to brown carbonate sands (Rhodes, 1998). In the southern Florida Canyon area an association with Zn and Fe oxides may be significant and possibly reflects earlier periods of flooding by meteoric Ca - and CO_3 - rich fluids as well as by the present groundwater system. Certainly some areas of significant dedolomitization can be attributed solely to recent oxidation and meteoric weathering.
In most MVT camps mineralization shows a spatial association with dolomitization but the coincidence is not normally on a one-to-one basis. Commonly, the areas of dolomitization are much more widespread laterally and vertically than the mineralization. Nonetheless, the likelihood is that the dolomitization marks the pathways of certain basinal fluids that, in some instances, dolomitize the rocks. Subsequently, more evolved basinal fluids utilizing the same pathways, locally deposited minerals. There is therefore a spatial link but not necessarily an exact temporal link, between the dolomitizing and mineralizing processes (Leach and Sangster, 1993).

At Florida Canyon there is a close spatial relationship between mineralization, carbonate dissolution and dolomitization, and strong structural control is evident. The dolomitization is clearly thickest adjacent to the Sam Fault, where the entire Chambara 2 is altered, but dolomitization also extends tens of meters into lower Chambara 1 lithologies as well as upward into the deeper fore-reef units of Chambara. About 800 meters laterally eastward from the fault, the dolomitization thins to an interfingering relationship, and is intersected throughout the Florida Platform in variable amounts, generally associated with intersecting structures. The most significant dolomitization appears to be confined marginal to structures, and this in turn has a direct correlation with both dissolution fabrics and mineralization. Dolomitization preferentially follows more porous horizons such as packstones and floatstones, and rudstones away from the main structures. Rhodes (1998) states that while dolomitization seems to be distinctly controlled by the Sam structure, the fault is also coincident with a facies transition from basinal mudstones to shoal packstones, fossil floatstones, and rudstones. In other carbonate settings in the world, this shelf-edge position is a common place to encounter enhanced dolomitization. Consequently while the fault would appear to be a major control, the role of the facies transition cannot be discounted. Though these thoughts by Rhodes have merit and should be seriously considered, the regional correlation between structure and Stage 1 and 2 dolomitization independent of facies change; such as in Floricita, lead the author to conclude that the dolomitization throughout the district is controlled primarily by structure and passively through permissive stratigraphy and its associated internal dissolution textures and porosity. A more detailed analysis of dolomitization and regional correlations is discussed in Paper Two of Reid (2001).

1.6.2 Dissolution Features

While dissolution features are common to, and perhaps a dominant characteristic of, MVT camps, there is no consensus as to their origin (Leach and Sangster, 1993; Rhodes, 1998). Some features seem to be relateable to meteoric karst and subaerial exposure of the carbonate platform during carbonate deposition, others to dissolution events accompanying mineralization, and still others to migrating fluids that are either meteoric or mineral associated. In this context, there is no evidence of true karst formation in the northern Pucara Group. For the purpose of this work all textural descriptions relating to dissolution and solution-collapse of carbonate is though to have developed via insitu dissolution along structures and major lineaments and does not imply meteoric dissolution during subaerial exposure.

At Florida Canyon there are distinct solution features that mark small to large-scale dissolution of the carbonates with variable removal of material and consequent foundering or collapse of the affected carbonate strata. These produced textures resemble those described for other MVT camps and they are a significant host to mineralization. At Florida Canyon they can be divided into localized small-scale cavities with fine geopetal, internal sediment fill and intervals in which solution has progressed to the extent that significant collapse breccias have occurred.
Often incipient dissolution of the carbonates occurs along contacts of anisotropy within the original carbonate such as stylolites, organic laminations or argillaceous seams. Commonly this incipient dissolution results in a micro-dissolution of carbonates along the contacts and a progressive buildup of insoluble residue components. Where dissolution continues the insoluble residue layers are often remobilized to provide material for internal sediments described below or, alternatively, the carbonates founder and fine chips of black solution residuum (bitumen and organic matter) form a common constituent of the resulting fine breccias and detritus. The presence of such black chips is a diagnostic indicator of the dissolution origins of the detritus breccias. Localized areas of 1 to 5 cm, thick bands and patches of dark grey to black, very finely crystalline dolomite often with subtle planar laminations are evident in many of the dolomitized intervals particularly where fluid flow as shown by pseudobreccias, has been most extreme. These areas of dolomite are clearly distinct from the host-dolomitized carbonate. Commonly small bands and patches of dolomite spar occur at the top of these dark dolomites. They are the result of small, open space cavitation and infill of the host dolomite by remobilized detritus.

These are internal sediments and include a significant organic, clay and insoluble residue component, resulting in the dark coloration.

In areas of more extreme dissolution there appears to be an ongoing process of dissolution and infill such that cycles of internal sediment layers capped by dolospar and later internal sediments are common (Rhodes, 1998). These may also be disrupted, brecciated and infilled by later generations of internal sediments and subsequently by very late dolomite spar. In some instances of small scale dissolution the host rocks have foundered and been reworked to create heterolithic rock composed of silt to fine gravel size clasts, often with abundant black solution residuum chips. These intervals lack the delicate infilling and sediment layering of the internal sediments and are referred to as solution detritus or trash zones.

Rhodes (1998) states that where significant strata have been removed by dissolution there will be some degree of brecciation and collapse resulting. Commonly, a significant throughgoing collapse shows the following textural variations downward in the collapse as a result of the maximum foundering at the base:

i) Crackle brecciation – Fine fractures radiate in a network through the carbonate and there is some solution enhancement of these fractures with perhaps a slight rotation of the carbonate fragments. Often the fracture network is partially or totally occupied by fine calcite or dolomite spar.

ii) Mosaic Breccia – Angular fragments of the host carbonate have a jigsaw aspect and can be fitted together but are separated by quite large, 1-5 cm. fracture networks that can be occupied by either fine silt to grit detritus or by dolomite or, less commonly, calcite spar. The fragments are oligomictic since they derive from beds in place.

iii) Coarse Collapse Breccia – Angular to subangular fragments between 5 cm and meters in size show distinct rotation and displacement. Fragments are relatively monolithic upwardly and become increasingly more heterolithic toward the base of the collapse. Matrix is most commonly fine rock detritus but can be spar or sulphides in mineralized situations.

iv) Fine Collapse breccia – Similar to the coarse collapse breccia but almost always a fine rock detritus matrix. Commonly, the fragments become progressively more comminuted towards the base of the collapse. Insoluble components of the stratigraphic column, such

as insoluable residues, shales, and cherts comprise a greater amount of the clasts and the breccia takes on a darker colour.

v) Solution detritus – In collapse breccias derived from relatively friable host rocks, the basal collapse is often composed of fine dolomite detritus of sand-to-grit material since the coarser components have broken down.

Various forms of the above have been identified not only in the main Florida Canyon area but regionally, in the Floricita and Maino areas. Other reports of significant dissolution collapse have been described in regional exploration work, but not observed by the author. Within the Florida Canyon area, the Sam Collapse breccia, confined spatially to the Sam Fault structure, shows all of the textural variations described above by Rhodes. The breccias for the most part are stratigraphically confined to the middle Chambara Formation and more specifically to those carbonates deposited in the high-energy shoal environment, specifically packstone, rudstone and floatstone lithofacies. These dissolution features are of significance as they are major indicators of throughgoing porosity that has both channeled ore fluid migration and been loci for ore deposition. Consequently, the mineralization is most abundant and of highest grade in areas that show preferential dissolution of porous lithologies. At Florida Canyon, dissolution features increase in abundance and intensity towards the Sam Fault in a similar manner to dolomitization. While significant areas of dissolutioned lithologies are not appreciably mineralized, the presence of these horizons is considered a favorable indicator of adequate ground preparation for mineralization.

The lack of consistent stratigraphically correlateable carbonate hard grounds across the Florida Canyon platform and/or throughgoing dissolution horizons distal from the main Sam Fault structure suggests that these dissolution features are not a result of true subaerial exposure and as such are not true karst features (Estaban and Klappa, 1983). However, exposure to either descending or circulating meteoric fluids could have been responsible for the textures observed in the Florida Canyon area. The difficulty in genetic identification of the processes responsible for the initial and continued dissolution of the host carbonate lies in the multi-episodic nature of the fluid system and the continuous overprinting of textures therein.

1.6.3 Mineralization

The best mineralization in the Bongara region is generally associated with strong ground preparation observed as pervasive dolomitization, pseudobrecciation, and carbonate dissolution. The ground preparation in Florida Canyon is controlled by the occurrence of carbonates deposited in high-energy environments of the middle Chambara Formation (Chambara 2), and by the proximity to major structures. To date significant mineralization has been observed along the Sam Fault structure and fault splays off the main structure. Significant mineralization has also been observed locally through drilling across the Florida Platform, usually associated with parallel and later crosscutting structures. To date economic mineralization has not been defined although a speculative resource of 7 million tons of approximately 7% combined zinc and lead has been suggested by exploration companies.

At Florida Canyon sulphide mineralization typically replaces rock fragments or fills open spaces in dissolved ground. Zinc mineralization consists of dark red to brown sphalerite with lesser dull yellow-beige sphalerite being identified locally. Sphalerite is observed as coarse euhedral to fine-grained (mm. to cm. scale) aggregates and locally colloformal zoned varieties. Lead mineralization is exclusively observed as galena, though oxide varieties of both zinc and lead mineralization have been observed in the district. Most commonly, zinc and lead sulphides are observed together as an intermeshed mosaic of sulphides, though galena veining has also been identified crosscutting early sphalerite phases. Pyrite is observed throughout the mineralizing sequence ranging from fine mm-scale disseminations to cm-scale massive replacement of the host. Later silicification and calcification is observed towards the waning stages of the mineralizing system. Mineralogy and paragenesis will be discussed below. Three textures of mineralization have been identified and defined as: i) bedding and/or small open-space replacement, ii) collapse breccia hosted and iii) minor zinc in vein, crackle and mosaic breccias in the upper Chambara Formation (Chambara 3).

I) Bedding and/or small scale open-space replacement (Plates 1.17 and 1.18)

Mineralization of this form is usually confined to porous rocks such as dolomitized packstones and rudstones. Sulphides (ZnS and PbS) typically fill porosity, as significant open space was never developed. Mineralization is typically fine grained, 0.1mm to 1mm, but ranges up to 5mm. This type of mineralization can be very high-grade up to 25% zinc, 3-5% lead and shows apparent stratigraphic control. Although the same stratigraphic horizons appear to be replaced by zinc and lead mineralization in drill holes up to several hundreds of meters apart, there is a disturbing lack of continuity in grade and thickness between the holes with respect to mineralization and dolomitization. The best developed example of this style of mineralization, is the intersection of drill holes FC33, 35 and 21 (Fig.1.14). This apparently bedding-controlled mineralization locally forms massive sulphide bodies comprising coarse crystalline red sphalerite, galena and pyrite as an intergrown sulphide mosaic. A dark-red to brown coloured sphalerite distinguishes this style of mineralization.

II) Collapse breccia-hosted mineralization (Plates 1.19 and 1.20)

Collapse breccia-hosted mineralization consists of zinc, lead and iron sulphides replacing clasts and fine solution detritus and filling open space in breccia bodies. Sphalerite occurs as botryoidal layers and replacement rinds on clasts. The highest grades occur near the bottom of the collapse breccias. The best example of this style of mineralization is the Sam breccia.

III) Vein and crackle breccia –hosted mineralization (Plates 1.21 and 1.22)

Vein and crackle breccia –hosted mineralization typically occur as thin veinlets hosted in upper Chambara Formation limestones (Chambara 3). Veins contain 0.1 to 3mm crystals of pale yellow sphalerite. This style of mineralization is not significant except that which may reflect mineralization at depth in the Chambara 2.

Throughout the Florida Canyon area, specifically proximal to the Sam Fault structure, a number of mineralized horizons have been identified that correlate with discovered surface showings as defined via drill testing. These horizons are associated with favorable dolomitization of the middle Chambara Formation, are centered stratigraphically about the coquina marker and include the Milagros, Nancy, and Karen zones (Fig.1.15). Mineralization within these zones

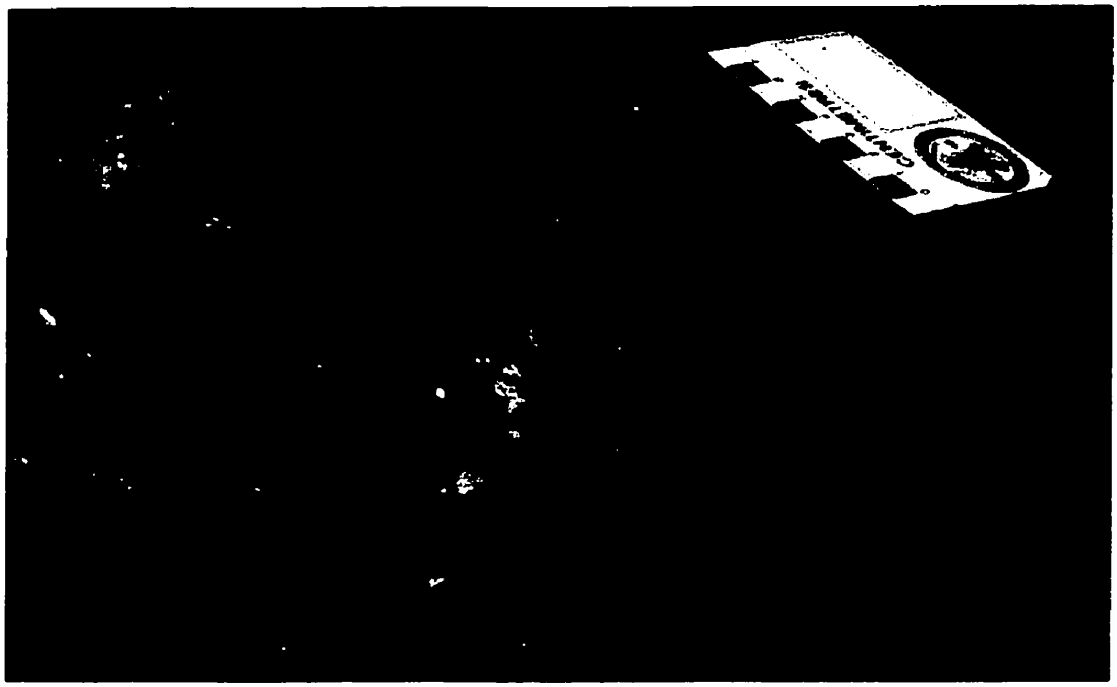

Plate 1.17 - Massive replacement of host carbonate by very-coarse grained sphalerite (2-phases), galena, and pyrite at the Karen Showing in Florida Canyon.

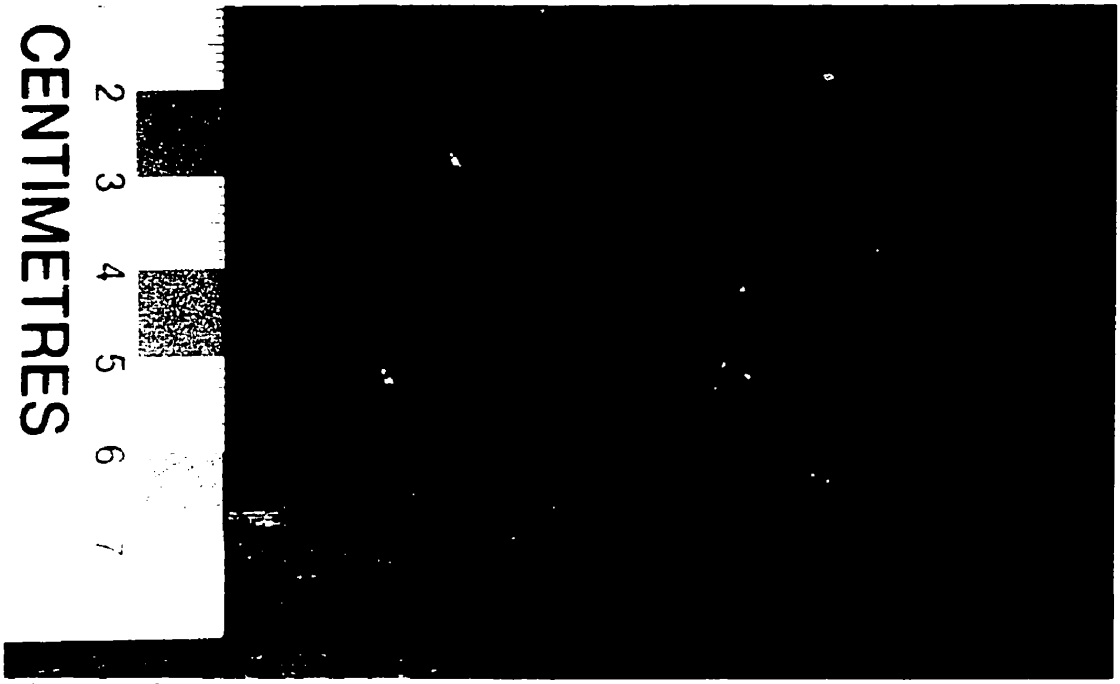

Plate 1.18 - Complete and massive replacement by coarse-grained, dark-red sphalerite and galena in Florida Canyon.

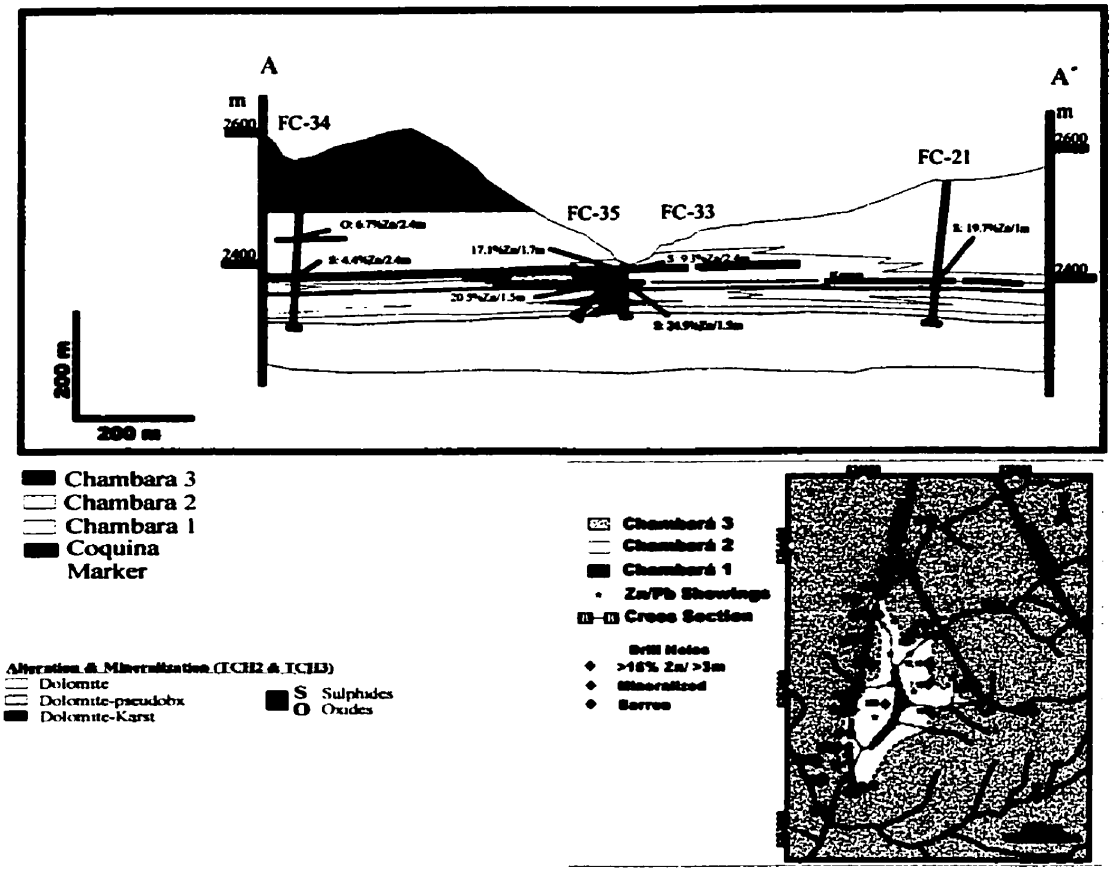

Figure 1.14 Cross section A-A' showing the principal mineralized corridors across the Florida Canyon platform.

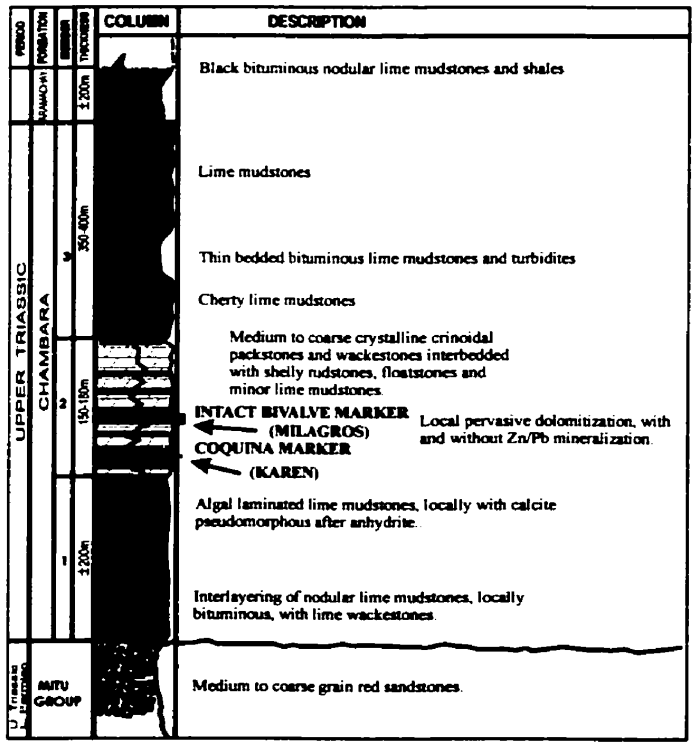

Figure 1.15 Stratigraphy of Florida Canyon showing the position of mineralized horizons within the Chambara 2.

Plate 1.19 - Coarse-grained sphalerite infilling open space, and replacing clast edges within a pseudobrecciated collapse system. Oxidation of sulphides has resulted in fine veining of smithsonite away from sulphides through open porosity.

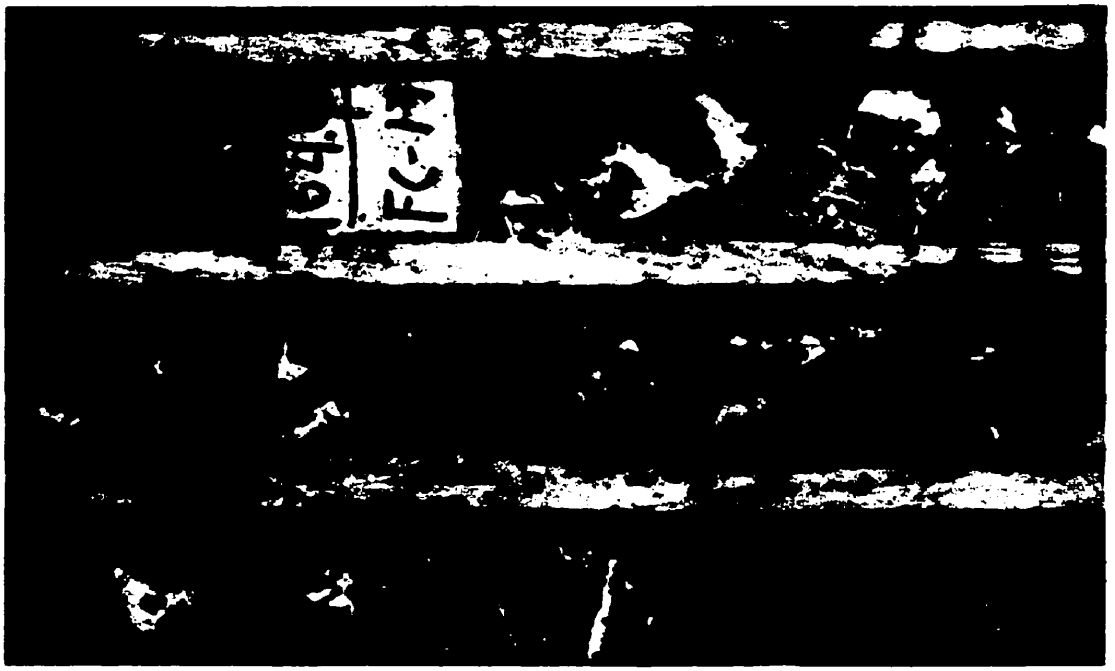

Plate 1.20- Mosaic to collapse breccia with coarse brown, partly botryoidal sphalerite rimming fragments, as fine disseminations within fine solution detritus.

Plate 1.21 - Crackle breccia with some dolospar and smithsonite/oxides after sphalerite.

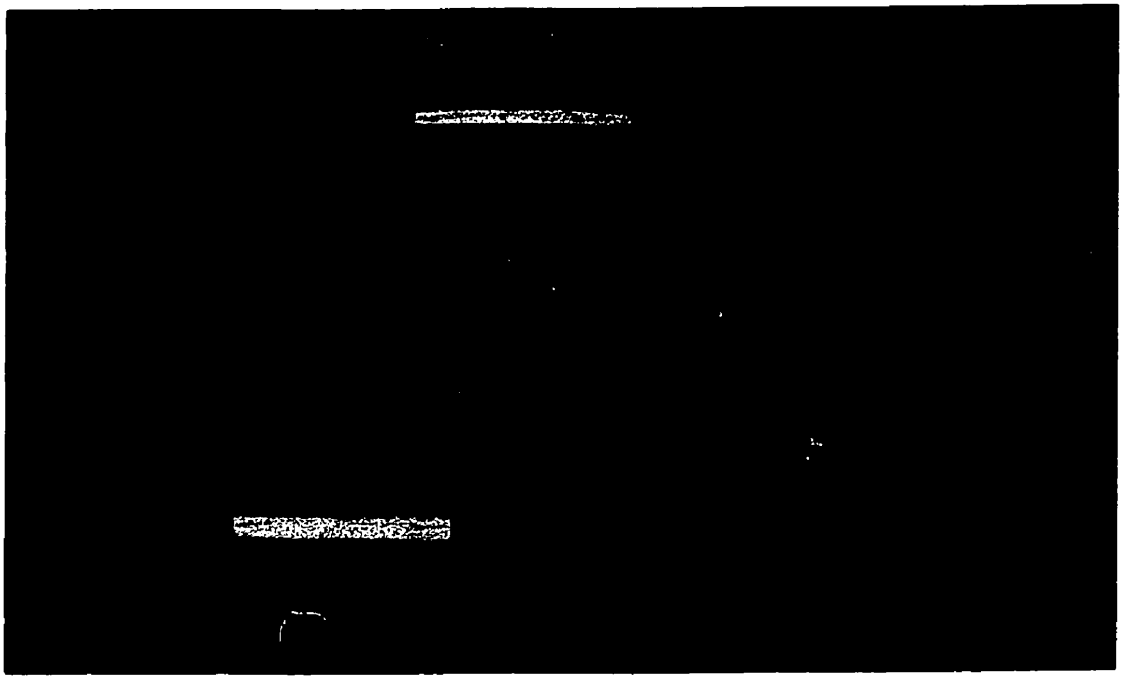

Plate 1.22- Crackle brecciated dolomitized Chambara 2 lithologies with dolospar matrix and orange smithsonite partially replacing sphalerite rimming fragments.

fluctuates vertically over a range of as much as 5 meters such that it is not planar and only broadly stratabound. Closer to the Sam Fault, dolomitization and ground preparation thickens to include much if not all of the Chambara 2 Formation, resulting in a series of stacked, stratabound, mineralized intervals within about 200 meters proximity of the Sam fault. These sulphide zones are at, or slightly above, the "intact bivalve marker"(IBM) and the Gordita and Raquel packstone beds. Of these only the IBM seems to consistently attain reasonable thicknesses of mineralization and zones of dissolution. While most of the mineralization occurs as massive replacement of internal sediment/solution detritus intervals there are some disseminated and patchy sulphides in pseudobreccias and weakly developed dissolution cavities.

The other area of significant mineralization studied by the author was at Floricita where sulphides occur at a pronounced unconformity between the Condorsinga member of the Pucara and Cretaceous Goyllarizquisga sandstones. The Condorsinga thins from 100 to 50 meters from south to north across the occurrence, but this may be a sloping erosional surface or a result of pre-Goyllarizquisga faulting. Major faults are oriented east-west through the deposit and there seems to be a very strong element of structural control to the mineralization. The relative contribution of active early Cretaceous carbonate dissolutioning to ore controls may be minor. Down-faulting of a significant volume of Goyllarizquisga into the Condorsinga appears to have been accomplished by large-scale structures and brittle fracturing of the Goyllarizquisga sandstones and the Condorsinga carbonates (Allen, 1997).

Mineralization comprises almost exclusively sphalerite and white dolomite spar in subequal proportions as open-space filling and rock fragment replacement within a large dissolution collapse system (Plates 1.23 and 1.24). Mineralization has a vertical extent of approximately 100 meters along a 100 to 150 m strike extent of crudely east-west oriented structures. Sulphides extend approximately 40 m up into the Goyllarizquisga and 60 m down into the Condorsinga. Neither the Goyllarizquisga sandstones nor Goyllarizquisga clasts are found below the unconformity surface suggesting that there was no significant solution collapse to the system. As the primary lithology of the Condorsinga is a dolomicrite rather than a micrite, the opportunity for significant late solution activity was diminished (Allen, 1997). Virtually all of the mineralization in the Goyllarizquisga comprises brittle veining of dolomite and sphalerite with parallel vein walls and little or no fragment rotation or solution rounding. Over the maximum 30 m. (vertical) range of mineralization in the Goyllarizquisga, the maximum open fracture space is perhaps 10-15%. Within the Condorsinga base metal sulphides make up plates

Plate1.23 - Open-space infill by coarse-grained black to dark-red sphalerite, with local fragment replacement in Condorsinga Formation dolomicrites of the upper Floricita adit.

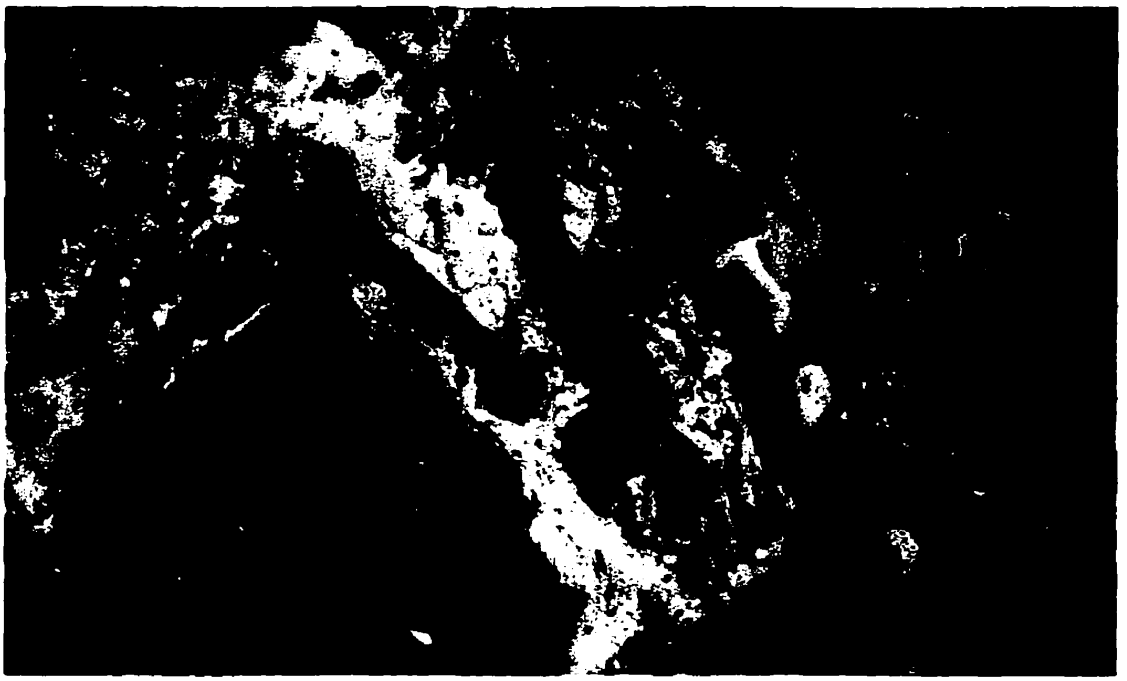

Plate 1.24 - Mineralization comprised almost exclusively of sphalerite and white dolomite spar as open space filling and rock fragment replacement within large dissolution collapse systems at Floricita.

approximately 50% parallel walled "stockwork" or crackle, fracture, vein mineralization with no solution enhancement and 50% stockwork of unrotated precursor dolomicrites with very modest solution enhancement and rounding. According to Allen (1997) the ground preparation or open space creation was largely structural expansion through faulting and includes only modest solution enlargement. There are portions along major bounding structures where increased solution activity is observed and hence dolomite plus sphalerite increases.

Throughout the rest of the study area a number of other zinc-lead base metal occurrences have been reported and documented. The majority of these are small in size with only-low grade disseminated sphalerite and galena with or without pyrite, or local high-grade veins of sphalerite that, as yet, have not been traced back to a larger volume of mineralization. The distribution of these showings is as variable as the mineralization observed at each. Most occur variably within the stratigraphic sequence and do not seem confined to any one lithotype or stratigraphic or structural setting. Of importance is the fact that all of these regional mineralized occurrences are structurally controlled and are associated with some form of early ground preparation or dolomitization.

In summary, the most significant mineralization observed within the study area is that of Florida Canyon. The mineralization is most pervasive proximal to predominant northeast and intersecting northwest structures across the Florida Canyon platform. The most important of these structures is the Sam fault that appears to control fluid movement. Associated with these structures are two phases of mineralization, dolomitization, local pyritization, and silicification. All of the above are observed best developed proximal to the structures in conjunction with high-energy carbonates of the middle Chambara Formation (Chambara 2), and diminishing in intensity away from this main structure.

1.6.4 Paragenesis

Through field observations, standard petrographic analysis and cathodoluminescence petrography, a general paragenetic sequence for mineralization has been identified by the author. Most of the studies were confined to material from the Florida Canyon area; however, similar results have been obtained on samples from the Floricita area. Details of the paragenesis and dolomite behavior are reported in detail in Paper 2 of Reid (2001).

The overall general paragenetic sequence is:

Dolomite Stage 1 → Pyrite → Sphalerite 1/Galena → Dolomite Stage 2 → Sphalerite 2 → Calcite 1 → Quartz/silicification → Calcite 2

Early fine-grained dolomite described as Stage 1 dolomite is observed to result from the earliest fluid event and was likely responsible for the initial ground preparation dissolution observed in Florida Canyon and for the dolomitization of the originally calcareous micrites of the Condorsinga Formation in the Floricita area. This phase of dolomitization was also identified in the southernmost Maino areas as the early dolomitization phase imposed upon fine-grained supratidal carbonates. Stage 1 dolomite has a characteristic dark red to brown – red luminescence and is easily distinguishable from the later Stage 2 dolomite. Commonly, Stage 1 dolomite replaces fossils and preserves their original shapes.

Stage 1 dolomite was followed by pyritization, which is observed occurring continuously throughout the mineralization. This is followed by the initial and most important sphalerite phase that consisted of various brown to red and dark yellow sphalerite that accounts for the majority of the mineralization observed in Florida Canyon, Floricita and other areas with significant mineralization. Usually this sphalerite is medium to coarse grained (0.5 mm. to 2 cm.) and is visible in a number of textural situations as described previously.

Stage 1 sphalerite is followed by Stage 2 dolomite which consists of the medium- to-coarse grained (mm to +5 cm) dolospar and saddle dolomites observed throughout the district. This dolomite phase appears to be more of a destructive open space filling with pervasive dissolution of intensely altered horizons and further expansion therein.

Sphalerite 2 occuring in trace amounts through the district is observed as pale yellow to light brown sphalerite overgrowing dolomite 2. This phase of sphalerite is likely the same pale yellow sphalerite observed in the Lower Chambara Formation (Chambara1) in Florida Canyon and sporadically through the upper Chambara Formation (Chambara 3) in both Florida and Tesoro Canyons.

Galena either grows with or in places crosscuts sphalerite 1. Pyrite also occurs as tiny inclusions in sphalerite 1, dolomite 1 and dolomite 2, or along contact of sphalerite 1/ dolomite 1 or

sphalerite 1/calcite 2. Calcite 1 is contemporaneous with or slightly later than dolomite 2, where as calcite 2 postdates every other mineral.

Authigenetic quartz replaces dolomite 1, dolomite 2, and sphalerite 1. The overall paragenetic sequence of the studied samples is shown in figure 1.16.

1.6.5 Mineralization Model

An early magnesium-rich fluid event, likely generated by basinal dewatering, leaching and tectonic expulsion, moved fluids through a basinal aquifer, probably the underlying Mitu red beds. Ultimately the fluids ascended through predominant northeast structures. Early dolomitizing fluids caused local dissolution and collapse of the middle Chambara Formation allowing for a lateral fluid movement within the high-energy lithofacies adjacent to the main structures. This ground preparation, replacement, dissolution and porosity increase may have been the initial fluid event or may have exploited existing zones of dissolution formed by earlier meteoric fluid flow through the sequence. With continued basinal dewatering, zinc saturated fluids ascended semi-vertical structures and followed paths of least resistance to the middle Chambara Formation where zinc and lead mineralization occured as the fluids came into contact with a reductant, most likely intraformational H_2S.

With continued fluid expulsion, a second coarse white dolospar phase was emplaced and the fluid system began to wane. Pyrite, sphalerite and later silica and calcite were deposited throughout the volume of dolomitized and mineralized rock as the hydrothermal system slowly cooled and choked itself off, or otherwise ceased to function (Fig.1.17).

Of importance to this study is the fact that all the fluid movement associated with the mineralizing system is structurally controlled. An appropriately porous horizon was capped by an aquitard such as the upper Chambara or Aramachay Formations, which could act as a significant seal to ascending fluids. In places like Floricita and Maino, though pervasive dolomitization is observed, and at Floricita significant mineralization has been discovered, the fact that no overlying aquitard was in place at the time of mineralization probably allowed ascending fluids to dissipate in the Cretaceous Goyllarizquisga Formation.

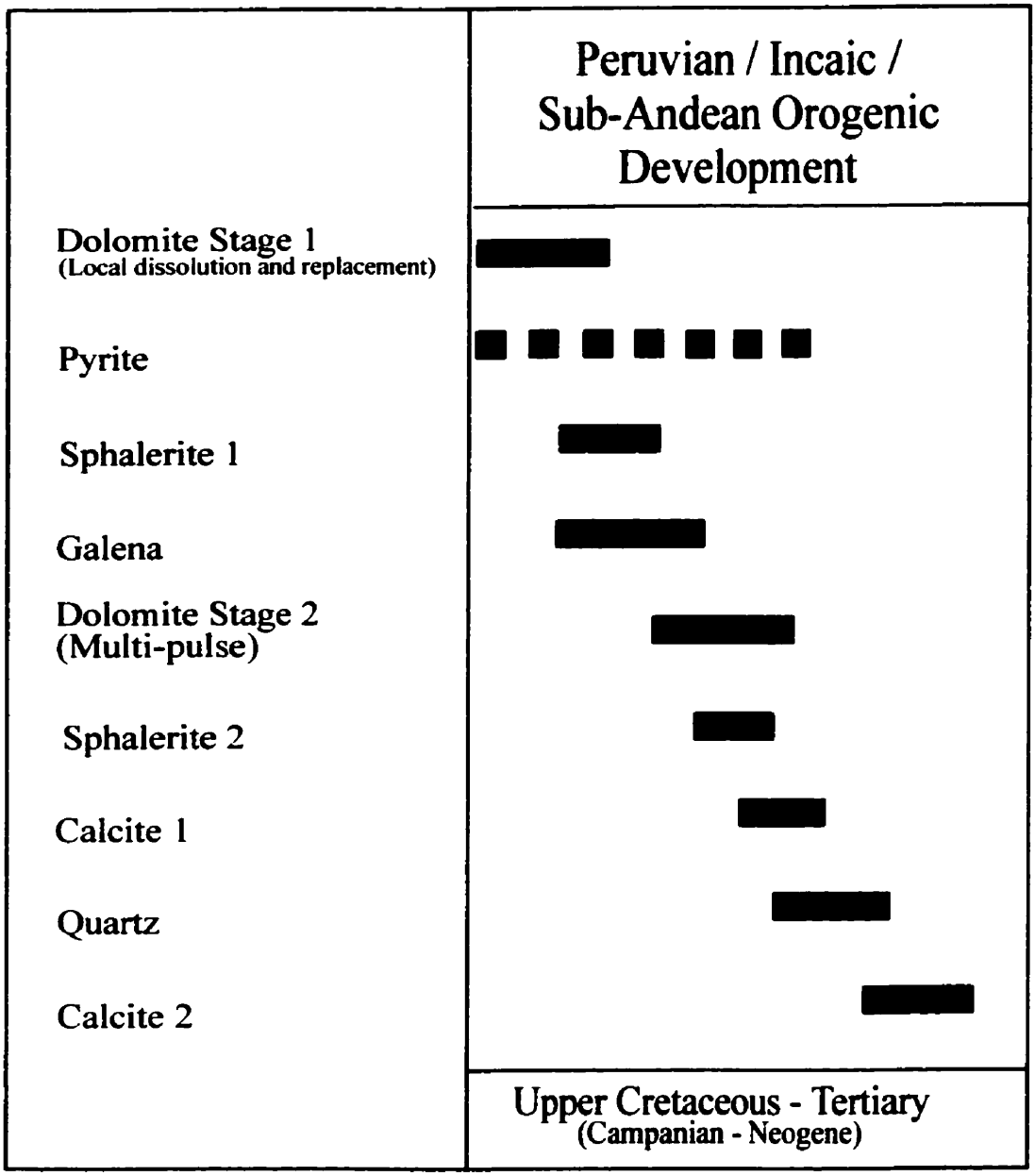

Figure 1.16 Paragenetic sequence for mineralization and alteration phases observed in Pucara Group carbonates from the Bongara area.

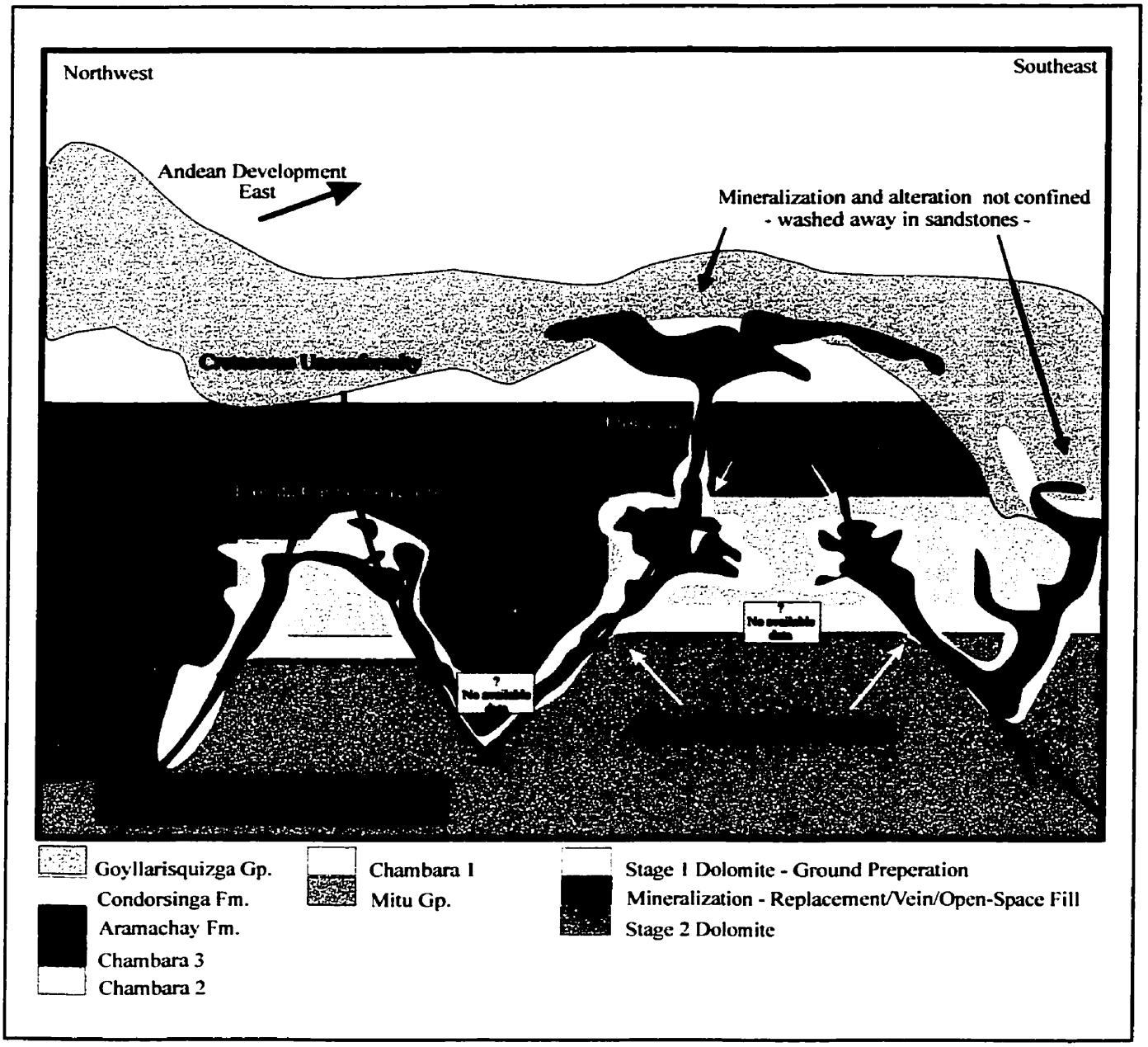

Figure 1.17 Schematic model for carbonate-hosted mineralization observed across the Utcubamba Valley. No attempt has been made to distinguish between textures of mineralization. Not to scale.

1.7 Comparison with Global MVT Districts

Leach and Sangster (1993) listed the most important geological characteristic associated with global MVT-style deposits. These characteristics include:

1. They occur primarily in dolostone, rarely in limestone or sandstone.
2. They are epigenetic and stratabound.
3. They are not associated with igneous activity.
4. They commonly occur at shallow depths at flanks of basins.
5. They occur in platform-carbonate sequences, located either in relatively undeformed rocks bordering foredeeps or in foreland thrust belts.
6. They typically occur in districts that cover hundreds of square kilometers, and a number of districts may even form a metallogenic province.
7. They form districts that are localized by geological features that permit upward migration of the ore fluids. Examples of these features are breccias, depositional margins of shale units, facies tracts, faults and basement highs (paleo-relief).
8. Their temperatures of deposition are low (75-200°C) but typically higher than can be accounted for by local basement-controlled thermal gradients; districts are generally in thermal equilibrium with respect to surrounding host rocks.
9. They are mineralogically simple; dominant minerals are sphalerite, galena, pyrite, maracasite, dolomite, calcite and quartz.
10. Associated alteration consists mainly of dolomitization, brecciation, dissolution of host rocks, and dissolution and crystallization of feldspar and clay.
11. There is always evidence of dissolution of carbonate host rocks, expressed as slumping, collapse, brecciation, or some combination of these.
12. The ore fluids were dense basinal brines, typically containing 10-30 wt.% salts.
13. Their isotopic compositions indicate crustal sources for both metal and reduced sulphur.
14. The sulphide textures are extremely varied, and the ores range from coarsely crystalline to fine-grained and from massive to disseminated.

Zinc-lead mineralization observed throughout the Bongara district accords with many of the above characteristics proposed by Leach and Sangster (1993). Almost all of the mineralization is associated with at least one of the two phases of dolomite identified, an early ground preparing phase and a later, post-sulphide phase. The mineralization is obviously epigenetic and locally has

stratabound morphology when associated with porous lithologies of the Chambara 2. No igneous activity has been identified within the region nor is there a genetic link inferred between regional volcanic events and the mineralization observed in this study.

The mineralization appears confined to a stable carbonate platform, within the Cretaceous Peruvian orogenic foreland fold-and-thrust belt. Of significance is that larger MVT districts show a fundamental relation to continent-orogen boundaries, being located along the flanks of the developing carbonate platform. In this case mineralization is located within the center of the carbonate platform, and within the orogenic belt.

Though at this time there is not sufficient regional mineralization to describe the Bongara region as a true MVT district, early exploration has defined significant, widespread mineralization, as of yet uneconomic. The regional presence of zinc-lead mineralization of very similar morphology suggests a district-wide interconnected hydrothermal plumbing system. This was likely controlled within the underlying horst and graben structures on which the Mitu Group was deposited while temporal reactivation of these structures during the Mid-Jurassic, forming a zone of uplift in the Utcubamba Valley, provided a structurally confined conduit for fluids to migrate.

The distribution of the Chambara 2 host lithologies is controlled by paleo-highs related to underlying piano-keyed horst and graben structures. The porous nature of these lithofacies prove the best host for all mineralization in the Chambara Formation and they appear to be limited to an elongate carbonate platform, confined to the Utcubamba Valley. These high-energy carbonates correspond to the high stand systems tract model that appears confined to areas of carbonate sedimentation on basement highs.

The sulphide mineralogy is very simple consisting of sphalerite, galena, and pyrite. With continued structural reactivation and exposure to meteoric fluids, significant zinc and lead oxides are observed regionally. These are common to MVT districts and indicative of oxidation of mineralization by various methods. Significant dolomite is associated with the system as an early and waning stage. There is both a temporal and spatial association between the metal and carbonate. Local calcification and silification occurs towards the close of the mineralizing event and is confined spatially to well-developed structural systems.

Alteration and ground preparation are very similar to those observed in other global MVT districts. Significant dissolution, collapse and brecciation are associated with both mineralization and dolomitization. Zinc and lead are confined to those areas showing the best ground preparation associated spatially with sub-vertical structures in Chambara 2 lithofacies, allowing for ingress and horizontal fluid flow.

Sulphide textures are varied. The majority of sphalerite occurs as coarse to medium grained, open space filling, mosaic intergrowths of large crystals. There is very little zoning or colloformal growth identified as coarse replacement of the original carbonate. Galena is always coarse-grained, euhedral, individual grains within the open space mosaic fill of sphalerite, and is rarely observed alone. Pyrite, the least common sulphide, is typically fine-to-medium grained and disseminated.

At Florida Canyon and throughout the areal extent of the Pucara Gp. in northern Peru, the carbonate section is underlain by the Permian red bed sandstones of the Mitu Gp. This thick sandstone unit has probably been of significant importance as a fluid aquifer and major source of metals.

Commonly in other MVT districts, an overlying shale or impermeable lithology acts as a stratigraphic cap to ascending ore fluids. There are no true shales of any significant thickness, in the upper Pucara Gp. However, it is possible that basinal lime mudstones at various levels have acted as significant aquitards to fluid flow and thus concentrated dolomitization, dissolution and mineralization at certain levels within the section. The only identifiable problem here is that the entire structural system remained active during carbonate deposition and later fluid expulsion and, as such, may have remained open for ascending fluids to dissipate through the Pucara Gp. and into the overlying Cretaceous sandstones, as seen at Floricita and Maino.

Leach (1999) compiled a diagram of the predominant global MVT districts and deposits in relation to age of mineralization and host rocks through Cambrian to Tertiary time (Fig.1.18). This compilation is based upon geological, paleomagnetic and radiometric data compiled from the literature. When the available data from the study area are plotted it can be seen that the age

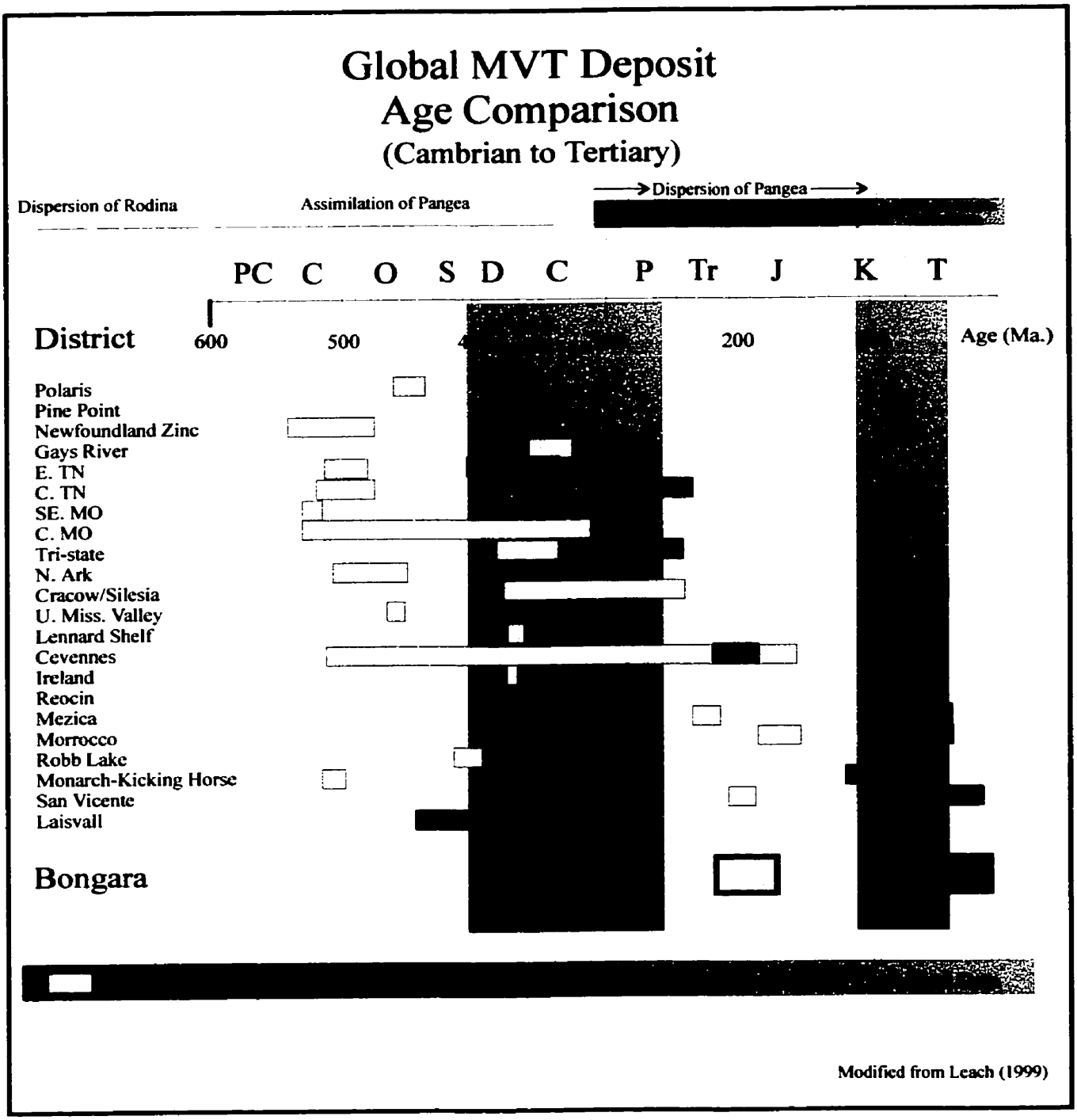

Figure 1.18 Global MVT deposit age comparison. Modified from Leach, 1999.

of the Pucara Gp. (Late Jurassic-Triassic) host rocks plot in the upper fifth of global deposits as being one of the youngest hosts identified. The Pucara Gp. is of course correlatable with San Vicente of southern Peru, but also to the host rocks of the Moroccan and Mezica districts.

Though no age dating has been attempted, mineralization occurred post Cretaceous unconformity, and after the deposition of the Goyllarizquisga Fm. sandstones, as identified in the Maino and Floricita areas. This would date the mineralization as less than 80-70 Ma, corresponding with either the Peruvian compressive event (84-79 Ma) or one of the later compressive pulses of the Incaic I (59-55 Ma), Incaic II (43-42 Ma), Incaic III (30-27 Ma), Incaic IV (22 Ma) or later Quechua period. These compressive intervals formed three major fold-and-thrust belts, the Peruvian (Campanian), the Incaic (Paleocene-Eocene) and the Sub-

Andean (Neogene). It is thought that the fluids responsible for the Bongara mineralization are related to the Peruvian Campanian orogeny, though they may be younger. In any rate, the fluids responsible for MVT-style mineralization can likely be considered one of the youngest MVT events studied. The age of mineralization is similar to those obtained via geological evidence from Pine Point, Cracow, Cevennes, Reocin, Mezica, Morroco and Robb Lake (Leach, 1999).

The Bongara district shows many of the criteria of an MVT district as proposed by Leach and Sangster (1993). Though to date no economic mineralization has been defined, exploration is still very young, and the terrain very difficult to explore thoroughly. With a little time the Bongara area could represent a significant emerging zinc-lead district.

1.8 Summary

Integrated sedimentological, and diagenetic studies of Pucara Group from barren, altered and mineralized carbonates indicate a complex, multi-phase depositional and mineralizing geological evolution for the Bongara district. Deposition of Chambara Fm. carbonates was controlled by the basinal position of paleo-highs formed within the Utcubamba Corridor along horst-and-graben structures of the underlying Permian Mitu redbeds. Distribution of Chambara 2 high-energy depositional lithofacies is confined to areas of elevated paleo-relief and provide depositional and spatial constraints for the formation of isolated carbonate platforms along the length of the study area.

The best mineralization in the Bongara region is generally associated with strong ground preparation observed as pervasive dolomitization, pseudobrecciation, and carbonate dissolution development. Three textures of mineralization have been identified and defined as: i) bedding and/or small cavity replacement, ii) collapse breccia hosted and iii) minor zinc in vein, crackle and mosaic breccias in the upper Chambara Formation (Chambara 3). Zinc mineralization consists of dark red to brown sphalerite with lesser dull yellow beige sphalerite being identified locally. Sphalerite is observed as coarse euhedral to fine-grained (mm to cm scale) aggregates with locally colloformal zoned varieties. Lead mineralization is exclusively observed as galena, though oxide varieties of both zinc and lead mineralization has been observed in the district. Most commonly zinc and lead sulphides are observed together as an intermeshed mosaic of sulphides, though galena veining has also been identified crosscutting early sphalerite phases. Pyrite is observed throughout the mineralizing sequence ranging from fine mm-scale disseminations to cm-scale massive replacement of the host. Later silicification and calcification is observed towards the waning stages of the mineralizing system.

Comparison with global MVT districts shows that the Bongara area possesses many of the necessary characteristics for classification as a true MVT –type deposit. The main differences appear confined to the placement of mineralization with the central basin, and not confined to the distal basinal edges as in the norm. Further exploration with focus on areas of known mineralization, those areas exhibiting Chambara 2 lithofacies and in areas of obvious paleo-relief may allow for new base metal discoveries through the region. Emphasis should be placed on the structural relationship between lithofacies, distribution of alteration, and proximity to known mineralization. The Bongara zinc-lead district is a good example of an under-explored emerging mining district containing several currently undefined MVT-style resources. With continued work in this difficult terrain new discoveries can be made.

1.19 Acknowledgements

Cominco and Cominco Peru Ltd. provided complete financial support for this study. The author would like to thank the Department of Geology at the University of Toronto, especially Professors Andrew Miall, Ed Spooner and Geoff Norris for their supervision, guidance and critical review of this work.

This study would not have been possible without the assistance and enthusiasm of Dr. Cameron Allen, Chief Geologist, Cominco Ltd. Wojtek Wodzicki, Manuel Montoya and Lino Ramirez are thanked for their assistance with project development and helping me to gain a better understanding of the geological complexities of the region.

Dereck Rhodes is thanked for his open idea-sharing and frank discussions regarding the geology of the Bongara area, and for his constant interest and enthusiasm for continued exploration within this under-explored district. Dereck's understanding of the MVT deposits and carbonate stratigraphy helped me to develop the scientific layout for this work. Dereck's original nomenclature and classifications used in the exploration process for the region proved remarkably accurate and were used as the starting point for this work.

Nurcahyo Basuki (Uki) is thanked for his insightful reviews, comments, and criticisms throughout the course of this study. John Pearson, Gary Delaney, and Barry Cook are thanked for their constant assistance with personal career decisions, professional development and for adequately preparing me for this undertaking. Barry Cook and David Robertson are thanked for their critical review of this manuscript. Darren Tisdale scanned all of the images within this work. The staff at the University of Waterloo are thanked for providing facilities for me to complete the cathodoluminescence work. Neil O'Brien and the staff at the Cominco Exploration Research Lab are thanked for all of the section preparation and XRD analysis.

Special thanks to my parents and especially to my wife Jodie, and daughter Jordan who have provided me with constant support, assistance, and a sense of life-meaning and purpose throughout this process.

PAPER 2.
DIAGENETIC AND EPIGENETIC EVOLUTION OF THE BONGARA MVT ZINC-LEAD DISTRICT, NORTHERN PERU

2.1 Abstract

The Bongara zinc-lead district is located within the sub-Andean fold-and-thrust belt of the northern Peruvian Eastern Foreland Basin. Pucara Group carbonates, host to MVT-style mineralization, form a craton-margin carbonate platform that represents the first marine transgression of the Andean Cycle. The northern Pucara Group developed discordantly over piano-key shaped horst-and-graben terrestrial sequences formed under extensional tectonic conditions. MVT-style zinc-lead mineralization occurs in Pucara carbonates with the most significant being associated with pervasive dolomitization and pseudobrecciation development in the Florida Canyon area. Mineralization is predominantly sphalerite, galena, and pyrite observed as various replacive and open-space filling textures. The paragenetic sequence preserved within the Pucara Group carbonates of the Utcubamba Valley includes early burial and compaction-related carbonate cements, and later diagenetic/epigenetic pre-mineralization and post-mineralization, zoned sparry dolomite and calcite. Petrographic, cathodoluminescent and carbonate isotope data suggest that both early diagenetic and late diagenetic/epigenetic alteration associated with zinc-lead mineralization throughout the Bongara district occurred through an interconnected, district wide, structurally controlled plumbing system. This suggests a genetic link between all metal occurrences independent of stratigraphic position.

2.2 Introduction

Mississippi Valley type (MVT) lead-zinc (Pb-Zn) mineralization, occurring in a variety of types, textures, and concentrations, has attracted the interest of exploration companies to the Bongara area. Mineralization is predominantly though not exclusively confined to the Chambara Formation of the Pucara Group and the most significant mineralization discovered to date is

around Florida Canyon (Fig. 2.1). Other significant mineralized occurrences have been identified in the Floricita, Naranjitos, and Cristal exploration areas. Significant dolomitization thought to be associated with or genetically related to zinc mineralization is observed throughout the study area in various forms, and may have implications with regard to the presence of mineralization in areas distal from the Florida Canyon core.

In this work, petrographic, cathodoluminescent and stable carbonate isotopic analysis was combined with regional geological investigations in an attempt to determine whether pervasive, early diagenetic and late-metal associated alteration was distributed regionally or, alternatively, was locally confined. If carbonate alteration phases associated with mineralization were correlatable with those of barren areas, then new areas for focused exploration could be defined. However, if drastic diagenetic and alteration phase differences existed across the district, exploration could be focused to those areas with favorable alteration characteristic of mineralized terrains.

2.2.1 Location

The Bongara study area is situated between 5°20' to 6°50' south and 78° to 77°30' west, within the Eastern Cordillera of the northern Peruvian Andes (Fig. 2.2) comprising an area approximately 90 km long and 20 km wide. The study area is located within the Bongara territory of the Amazonas Department.

Access to the area is by paved highway from the city of Chiclayo via the town of Bagua Grande to the village of Pedro Ruiz. Pedro Ruiz was the central logistic base for the study and exploration work carried out in the region. The paved highway continues east of Pedro Ruiz to the jungle towns of Rioja and Tarapoto. There are daily commercial flights from Lima to both Chicalyo and Tarapoto. Driving time from both cites to Pedro Ruiz is approximately 6 hours. An unpaved road connects Pedro Ruiz with Chachapoyas, the capital of the department of Amazonas, and continues south to Cajamarca. Access to the area is relatively easy by road; however, travel within the property is arduous due to its elevation, and jungle cover requiring helicopter support or local guides with knowledge of the jungle areas and passes.

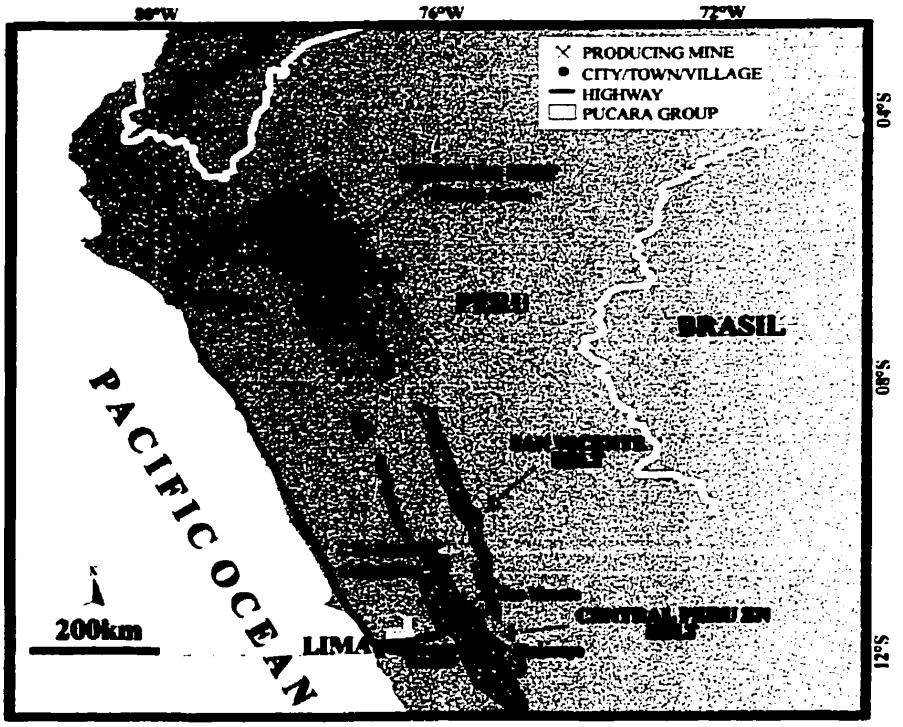

Figure 2.1 Location of the Bongara, San Vicente, and Central Peru CRD zinc districts.

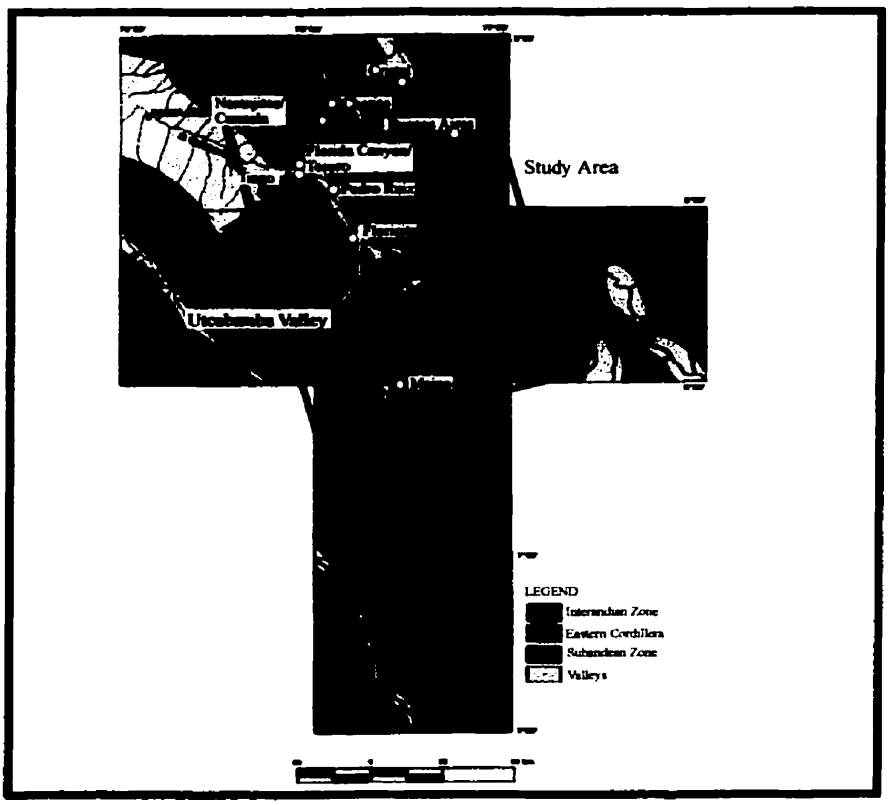

Figure 2.2 Locations of major villages, zinc occurences, and measured stratigraphic sections in relation to major physiographic divisions. Modified from Fig. 2.1 of Ingemmet Boletin No.56, 1995.

2.3 Geotectonic Setting

The description here is a summary of geological work emphasizing the tectonic development and morphological division of the Peruvian Andes. The work of the author is confined to a very well defined segment of the Eastern Foreland Basin located in the northern portion of the Sub-Andean zone (Fig.2.3).

The Andean Cordillera, a major mountain range located between the Peru-Chile oceanic trench in the west and the Brazilian shield in the east, forms the western-central part of Peru. The formation of the Andes is a result of the Mariana-type subduction of the Nazca Plate beneath the ensialic South American Plate. Along the western margin of the plate the development of over 70 km. of crustal thickening has led to cordilleran uplift of approximately 4000 meters from the Late Triassic to Present (Benavides-Caceres, 1999; Megard, 1987).

The Andean Cordillera is a result of three geodynamic pulses (Benevides-Caceres, 1999): Precambrian; Paleozoic to Early Triassic; and Late Triassic to Present. The Cordillera can be divided into two dominant ranges: the Western Cordillera, resulting from the formation of a magmatic arc, and the Eastern Cordillera, representing the zone of uplift or lesser subsidence. Between these ranges is the Altiplano, a zone between the Pacific margin of the magamatic arc and the oceanic trench.

Prominent features of the Andes include the Cretaceous-Paleocene Coastal Batholith, which is bounded to the east by the Incaic fold-and-thrust belt, the site of a series of compressive events. East of the eastern Cordillera horst is the Sub-Andean fold-and-thrust belt formed during the Late Miocene. The Eastern Foreland Basin marks the eastern edge of the Andean Cordillera with a thinning sedimentary package unconformably overlying the Brazilian Shield.

By the end of the Paleozoic, the Andean region was part of the western Pangean margin. It is thought that during Middle Triassic time intense intracontinental rifting formed a large horst-and graben-system occupying the present Andean trend. The most dramatic of these systems was the Mitu Graben, which received over 3000 meters of continental red beds, volcaniclastic, and alkaline volcanic rocks (Benvadies-Caceres, 1999; Megard, 1987). Pucara Group carbonate deposition is spatially confined to the distribution of these underlying redbeds throughout the study area.

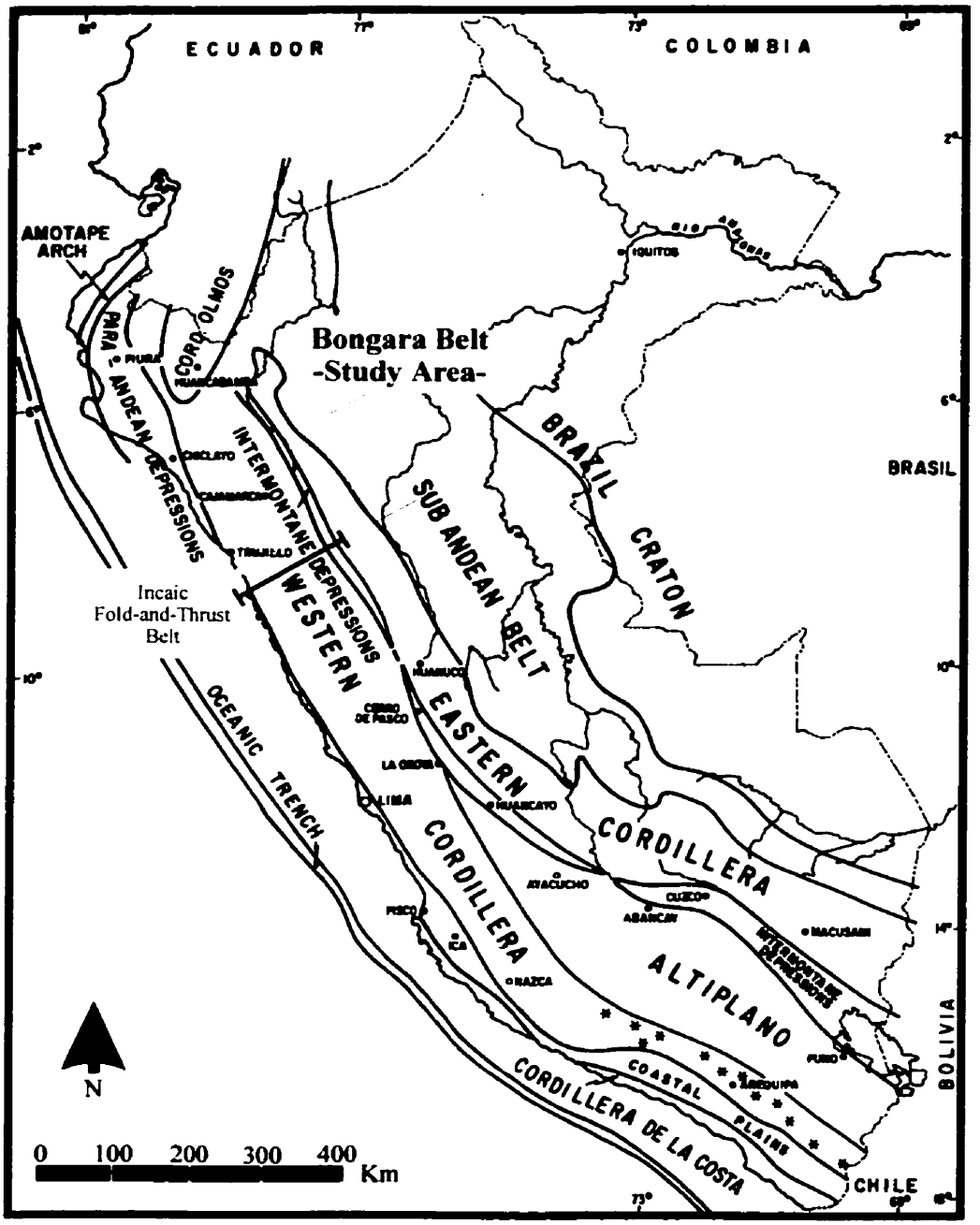

Figure 2.3 Main morphostructural units of Peru. Modified from Benavides-Caceres, 1999.

2.4 Basinal Setting

The Pucara Basin is a craton-margin carbonate platform that represents the first marine transgression of the Andean Cycle over continental clastic sediments, volcanic and volcaniclastic rocks of the Permian-Triassic Mitu Group, and other Paleozoic rocks (Fig.2.4). The wide carbonate platform of the Pucara Group (Gp.) developed discordantly over piano-key shaped horst-and-graben terrestrial sequences formed under extensional tectonic conditions, on the western margin of the Brazilian Shield in northern and central Peru (Fontbote, 1990; Megard, 1987).

The Pucara carbonate platform has been best studied in the Altiplano region of central and south central Peru where it has been subdivided into three formations: Chambara, Aramachay, and Condorsinga (Fontbote, 1990; Rosas, 1994). This study is confined to a small area of the Utcubamba Valley in northern Peru. Other investigations of the Pucara in northern Peru include that of Wilson and Reyes (1964) near Pataz, and the Utcubamba Valley by Prinz (1985). Other studies of Pucara Gp. stratigraphy in the sub Andean region of central Peru include those of Levin (1974) and Palcios (1980).

Many models have been proposed concerning the development of the Pucara basin. Loughman and Hallam (1982) proposed an unrestricted open shelf to the Paleo-Pacific in the west. Szekely and Grose (1972) and Megard (1978) proposed the existence of a structural high with emergent areas between the Pucara basin and the Paleo-Pacific. Fontbote (1990) suggests that the evolution of the Triassic-Liassic Pucara Basin has more similarities to basins in the Triassic of the Alpino-type lithofacies than to the Andean basins related to paired magmatic arc-back-arc. These similarities include high subsidence rates, predominant carbonate sedimentation, and the paleogeographic situation at the margin of an emerged continent.

The Pucara Gp. of the northern Pucara basin can be divided stratigraphically into the Chambara, Aramachay and Condorsinga Formations, as described from studies of the Pucara Gp. from the central Altiplano region of Peru. However, marked lithofacie differences, especially in the Chambara Formation, have allowed informal subdivisions to be applied locally. These lithofacie differences (discussed below) likely resulted from a differentiated extensional basin controlled by localized paleogeographic highs exhibiting substantial vertical and spatial variation over kilometer-scale distances. As well, syndepositonal tectonic, structural modification of this

original paleo-relief may have affected the stratigraphic character and distribution of the Pucara carbonates throughout the study area.

The study area is confined to an elongate northeast corridor that extends from the southern Maino region northeast through the Utcubamba valley and terminates north of Florida Canyon in the Naranjitos area, approximately 90 kilometers in length and 12-20 kilometers in width. The Utcubamba Valley continues to the southeast for at additional 40 kilometers through the Leimebamba area.

Unlike most global MVT districts, the Bongara area is located centrally within a moderately stable carbonate platform rather than along the basin margins. Within the study area the formal stratigraphic division of the Pucara Group (Gp.) as suggested by Harrison (1943) and Megard (1968) can be identified, though regional lithofacies correlation is difficult due to depositional controls, structural modification, and lack of exposure. The Pucara sequences of this area provide a unique stratigraphic study because active tectonism and structural movements were prevalent during and after Pucara Gp. deposition. This structural movement was both local and regional, and variable in intensity. The end result is a northwest-southeast corridor of structural highs and lows preserved in an elongate structural belt. This belt corresponds grossly with the horst-and-graben structures of the underlying Mitu graben, and is elongate perpendicular to later Andean thrust movements. These variable basement structures provided an antecedent surface on which carbonate deposition was initiated, and appear confined within the Utcubamba Valley, an area of significant basement uplift. The distribution of carbonate facies observed in the area is a function of original Mitu basement topography, depth of water during carbonate production, and distribution of structural reactivation of basement structures through the sediment pile during active deposition. The end result is a structurally-controlled depositional pattern that closely conforms to the distribution of paleo-highs formed as a result of extensional tectonics and the associated structural reactivation along these topographic margins.

The best applicable depositional model is one of a series of stepped, piano-keyed, isolated, carbonate platforms distributed within a much larger platform that extends the length of the study area (Fig.2.5a and 2.5b).

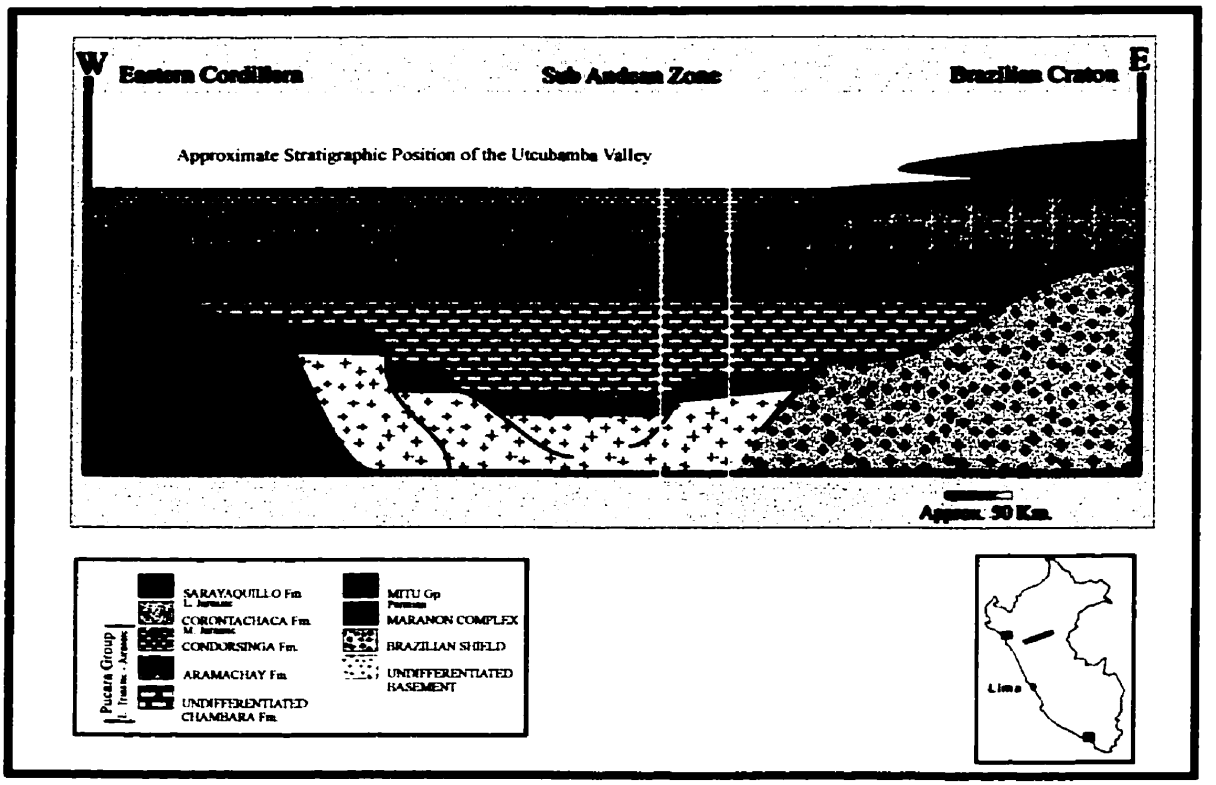

Figure 2.4 Schematic W-E profile of the Pucara encompassing the Utcubamba Study area. Modified from Fontbote, 1990. Based upon data from Ingemmet Boletin No.60, 1995 and stratigraphic data collected by the author.

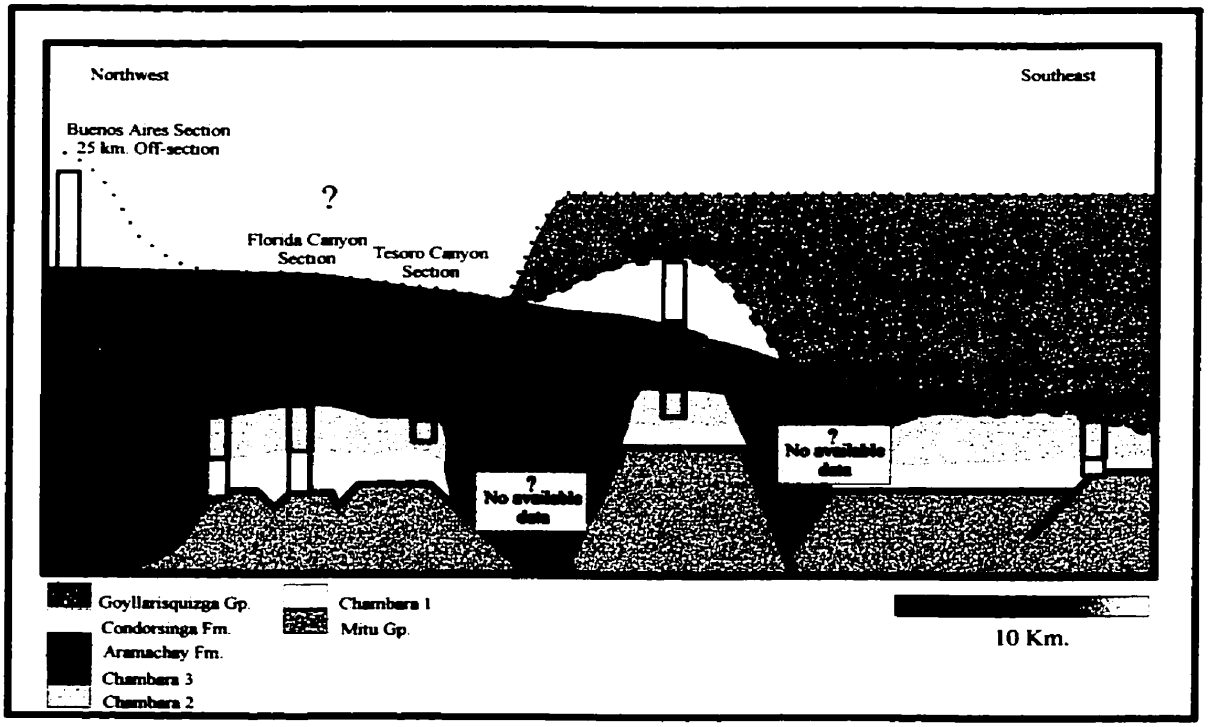

Figure 2.5a Schematic section, looking northeast across the Utcubamba Valley. This figure attempts to put all measured sections into a basinal and depositional framework. Correlation proves difficult due to the lack of identifiable surfaces resulting from poor regional stratigraphic exposure. Not to scale.

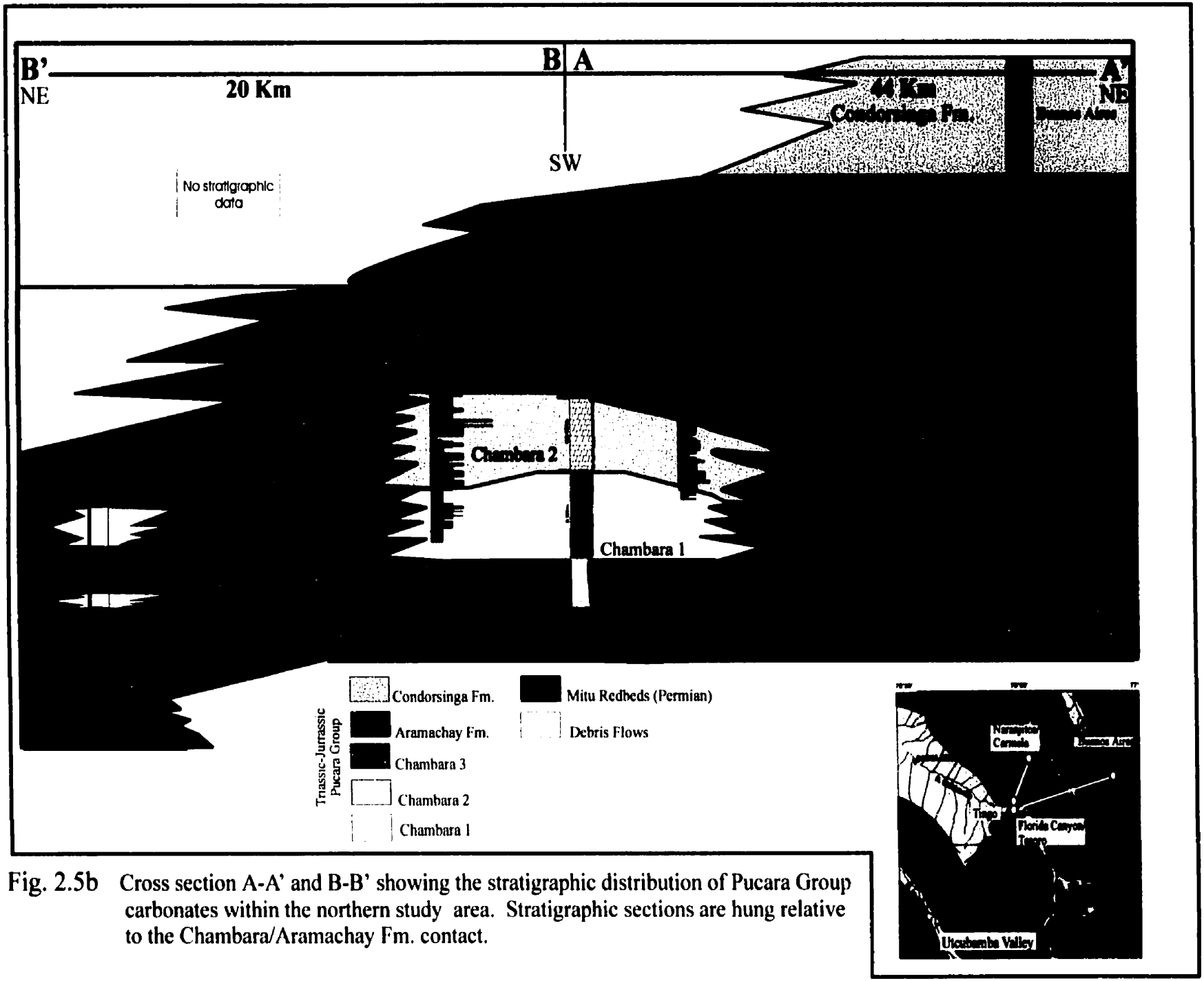

Fig. 2.5b Cross section A-A' and B-B' showing the stratigraphic distribution of Pucara Group carbonates within the northern study area. Stratigraphic sections are hung relative to the Chambara/Aramachay Fm. contact.

2.4.1 Stratigraphy of the Utcubamba Corridor

2.4.1.1 Basement

The oldest rocks in the study area are Precambrian gneisses of the Maranon complex, exposed in elongate, NW-trending, fault bounded blocks which outcrop to the north of the study area.

The Permian Mitu red beds unconformably overlie the Maranon Complex and are well exposed throughout the area, predominantly on the main road between the towns of Bagua Grande east to Pedro Ruiz in the north. In the study area the Mitu Formation consists of coarse-grained ferruginous sandstones and both monomictic and polymictic conglomerates and/or local debris flows (Plates 2.1 and 2.2). These rocks are associated with horst-and-graben structures related to an aborted ensialic rift (Noble et al, 1978; Kontak et al, 1985). Stratabound copper deposits and occurrences have been reported in the Mitu within central Peru (Amstutz, 1956; Kobe, 1960, 1990). The rift-related horst-and-graben structures of the Mitu provide the differentiated piano-key-shaped basin surface, or paleo relief, in which the carbonates of the Pucara Group were deposited.

2.4.1.2 Local Pucara Group

Through the studied area, the Pucara Group can be observed from the basal Chambara Formation unconformably overlying the Mitu redbeds through the Aramachay Formation and in places where preserved, the Condorsinga Formation (Fig.2.6).

2.4.1.2.1 Chambara Formation

Weaver (1942) applied different names to various intervals of the Chambara Formation, including the Utcubamba Fm. within this study area. The Upper Triassic limestones were named the Chambara Formation by Grose (1961) based upon outcrops near the Chambara village, about 20 km. northwest of the town of Huancayo. Stratigraphic correlations made between central and northern Peru have ensured the acceptance of the Grose (1961) nomenclature for the Chambara Fm. and has become the scientific standard. Though persistent through the study area, the

Plate 2.1 - Mitu Conglomerate; fragments of Proterozoic Maranon Complex gneisses supported within coarse-grained, well-sorted, consolidated ferriginous sand.

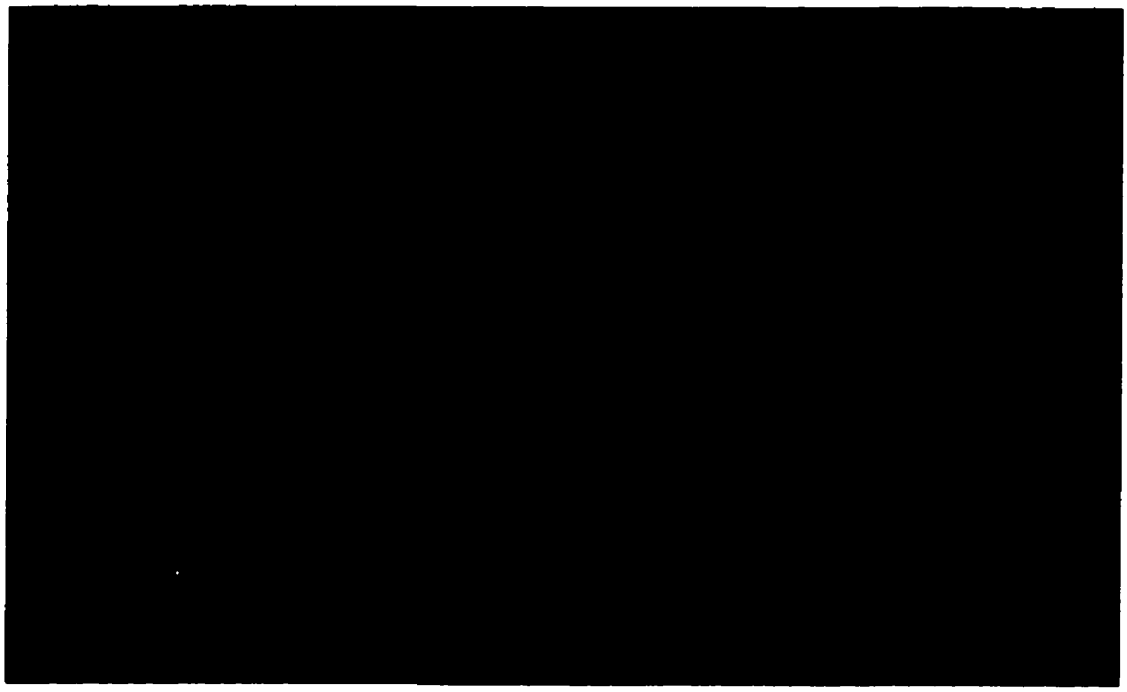

Plate 2.2 - Mitu Sandstones; laminated and cross-bedded,composed of well-sorted, consolidated, ferruginous sand.

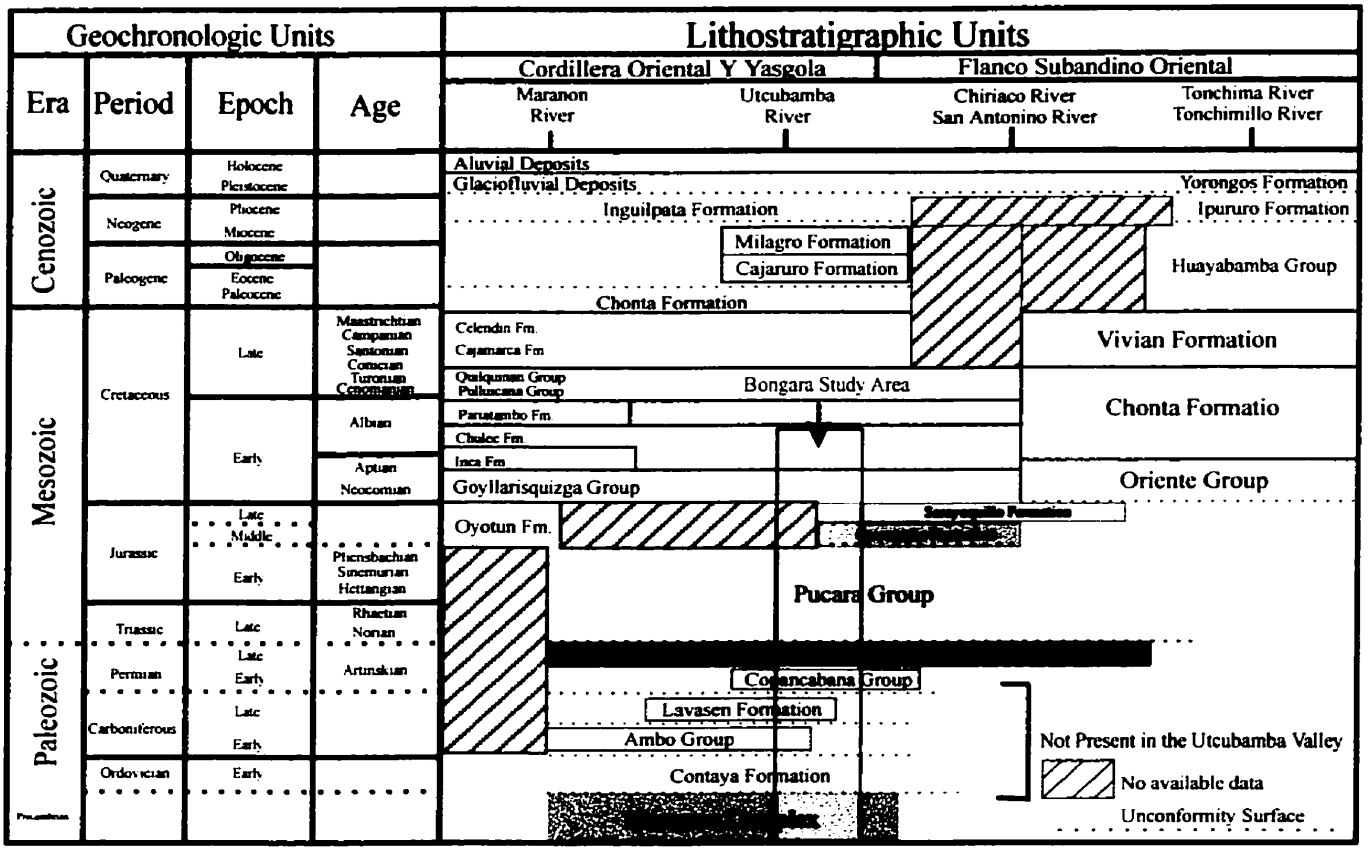

Figure 2.6 Time-space stratigraphic tabulation for the Maranon, Utcubamba, Chiriaco, San Antonio, Tonchima and Tonchimillo River Valleys of Northern Peru. Modified from Ingemmet Boletin No.56, 1995.

Chambara exhibits laterally variable lithofacies, depending on the depth and location of the carbonate depositional environment in relation to basement paleo highs. For the purpose of this discussion the "reference" section for the Chambara Fm. will be the one at Florida Canyon, which is the best exposed and which also has the most associated diamond drill core information of the studied areas. As a consequence, the Chambara has been informally divided into three sub-members designated Chambara 1,2, and 3 as described below. It should be noted at this point that throughout the Bongara region, carbonate stratigraphy has been overprinted by local and regional multiphase dolomitization.

The Chambara 1 lies unconformably on Mitu Gp. redbeds and where identified is composed predominantly of algal limestones and lime mudstones, deposited in a very shallow, hypersaline, sea with algal mats being common and evaporitic conditions being sufficient to precipitate anhydrite nodules within the lime muds. Substantial facies variations exist ranging from algal lime mudstones to local wackestones and storm deposits.

The Chambara 2 is composed predominantly of high-energy depositional carbonate environments. Lithologies range from nodular, bituminous lime mudstones through skeletal wackestones and packstones, fossiliferous floatstones, and rudstones. Where exposed, the Chambara 2–type lithologies remain relatively consistent and locally correlatable based upon a series of markers identified within the Florida Canyon, Tingo and Tesoro areas. These markers include the first appearance of a Sponge rudstone separating the Chambara 1 from the Chambara 2, a black star crinoid marker, a well developed and locally consistent coquina marker, and an intact bivalve marker. Centimetric to decimetric chert nodules are commonly observed within the Chamabara 2; however, due to lack of regional continuity, chert is of no use when attempting stratigraphic correlation.

The Chambara 3 is predominantly deep basinal lime mudstones and bituminous lime mudstones with minor shale interbeds, turbidites, and debris flows identified. Local work by exploration companies centrally within the study area has defined a five-fold subdivision for the Chambara 3. The Chambara 3A is observed as a nodular textured lime mudstone. The Chambara 3B is a deep basinal turbiditic unit: The Chambara 3C is dominantly a lime mudstone, with lesser shales, common bivalve debris, and is observed locally interbedded with 3B equivalents. Chambara 3D is dominantly silt-laminated lime mudstones, and turbiditic mudstones with minor interbedded shales. The 3E is very similar to D with the exception of predominance of variable sized

concretions developed within the strata. The observation of concretions within the Chambara 3 marks the transitional contact into the Aramachay Formation.

2.4.1.2.2 Aramachay Formation

Megard (1968) named the Aramachay Formation based upon an exposed shaley succession at the site of the Ichpachi mine, 2 km. SW of the village of Aramachay, about 30 km. NW of the town of Hyancayo. Within the Bongara region the Aramachay is observed with various stratigraphic thicknesses throughout the district and is composed predominantly of deep basinal lime mudstones, calcareous shales and variable turbidites. The contact between the Aramachay and the upper Chambara Fm. is gradational over tens of meters and at times is difficult to pick. The contact with the overlying Condorsinga, where exposed, is sharp and well-defined.

2.4.1.2.3 Condorsinga Formation

Megard (1968) named the upper limestone unit of the Pucara Group the Condorsinga Formation. Within the Bongara area there is a marked difference in stratigraphic thickness regionally. Measured sections range from approximately 100 meters in the Floricita area (discussed below) to greater than 180 meters in the distal northeastern Buenos Aires section. Rhodes (1998) discussed the regional variations observed within the Condorsinga Formation with regards to both facies distribution and thickness. At Minas Grande, Rhodes observed coarsely pelletal lime mudstones, which overlie chicken-wire-textured gypsum (after anhydrite). In the Floricita area the Condorsinga is predominantly medium-to-thin bedded limestones and dolomitized (mineralization-related) equivalents. In the Buenos Aires section the thickest exposures of Condorsinga examined are over 200 meters in thickness. Here the Condorsinga is predominantly a thin to fine bedded, bituminous, black to dark grey, fine-grained nodular lime mudstone. The Minas Grande area (Rhodes, 1998), and the Floricita area appear to represent a very shallow water depositional environment characteristic of a shallow hypersaline and restricted environment. The northeastern and eastern equivalents, on the other hand, mark a deeper basinal environment. This is a function of proximity to the general corridor of uplift within the Utcubamba Valley. The contact between the deeper basinal Aramachay and the Condorsinga in the central corridor of the area is much sharper than the eastern equivalents, which appear to be a more inter-tonguing, transitional depositional center.

2.4.1.2.4 Post-Pucara Units

To the east of the Utcubamba Valley the Corontochaca and Sarayaquillo formations are variably observed and pinch-out against a narrow high(s) formed by the uplifted Pucara Group, and rapidly thicken away from it. Both units indicate a substantial degree of uplift, subaerial exposure, and erosion of the Pucara Group (Pardo and Sanz, 1979; Prinz, 1985; Rosas, 1994). The Corontochaca varies from very coarse-scarp derived boulder conglomerates to more sorted conglomerates, sandstones and silts of fluvial/deltaic character. The Sarayaquillo Formation is dominantly red bed shales, sandstones and marls, with some gypsum beds. The contact with underlying stratigraphy in the Bongara region is unique, and locally a strong angular unconformity is observed between the Pucara Group and the Corontochaca and Sarayaquillo Formations. This suggests a substantial degree of uplift and deformation, subaerial exposure, and erosion of the Pucara Group rocks during the mid-Jurassic, confined within the Utcubamba Corridor.

The Lower Cretaceous clastic Goyllarizquisga Formation unconformably overlies the Pucara Group within the study area and the Sarayaquillo Formation locally. The Goyllarizquisga Formation consists mainly of delta and shallow-marine clastic sediments (Wilson, 1963; Rosas, 1986). These continental siliciclastics are interpreted as synorogenic products of the Nevadian Orogeny and overlie a regional stratigraphic unconformity. Elsewhere within the study area, the unconformity surface cuts variably through different stratigraphic levels of the Pucara Group, and in places near Maino, rests upon the Mitu, suggesting complete erosion of the Pucara.

2.5 Mineralization and Associated Features

The most abundant information collected thus far has been from Florida Canyon. The best mineralization in the Bongara region is generally associated with strong ground preparation observed as pervasive dolomitization, pseudobrecciation, and carbonate dissolution. The ground preparation in Florida Canyon is controlled by the occurrence of carbonates deposited within high-energy environments of the middle Chambara Fm. (Chambara 2), and by the proximity to major structures (Wodzicki, 1998). To date, significant mineralization has been observed along the Sam Fault structure and fault splays off the main structure. Significant mineralization has also been observed locally through drilling across the Florida Platform, usually associated with parallel and later crosscutting structures. To date, economic mineralization has not been defined,

although a speculative resource of 7 million tons of approximately 7% combined zinc and lead has been suggested by exploration companies.

At Florida Canyon sulphide mineralization typically replaces rock fragments or fills open spaces in dissolutioned ground. Three textures of mineralization have been identified and defined as: i) bedding and/or open-space replacement, ii) collapse breccia hosted and iii) minor zinc in vein, crackle and mosaic breccias in the upper Chambara Formation (Chambara 3) (Plates 2.3, 2.4 and 2.5). Zinc mineralization consists of dark red-to-brown sphalerite with lesser dull yellow-beige sphalerite being identified locally. Sphalerite is observed as coarse euhedral to fine-grained (mm to cm scale) aggregates and locally colloformal zoned varieties. Lead mineralization is exclusively observed as galena, though oxide varieties of both zinc and lead mineralization have been observed in the district. Most commonly, zinc and lead sulphides are observed together as an intermeshed mosaic of sulphides, though galena veining has also been identified crosscutting early sphalerite phases. Pyrite is observed throughout the mineralizing sequence ranging from fine mm.-scale disseminations to cm.-scale massive replacement of the host. Later silicification and calcification is observed towards the waning stages of the mineralizing system.

Throughout the Florida Canyon area, specifically proximal to the Sam Fault structure a number of mineralized horizons have been identified that correlate with discovered surface showings as defined via drill testing. These horizons are associated with favorable dolomitization of the middle Chambara Fm., are centered stratigraphically about the coquina marker and include the Milagros, Nancy, and Karen zones (Fig.2.7). Mineralization within these zones fluctuates vertically over a range of as much as 5 meters to the extent that it is not planar and only broadly stratabound. Closer to the Sam Fault, dolomitization and zones of dissolutioned carbonate thickens to include much if not all of the Chambara 2 Fm., resulting in a series of stacked, stratabound, mineralized intervals within about 200 meters proximity of the Sam Fault. These sulphide zones are at or slightly above the "intact bivalve marker"(IBM) and the Gordita and Raquel packstone beds. Of these, only the IBM seems consistently to attain reasonable thicknesses of mineralization and dissolution. While most of the mineralization occurs as massive replacement of internal sediment/solution detritus intervals there is some disseminated and patchy sulphides in pseudobreccias and weakly-developed dissolution zones.

Plate 2.3 - Massive replacement of host carbonate by very-coarse grained sphalerite (2-phases), galena, and pyrite at the Karen Showing in Florida Canyon.

Plate 2.4 - Coarse-grained sphalerite infilling open space, and replacing clast edges within a psuedobrecciated collapse system. Oxidation of sulphides has resulted in fine veining of smithsonite away from sulphides through open porosity.

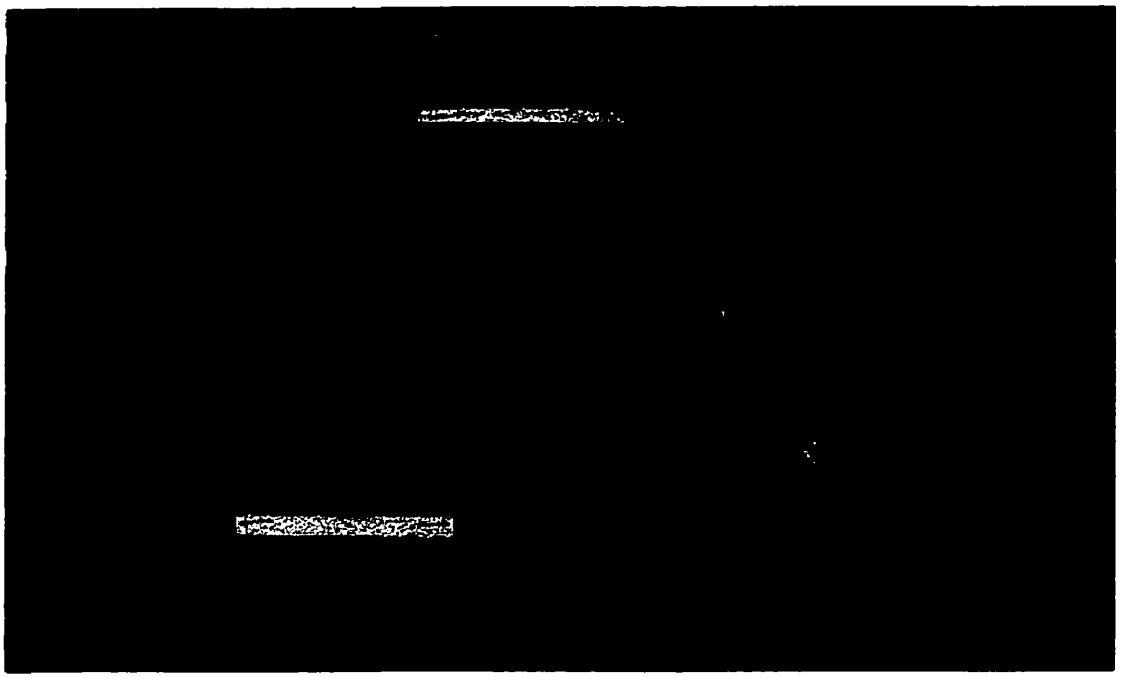

Plate 2.5- Crackle brecciated dolomitized Chambara 2 lithologies with dolospar matrix and orange smithsonite partially replacing sphalerite rimming fragments.

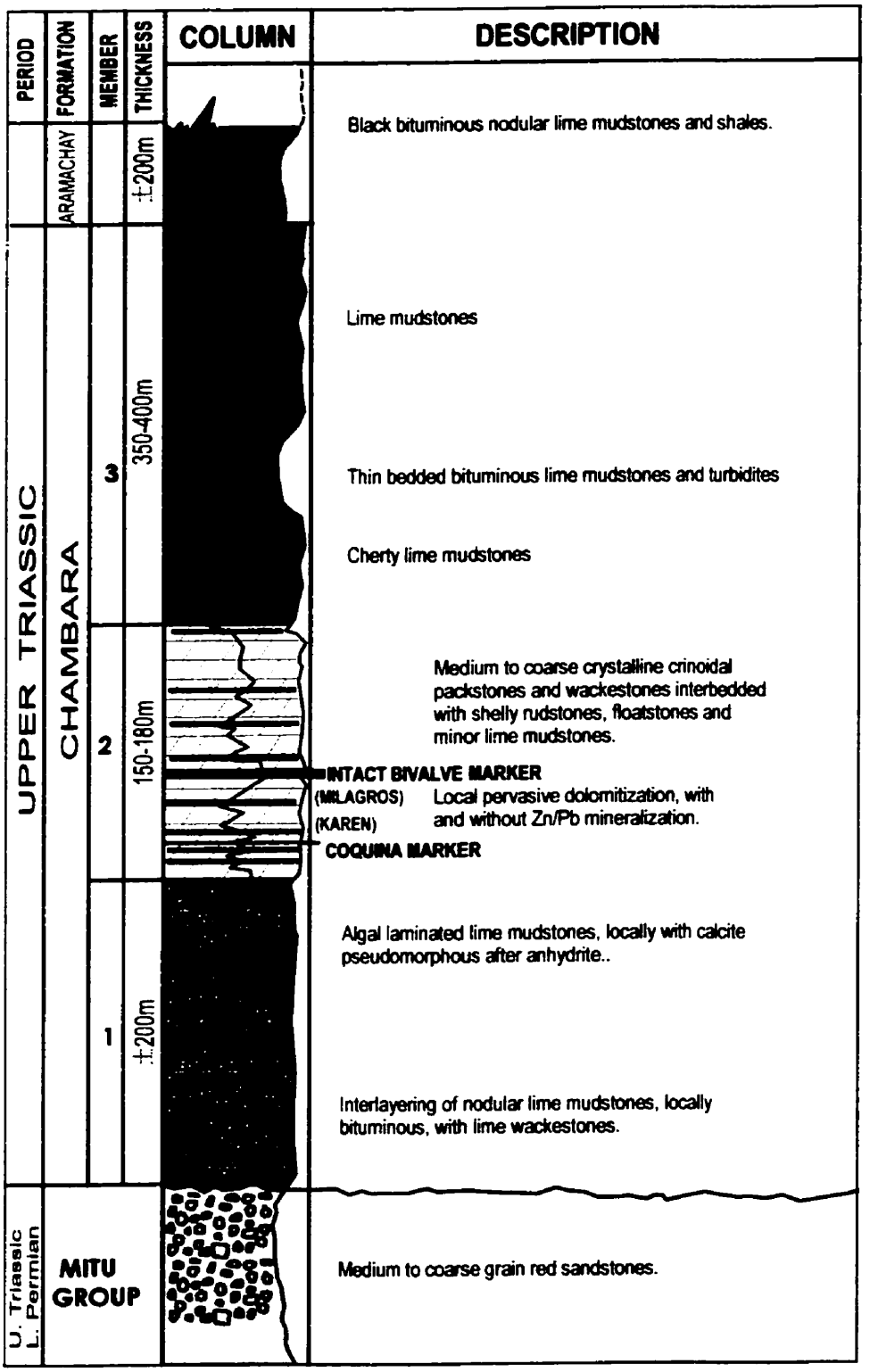

Figure 2.7 Stratigraphy of Florida Canyon showing the position of mineralized horizons within the Chambara 2.

The other area of significant mineralization studied by the author was at Floricita where sulphides occur at a pronounced unconformity between the Condorsinga member of the Pucara and Cretaceous Goyllarizquisga sandstones. The Condorsinga thins from 100 to 50 meters from south to north across the occurrence, but this may be a sloping erosional surface or a result of pre-Goyllarizquisga faulting. Major faults are oriented east-west through the deposit and there seems to be a very strong element of structural control to the mineralization. The relative contribution of active early Cretaceous dissolution to ore controls may be minor. Down-dropping of a significant volume of Goyllarizquisga into the Condorsinga appears to have been accomplished by large-scale structures and brittle fracturing of the Goyllarizquisga sandstones and the Condorsinga carbonates (Allen, 1997).

Mineralization is composed almost exclusively of sphalerite and white dolomite spar in subequal proportions, as open-space filling and rock fragment replacement within a large dissolution collapse system (Plate 2.6). Mineralization has a vertical extent of approximately 100 meters along a 100 to 150 m. strike extent of crudely east-west orientated structures. Sulphides extend approximately 40 m. up into the Goyllarizquisga and 60 m down into the Condorsinga. Neither the Goyllarizquisga sandstones nor Goyllarizquisga clasts are found below the unconformity surface, suggesting that there was no significant solution collapse to the system. As the primary lithology of the Condorsinga is a dolomicrite rather than a lime micrite, the opportunity for significant late solution activity was diminished (Allen, 1997). Virtually all of the mineralization in the Goyllarizquisga comprises brittle veining of dolomite and sphalerite with parallel vein walls and little or no fragment rotation or solution rounding. Over the maximum 30 m. (vertical) range of mineralization in the Goyllarizquisga, the maximum open fracture space, which was generated, is perhaps 10-15%. Within the Condorsinga, base metal sulphides make up approximately 50% parallel walled "stockwork" or crackle, fracture, vein mineralization with no solution enhancement and 50% stockwork of unrotated precursor dolomicrites with very modest solution enhancement and rounding (Plate 2.7). According to Allen (1997) the ground preparation or open space creation was largely structural expansion through faulting and only modest solution enlargement. There are portions along major bounding structures where increased solution activity is observed; hence, dolomite and sphalerite increases (Allen, 1997).

Throughout the rest of the study area a number of other zinc-lead base metal occurrences have been reported and documented. The majority of these are small in size with only low-grade disseminated sphalerite and galena with or without pyrite, or local high-grade veins of sphalerite

Plate 2.6 - Open-space infill by coarse-grained black to dark-red sphalerite, with local fragment replacement in Condorsinga Formation dolomicrites of the upper Floricita adit.

Plate 2.7 - Mineralization comprised almost exclusively of sphalerite and white dolomite spar as open space filling and rock fragment replacement within large dissolution collapse systems at Floricita.

that as of yet have not been related to a larger expanse of mineralization. The distribution of these showings is as variable as the mineralization observed at each. Most occur variably within the stratigraphic sequence and do not seem confined to any one lithotype or stratigraphic or structural setting. Of importance is the fact that all of these regional mineralized occurrences are structurally controlled and are associated with some form of early ground preparation or dolomitization.

The following model was proposed by to account for the mineralization in the Bongara region. An early magnesium-rich fluid event, likely generated by basinal dewatering, leaching and tectonic expulsion, moved fluids through a basinal aquifer, probably the underlying Mitu red beds. Ultimately the fluids ascended through predominant northeast structures. Early dolomitizing fluids caused local dissolution and collapse of the middle Chambara Formation allowing for a lateral fluid movement within the high-energy lithofacies adjacent to the main structures. This ground preparation, replacement, dissolution and porosity increase may have been the initial fluid event or may have exploited existing zones of dissolution formed by earlier meteoric fluid flow through the sequence. With continued basinal dewatering, zinc saturated fluids ascended semi-vertical structures and followed paths of least resistance to the middle Chambara Formation where zinc and lead mineralization occured as the fluids came into contact with a reductant, most likely intraformational H_2S (Fig.2.8)

With continued fluid expulsion, a second coarse white dolospar phase was emplaced and the fluid system began to wane. Pyrite, sphalerite and later silica and calcite were deposited throughout the volume of dolomitized and mineralized rock as the hydrothermal system slowly cooled and choked itself off, or otherwise ceased to function.

Of importance to this study is the fact that all the fluid movement associated with the mineralizing system is structurally controlled. An appropriately porous horizon was capped by an aquitard such as the upper Chambara or Aramachay Formations, which could act as a significant seal to ascending fluids. In places like Floricita and Maino, though pervasive dolomitization is observed, and at Floricita significant mineralization has been discovered, the fact that no overlying aquitard was in place at the time of mineralization probably allowed ascending fluids to dissipate in the Cretaceous Goyllarizquisga Formation.

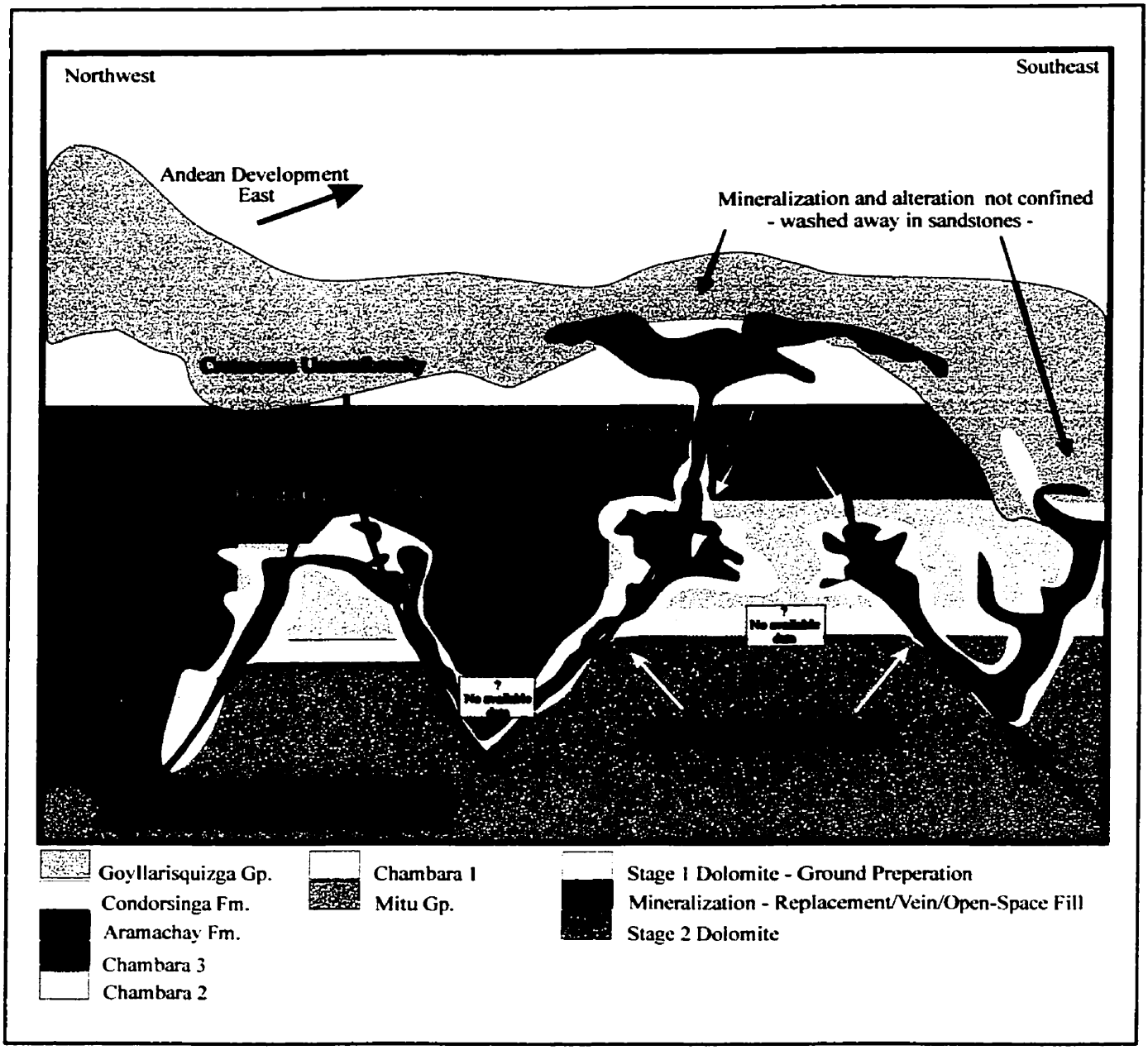

Figure 2.8 Schematic model for carbonate-hosted mineralization observed across the Utcubamba Valley. No attempt has been made to distinguish between textures of mineralization. Not to scale.

2.6 Paragenesis

The paragenetic sequence recorded in the Pucara Group carbonates includes early burial and compaction-related carbonate cements, and later diagenetic/epigenetic premineralization replacement and post-mineralization zoned sparry dolomite and calcite (Fig.2.9). This work will focus on the differentiation of later dolomite phases temporally associated with pre-and post-mineralization based predominantly on plane-light and cathodoluminescent (CL) characteristics. The stable isotope geochemistry of the dolomite will be discussed later, in section (2.7). All diagenetic processes observed in the Pucara Group occurred during the post-depositional history of the carbonates. All carbonates within the study area were deposited originally as limestones.

The subdivision of shallow burial diagenesis and intermediate-to-deep burial diagenesis used in this work is as suggested by Choquette and James (Fig.2.10)(1990). Shallow burial diagenesis comprises all the processes that occur immediately after the sedimentation on the submarine floor, in the meteoric environment, and up to a few tens of meters of burial. Intermediate-to-deep burial diagenesis occurs from a few tens of meters of burial up to the realm of low-grade metamorphism. There are not certain limits for these diagenetic fields, as they vary from one sedimentary basin to another or even within a single basin. The factors which influenced these limits are changes in hydrology, pore-water chemistry, pressure, temperature, and burial beneath younger strata (Choquette and Pray, 1970; James and Choquette, 1984; Choquette and James, 1990).

Early diagenetic phases include processes such as micritization and submarine cementation, chert formation and possible dissolution associated with shallow burial diagenetic environments. Intermediate-to-deep burial diagenetic processes occur later and include typical compaction features such as burial calcite cement and neomorphism and local pressure-solution features and veinlets (James and Choquette, 1990).

Late diagenetic/epigenetic phases include dolomite associated with early pre-mineralization ground preparation, and post-mineralization zoned sparry white saddle dolomites and calcites that post-date all carbonate dissolution. Precipitation of regionally developed, late diagenetic carbonates appears to be confined to the development of significant secondary porosity, well-developed dissolution, tectonic faults, fractures and breccias. Thus, late-diagenetic/epigenetic

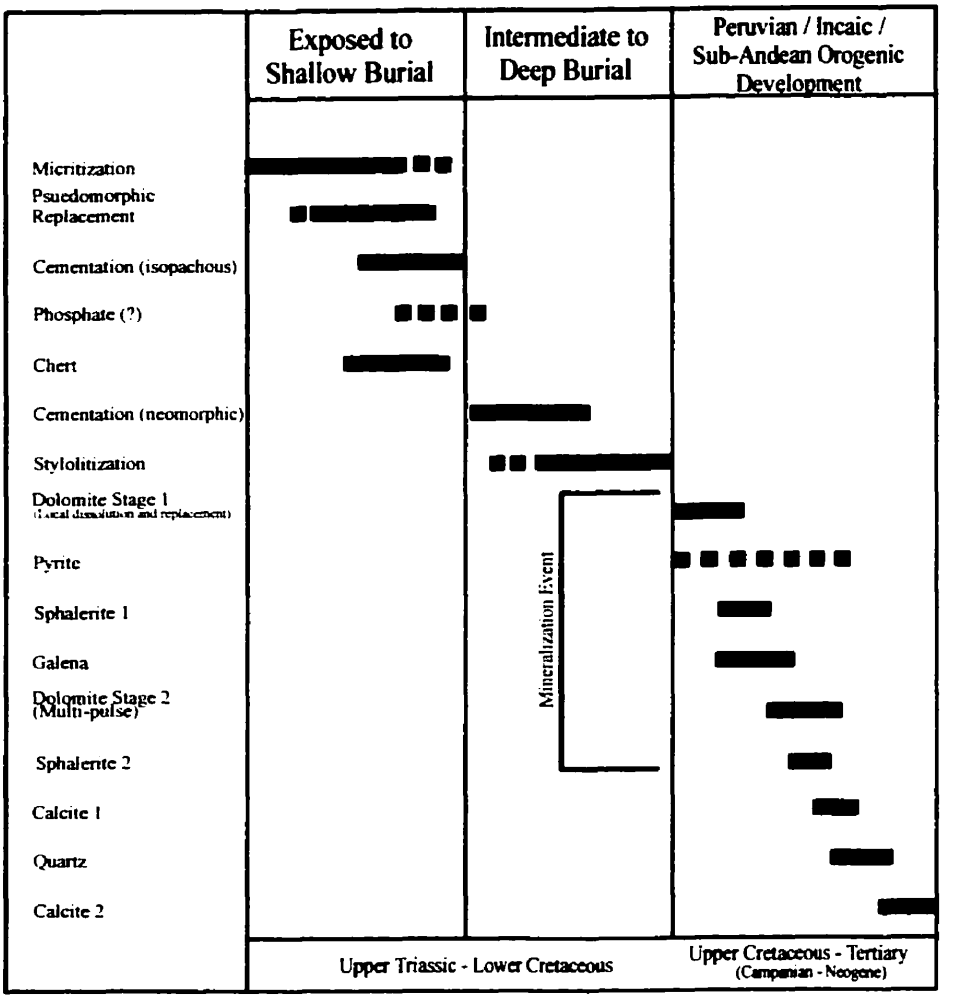

Figure 2.9 Paragenetic relationships observed in Pucara Group carbonates of the Utcubamba Valley.

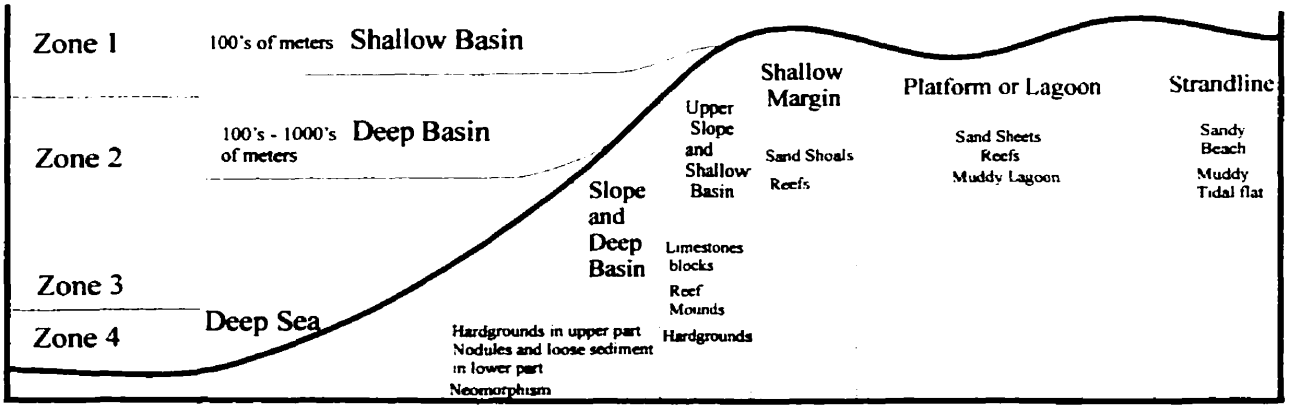

Figure 2.10 The locations of sea-floor precipitation and neomorphism on a shallow carbonate platform and in adjacent deep-water settings. Modified from James and Choquette, 1990.

carbonate alteration provides a spatial and temporal framework in which to interpret regional diagenetic events and their paragenetic relation to MVT-style zinc-lead mineralization.

2.6.1 Early Diagenetic Phases

A variety of early marine diagenetic processes were observed in the studied Pucara sample suite. They correspond with zone I of James and Choquette (1990), and include micritization, cementation and chertification. Micritization was best-observed in the algal laminated lithofacies of the Chambara 1 Formation in Florida Canyon and in the fine-grained micrites of the lower Condorsinga Formation in the Floricita area. Oolitic wackestones and packstones of the Chambara 2 in the Maino area show micritization of the original carbonate, that was in turn replaced by late-diagenetic dolomites (Reid, 2001). The light colouration of the algal mats can be attributed to the digestion of the original organic matter by bacteria. The micritization of ooids (Plate 2.8) can be attributed to encrusting algal perforation (boring endolithic microorganisms; such as algae, cyano bacteria, and fungi). The individual borings, that are only a few microns long, become filled with micritic cement when they were vacated (Margolis and Rex, 1971; Budd and Perkins, 1980; Greensmith, 1989; Tucker and Wright, 1990; Rosas, 1994). The micritization observed within the study area correlates well with observations by Rosas (1994) in her large-scale study of the southern Pucara in Peru.

Rosas (1994) observed finely-to-very-finely crystalline dolomite as well as displacive gypsum crystals and anhydrite nodules in supratidal breccias, mudstones, biomicrites, peloidal packstones, grapestones and oolitic grainstones of the southern Pucara. In this work the author has not identified any early-diagenetic dolomite precipitation within the studied Pucara carbonates, though speculation remains in the lower Chambara 1 of the Maino area. However, gypsum and calcite psuedomorphs are observed replacing inferred anhydrite or evaporite pseudomorphs deposited within algal-laminated and micritized Chambara 1 and lower Condorsinga formations in the Florida Canyon, Floricita, Maino and Buenos Aries sections (Tucker and Wright, 1990; Rosas, 1994). All dolomitization can be attributed to late diagenetic alteration associated with the mineralization process (discussed below).

Early diagenetic cements were observed in unmineralized and altered lithologies of Chambara 2 in Florida Canyon, and in indivisible Chambara carbonates of the Buenos Aires section. The

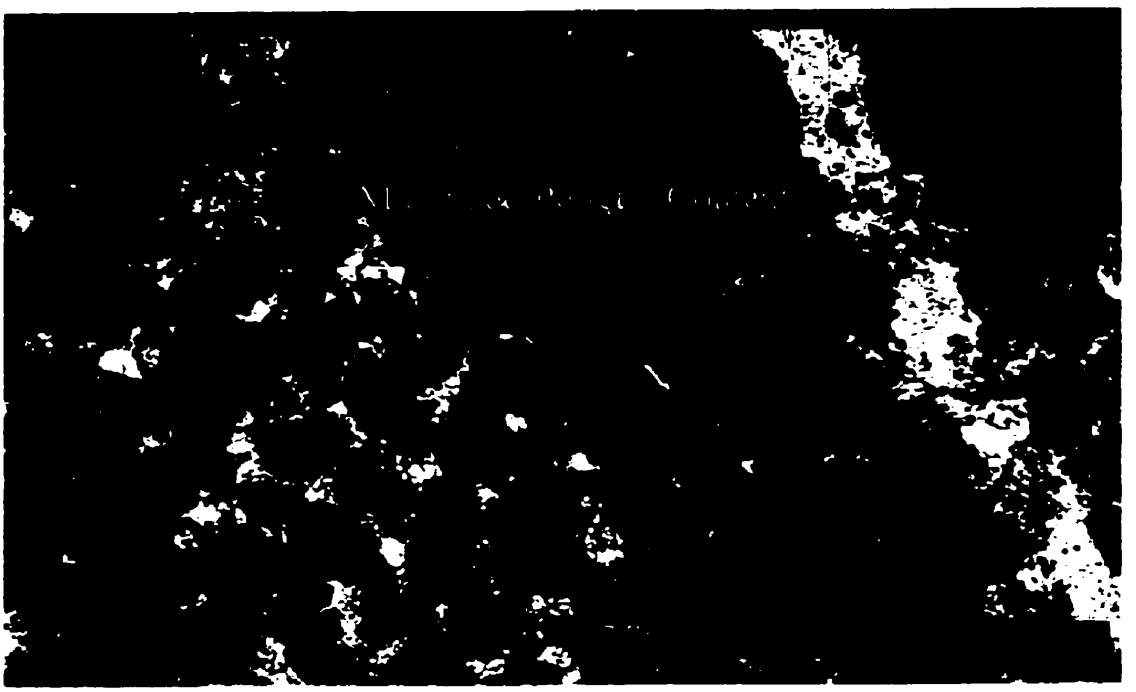

Plate 2.8 - Micritization of ooids by encrusting algae perforation, in shallow water facies of Chambara 1 equivalent lithofacies from the Maino area.

Plate 2.9 - Medium-grained calcite spar interpreted to be a intermediate burial diagenetic process. Observed here infilling available porosity within a micritic lime wacke-packstone of Chambara 2 equivalent lithofacies from the Maino area.

best examples were observed in carbonates deposited in relatively high-energy environments with substantial original porosity such as wackestones, packstones and, in Florida Canyon, local rudstones. The submarine cements include isopachous fringes of calcite around bioclasts, pelletal constituents, or coating fenestral pore spaces. As suggested by Rosas (1994), due to the isopachous-morphology of this cement it can be assumed that an original composition of aragonite or Mg-calcite precipitated as crusts in the sea-floor environment. Tucker and Hollingworth (1986) describe such cements for the Permian Reef Complex of Northeast England. Generally, the calcite cement is dull-to-faint yellow luminescent and easily distinguishable from typical surrounding limestone carbonate fabrics.

Not studied by the author, but well-documented by Loughman and Hallam (1982) and Loughman (1984), in the Aramachay Formation, is a phosphate content of up to 8.6 wt. %. Rosas (1984) has also observed phosphate in the southern Pucara. Phosphate is described as occurring mainly as secondary minerals, replacing allochems – mainly bioclasts. This replacement is assumed to correlate with early diagenetic processes. Although the internal structure of the bioclasts is normally not preserved, the outer shape of the bioclasts is better preserved when they are phosphatized than when they have suffered recrystallization or burial diagenetic replacement by calcite or dolomite.

Scattered chert nodules are a typical field characteristic of the Chambara Formation in all of the studied areas, especially pervasive in middle Chambara 2 and locally in Chambara 3. Chert nodules are variable in size (locally 5-10 cm.) and are usually observed concordant to bedding planes as dark grey to black, ovoid masses, rarely accounting for more than 2 to 3 % of total rock volume. Rosas (1994) observed chalcedony and probable quartzine in evaporite pseudomorphs as well as a predominance of microquartz. In the study area most of the chert is microquartz with no true chalcedony being observed. In Florida Canyon, quartz is observed as megacrystic intergranular cements locally within porous grainstones of the Chambara 2. Additional chert nodules have been observed sporadically throughout the lower Aramachay Formation in Buenos Aires and in the lower Condorsinga of the Floricita area. Late silicification appears to be locally confined to dominant structures and lacks stratigraphic continuity, suggesting that intergranular silicification, unlike chert formation, is a later diagenetic or epigenetic event and not associated with chert microquartz formation.

Most studies of Phanerozoic occurrences suggest an ultimately biogenic origin for chert (e.g. Meyers, 1977; Geeslin and Chafetz, 1982; DeCelles and Gutschick, 1983; Bustillo and Ruiz Ortiz, 1987; Coniglio, 1987; Rosas, 1994). Siliceous sponge spicules have been identified within the Chambara 2, Aramachay, and Condorsinga Fm.'s and likely acted as the main silica source. Rosas (1994) suggests than an additional source for the chert could be the alteration of volcanic glass from pyroclastic rocks intercalated with the sediments in southern Peru. Due to the lack of any volcanics in the study area, this is not an option for this study.

The only intermediate to possibly deep diagenetic process observed is the formation of intergranular calcite spar and the presence of fine-grained neomorphic calcite, interpreted to be a process from an intermediate diagenetic environment (James and Choquette, 1990). In samples studied away from alteration associated with mineralization, calcite spar is observed between allochems in some coarse-grained, porous lithofacies of the Chambara 2 Formation. Usually the calcite spar is medium-to-fine grained and is interpreted to be a neomorphism from micritic calcite (Plate 2.9). Other examples of calcite neomorphism are observed in the replacement of bioclast-shells, where neomorphic spar-calcite crystals replace the shell while preserving its microarchitecture (Plate 2.10). Usually, neomorphic calcite cements are dull to non-luminescent, showing very little to no internal crystal zonation. The original sedimentary textures are commonly obliterated, though, as described above, rare examples of preservation exist.

Pressure solution features are well documented throughout the sedimentary record of the Pucara Group. In the study area, stylolites are frequently observed in the supratidal facies of the Chambara 1 and 3, Aramachay, and Condorsinga Formations. These are well documented in Florida Canyon and Maino, and have been observed in Buenos Aires. In all cases they occur parallel to lamination. They can be classified after Wanless (1979) and Choquette and James (1990) as bedding-parallel swarms of stylolites of small amplitude. The stylolite surfaces are often coated by organic matter.

2.6.2 Late Diagenetic Phases and MVT Mineralization

The focus of the carbonate study is on the morphology and cathodoluminescence of dolomite and calcite in late diagenetic stages associated temporally and spatially with MVT-style zinc-lead

Plate 2.10- Replacement of bioclasts by neomorphic spar-calcite crystals while preserving the shells' original microarchitecture. Bright yellow luminescence is indicative of typical spar-calcite, and is easily distinguished from original orange dull-red luminescent grainstones of Chambara 2.

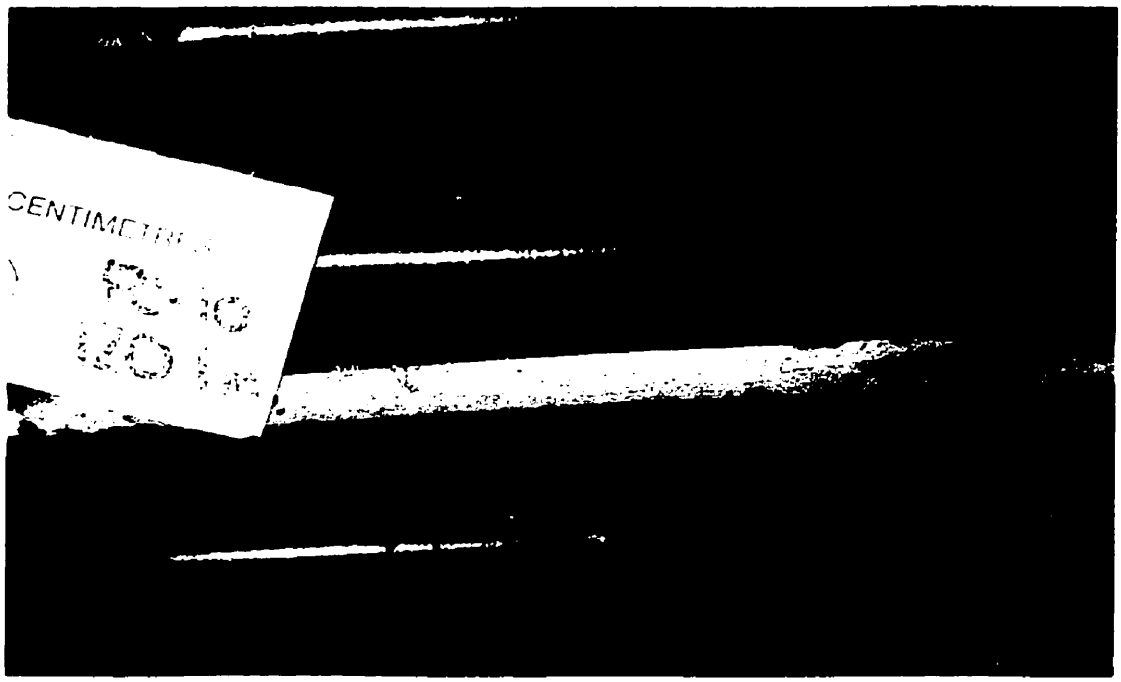

Plate 2.11 - Stage 1 dolomite observed exploiting available open space and porosity in a solution collapse breccia of the Chambara 2 at Florida Canyon.

mineralization observed throughout the Bongara study area. For the most part these cements are confined to the Chambara 2 Formation in the Florida Canyon area and to the Chambara and lower Condorsinga Formation in the Floricita areas. The southern Maino area shows the most stratigraphically and spatially pervasive late carbonate alteration not associated with known significant mineralization. Correlation of late diagenetic/epigenetic processes between areas allows for a regional, basin-wide homogeneity to be inferred. Most of the mineralization and alteration studied away from these three dominant areas are confined to various stratigraphic levels within the Chambara Formation as discussed in Reid (2001).

Late diagenetic alteration and MVT-style zinc-lead mineralization is interpreted to have been derived via basinal fluid dewatering resulting from the compressive tectonic formation of the Andes during either the Peruvian, Incaic, or sub-Andean fold-and-thrust belts. These belts have been dated as occurring between Campanian and Neogene time as a series of nine compressive events (Megard, 1984, 1987; Benavides-Caceres, 1999). Though paragenetic sequences vary slightly from area to area, the general paragenetic sequence as portrayed in figure 2.8 remains consistent. It is as defined by an early dolomite (dolomite Stage 1), followed by pyrite, the dominant zinc event (sphalerite 1), galena, a second dolomite event (dolomite Stage 2), and a second less significant sphalerite pulse. This mineralization event is followed by two calcite events with an intervening quartz/silicification event. Though sedimentary facies that host mineralization are variable throughout the area, diagenetic processes remain texturally and petrographically very similar, suggesting a regional genetic correlation. Cathodoluminescence studies allow for regional comparisons to be made and are suggestive of an interconnected plumbing system responsible for fluid migration to sites of deposition. As figure 2.9 depicts, the development of diagenetic alteration events was not spatially or temporally exclusive, as significant overgrowth of textures can be observed. In places, not all textural overgrowths are observed, though enough evidence has been collected to suggest that the processes are regional in extent.

The initial dolomite replacement event (Stage 1) is thought to have been associated with all early ground preparation, premineralizing carbonate replacement and dissolution in the Bongara region. Stage 1 dolomite is a fine-to-medium grained, subhedral to euhedral dolomite that overprints and replaces original sedimentary structures of the Chambara and Condorsinga Formations. Stage 1 dolomite is observed replacing both intact original depositional features, as

open space porosity infilling and local veining. Replacement involves an insitu substitution of original rock fabric with grain size ranging from less than 0.2 mm. to 5 mm. depending on the original sedimentary texture of the carbonate. It produces a rock whose primary constituents and textures are still recognizable but which is slightly darker and tends to have a variable degree of fine pinpoint (<0.1-1mm) and occasionally finely vuggy (1-5 mm) porosity. The darker colour of this dolomite is likely a result of dark insoluble organic residue components formed during the replacement process (Plate 2.11).

Stage 1 dolomites do not pervasively replace the stratigraphic interval in which they are identified. In Florida Canyon, replacement is most pervasive proximal to major lineaments such as the Sam and Tesoro fault systems (Reid, 2001). Replacement is incomplete and situated in lithofacies of Chambara 2 that have substantial amount of available porosity and local carbonate dissolution. Stage 1 dolomites are characterized by a relatively fine-to-medium-grained mosaic intergrowth of euhedral to subhedral crystals that exhibit a dark-red to dull-red luminescence during cathodoluminescent analysis (Plates 2.12 and 2.13). Commonly these show little to no internal zonation, likely due to the smaller crystal size. Rare crystal zonation is observed where replacement is complete and available porosity is infilled. Early dolomite replacement in Florida Canyon, Floricita, Maino, Charito and Buenos Aires all show a very similar luminescent pattern regionally. During stage 2 dolomitization (discussed below), relict cores of this dolomite phase are preserved and overprinted by later diagenetic events. Dolomitization is not stratigraphically exclusive to the Chambara 2 Formation. In the Florida Canyon area local dolomitization is observed in the Chambara 1 algal laminated mudstones and is observed extending through the lower Chambara 3 mudstones, predominantly as thin veins. In Floricita, complete replacement of micritic lime mudstones of the Condorsinga is observed, with local early dolomitization also within vertical structures acting as hydrothermal fluid feeders for the mineralization in the area.

Stage 1 dolomite is followed by pyrite precipitation. This sulphide phase is observed variably through the paragenetic sequence suggesting that iron precipitation was concurrent with Stage 1 dolomite and continued through the waning of the main mineralizing system. Pyrite is observed as fine, mm-scale disseminated sulphide grains throughout the Chambara formation in Florida Canyon, as well as massive, replacement, iron sulphide rock locally within the main Sam Fault structure. Zinc mineralization has no identifiable spatial association with pyrite and has been observed with or without an iron sulphide component.

Plate 2.12- Open space infill by both coarse-grained euhedral Stage 1dolomite (dark-red luminescence) and euhedral calcite spar (bright-yellow luminescence) showing beautiful crystal zonations.

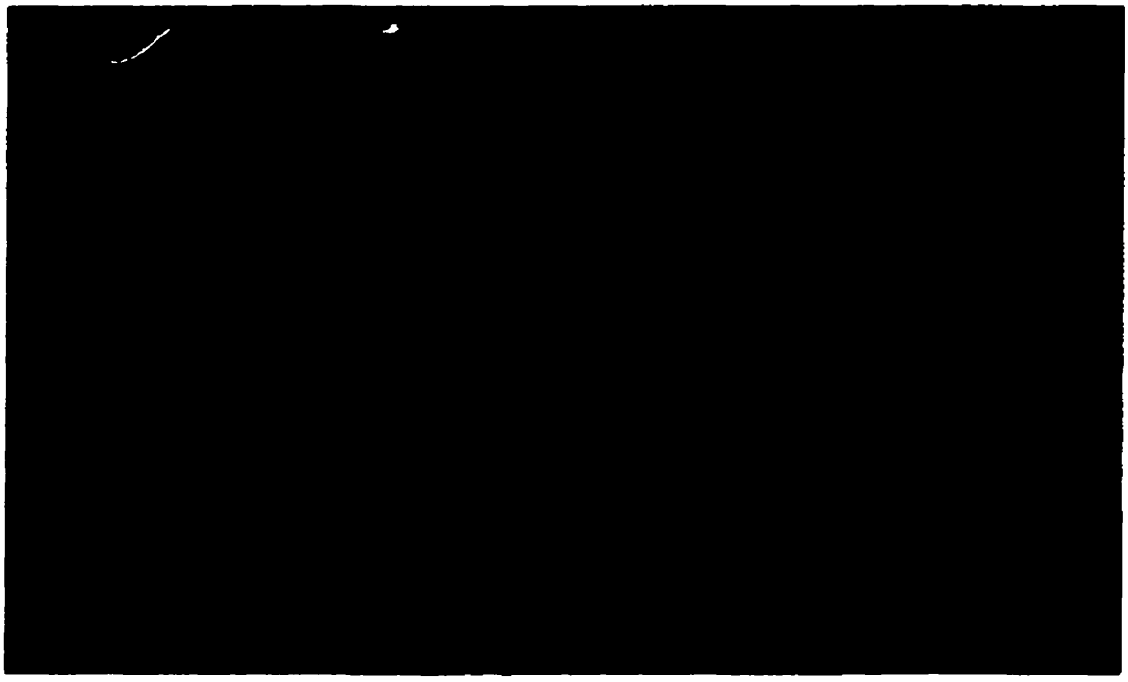

Plate 2.13 - Complete replacement of original micritic limestone by fine-grained, red-to-dull-red Stage 1 dolomite in the Condorsinga Formation of Floricita. Stage 1 dolomite is typically very-fine grained and can be observed replacing various lithofacies independent of original sedimentary structure and porosity..

Plate 2.14 - Open space infill by both coarse-grained euhedral dolospar and brown-to-reddish sphalerite (Sphalerite Stage 1). Sample was taken from Florida Canyon DDH FC21 at a depth of 161.35 meters.

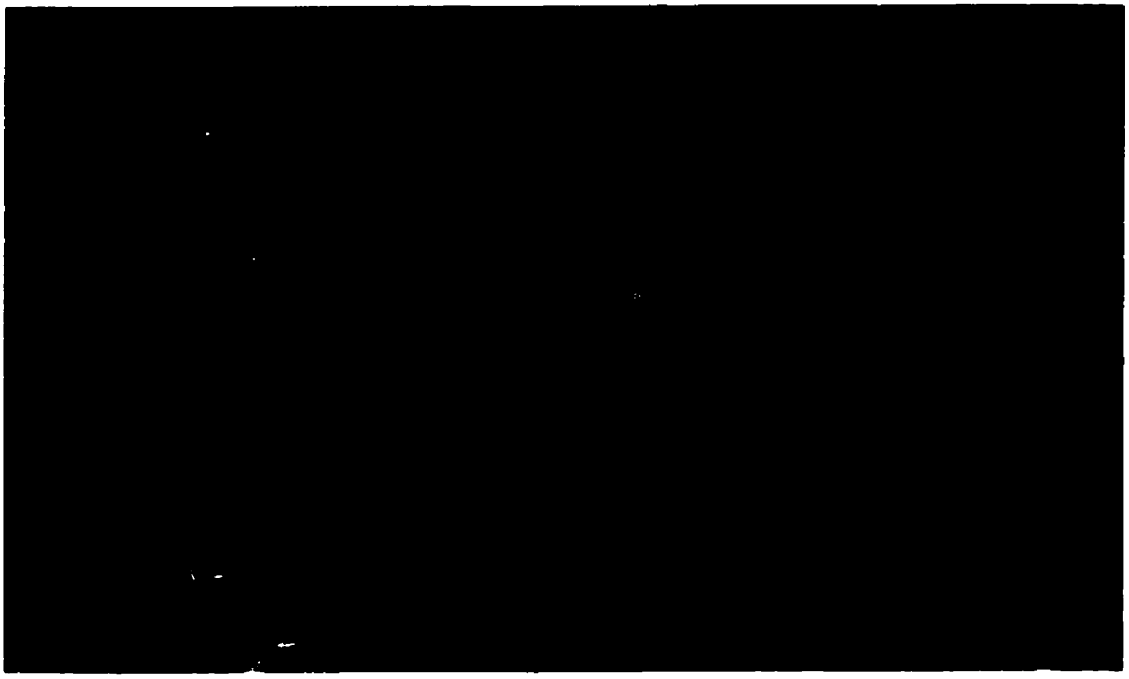

Plate 2.15 - As above: Sphalerite is non-luminescent as black-to-dark brown euhedral crystals. Dolospar infill shows both Stage1 and Stage2. Stage 1, is observed as fine-grained, darker-red luminescent zones within cores of bright-red luminescent Stage 2 dolomites.

Following the initiation of pyrite mineralization, the main zinc phase (sphalerite 1) developed. Zinc mineralization has been identified as bedding and/or small cavity replacements, collapse breccia hosted, minor zinc in veins and minor zinc in vein, crackle and mosaic breccias throughout the Florida Canyon area, and as parallel-walled "stockwork", crackle, fracture and vein mineralization in the Floricita area. This phase consists of dark-red-to-brown sphalerite. Sphalerite is observed as coarse euhedral to fine grained aggregates varying in size from mm. to cm scale, locally showing colloformal zonation, and /or massive coarse grained mosaics of open crystal infilling (Plates 2.14 and 2.15). For a complete description of mineralization the reader is referred to Reid (2001).

Galena is observed as medium-grained euhedral crystal aggregates intergrown with open space sphalerite mosaics and veining. Rich galena veins are observed cross-cutting sphalerite zones, especially in exposed sulphide-rock occurrences within the walls of Florida Canyon. Galena is also identified as veining and thin stockwork-textured zones within areas spatially associated with significant zinc mineralization. Galena is not commonly observed without a significant zinc association. In Florida Canyon the Irene showing is extremely lead-rich and shows a NE (030°) structural trend that cross-cuts the NW trend of the canyon. This may suggest that galena is controlled by a different structural system than the zinc, though this has not been identified elsewhere.

Initial sphalerite and galena precipitation is followed by Stage 2 dolomitization which is characterized by rocks with greater than five percent coarsely crystalline white dolomite spar observed mottling the original dolomite in an in situ replacive pattern. This texture has been called pseudobrecciation in the MVT literature and is a term commonly used to describe this coarse replacement and vuggy porosity-generating event by sparry-to-saddle white dolomites. Stage 2 dolomite crystals are generally large (mm-cm scale), mottled, showing cannibalistic replacement and open space filling of porous horizons throughout the Pucara carbonates proximal to major lineaments (Plates 2.16 and 2.17). Commonly Stage 2 dolomites will show internal crystal zonation in plain polarized light. A dull orange to bright red luminescence is observed in these dolomites, showing a regional well-defined crystal zonation pattern. Dolomite crystals, associated with replacement Stage 2 dolomites in a relatively fine-grained lithofacies will exhibit a consistent red-to-bright–red luminescence that is constant across the sample, representing complete replacement and pinpoint porosity infill (Plate 2.18). Open-space dolomite infilling shows a well-developed crystal zonation. Commonly 3-5 sub-zones can be

Plate 2.16 - Stage 2 dolomite forming a pseudobreccia texture within Chambara 2 lithofacies in the Maino area. Most of the original sedimentary features have been completely obliterated. Replacement appears to follow bedding.

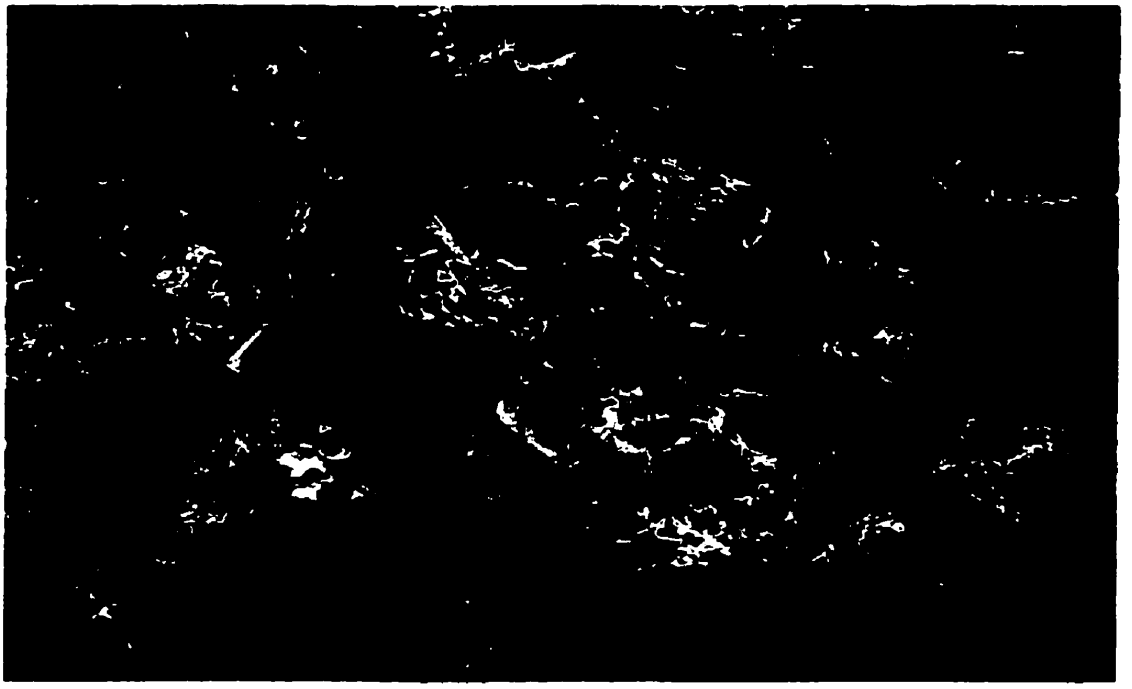

Plate 2.17 - Stage 2 dolomite forming a pseudobreccia texture within Chambara 2 lithofacies in the Maino area. Most of the original sedimentary features have been completely obliterated. Open vuggy porosity is a result of recent oxidation of calcite cores and erosion.

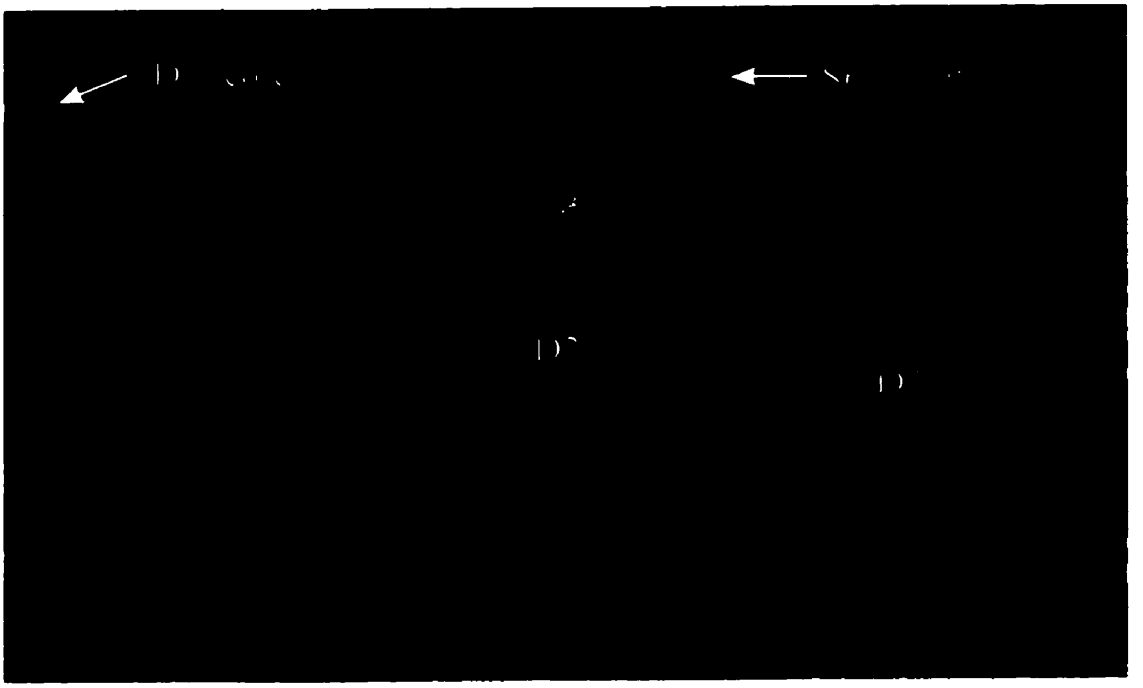

Plate 2.18 - Replacement of fine-grained mud-wackestone fragments within a dissolution breccia from the Nancy Showing of Florida Canyon. Brighter-red luminescent D2 can be distinguished from dark-red to blackish luminescent D1 cores.

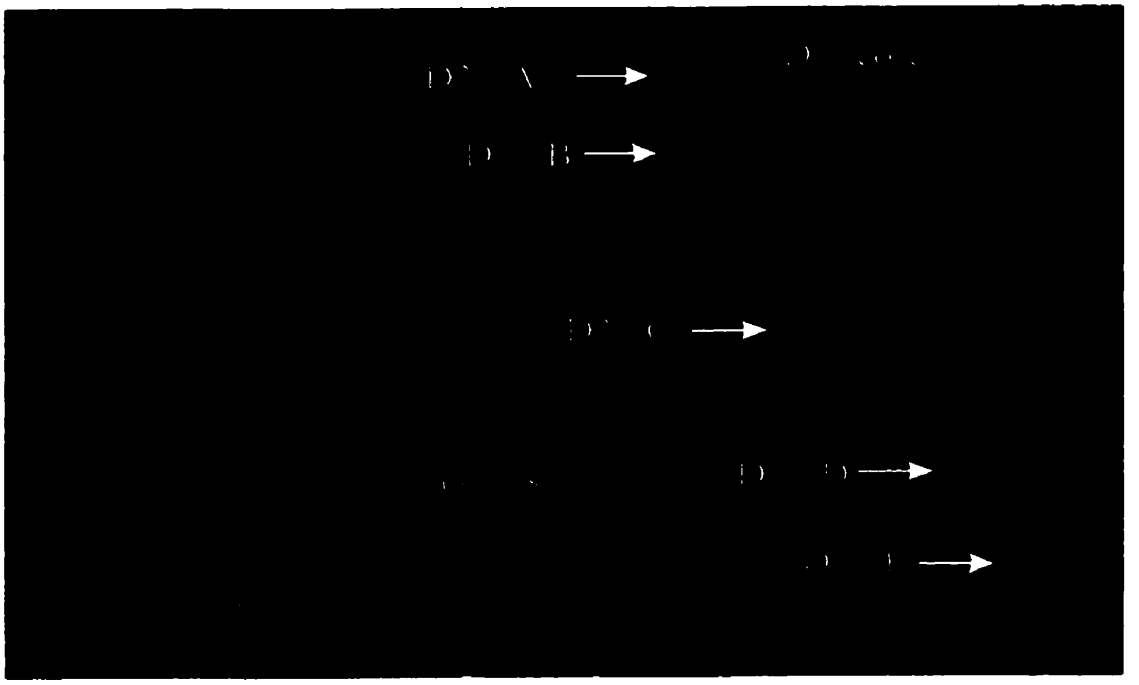

Plate 2.19 - Very-coarse grained open-space fill by Stage D2 dolomite. D2 dolomite crystals appear nucleated on preexisting D1 cores. D2 dolomite shows stages A through E.

identified (Stage 2A-2E) and represent the prolonged open space precipitation of the mineral. Commonly dark red to black/brown cores of Stage 1 dolomite are preserved within the central crystal core and represent the initial point of nucleation (Plates 2.19 and 2.20). Late dolomite precipitation is correlatable regionally from area to area, based upon the consistent luminescent patterns of the crystals, and the internal zonation hierarchy observed.

Sphalerite 2 is subordinate to Sphalerite 1 and is commonly identified as small mm.-scale sulphide aggregates of light-brown to yellow sphalerite associated with late open space infilling, veining, rare dissemination, and secondary replacement of coarser sphalerite 1 proximal to major structures in Florida Canyon. Most Sphalerite 2 is associated with fine-grained, non-porous, algally laminated mudstones of the Chambara and upper Chambara 3 basinal mudstones, as fine veins and radiating sulphide networks along small dissolution and breccia zones. To date this sphalerite phase does not account for any significant mineralization in the district. The paragenetic sequences from initial dolomite Stage 1 through to Sphalerite 2 accounts for the fluid or fluid systems responsible for the main mineralization event in the area.

These stages are followed by two calcite phases (calcite 1 and 2). Calcite 1 is commonly associated with dolomite, whereas the second calcite fills residual pores and veins, or replaces other minerals. Calcite 1 commonly shows a dull-to-slightly luminescent, non-zoned yellow cathodoluminescence (Plate 2.21), usually as pervasive replacement of the rock. Clacite 1 can be distinguished from the original limestones, as the host carbonates commonly show a dull orange to dull yellow brown luminescence that is easily identifiable when in contact with Calcite 1 (Plate 2.22). Calcite 2 has a bright-to-very-bright luminescence, commonly with internal zonations suggesting the fluid had significant time to develop advanced crystallinity. Both calcite phases have been identified regionally and are suggestive of a regional diagenetic alteration pattern. Late diagenetic calcite appears not to be confined to major structural zones, or confined to preferential lithofacies. Calcite 1 and 2 can be identified in all lithofacies of all formations spatially across the carbonate platform.

During calcite alteration, silicification occurred. This has been observed as pervasive silicification confined to local zones along major structures associated with mineralization and dolomitization, and confined stratigraphically to the Chambara formation in the Florida Canyon area. Though not pervasive, silicification commonly follows an inferred interconnected

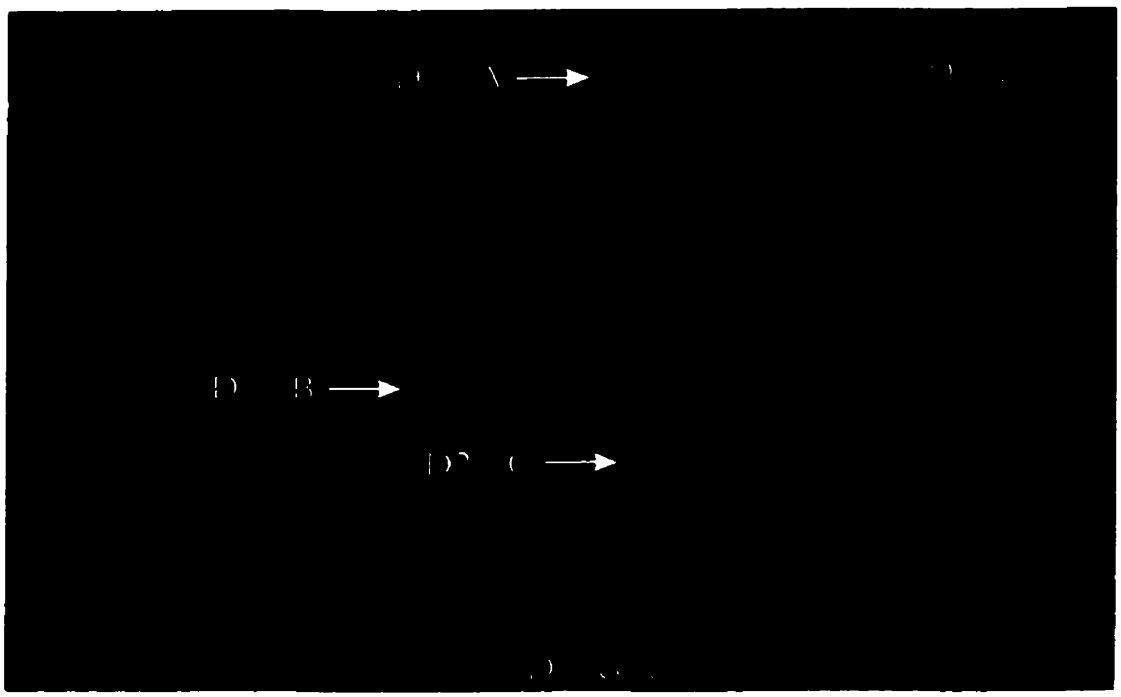

Plate 2.20 - Very coarse- grained open-space fill by Stage D2 dolomite. D2 dolomite crystals appear nucleated on preexisting D1 cores. Sample shows D2 stages A through C.

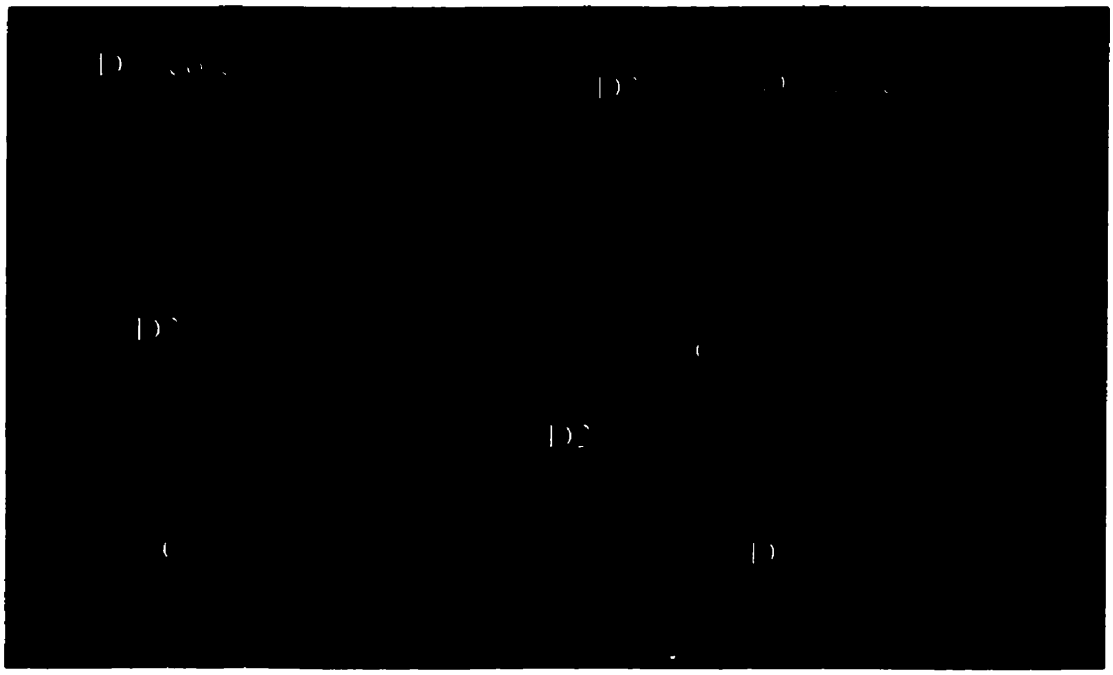

Plate 2.21- Dull-to-slightly luminescent yellow C1 calcite commonly observed, as fine-grained replacement of host lithologies to massive non-zoned, open-space crystal infill.

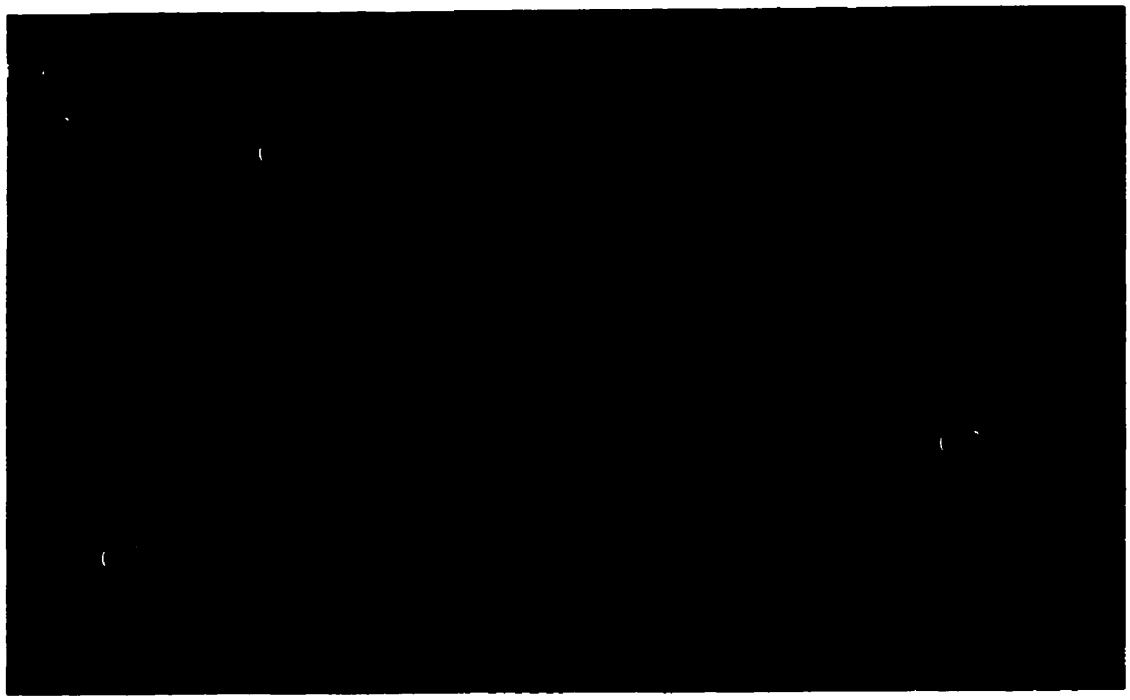

Plate 2.22- Very coarse-grained open-space infill of C2 calcite. C2 calcite can be distinguished from C1 by the presence of beautiful internal crystal zonations and a much brighter yellow luminescence.

dissolution path confined to major faults, and regional structures, through porous horizons ranging from cm. to m. intervals in thickness. Minor silicification has been studied in Maino and locally in Floricita, Buenos Aires and Naranjitos. The author believes that observed silicification is more an indication of open, structural, controlled fluid flow through the basin, than representing a genetic link to mineralization for use as a pathfinder by exploration companies as it is not consistently associated with mineralization, and has been identified in strata devoid of alteration.

2.7 Stable Carbonate Isotope Geochemistry

Stable isotope studies of carbonates from Mississippi Valley-Type (MVT) deposits can provide valuable information on sources of the mineralizing solutions, temperature of the mineralization, and fluid pathways (e.g. Hannah and Stein, 1984; Haefner et al., 1988; Gregg and Shelton, 1989; Nesbitt and Muehlenbachs, 1994). Furthermore, they may put physicochemical constraints on the mechanism of precipitation of ore and gangue carbonates, chemical evolution of the mineralizing fluids, and on fluid-mixing and fluid-rock interaction processes (Sverjensky, 1981; Gregg, 1985; Frank and Lohmann, 1986; Gregg and Shelton, 1989; Banner et al., 1989; Ghazban et al., 1991; Far, 1992; Qing and Mountjoy, 1992; Garvin and Ludvigson, 1993; Spangenberg, 1995). The $\delta^{13}C$ and $\delta^{18}O$ values of Stage 1 and 2 dolomites and calcites associated with mineralization in the Bongara district show a strong regional homogeneity. These results, coupled with strong mineralogical and petrographic similarities of mineralization and alteration phases regionally, perhaps reflect the fact that the mineralizing processes were similar for Florida Canyon, Floricita, and the other zinc occurrences district wide, as well suggesting the existence of a common regional mineralizing hydrothermal system with interconnected structurally controlled plumbing. Work by Spangenberg (1995) on this subject in the San Vicente belt 300 kms to the south studies this question in great detail. Spangenberg's study takes the use of regional isotopic studies beyond the scope of this author's work. A close correlation exists between the analyzed data from the Bongara area and the results obtained by Spangenberg. The focus of this work is to determine whether an interconnected plumbing system can be assumed for the Bongara area, and whether a regional correlation can be attributed and used in future exploration of the district.

Samples were divided based upon the above paragenetic division of Dolomite stages 1 and 2 (D1 and D2), and calcite stages 1 and 2 (C1 and C2) (Fig.2.9). Different carbonate generations were selected after detailed hand-sample and petrographic analysis. The mineralogical composition of

the sample set was determined using X-ray powder diffractometry (Appendix 3). Isotopic analysis was conducted at the Environmental Isotope Lab at the University of Waterloo using standard mass spectrometry for carbonates following the conventional method by McCrea (1950).

The carbon and oxygen isotope ranges determined in the D1, D2, C1, C2 and Pucara carbonates are given in Appendix 4. Obtained values closely compare with values from similar paragenetic phases obtained by Spangenberg (1995). The $\delta^{13}C$ and $\delta^{18}O$ values of D1 ($\delta^{13}C$ =-3.9 to 1.85 $^{0}/_{00}$; $\delta^{18}O$ = -11.6 to -2.94 $^{0}/_{00}$) and D2 ($\delta^{13}C$ =-1.7 to 1.35 $^{0}/_{00}$; $\delta^{18}O$ = -12.25 to -7.15 $^{0}/_{00}$) vary within a close range across the district. At a local scale the two main dolomite generations (D1 and D2) are isotopically very similar with certain D1 samples showing slightly heavier $\delta^{13}C$ and $\delta^{18}O$ values (Fig.2.11 and 2.12). The $\delta^{13}C$ and $\delta^{18}O$ values from twelve samples of late filling calcite (C1 and C2) have scattered values from -9.92 to 1.03 $^{0}/_{00}$ $\delta^{13}C$ and -13.53 to -6.32 $^{0}/_{00}$ $\delta^{18}O$, respectively. The carbonate generations show a general tendency towards lighter isotopic compositions with advancing paragenetic stage. The regional homogeneity of the isotopic composition of the altered gangue dolomites suggests that the physicochemical conditions and the fluid-rock interaction processes were uniform and almost constant during gangue precipitation.

At San Vicente, Spangenberg (1995) states that the deposit displays a general tendency toward lighter isotopic compositions in the following sequence: dark replacement dolomite – white sparry dolomite – late filling dolomite – late filling calcite – carbonates replacing evaporitic sulfates. This trend conforms with previous C and O isotopic studies from the San Vicente deposit (Fontbote and Gorawski, 1990) and is similar to those found in studies from other MVT deposits (e.g. Frank and Lohmann, 1986; Ghazban et al., 1990; Farr, 1992; Nesbitt and Muehlenbachs, 1994; Spangenberg, 1995), which report lighter isotopic compositions in paragenetically late carbonates compared to the unaltered host carbonates.

Spangenberg (1995) states that the wide isotopic ranges of the hydrothermal carbonates from San Vicente cannot be due to simple thermally-induced isotopic reequilibrium, which affects the oxygen more than the carbon isotopes. Therefore, simple cooling cannot account for the measured isotopic variations of carbonates at San Vicente, indicating that multiple fluids were involved in their precipitation. This conclusion may hold true for the Bongara district as isotopic patterns from the Bongara district closely follow those of San Vicente and may in fact represent a northern extension of that hydrothermal regime.

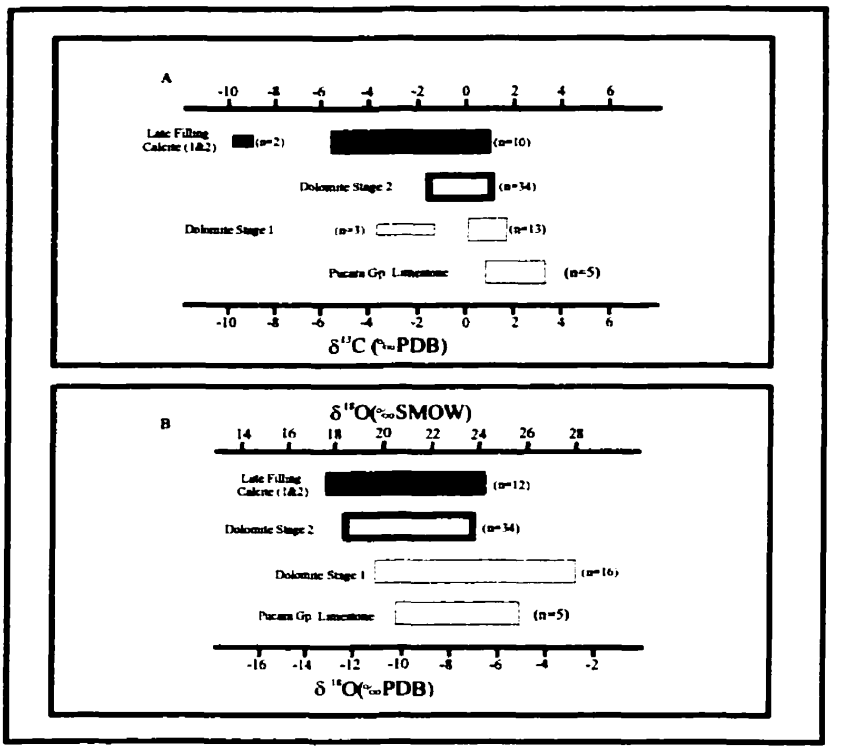

Figure 2.11 Carbon (A) and Oxygen (B) isotope variations of host and gaunge carbonates from the Bongara study area. .

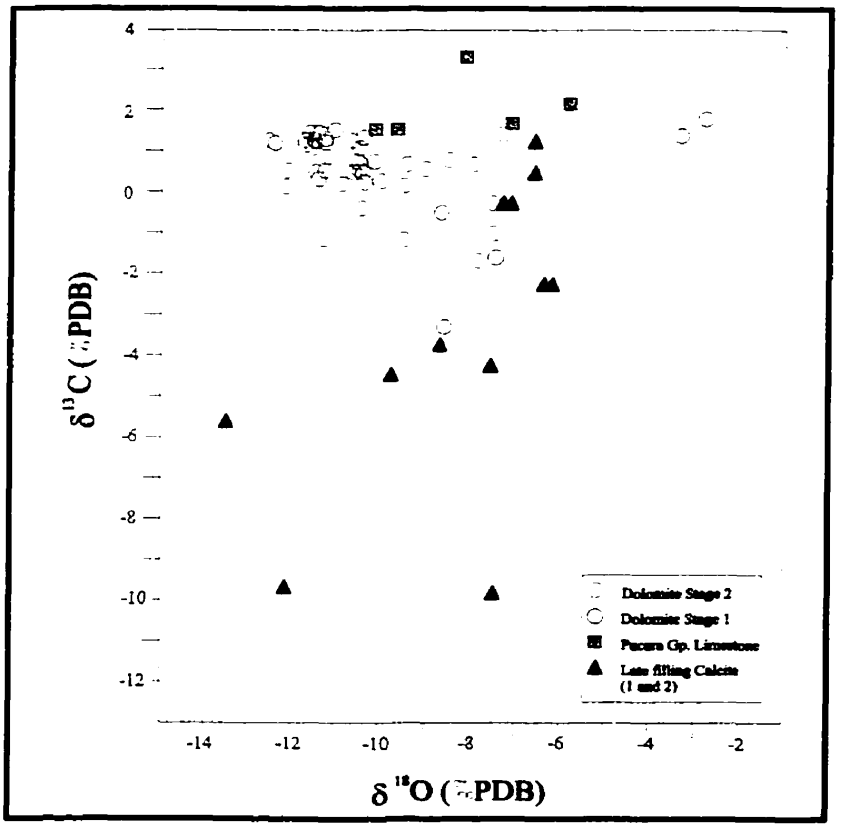

Figure 2.12 $\delta^{18}O$ versus $\delta^{13}C$ of Carbonates from the Bongara Study Area.

The median $\delta^{13}C$ and $\delta^{18}O$ values of gangue carbonate phases of all the samples collected from the district are shown in figure 2.13. Both the altered D1 and D2 display a significant correlation in $\delta^{13}C$ vs. $\delta^{18}O$ space. The D1 represents the heaviest end member, with a general isotopic lightening throughout the D2 and C paragenetic stages. Isotopic compositions of the carbonates of the Bongara district show variation trends which are regionally similar. These variation trends do not have any correlation with the stratigraphic sequence and do not show any zonation at a district scale, (Fig.2.13) suggesting common mineralizing events. It was concluded that ore and hydrothermal carbonates in the San Vicente district were precipitated from fluids of specific isotopic composition by regionally unvarying and stratigraphic independent fluids within a regional mineralizing hydrothermal system with interconnected plumbing. Data correlation with those of Spangenberg's from San Vicente lead the author to postulate that on some large scale the Bongara and San Vicente systems are genetically similar. Further detailed analysis of the Bongara isotopic data may clarify this.

2.8 Summary

The paragenetic sequence preserved within the Pucara Gp. carbonates of the Utcubamba Valley includes early burial and compaction-related carbonate cements, and later diagenetic/epigenetic pre-mineralization and post-mineralization, zoned sparry dolomite and calcite. Early diagenetic phases include processes such as micritization and submarine cementation, chert formation and possible dissolution associated with shallow burial diagenetic environments. Intermediate-to-deep burial diagenetic processes are observed temporally later, and include typical compaction features such as calcite cement and neomorphism and local pressure-solution features and veinlets. All early diagenetic features are regional in distribution and correlatable across the study area, suggesting that basinal processes were, for the most part, homogeneous across the study area.

Late diagenetic/epigenetic phases include dolomite associated with early pre-mineralization ground preparation, and post-mineralization zoned sparry white saddle dolomites and calcites that post-date all carbonate dissolution. Precipitation of regionally developed, late diagenetic carbonates appears to be confined to the development of significant secondary porosity, well-developed dissolution, tectonic faults, fractures and breccias. Detailed cathodoluminescent analysis of the late diagenetic paragenetic sequence show a distinct correlatability with regard to the characteristics of gangue carbonates from both barren and mineralized areas. This feature suggests that carbonate phases precipitated during the mineralizing event in the region are

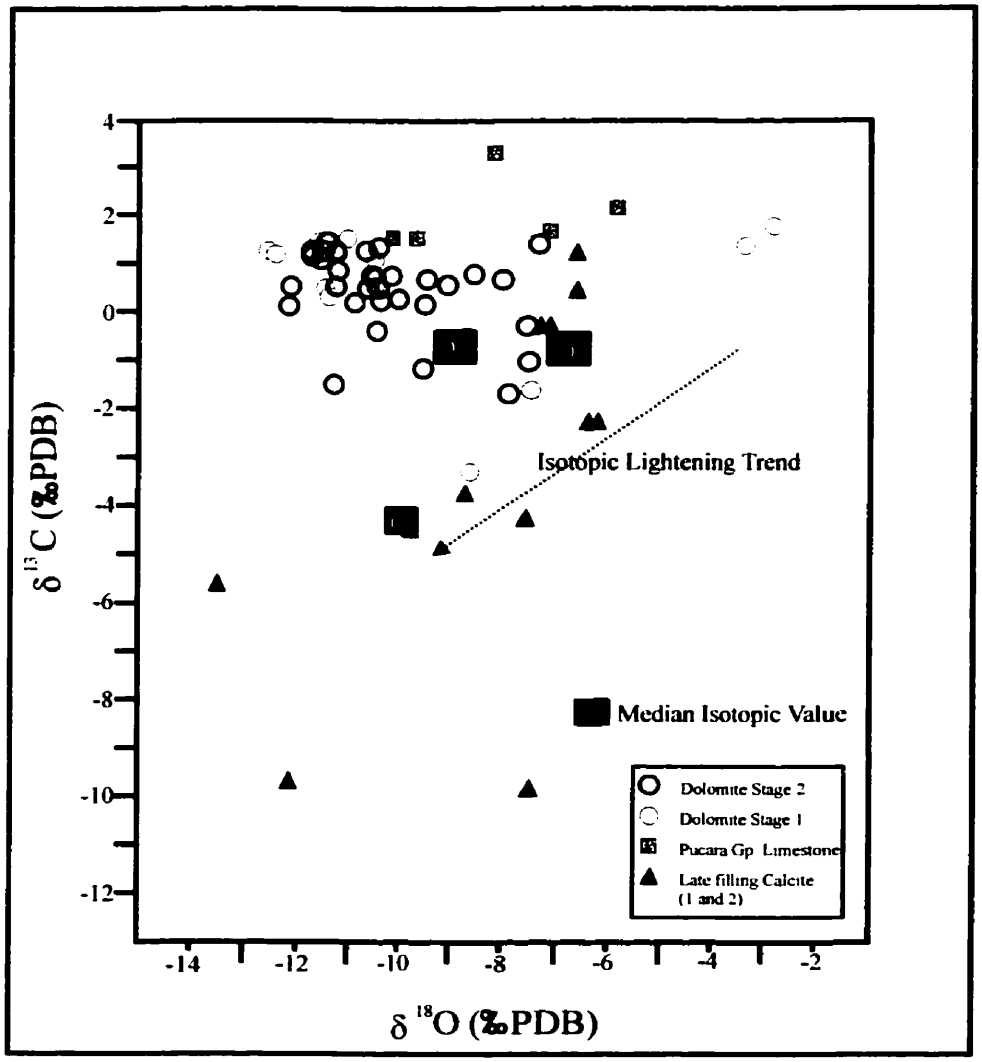

Figure 2.13 $\delta^{18}O$ versus $\delta^{13}C$ of carbonates from the Bongara Study Area, showing median isotopic values.

genetically related, and were transported to the depocenter through a linked structurally controlled plumbing system.The $\delta^{13}C$ and $\delta^{18}O$ values of Stages 1and 2 dolomites and calcites associated with mineralization in the Bongara district show a strong regional homogeneity. These results, coupled with strong mineralogical and petrographic similarities of mineralization and alteration phases regionally, perhaps reflect the fact that the mineralizing processes were similar for Florida Canyon and Floricita, as well as the other zinc occurrences district wide. They also suggest the existence of a common regional mineralizing hydrothermal system with interconnected plumbing.

The carbonate generations show a general tendency towards lighter isotopic compositions with advancing paragenetic stage. The regional homogeneity of the isotopic composition of the altered gangue dolomites suggests that the physicochemical conditions and the fluid-rock interaction processes were uniform and almost constant during gangue precipitation. The $\delta^{13}C$ and $\delta^{18}O$ values obtained from the Bongara region correlate well with published data from the San Vicente deposit in central Peru. The lightening of isotopic compositions through the paragenetic sequence compares well with general trends observed within global MVT districts and adds further support that Bongara represents an emerging MVT district for continued exploration.
Standard petrographic, cathodoluminescent and carbonate isotopic analysis suggest that both early diagenetic and late diagenetic/epigenetic alteration associated with zinc-lead mineralization throughout the Bongara district was emplaced through an interconnected, district-wide, structurally controlled plumbing system. This observation suggests a genetic link between all metal occurrences independent of stratigraphic position.

2.9 Acknowledgments

Cominco and Cominco Peru Ltd. provided complete financial support for this study. The author would like to thank the Department of Geology at the University of Toronto, especially Professors Andrew Miall, Ed Spooner and Geoff Norris for their supervision, guidance and critical review of this work.

This study would not have been possible without the assistance and enthusiasm of Dr. Cameron Allen, Chief Geologist, Cominco Ltd. Wojtek Wodzicki, Manuel Montoya and Lino Rameriz are thanked for their assistance with project development and helping me to gain a better understanding of the geological complexities of the region.

Dereck Rhodes is thanked for his open-idea sharing and frank discussions regarding the geology of the Bongara area, and for his constant interest and enthusiasm for continued exploration within this under-explored district. Dereck's understanding of the MVT deposits and carbonate stratigraphy helped me to develop the scientific layout for this work. Dereck's original nomenclature and classifications used in the exploration process for the region proved remarkably accurate and were used as the starting point for this work.

Nurcahyo Basuki (Uki) is thanked for his insightful reviews, comments, and criticisms throughout the course of this study. John Pearson, Gary Delaney, and Barry Cook are thanked for their constant assistance with personal career decisions, professional development and for adequately preparing me for this undertaking. Barry Cook and David Robertson are thanked for their critical review of this manuscript. Darren Tisdale scanned all of the images within this work. The staff at the University of Waterloo are thanked for their assistance with the isotopic analysis and for providing facilities for me to complete the cathodoluminescence work. Neil O'Brien and the staff at the Cominco Exploration Research Lab are thanked for all of the section preparation and XRD analysis.

Special thanks to my parents and especially to my wife Jodie and daughter Jordan who have provided me with constant support, assistance and a sense of life meaning and purpose.

THESIS CONCLUSIONS

The following summarizes the major scientific findings resulting from this work.

Integrated sedimentological and diagenetic studies of the Pucara Group from barren, altered and mineralized carbonates indicate a complex, multi-phase depositional and mineralizing geological evolution for the Bongara district. Deposition of Chambara Fm. carbonates was controlled by the basinal position of paleo-highs formed within the Utcubamba Corridor along horst-and-graben structures of the underlying Permian Mitu redbeds. Distribution of Chambara 2 high-energy depositional lithofacies was confined to areas of elevated paleo-relief and provides depositional and spatial constraints for the formation of isolated carbonate platforms along the length of the study area.

Mineralization in the Bongara region is generally associated with strong ground preparation observed as pervasive dolomitization, pseudobrecciation, and carbonate dissolution. Three textures of mineralization have been identified and defined as: i) bedding and/or small cavity replacement, ii) collapse breccia hosted and iii) minor zinc in vein, crackle and mosaic breccias in the upper Chambara Formation (Chambara 3). Zinc mineralization consists of dark red to brown sphalerite with lesser dull yellow beige sphalerite locally. Sphalerite is observed as coarse euhedral to fine-grained (mm to cm scale) aggregates and locally colloformal zoned varieties. Lead mineralization is observed as galena, and oxide varieties of both zinc and lead mineralization have been observed in the district. Most commonly zinc and lead sulphides are observed together as an intermeshed mosaic of sulphides, though galena veining has also been identified crosscutting early sphalerite phases. Pyrite is observed throughout the mineralizing sequence ranging from fine mm-scale disseminations to cm-scale massive replacement of the host. Later silicification and calcification is observed towards the waning stages of the mineralizing system.

Comparison with global MVT districts shows that the Bongara area possesses many of the necessary characteristics for classification as a true MVT–type district. The paragenetic sequence preserved within Pucara Group carbonates of the Utcubamba Valley includes early burial and compaction-related carbonate cements, later diagenetic/epigenetic pre-mineralization and post-mineralization, zoned sparry dolomite and calcite. Early diagenetic phases include processes such as micritization and submarine cementation, chert formation and possible

dissolution associated with shallow burial diagenetic environments. Intermediate to deep burial diagenetic processes include typical compaction features such as neomorphic calcite cement and local pressure-solution features and veinlets. All early diagenetic features are regional in distribution and correlatable across the study area, suggesting that most basinal process were, for the most part, homogeneous.

Late diagenetic/epigenetic phases include dolomite associated with early pre-mineralization ground preparation, and post-mineralization zoned sparry white saddle dolomites and calcites that post-date all carbonate dissolution. Precipitation of regionally extensive, late diagenetic carbonate appears confined to strata or areas showing the development of significant secondary porosity, well-developed dissolution, tectonic faults, fractures and breccias. Detailed cathodoluminescent analysis of the late diagenetic paragenetic sequence show a distinct correlation of gangue carbonates from both barren and mineralized areas. This observation suggests that carbonate phases precipitated during the mineralizing event are genetically related, and transported to the site of deposition through a linked structurally controlled plumbing system.

$\delta^{13}C$ and $\delta^{18}O$ values from Stages 1and 2 dolomites and calcite associated with mineralization show a strong regional homogeneity. These results coupled with strong mineralogical and petrographic similarities of mineralization and alteration phases regionally, suggest a single process at Florida Canyon, Floricita, and the other local zinc occurrences.

Carbonate generations show a general tendency towards lighter isotopic compositions with advancing paragenetic stage. The regional homogeneity of the isotopic composition from altered gangue dolomites suggests that the physicochemical conditions and fluid-rock interaction processes were uniform and almost constant during gangue precipitation. $\delta^{13}C$ and $\delta^{18}O$ values correlate well with published data from the San Vicente deposit approximatley 600 km SE in central Peru. The lightening of isotopic compositions through the paragenetic sequence compares well with general trends observed within global MVT districts and adds further support that Bongara may represent an emerging MVT district.

Standard petrographic, cathodoluminescent and carbonate isotopic analysis techniques suggest that both early diagenetic and late diagenetic/epigenetic alteration associated with zinc-lead mineralization throughout the Bongara district was emplaced through an interconnected, district

wide, structurally controlled plumbing system. This observation suggests a genetic link between all metal occurrences independent of stratigraphic position.

REFERENCES

Allen, C.R., 1997, Visit to Bongara, Peru, Internal Cominco Correspondence, p.7.

Amstutz, G.C., 1956, A note on a peculiar association of copper with fossil plants in central Peru, Bol Soc Geol Peru 30, p. 5-11.

Atherton, M.P., 1990, The Coastal batholith of Peru: The product of rapid recycling of "new" crust formed within rifted continental margin: Geological Journal, v. 25, p. 337-349.

Banner, J.L., Wasserburg, G.J., Dobson, P.F., Carpenter, A.B., Moore, C.H., 1989, Isotopic and trace element constraints on the origin and evolution of saline groundwaters from central Missouri, Geochimica et Cosmochimica Acta, 53, p. 383-398.

Benavides-Caceres, V., 1999, Orogenic Evolution of the Peruvian Andes: The Andean Cycle, *in* Skinner, B. J., ed., Geology and Ore Deposits of the Central Andes: Society of Economic Geologists Special Publication Number 7, p. 61-107.

Budd, D.A., and Perkins, R.D., 1980, Bathymetric zonation and paleoecological significance of microboring in Puerto-Rican shelf and slope sediments, Journal of Sedimentary Petrology, v. 50, p. 881-905.

Bustillo, M.A., and Ruiz Ortiz, P.A., 1987, Chert occurrences in carbonate turbidites: examples from the Upper Jurassic of the Betic Mountains (southern Spain). Sedimentology, 34, p. 611-621.

Choquette, P.W., and James, N.P., 1990, Limestones—The burial diagenetic environment, *in* McIlreath, I.A., and Morrow, D.W., eds., Diagenesis, Geoscience Canada reprint series 4, p. 75-111.

Choquette, P.W., and Pray, L.C., 1970, Geologic nomenclature and classification of porosity in sedimentary carbonates, American Association of Petroleum Geologists Bulletin, 54, p.250-297.

Cobbing, E.J., Pitcher, W.S., Wilson, J.J., Baldock, J., Taylor, W., McCourt, W., and Snelling, N.J., 1981, Estudio geologico de la Cordillera Occidental del norte del Peru: Boletin Instituto Geologico Minero y Metalurgico, LiMa, v. 10D, 252 p.

Coniglio, M., 1987, Biogenic chert in the Cow Head Group (Cambro-Ordovician), western Newfoundland, Sedimentology, 34, p. 813-823.

De Celles, P.G., and Gutschick, R.C., 1983, Mississippian wood-grained cherts and its significance in the Western Interior United States, Journal of Sedimentary Petrology, v. 53, p. 1175-1191.

Dorbath, C., Granet, M., Poupinet, G., and Martlnez, C., 1993, A seismic study of the Altiplano and the Eastern Cordillera in northern Bolivia: New constraints on a lithospheric model: Second Symposium International Geodynamique Andine, ISAG 93, Editions de l'ORSTOM, Collection Colloques et Deminaires, Paris, 1993, p. 7-10.

Enos, P., 1983, Shelf Environment, *in* Scholle, P.A., Bebout, D.G., and Moore, C.H., eds., Carbonate depositional environments, American Association of Petroleum Geologists Memoire, 33, p. 268-295.

Esteban, M., and Klappa, C.F., 1983, Subaerial Exposure, , *in* Scholle, P.A., Bebout, D.G., and Moore, C.H., eds., Carbonate depositional environments, American Association of Petroleum Geologists Memoire, 33, p. 1-54.

Farr, M.R., 1992, Geochemical variation of dolomite cement within the Cambrian Bonneterre Formation, Missouri: evidence for fluid mixing, Journal of Sedimentary Petrology, v. 62, p. 636-651.

Fontbote, L., 1990, Stratabound ore deposits in the Pucara Basin – an overview, *in* Fontbote, L., Amstutz, G.C., Cardozo, M., Cedillo, E., Frutos, J., eds., Stratabound Ore Deposits in the Andes, 1990, Spinger-Verlag, Berlin, Heidelberg, p.255-266.

Fontbote, L., Gorzawski, H., 1990, Genesis of the Mississippi Valley-type Zn-Pb deposit of San Vicente, Central Peru: geological and isotopic (Sr, O, C, S) evidences, Economic Geology, v.

85, p. 1402-1437.

Frank, M.H., and Lohmann, K.C., 1986, Textural and chemical alteration of dolomite: Interaction of mineralizing fluids and host rock in a Mississippi Valley-type deposit, Bonneterre Formation, Viburnum Trend, *in* Hagni, R.D., ed., Process Mineralogy VI, The Metallurgy Society, Varrendale, PA, p. 103-116.

Fukao, Y., and Yamamoto, A., 1989, Gravity anomaly across the Peruvian Andes: Journal of Geophysical Research, v. 94, no. B4, p. 3867-3890

Garvin, P.L., and Ludvigson, G.A., 1993, Epigenetic sulfide mineralization associated with Pennsylvanian paleokarst in eastern Iowa, U.S.A., Chemical Geology, v. 105, p. 271-290.

Geeslin, J.H., and Chafetz, H.S., 1982, Ordoviacian Aleman ribbon cherts; an example of silicfication prior to carbonate lithification, Journal of Sedimentary Petrology, v. 52, p.1283-1293.

Ghazban, F., Schwarcz, H.P., and Ford, D.C., 1990, Carbon and sulfur isotope evidence for in situ reduction of sulfate, Nanisivik lead-zinc deposits, Northwest Territories, Baffin Island, Canada, Economic Geology, v. 85, p. 360-375.

Ghazban, F., Schwarcz, H.P., and Ford, D.C., 1991, Correlated strontium, carbon and oxygen isotopes in carbonate gangue at the Nanisivik zinc-lead deposits, northern Baffin Island, N.W.T., Canada, Chemical Geology (Isotope Geoscience Section), v. 87, p. 137-146.

Gregg, J.M., and Shelton K.L., 1989, Geochemical and petrographic evidence for fluid sources and pathways during dolomitization and lead-zinc mineralization in Southeast Missouri: a review, Carbonates and Evaporites, v. 4. P.153-175.

Greensmith, J.T., 1989, Petrology of the sedimentary rocks, Unwin Hyman Ltd., Oxford, 262 p.

Grose, L.T., 1961, Geology of the vanadiferous, seleniferous, and phosphatic rocks of the Sincos region, Peru, Private Report, Compania Minera Manataro.

Haefner, R.J., Mancuso, J.J., Frizado, J.P., Shelton, K.L., and Gregg, J.M., 1988, Crystallization temperatures and stable isotope composition of Mississippi Valley-Type carbonates and sulfides of the Trenton limeston, Wyandot County, Ohio, Economic Geology, v. 83, p. 1061-1069.

Halley, R.B., Harris, P.M., Hine, A.C., 1983, Bank Margin, *in* Scholle, P.A., Bebout, D.G., and Moore, C.H., eds., Carbonate depositional environments, American Association of Petroleum Geologists Memoire, 33, p. 453-506.

Ham, C.K., and Herrera, L. J., 1963, Role of sub-Andean fault system in tectonics of eastern Peru and Ecuador, *in* Childs, O.E., and Beebe, B.W., eds., Backbone of the Americas: American Association of Petroleum Geologists Memoir 2, p. 47-61.

Hannah, J.L., and Stein, H., 1984, Evidence for changing ore fluid composition: stable isotope analysis of secondary carbonates, Bonneterre Formation, Missouri, Economic Geology, v. 79, p.1930-1935.

Harrison, J.V., 1943, The geology of the central Andes in part of the Province of Junin, Peru: Quarterly Journal of the Geological Society of London, v. 99, p. 1-36

Hillebrandt, A. von, 1973, Neue Ergebnisse uber den Jura in Chile und Argentinien, Munster, Forsch, Geol., Palaont, v. 31/32 p.167-199.

Hillebrandt, A. von, Groschke, M., Prinz, P., and Wilke, H.G., 1986, Marines Mesozoikum in Nordchile zwischn 21° und 26°S, Berliner geowissenschaftlicher Abhandlungen, A, 66, p.169-190.

James, N.P., 1983, Reef, *in* Scholle, P.A., Bebout, D.G., and Moore, C.H., eds., Carbonate depositional environments, American Association of Petroleum Geologists Memoire, 33, p. 345-462.

James, N.P., and Choquette, P.W., 1990, Limestones—the sea floor diagenetic environment, *in* McIlreath, I.A., and Morrow, D.W., eds., Diagenesis, Geoscience Canada reprint series 4, p.13-34.

Kobe, H.W., 1960, Cu-Ag deposits of the red-bed type at Negra Huanusha in central Peru, Schweizeerische mineralogische und Petrographische mitteilungen, 40, p. 163-176.

----1990a, Stratabound Cu-(Ag) deposits in the Permian red-bed Formation, Central Peru, *in* Fontbote, L., Amstutz, G.C., Cardozo, M., Wauschkuhn, A., eds., Stratabound Ore Deposits in the Andes, Springer, Berlin-Heidelberg, New York, p. 113-122.

Kontak, D.J., Clark, A.H., Farrar, E., Strong, D.F., 1985, The rift associated Permo-Triassic magmatism of the Eastern Cordillera: a precursor of the Andean orogeny, *in* Pitcher, W.S., Atherton, M.P., Cobbing, E.J., Beckinsale, R.D., eds., Magmatism at a plate edge: the Peruvian Andes, Blackie, Glasgow and London and Halsted Press, New York, p. 36-44.

Laubacher, G., and Naeser, C.W., 1994, Fission-track dating of granite rocks from the Eastern Cordillera of Peru: Evidence for Late Jurassic and Cenozoic cooling: Journal of the Geological Society, v. 151, p. 473-483.

Leach, D.L., 1999, PDAC Short Course, MVT Deposits, Toronto.

Leach, D.L., and Sangster, D.F., 1993, Mississippi Valley-type lead-zinc deposits, *in* Kirkham, R.V., Sinclair, W.D., Thorpe, R.I., and Duke, J.M., eds., Mineral Deposit Modeling, Geological Association of Canada Special Paper 40, p.289-314.

Levin, P., 1974, Die Pucara-Sedimente im Chanchamayo-Gebiet in Ost-Peru, Geol Rundsch 63: p.345-356.

Loughman, D.L., 1984, Phosphate authigenesis in the Aramachay Formation (Lower Jurassic) of Peru, Journal of Sedimentary Petrology, 54, p. 1147-1156.

Loughman, D.L., and Hallam, A., 1982, A facies analysis of the Pucara Group (Norian to Toarcian carbonates, organic-rich shale and phosphate) of central and northern Peru, Sediment Geology 32, p. 161-194.

Margolis, S. and Rex, R.W., 1971, Endolithic algae and micrite envelope formation in Bahaman oolites as revealed by scanning electron microscopy, Geological Society of America Bulletin, 82, p. 843-852.

McCrea, J.M., 1950, On the isotopic chemistry of carbonates and a paleotemperature scale, Journal of Chemical Physics, v. 18, p. 849-857.

Megard, F., 1968, Geologia del cuadrangulo de Huancayo: Boletin Servicio de Geologia y Mineria, Lima, no. 18, 123 p.

----1978, Etude geologique des Andes du Perou central, Mem ORSTOM, Paris, v. 86, 310p.

----1984, The Andean orogenic period and its major structures in central and northern Peru: Journal of the Geological Society of London, v.141, p. 893-900

----1987, Structure and evolution of the Peruvian Andes, *in* Schaer, J. P., and Rodgers, J., The anatomy of mountain ranges, Princeton, New Jersey, Princeton University Press, p. 179-210.

Meyers, W.J., 1977, Chertification in the Mississippi Lake Valley Formation, Sacramento Mountains, New Mexico, Sedimentology, 24, p. 75-105.

Myers, J.S., 1974, Cretaceous stratigraphy and structure, western Andes of Peru between latitudes 10°-10°30': American Association of Petroleum Geologists Bulletin, v. 58, no. 3, p. 474-487.

----1980, Geologia de los cuadrangulos de Huarmey y Huayllapampa: Boletin Instituto Geologico Minero y Metalurgico, v. 33, 153 p.

Nesbitt, B.E., and Muehlenbachs, K., 1994, Paleohydrogeology of the Canadian Rockies and origins of brines, Pb-Zn deposits and dolomitization in the Western Canada Sedimentary Basin, Geology, v. 22, p.243-246.

Noble, D.C., McKee, E.H., and Megard, F., 1978, Eocene uplift and unroofing of the Coastal batholith near Lima, central Peru: Journal of Geology, v. 86, p. 403-405.

Noble, D.C., McKee, E.H., and Megard, F., 1979b, Early Tertiary "Incaic" tectonism, uplift and volcanic activity, Andes of Central Peru: Geological Society of America Bulletin, v. 90, p. 903-907.

Noble, D.C., Sebrier, M., Megard, F., and McKee, E.H., 1985, Demonstration of two pulses of Paleogene deformation in the Andes of Peru: Earth and Planetary Science Letters, v.73, p. 345-349.

Noble, D.C., McKee, E. H., Mourier, T., and Megard, F., 1990, Cenozoic stratigraphy, magmatic activity, compressive deformation and uplift in northern Peru: Geological Society of American Bulletin, v.102, p. 1105-1113.

Palacios, O., 1980, El Grupo Pucara en la region Subandina (Peru Central), Bol Soc Geol Peru 67, p. 153-162.

Pardo, A., and Sanz, V., 1979, Estratigrafia del curso medio del Rio La Leche, Departmento de Lambayeque, Boletin de la Sociedad geologica del Peru, 67, p. 153-162.

Paredes, J., 1980, Estudio del distrito Minero de Hualgayoc-Cajamarca, v. II: Informe final geologico-economico: Bureau de Recherches Geologiques et Minieres, Cooperacion Minera Franco-Peruna, Lima, 97 p.

Prinz, P., 1985a, Stratigraphic und Ammonitenfauna der Pucara-Gruppe (Obertrias-Unterjura) von Nord-Peru. Paleontographica, Stuttgart, Abt A 188:153 – 197.

Qing, H. and Mountjoy, E., 1992, Large-scale fluid flow in the Middle Devonian Presquile barrier, Western Canada Sedimentary Basin, Geology, v. 20, p. 903-906.

Reid, C. J., 2001, Stratigraphy and Mineralization of the Bongara Zinc-Lead District, Northern Peru, Unpublished Masters Thesis, Toronto, Ontario, University of Toronto,

Rhodes, D., 1998, Report on Florida Canyon with emphasis on drill sections, Internal Cominco Correspondance, p.45.

Roeder, D., and Chamberlain, R.I., 1995, Structural geology of sub-Andean fold and thrust belt in northwestern Bolivia, *in* Tankard, A.J., Suarez S., R., and Welsink, H.J., Petroleum basins of South America, American Association of Petroleum Geologists Memoir 62, p. 459-479.

Rosas, S., 1994, Facies, diagenetic evolution and sequence analysis along a SW-NE profile in the southern Pucara basin (Upper Triassic-Lower Jurassic), central Peru: Unpublished dissertation thesis, Heidelberg, Universitat Heidelberg, Heidelberger Geowissenschaftliche Abhhandlungen, v. 80, 330 p.

Sanchez, A.F., 1995, Geologia de los Cuadrangulos de Bagua Grande, Jumbilla, Lonya Grande, Chachapoyas, Rioja, Leimebamba y Bolivar, Instituto Geologico Minero y Metalurgico, Boletin 56, p. 285.

Shinn, E. A., 1983, Tidal flat environment, *in* Scholle, P.A., Bebout, D.G., and Moore, C.H., eds., Carbonate depositional environments, American Association of Petroleum Geologists Memoire, 33, p. 172-210.

Soler, P., 1989, Petrography and geochemistry of Lower Cretaceous alkali basalts from the high plateaus of central Peru and their tectonic significance: Zentralblatt fur Geologie und Palaontologie, part I, H. 5/6, p. 1053-1064.

----1991, Contribution a l'etude du magmatism associe aux marges actives—petrographie, geochimie et geochimie isotopique du magmatisme Cretace a Pliocene le long d'une transeversale des Andes du Perou ventral—implications geodynamiques et metallogeniques: Unpublished these de Doctorat des Sciences Naturelles, Paris, UniversitE Pierre et Marie Curie, Paris VI, 832 p.

Spangenberg, J., 1995, Geochemical (elemental and isotopic) constraints on the genesis of the Mississipps Valley-type zinc-lead deposit of San Vicente, central Peru, Ph.D. dissertation, University of Geneva, Switzerland (in press).

Steinmann, G., 1929, Geologie von Peru: Heidelberg, Carl Winterss Universitats Buch Handlung, 448 p.

Suarez, G., Molnar, P., and Clark, B.B., 1983, Seismicicity, fault plane solutions, depth of faulting, and active tectonics of the Andes of Peru, Ecuador and southern Columbia, Journal of Geophysical Research, v. 88, no. B12, p. 10403-10428

Suarez, G., Gagnepain, J., Cisternas, A., Hatzfeld, D., Molnar, P., Ocola, L., Roecker, S.W., and Viode, J.P., 1990, Tectonic deformation of the Andes and the configuration of the subducted slab in central Peru: Results from a microseismic experiment, Geophysical Journal International, v. 103, p. 1-12.

Sverjensky, D.A., 1981, Isotopic alteration of carbonate host rocks as a function of water to rock ratio-An example from under the Upper Mississippi Valley zinc-lead district, Economic Geology, v. 76, p. 154-172.

Szekely, T.S., and Grose, L.T., 1972, Stratigraphy of the carbonate black shale and phosphate of the Pucara Group (Upper Triassic-Lower Jurassic), Central Andes, Peru, Geol Soc Am Bull 83, p. 407-428.

Szybinski, A., 1998, Notes on structural geology of the Florida Canyon area, Internal Cominco Correspondence, p.7.

Tucker, M.E., ed., 1988, Techniques in Sedimentology, Blackwells, Oxford, 394 p.

Tucker, M.E. and Hollingworth, N.T.J., 1986, The Upper Permian reef complexes (EZ1) of North East England: Diagenesis in a marine to evaporitic setting, *in* Schroeder, J.H., and Purser, B.H., eds., Reef Diagenesis, Springer, Berlin-Heidelberg, p. 270-290.

Tucker, M.E., and Wright, V.P., 1990, Carbonate sedimentology, Blackwell, Oxford-London-Edinburgh-Boston-Melbourne, 482 p.

Wanless, H.R., 1979, Limestone response to stress – pressure solution and dolomitization, Journal of Sedimentary Petrology, 49, p. 437-462.

Weaver, Ch., E., 1942, A general summary of the Mesozoic of South America, Proc. 8th American Scientific Congress, 4 (Geol. Sci.), p. 149-193

Wilson, J.J., 1963, Cretaceous stratigraphy of central Andes of Peru, American Association of Petroleum Geologists Bulletin, 47, p. 1-34.

Wilson, J.J., and Reyes, R., L., 1964, Geologia del cuadrangulo de Pataz: Boletin Comision Carta Geologia Nacional, Lima, v. 9, 91 p.

Wilson, J.L., 1975, Carbonate Facies in Geologic History, New York: Springer – Verlag, 471p.

Wodzicki, W., 1998, Bongara Year End Report, Internal Cominco Correspondence, p.47.

Yates, R.G., Dean, F. K., and Fernandez Concha, J., 1951, Geology of the Huancavelica Quicksilver district, Peru: U.S. Geological Survey Bulletin, v. 975-A, 45 p.

Appendix 1 - Bongara Sample Database

Date Collected	Section/ddh	Smpl#	Meterage From:	To:	Notes:	Total
Orientation						
04/29/99	El Tingo Orientation	cjr 04/29/1	na	na	maranon complex	1
04/29/99	El Tingo Orientation	cjr 04/29/1a	na	na	maranon complex	2
04/29/99	El Tingo Orientation	cjr 04/29/1b	na	na	maranon complex	3
04/29/99	El Tingo Orientation	cjr 04/29/1c	na	na	maranon complex	4
04/29/99	El Tingo Orientation	cjr 04/29/2	na	na	mitu	5
04/29/99	El Tingo Orientation	cjr 04/29/3	na	na	mitu	6
04/29/99	El Tingo Orientation	cjr 04/29/4	na	na	mitu	7
Buenos Aires Section						
4/5/99	Buenos Aires Sect	BA-01	1.70	na		8
4/5/99	Buenos Aires Sect	BA-02	6.80	na		9
4/5/99	Buenos Aires Sect	BA-03	8.50	na		10
4/5/99	Buenos Aires Sect	BA-04	10.50	na		11
4/5/99	Buenos Aires Sect	BA-05	13.00	na		12
4/5/99	Buenos Aires Sect	BA-06	17.80	na		13
4/5/99	Buenos Aires Sect	BA-07	35.00	na		14
4/5/99	Buenos Aires Sect	BA-08	47.00	na		15
4/5/99	Buenos Aires Sect	BA-09	53.00	na		16
4/5/99	Buenos Aires Sect	BA-10	69.00	na		17
4/5/99	Buenos Aires Sect	BA-11	74.00	na	in tertiary bx	18
4/5/99	Buenos Aires Sect	BA-12	74.00	na	in tertiary bx	19
4/5/99	Buenos Aires Sect	BA-13	74.00	na	in tertiary bx	20
4/5/99	Buenos Aires Sect	BA-14	85.00	na		21
4/5/99	Buenos Aires Sect	BA-15	92.50	na		22
4/5/99	Buenos Aires Sect	BA-16	98.00	na		23
4/5/99	Buenos Aires Sect	BA-17	102.00	na		24
4/5/99	Buenos Aires Sect	BA-18	112.40	na		25
4/5/99	Buenos Aires Sect	BA-19	127.00	na		26
4/5/99	Buenos Aires Sect	BA-20	136.00	na		27
4/5/99	Buenos Aires Sect	BA-21	150.00	na		28
4/5/99	Buenos Aires Sect	BA-22	158.00	na		29
4/5/99	Buenos Aires Sect	BA-23	169.00	na		30
4/5/99	Buenos Aires Sect	BA-24	177.00	na		31
4/5/99	Buenos Aires Sect	BA-25	185.00	na		32
4/5/99	Buenos Aires Sect	BA-26	187.00	na		33
4/5/99	Buenos Aires Sect	BA-27	194.00	na		34
4/5/99	Buenos Aires Sect	BA-28	198.00	na		35
4/5/99	Buenos Aires Sect	BA-29	218.00	na		36
5/5/99	Buenos Aires Sect	BA-30	?	na	lost in tertiary bx	37
5/5/99	Buenos Aires Sect	BA-31	?	na	lost in tertiary bx	38
5/5/99	Buenos Aires Sect	BA-32	1.00	na		39
5/5/99	Buenos Aires Sect	BA-33	4.00	na		40
5/5/99	Buenos Aires Sect	BA-34	6.00	na		41
5/5/99	Buenos Aires Sect	BA-35	8.00	na		42
5/5/99	Buenos Aires Sect	BA-36	10.00	na		43
5/5/99	Buenos Aires Sect	BA-37	13.50	na		44
5/5/99	Buenos Aires Sect	BA-38	16.00	na		45
5/5/99	Buenos Aires Sect	BA-39	18.00	na		46
5/5/99	Buenos Aires Sect	BA-40	20.00	na		47
5/5/99	Buenos Aires Sect	BA-41	22.00	na		48
5/5/99	Buenos Aires Sect	BA-42	24.00	na		49
5/5/99	Buenos Aires Sect	BA-43	44.00	na		50
5/5/99	Buenos Aires Sect	BA-44	49.00	na		51
5/5/99	Buenos Aires Sect	BA-45	59.00	na		52
5/5/99	Buenos Aires Sect	BA-46	64.00	na		53
5/5/99	Buenos Aires Sect	BA-47	71.00	na		54
5/5/99	Buenos Aires Sect	BA-48	75.00	na		55
5/5/99	Buenos Aires Sect	BA-49	79.50	na		56

5/5/99	Buenos Aires Sect	BA-50	87.00	na		57
5/5/99	Buenos Aires Sect	BA-51	2.00	na		58
5/5/99	Buenos Aires Sect	BA-52	8.00	na		59
5/5/99	Buenos Aires Sect	BA-53	14.50	na		60
5/5/99	Buenos Aires Sect	BA-54	26.00	na		61
5/5/99	Buenos Aires Sect	BA-55	28.50	na		62
5/5/99	Buenos Aires Sect	BA-56	1.00	na		63
5/5/99	Buenos Aires Sect	BA-57	10.00	na		64
5/5/99	Buenos Aires Sect	BA-58	30.00	na		65
5/5/99	Buenos Aires Sect	BA-59	34.00	na		66
5/5/99	Buenos Aires Sect	BA-60	45.00	na		67
5/5/99	Buenos Aires Sect	BA-61	54.50	na		68
5/5/99	Buenos Aires Sect	BA-62	86.00	na		69
5/5/99	Buenos Aires Sect	BA-63	94.50	na		70
5/5/99	Buenos Aires Sect	BA-64	95.50	na		71
5/5/99	Buenos Aires Sect	BA-65	112.00	na		72
5/5/99	Buenos Aires Sect	BA-66	135.00	na	ammonite sample	73
5/5/99	Buenos Aires Sect	BA-67	135.00	na	ammonite sample	74
5/5/99	Buenos Aires Sect	BA-68	145.00	na		75
5/5/99	Buenos Aires Sect	BA-69	159.00	na		76
5/5/99	Buenos Aires Sect	BA-70	205.00	na		77
5/5/99	Buenos Aires Sect	BA-71	215.00	na		78
5/5/99	Buenos Aires Sect	BA-72	220.00	na	ammonite sample	79
5/5/99	Buenos Aires Sect	BA-73	220.00	na	ammonite sample	80
5/5/99	Buenos Aires Sect	BA-74	220.00	na	ammonite sample	81
5/5/99	Buenos Aires Sect	BA-75	2.00	na		82
5/5/99	Buenos Aires Sect	BA-76	8.00	na		83
5/5/99	Buenos Aires Sect	BA-77	22.00	na		84
5/5/99	Buenos Aires Sect	BA-78	30.00	na		85
5/5/99	Buenos Aires Sect	BA-79	38.00	na		86
5/5/99	Buenos Aires Sect	BA-80	42.00	na		87
5/5/99	Buenos Aires Sect	BA-81	50.00	na		88
5/5/99	Buenos Aires Sect	BA-82	52.00	na		89
5/5/99	Buenos Aires Sect	BA-83	56.00	na		90
5/5/99	Buenos Aires Sect	BA-84	59.00	na		91
5/5/99	Buenos Aires Sect	BA-85	65.00	na		92
6/5/99	Buenos Aires Sect	BA-86	63.00	na		93
6/5/99	Buenos Aires Sect	BA-87	82.00	na		94
6/5/99	Buenos Aires Sect	BA-88	86.00	na		95
6/5/99	Buenos Aires Sect	BA-89	96.00	na		96
6/5/99	Buenos Aires Sect	BA-90	108.00	na		97
6/5/99	Buenos Aires Sect	BA-91	115.00	na		98
6/5/99	Buenos Aires Sect	BA-92	118.00	na		99
6/5/99	Buenos Aires Sect	BA-93	124.00	na		100
6/5/99	Buenos Aires Sect	BA-94	129.00	na		101
6/5/99	Buenos Aires Sect	BA-95	138.00	na		102
6/5/99	Buenos Aires Sect	BA-96	145.00	na		103
6/5/99	Buenos Aires Sect	BA-97	150.00	na		104
6/5/99	Buenos Aires Sect	BA-98	157.00	na		105
6/5/99	Buenos Aires Sect	BA-99	161.00	na		106
6/5/99	Buenos Aires Sect	BA-100	169.00	na		107
6/5/99	Buenos Aires Sect	BA-101	176.00	na		108
6/5/99	Buenos Aires Sect	BA-102	184.00	na		109
6/5/99	Buenos Aires Sect	BA-103	185.00	na		110
6/5/99	Buenos Aires Sect	BA-104	194.00	na		111
6/5/99	Buenos Aires Sect	BA-105	204.00	na		112
6/5/99	Buenos Aires Sect	BA-106	212.00	na		113
6/5/99	Buenos Aires Sect	BA-107	219.00	na		114
6/5/99	Buenos Aires Sect	BA-108	224.50	na		115
6/5/99	Buenos Aires Sect	BA-109	232.00	na		116
6/5/99	Buenos Aires Sect	BA-110	243.00	na		117
6/5/99	Buenos Aires Sect	BA-111	248.00	na		118
6/5/99	Buenos Aires Sect	BA-112	257.00	na		119
6/5/99	Buenos Aires Sect	BA-113	268.00	na		120

6/5/99	Buenos Aires Sect	BA-114	283.00	na		121
6/5/99	Buenos Aires Sect	BA-115	290.00	na		122
6/5/99	Buenos Aires Sect	BA-116	300.00	na		123
6/5/99	Buenos Aires Sect	BA-117	310.00	na		124
6/5/99	Buenos Aires Sect	BA-118	318.00	na	total 118 smpls	125
Maino Section						
7/5/99	Maino Sect	My-0	1.00	na		126
7/5/99	Maino Sect	My-1	7.00	na		127
7/5/99	Maino Sect	My-2	9.50	na		128
7/5/99	Maino Sect	My-3	13.50	na		129
7/5/99	Maino Sect	My-4	20.00	na		130
7/5/99	Maino Sect	My-5	24.50	na		131
7/5/99	Maino Sect	My-6	30.00	na		132
7/5/99	Maino Sect	My-7	30.50	na		133
7/5/99	Maino Sect	My-8	40.50	na		134
7/5/99	Maino Sect	My-9	47.50	na		135
7/5/99	Maino Sect	My-10	55.00	na		136
7/5/99	Maino Sect	My-11	60.00	na		137
7/5/99	Maino Sect	My-12	75.00	na		138
7/5/99	Maino Sect	My-13	77.00	na		139
7/5/99	Maino Sect	My-14	80.00	na		140
7/5/99	Maino Sect	My-15	87.00	na		141
7/5/99	Maino Sect	My-16	92.00	na		142
7/5/99	Maino Sect	My-17	94.00	na		143
7/5/99	Maino Sect	My-18	91.00	na	smpl taken out of sequence	144
7/5/99	Maino Sect	My-19	102.00	na		145
7/5/99	Maino Sect	My-20	112.00	na		146
7/5/99	Maino Sect	My-21	119.00	na		147
8/5/99	Maino Sect	My-22	121.00	na		148
8/5/99	Maino Sect	My-23	124.00	na		149
8/5/99	Maino Sect	My-24	127.00	na		150
8/5/99	Maino Sect	My-25	129.00	na		151
8/5/99	Maino Sect	My-26	143.00	na		152
8/5/99	Maino Sect	My-27	152.00	na		153
8/5/99	Maino Sect	My-28	167.00	na		154
8/5/99	Maino Sect	My-29	170.00	na		155
8/5/99	Maino Sect	My-30	174.00	na		156
8/5/99	Maino Sect	My-31	183.00	na		157
8/5/99	Maino Sect	My-32	190.00	na		158
8/5/99	Maino Sect	My-33	196.00	na		159
8/5/99	Maino Sect	My-34	202.00	na		160
8/5/99	Maino Sect	My-35	218.00	na		161
8/5/99	Maino Sect	My-36	226.00	na		162
8/5/99	Maino Sect	My-37	233.00	na		163
8/5/99	Maino Sect	My-38	246.00	na		164
8/5/99	Maino Sect	My-39	265.00	na		165
8/5/99	Maino Sect	My-40	273.00	na		166
8/5/99	Maino Sect	My-41	280.00	na		167
8/5/99	Maino Sect	My-42	285.00	na		168
8/5/99	Maino Sect	My-43	293.00	na		169
8/5/99	Maino Sect	My-44	302.00	na		170
8/5/99	Maino Sect	My-45	310.00	na		171
8/5/99	Maino Sect	My-46	325.00	na		172
8/5/99	Maino Sect	My-47	335.00	na		173
8/5/99	Maino Sect	My-48	347.00	na		174
8/5/99	Maino Sect	My-49	360.00	na		175
8/5/99	Maino Sect	My-50	370.00	na		176
8/5/99	Maino Sect	My-51	?	na	smpls taken 400m up trail beyond measurable section	177
8/5/99	Maino Sect	My-52	?	na	total 52 smpls taken	178
8/6/99	Maino Sect	My-53	?	na		
Lemebamba Evaluation						
05/12-15/1999	Lemebamba	LL-0		na	cave	179

Appendix 1 - Sample Database

05/12-15/1999	Lemebamba	LL-1	sh5	na		180
05/12-15/1999	Lemebamba	LL-2	sh5	na		181
05/12-15/1999	Lemebamba	LL-3	sh5	na	sh5 coords 198924E 9241935N	182
05/12-15/1999	Lemebamba	LL-4	sh5	na		183
05/12-15/1999	Lemebamba	Alfonso		na	hydrothermal dolomite from trail	184
Florida DDH 04						
05/19/99	FC-04	FC4-01	10.50	10.60		185
05/19/99	FC-04	FC4-02	13.20	13.35		186
05/19/99	FC-04	FC4-03	15.80	16.00		187
05/19/99	FC-04	FC4-04	18.00	18.20		188
05/19/99	FC-04	FC4-05	21.85	22.00		189
05/19/99	FC-04	FC4-06	24.25	24.40		190
05/19/99	FC-04	FC4-07	32.55	32.70		191
05/19/99	FC-04	FC4-08	38.35	38.50		192
05/19/99	FC-04	FC4-09	42.30	42.50		193
05/19/99	FC-04	FC4-10	51.40	51.60		194
05/19/99	FC-04	FC4-11	55.45	55.60		195
05/19/99	FC-04	FC4-12	59.85	60.00		196
05/19/99	FC-04	FC4-13	66.50	66.65		197
05/19/99	FC-04	FC4-14	72.00	72.15		198
05/19/99	FC-04	FC4-15	74.30	74.45		199
05/19/99	FC-04	FC4-16	78.05	78.25		200
05/19/99	FC-04	FC4-17	81.90	82.05		201
05/19/99	FC-04	FC4-18	83.85	84.10		202
05/19/99	FC-04	FC4-19	91.45	91.65		203
05/19/99	FC-04	FC4-20	95.80	96.00		204
05/19/99	FC-04	FC4-21	100.20	100.35		205
05/19/99	FC-04	FC4-22	101.55	101.70		206
05/19/99	FC-04	FC4-23	105.35	105.50		207
05/19/99	FC-04	FC4-24	118.30	118.45		208
05/19/99	FC-04	FC4-25	121.60	121.80		209
05/19/99	FC-04	FC4-26	127.70	127.85		210
05/19/99	FC-04	FC4-27	137.85	138.00		211
05/19/99	FC-04	FC4-28	148.85	149.00		212
05/19/99	FC-04	FC4-29	158.20	158.40		213
05/19/99	FC-04	FC4-30	161.05	161.20		214
05/19/99	FC-04	FC4-31	161.30	161.40		215
05/19/99	FC-04	FC4-32	165.70	165.85		216
05/19/99	FC-04	FC4-33	170.40	170.55		217
05/19/99	FC-04	FC4-34	176.50	176.65		218
05/19/99	FC-04	FC4-35	179.30	179.50		219
05/19/99	FC-04	FC4-36	185.45	185.60		220
05/19/99	FC-04	FC4-37	191.55	191.70		221
05/19/99	FC-04	FC4-38	197.80	197.95		222
05/19/99	FC-04	FC4-39	202.55	202.70		223
05/19/99	FC-04	FC4-40	206.85	207.00	total 40 smpls	224
Florida DDH 21						
05/20/99	FC-21	FC21-01	3.10	3.20		225
05/20/99	FC-21	FC21-02	9.05	9.20		226
05/20/99	FC-21	FC21-03	11.60	11.75		227
05/20/99	FC-21	FC21-04	12.70	12.80		228
05/20/99	FC-21	FC21-05	19.25	19.40		229
05/20/99	FC-21	FC21-06	23.00	21.50		230
05/20/99	FC-21	FC21-07	32.00	32.15		231
05/20/99	FC-21	FC21-08	34.35	34.50		232
05/20/99	FC-21	FC21-09	39.30	39.45		233
05/20/99	FC-21	FC21-10	43.50	43.65		234
05/20/99	FC-21	FC21-11	46.35	46.50		235
05/20/99	FC-21	FC21-12	52.80	52.95		236
05/20/99	FC-21	FC21-13	60.25	60.40		237
05/20/99	FC-21	FC21-14	61.60	61.75		238
05/20/99	FC-21	FC21-15	66.05	66.20		239
05/20/99	FC-21	FC21-16	78.60	78.70		240

05/20/99	FC-21	FC21-17	83.85	84.00		241
05/20/99	FC-21	FC21-18	84.90	85.05		242
05/20/99	FC-21	FC21-19	92.80	92.95		243
05/20/99	FC-21	FC21-20	97.10	97.25		244
05/20/99	FC-21	FC21-21	100.30	100.45		245
05/20/99	FC-21	FC21-22	103.40	103.55		246
05/20/99	FC-21	FC21-23	112.25	112.35		247
05/20/99	FC-21	FC21-24	115.45	115.60		248
05/20/99	FC-21	FC21-25	120.75	120.80		249
05/20/99	FC-21	FC21-26	128.50	128.65		250
05/20/99	FC-21	FC21-27	133.90	134.05		251
05/20/99	FC-21	FC21-28	142.10	142.35		252
05/20/99	FC-21	FC21-29	145.65	145.80		253
05/20/99	FC-21	FC21-30	149.80	149.95		254
05/20/99	FC-21	FC21-31	151.50	151.65		255
05/20/99	FC-21	FC21-32	151.90	152.05		256
05/20/99	FC-21	FC21-33	155.75	155.80		257
05/20/99	FC-21	FC21-34	158.10	158.30		258
05/20/99	FC-21	FC21-35	161.20	161.35		259
05/20/99	FC-21	FC21-36	161.35	161.50		260
05/20/99	FC-21	FC21-37	162.80	162.95		261
05/20/99	FC-21	FC21-38	166.10	166.25		262
05/20/99	FC-21	FC21-39	172.60	172.75		263
05/20/99	FC-21	FC21-40	175.80	175.95		264
05/20/99	FC-21	FC21-41	184.30	184.45		265
05/20/99	FC-21	FC21-42	187.35	187.50		266
05/20/99	FC-21	FC21-43	194.00	194.15		267
05/20/99	FC-21	FC21-44	198.85	199.00		268
05/20/99	FC-21	FC21-45	200.35	200.50		269
05/20/99	FC-21	FC21-46	205.15	205.30		270
05/20/99	FC-21	FC21-47	215.05	215.20		271
05/20/99	FC-21	FC21-48	220.00	220.15	total 48 smpls	272
Florida DDH 10						
05/21/99	FC-10	FC10-01	18.05	18.20		273
05/21/99	FC-10	FC10-02	37.00	37.15		274
05/21/99	FC-10	FC10-03	40.60	40.75		275
05/21/99	FC-10	FC10-04	55.80	55.95		276
05/21/99	FC-10	FC10-05	108.60	108.75		277
05/21/99	FC-10	FC10-06	120.10	120.25		278
05/21/99	FC-10	FC10-07	128.00	128.15		279
05/21/99	FC-10	FC10-08	137.10	137.25		280
05/21/99	FC-10	FC10-09	140.30	140.45		281
05/21/99	FC-10	FC10-10	143.40	143.55		282
05/21/99	FC-10	FC10-11	145.30	145.45		283
05/21/99	FC-10	FC10-12	163.90	164.05		284
05/21/99	FC-10	FC10-13	176.80	176.95		285
05/21/99	FC-10	FC10-14	195.10	195.25		286
05/21/99	FC-10	FC10-15	211.40	211.55		287
05/21/99	FC-10	FC10-16	250.85	251.00		288
05/21/99	FC-10	FC10-17	261.30	261.45		289
05/21/99	FC-10	FC10-18	268.15	268.30		290
05/21/99	FC-10	FC10-19	269.30	269.45		291
05/21/99	FC-10	FC10-20	271.30	271.45		292
05/21/99	FC-10	FC10-21	275.40	275.55		293
05/21/99	FC-10	FC10-22	286.60	286.75		294
05/21/99	FC-10	FC10-23	287.40	287.55		295
05/21/99	FC-10	FC10-24	288.40	288.55		296
05/21/99	FC-10	FC10-25	289.75	289.90		297
05/21/99	FC-10	FC10-26	292.40	292.55		298
05/21/99	FC-10	FC10-27	294.40	294.60		299
05/21/99	FC-10	FC10-28	297.90	298.15		300
05/21/99	FC-10	FC10-29	302.80	302.95		301
05/21/99	FC-10	FC10-30	309.00	309.15		302

05/21/99	FC-10	FC10-31	317.10	317.25	303
05/21/99	FC-10	FC10-32	322.85	323.00	304
05/21/99	FC-10	FC10-33	328.50	328.65	305
05/21/99	FC-10	FC10-34	338.30	338.40	306
05/21/99	FC-10	FC10-35	342.30	342.45	307
05/21/99	FC-10	FC10-36	358.75	358.90	308
05/21/99	FC-10	FC10-37	368.65	368.80	309
05/21/99	FC-10	FC10-38	383.05	383.20	310
05/21/99	FC-10	FC10-39	384.20	384.40	311
05/21/99	FC-10	FC10-40	387.40	387.60	312
05/21/99	FC-10	FC10-41	393.30	393.45	313
05/21/99	FC-10	FC10-42	411.40	411.60	314
05/21/99	FC-10	FC10-43	413.10	413.35 total 43 samples	315
Florida DDH 29					
05/22/99	FC-29	FC29-01	16.00	16.10	316
05/22/99	FC-29	FC29-02	47.00	47.15	317
05/22/99	FC-29	FC29-03	53.00	53.15	318
05/22/99	FC-29	FC29-04	75.30	75.45	319
05/22/99	FC-29	FC29-05	85.80	85.95	320
05/22/99	FC-29	FC29-06	93.85	94.00	321
05/22/99	FC-29	FC29-07	118.60	118.75	322
05/22/99	FC-29	FC29-08	124.05	124.20	323
05/22/99	FC-29	FC29-09	135.45	135.60	324
05/22/99	FC-29	FC29-10	139.70	139.85	325
05/22/99	FC-29	FC29-11	145.00	145.15	326
05/22/99	FC-29	FC29-12	146.80	146.95	327
05/22/99	FC-29	FC29-13	151.90	152.05	328
05/22/99	FC-29	FC29-14	160.95	161.10	329
05/22/99	FC-29	FC29-15	173.05	173.20	330
05/22/99	FC-29	FC29-16	185.00	185.15	331
05/22/99	FC-29	FC29-17	186.90	187.05	332
05/22/99	FC-29	FC29-18	198.60	198.75	333
05/22/99	FC-29	FC29-19	212.00	212.15	334
05/22/99	FC-29	FC29-20	215.00	215.15	335
05/22/99	FC-29	FC29-21	227.75	227.90	336
05/22/99	FC-29	FC29-22	235.85	236.00	337
05/22/99	FC-29	FC29-23	242.40	242.55	338
05/22/99	FC-29	FC29-24	246.90	247.05	339
05/22/99	FC-29	FC29-25	249.50	249.65	340
05/22/99	FC-29	FC29-26	250.70	250.85	341
05/22/99	FC-29	FC29-27	252.25	252.40	342
05/22/99	FC-29	FC29-28	254.80	255.00	343
05/22/99	FC-29	FC29-29	256.60	256.75	344
05/22/99	FC-29	FC29-30	265.80	265.95	345
05/22/99	FC-29	FC29-31	274.10	274.35	346
05/22/99	FC-29	FC29-32	292.55	292.70	347
05/22/99	FC-29	FC29-33	295.30	295.45	348
05/22/99	FC-29	FC29-34	308.60	308.75	349
05/22/99	FC-29	FC29-35	316.70	316.90	350
05/22/99	FC-29	FC29-36	318.75	318.90	351
05/22/99	FC-29	FC29-37	321.85	322.00	352
05/22/99	FC-29	FC29-38	354.20	354.35	353
05/22/99	FC-29	FC29-39	355.00	355.20	354
05/22/99	FC-29	FC29-40	359.05	359.20	355
05/22/99	FC-29	FC29-41	363.95	364.10	356
05/22/99	FC-29	FC29-42	367.50	367.64 total 42 sampls	357
Florida DDH 27					
05/24/99	FC-27	FC27-01	23.85	24.00 excellent x-section through hydrothermal	358
05/24/99	FC-27	FC27-02	24.85	25.00 dolomite envelope	359
05/24/99	FC-27	FC27-03	31.90	32.05	360
05/24/99	FC-27	FC27-04	40.00	40.15	361
05/24/99	FC-27	FC27-05	43.50	43.65	362
05/24/99	FC-27	FC27-06	47.50	47.65	363

05/24/99	FC-27	FC27-07	58.00	58.15	364
05/24/99	FC-27	FC27-08	64.20	64.35	365
05/24/99	FC-27	FC27-09	68.40	68.55	366
05/24/99	FC-27	FC27-10	72.00	72.20	367
05/24/99	FC-27	FC27-11	78.15	78.30	368
05/24/99	FC-27	FC27-12	81.70	81.85	369
05/24/99	FC-27	FC27-13	96.00	96.15	370
05/24/99	FC-27	FC27-14	105.70	105.85	371
05/24/99	FC-27	FC27-15	119.90	120.05	372
05/24/99	FC-27	FC27-16	124.00	124.15	373
05/24/99	FC-27	FC27-17	130.10	130.25	374
05/24/99	FC-27	FC27-18	136.20	136.35	375
05/24/99	FC-27	FC27-19	143.30	143.45	376
05/24/99	FC-27	FC27-20	151.50	151.65	377
05/24/99	FC-27	FC27-21	151.85	152.00	378
05/24/99	FC-27	FC27-22	156.60	156.75	379
05/24/99	FC-27	FC27-23	160.60	160.75	380
05/24/99	FC-27	FC27-24	172.80	173.00	381
05/24/99	FC-27	FC27-25	175.90	176.05	382
05/24/99	FC-27	FC27-26	176.15	176.30	383
05/24/99	FC-27	FC27-27	178.75	178.90	384
05/24/99	FC-27	FC27-28	184.30	184.45	385
05/24/99	FC-27	FC27-29	187.95	188.10	386
05/24/99	FC-27	FC27-30	190.10	190.25	387
05/24/99	FC-27	FC27-31	194.20	194.35	388
05/24/99	FC-27	FC27-32	197.20	197.35	389
05/24/99	FC-27	FC27-33	198.20	198.35	390
05/24/99	FC-27	FC27-34	198.45	198.60	391
05/24/99	FC-27	FC27-35	200.00	200.15	392
05/24/99	FC-27	FC27-36	200.50	200.65	393
05/24/99	FC-27	FC27-37	201.30	201.45	394
05/24/99	FC-27	FC27-38	202.30	202.45	395
05/24/99	FC-27	FC27-39	203.50	203.65	396
05/24/99	FC-27	FC27-40	205.40	205.55	397
05/24/99	FC-27	FC27-41	206.40	206.55	398
05/24/99	FC-27	FC27-42	207.70	207.85	399
05/24/99	FC-27	FC27-43	211.50	211.65	400
05/24/99	FC-27	FC27-44	213.50	213.65	401
05/24/99	FC-27	FC27-45	221.70	221.85	402
05/24/99	FC-27	FC27-46	228.60	228.85 total 46 smpls	403
Florida DDH 36					
05/26/99	FC-36	FC36-01	6.10	6.25	404
05/26/99	FC-36	FC36-02	9.35	9.50	405
05/26/99	FC-36	FC36-03	12.20	12.35	406
05/26/99	FC-36	FC36-04	15.40	15.65	407
05/26/99	FC-36	FC36-05	16.40	16.55	408
05/26/99	FC-36	FC36-06	18.60	18.75	409
05/26/99	FC-36	FC36-07	21.10	21.35	410
05/26/99	FC-36	FC36-08	23.40	23.55	411
05/26/99	FC-36	FC36-09	24.80	24.95	412
05/26/99	FC-36	FC36-10	26.05	26.20	413
05/26/99	FC-36	FC36-11	27.80	27.95	414
05/26/99	FC-36	FC36-12	29.75	29.90	415
05/26/99	FC-36	FC36-13	33.55	33.70	416
05/26/99	FC-36	FC36-14	36.60	36.75	417
05/26/99	FC-36	FC36-15	39.65	39.80	418
05/26/99	FC-36	FC36-16	41.85	42.00	419
05/26/99	FC-36	FC36-17	54.75	54.90	420
05/26/99	FC-36	FC36-18	55.95	56.10	421
05/26/99	FC-36	FC36-19	61.40	61.55	422
05/26/99	FC-36	FC36-20	73.75	73.90	423
05/26/99	FC-36	FC36-21	83.00	83.15	424
05/26/99	FC-36	FC36-22	88.30	88.45	425

05/26/99	FC-36	FC36-23	91.70	91.85		426
05/26/99	FC-36	FC36-24	97.45	97.60		427
05/26/99	FC-36	FC36-25	101.85	102.00		428
05/26/99	FC-36	FC36-26	103.00	103.23		429
05/26/99	FC-36	FC36-27	105.00	105.20		430
05/26/99	FC-36	FC36-28	105.75	105.90		431
05/26/99	FC-36	FC36-29	111.95	112.10		432
05/26/99	FC-36	FC36-30	121.00	121.15		433
05/26/99	FC-36	FC36-31	123.00	123.15		434
05/26/99	FC-36	FC36-32	136.25	136.40		435
05/26/99	FC-36	FC36-33	138.20	138.50		436
05/26/99	FC-36	FC36-34	140.80	140.95		437
05/26/99	FC-36	FC36-35	142.80	142.95		438
05/26/99	FC-36	FC36-36	143.55	143.77		439
05/26/99	FC-36	FC36-37	144.70	144.85		440
05/26/99	FC-36	FC36-38	149.45	149.60		441
05/26/99	FC-36	FC36-39	152.35	152.50		442
05/26/99	FC-36	FC36-40	154.05	154.20		443
05/26/99	FC-36	FC36-41	157.25	157.40		444
05/26/99	FC-36	FC36-42	167.60	167.75		445
05/26/99	FC-36	FC36-43	167.75	167.90		446
05/26/99	FC-36	FC36-44	173.70	173.85		447
05/26/99	FC-36	FC36-45	180.80	180.95		448
05/26/99	FC-36	FC36-46	183.85	184.00		449
05/26/99	FC-36	FC36-47	186.85	187.05		450
05/26/99	FC-36	FC36-48	188.75	188.90		451
05/26/99	FC-36	FC36-49	196.90	197.05		452
05/26/99	FC-36	FC36-50	197.80	197.95		453
05/26/99	FC-36	FC36-51	199.25	199.40		454
05/26/99	FC-36	FC36-52	203.85	204.00		455
05/26/99	FC-36	FC36-53	208.40	208.55		456
05/26/99	FC-36	FC36-54	225.80	225.95		457
05/26/99	FC-36	FC36-55	226.80	226.95		458
05/26/99	FC-36	FC36-56	227.80	227.95	total 56 smpls	459
Florida DDH 26						
05/27/99	FC-26	FC26-01	21.50	21.65		460
05/27/99	FC-26	FC26-02	22.50	22.65		461
05/27/99	FC-26	FC26-03	23.50	23.65		462
05/27/99	FC-26	FC26-04	24.90	25.05		463
05/27/99	FC-26	FC26-05	27.85	28.00		464
05/27/99	FC-26	FC26-06	30.90	31.05		465
05/27/99	FC-26	FC26-07	37.30	37.45		466
05/27/99	FC-26	FC26-08	43.20	43.35		467
05/27/99	FC-26	FC26-09	47.10	47.25		468
05/27/99	FC-26	FC26-10	53.70	53.85		469
05/27/99	FC-26	FC26-11	59.60	59.75		470
05/27/99	FC-26	FC26-12	63.40	63.55		471
05/27/99	FC-26	FC26-13	67.60	67.75		472
05/27/99	FC-26	FC26-14	80.10	80.35		473
05/27/99	FC-26	FC26-15	86.80	86.95		474
05/27/99	FC-26	FC26-16	90.70	90.85		475
05/27/99	FC-26	FC26-17	91.50	91.75		476
05/27/99	FC-26	FC26-18	92.30	92.45		477
05/27/99	FC-26	FC26-19	95.15	95.30		478
05/27/99	FC-26	FC26-20	103.35	103.50		479
05/27/99	FC-26	FC26-21	104.00	104.50		480
05/27/99	FC-26	FC26-22	118.30	118.45		481
05/27/99	FC-26	FC26-23	125.90	126.05		482
05/27/99	FC-26	FC26-24	132.20	132.35		483
05/27/99	FC-26	FC26-25	151.55	151.70		484
05/27/99	FC-26	FC26-26	157.40	157.55		485
05/27/99	FC-26	FC26-27	199.45	199.60		486
05/27/99	FC-26	FC26-28	200.60	200.75		487

05/27/99	FC-26	FC26-29	202.10	202.25	488
05/27/99	FC-26	FC26-30	203.50	203.65 total 30 smpls	489
Florida DDH 39					
05/28/99	FC-39	FC39-01	14.10	14.25	490
05/28/99	FC-39	FC39-02	14.60	14.75	491
05/28/99	FC-39	FC39-03	21.10	21.35	492
05/28/99	FC-39	FC39-04	30.15	30.30	493
05/28/99	FC-39	FC39-05	35.30	35.45	494
05/28/99	FC-39	FC39-06	37.25	37.40	495
05/28/99	FC-39	FC39-07	43.10	43.25	496
05/28/99	FC-39	FC39-08	60.85	61.00	497
05/28/99	FC-39	FC39-09	70.00	70.15	498
05/28/99	FC-39	FC39-10	78.30	78.45	499
05/28/99	FC-39	FC39-11	100.65	100.80	500
05/28/99	FC-39	FC39-12	103.70	103.85	501
05/28/99	FC-39	FC39-13	107.75	107.90	502
05/28/99	FC-39	FC39-14	116.25	116.40	503
05/28/99	FC-39	FC39-15	127.10	127.25	504
05/28/99	FC-39	FC39-16	133.80	133.95	505
05/28/99	FC-39	FC39-17	139.30	139.45	506
05/28/99	FC-39	FC39-18	151.70	151.85	507
05/28/99	FC-39	FC39-19	161.50	161.65	508
05/28/99	FC-39	FC39-20	164.90	165.05	509
05/28/99	FC-39	FC39-21	179.95	180.10	510
05/28/99	FC-39	FC39-22	182.00	182.15	511
05/28/99	FC-39	FC39-23	198.30	198.45	512
05/28/99	FC-39	FC39-24	206.10	206.25	513
05/28/99	FC-39	FC39-25	213.10	213.25	514
05/28/99	FC-39	FC39-26	218.60	218.75	515
05/28/99	FC-39	FC39-27	219.60	219.75	516
05/28/99	FC-39	FC39-28	226.50	226.65	517
05/28/99	FC-39	FC39-29	233.70	233.85	518
05/28/99	FC-39	FC39-30	240.00	240.15	519
05/28/99	FC-39	FC39-31	241.80	241.95	520
05/28/99	FC-39	FC39-32	250.10	250.25	521
05/28/99	FC-39	FC39-33	258.40	258.55	522
05/28/99	FC-39	FC39-34	262.15	262.30	523
05/28/99	FC-39	FC39-35	268.60	268.75	524
05/28/99	FC-39	FC39-36	278.60	278.75	525
05/28/99	FC-39	FC39-37	292.80	292.95	526
05/28/99	FC-39	FC39-38	302.85	303.00	527
05/28/99	FC-39	FC39-39	306.50	306.65	528
05/28/99	FC-39	FC39-40	309.50	309.65	529
05/28/99	FC-39	FC39-41	311.15	311.30	530
05/28/99	FC-39	FC39-42	324.20	324.35	531
05/28/99	FC-39	FC39-43	347.70	347.85	532
05/28/99	FC-39	FC39-44	350.60	350.75	533
05/29/99	FC-39	FC39-45	356.70	356.85	534
05/29/99	FC-39	FC39-46	359.65	359.80	535
05/29/99	FC-39	FC39-47	365.00	365.15	536
05/29/99	FC-39	FC39-48	367.90	368.05	537
05/29/99	FC-39	FC39-49	372.10	372.25	538
05/29/99	FC-39	FC39-50	378.20	378.45	539
05/29/99	FC-39	FC39-51	381.25	381.40	540
05/29/99	FC-39	FC39-52	384.15	384.30	541
05/29/99	FC-39	FC39-53	387.20	387.35	542

05/29/99	FC-39	FC39-54	390.40	390.55		543
05/29/99	FC-39	FC39-55	393.45	393.60		544
05/29/99	FC-39	FC39-56	399.35	399.50		545
05/29/99	FC-39	FC39-57	402.60	402.75		546
05/29/99	FC-39	FC39-58	403.60	403.75		547
05/29/99	FC-39	FC39-59	420.90	421.05		548
05/29/99	FC-39	FC39-60	423.95	424.10		549
05/29/99	FC-39	FC39-61	427.00	427.15	total 61 sampl	550
Florcita Section						
06/25/99	Florcita (fluid/min smpl)	cjr 25/06/99 - 1	na	na	smpl from upper adit at florcita, near base of karst	551
06/25/99	Florcita (fluid/min smpl)	cjr 25/06/99 - 2	na	na	pyritized, sphal, dol. breccia from upper florcita adit	552
06/25/99	Florcita (fluid/min smpl)	cjr 25/06/99 - 3	na	na	fine-med grained dolo mudstone from upper adit	553
06/25/99	Florcita (fluid/min smpl)	cjr 25/06/99 - 4	na	na	fine-med grained dolo mud of condorsinga - at level of upper adit imediately to south out of collapse - same elevation as upper adit approx. 50 m	554
06/25/99	Florcita (fluid/min smpl)	cjr 25/06/99 - 5	na	na	50 m s of adit at same elevation in system.	555
06/25/99	Florcita (fluid/min smpl)	cjr 25/06/99 - 6	na	na	12 m elev above adit	556
06/25/99	Florcita (fluid/min smpl)	cjr 25/06/99 - 7	na	na	coarse sphal from upper adit	557
06/25/99	Florcita (fluid/min smpl)	cjr 25/06/99 - 8	na	na	coarse sphal from upper adit	558
06/25/99	Florcita (fluid/min smpl)	cjr 25/06/99 - 9	na	na	vein of dolo and sph in fine unaltered dolo 14 above adit 20 m to north. Near goya contact	559
06/25/99	Florcita (fluid/min smpl)	cjr 25/06/99 - 10	na	na	from 25 m above adit (old reference cominco 467364)	560
06/25/99	Florcita (fluid/min smpl)	cjr 25/06/99 - 11	na	na	odd fe oxide, py , dolo, gerrisite/hematite - goya/condorsinga shear contact	561
06/25/99	Florcita (fluid/min smpl)	cjr 25/06/99 - 12	na	na	200 m n of upper adit	562
06/25/99	Florcita (fluid/min smpl)	cjr 25/06/99 - 13	na	na	200 m n of upper adit	563
06/25/99	Florcita (fluid/min smpl)	cjr 25/06/99 - 14	na	na	200 m n of upper adit	564
06/26/99	Florcita Section	FL-1	1.50	na	bituminous dk grey l mdst	565
06/26/99	Florcita Section	FL-2	12.00	na	coarse calcite veining in oc, med bedded lst	566
06/26/99	Florcita Section	FL-3	24.00	na		567
06/26/99	Florcita Section	FL-4	47.00	na		568
06/26/99	Florcita Section	FL-5	54.00	na		569
06/26/99	Florcita Section	FL-6	63.00	na		570
06/26/99	Florcita Section	FL-7	72.00	na		571
06/26/99	Florcita Section	FL-8	85.00	na		572
06/26/99	Florcita Section	FL-9	91.00	na		573
06/26/99	Florcita Section	FL-10	100.00	na		574
06/26/99	Florcita Section	FL-11	112.00	na		575
06/26/99	Florcita Section	FL-12	121.00	na		576
06/26/99	Florcita Section	FL-13	126.00	na		577
06/26/99	Florcita Section	FL-14	134.00	na		578
06/26/99	Florcita Section	FL-15	141.00	na		579
06/26/99	Florcita Section	FL-16	150.00	na		580
06/26/99	Florcita Section	FL-17	157.00	na		581
06/26/99	Florcita Section	FL-18	172.00	na		582
06/26/99	Florcita Section	FL-19	178.00	na		583
06/26/99	Florcita Section	FL-20	190.00	na		584
06/26/99	Florcita Section	FL-21	200.00	na		585
06/26/99	Florcita Section	FL-22	212.00	na		586
06/26/99	Florcita Section	FL-23	223.00	na		587
06/26/99	Florcita Section	FL-24	232.00	na		588
06/26/99	Florcita Section	FL-25	254.00	na	39 total samples	589
Tingo Section						
06/29/99	Tingo Section	TG-1	0.00	na		590

06/29/99	Tingo Section	TG-2	6.00	na		591
06/29/99	Tingo Section	TG-3	21.00	na		592
06/29/99	Tingo Section	TG-4	32.00	na		593
06/29/99	Tingo Section	TG-5	44.00	na		594
06/29/99	Tingo Section	TG-6	53.00	na		595
06/29/99	Tingo Section	TG-7	65.00	na		596
06/29/99	Tingo Section	TG-8	77.00	na		597
06/29/99	Tingo Section	TG-9	87.00	na		598
06/29/99	Tingo Section	TG-10	101.00	na		599
06/29/99	Tingo Section	TG-11	128.00	na		600
06/29/99	Tingo Section	TG-12	152.00	na		601
06/29/99	Tingo Section	TG-13	157.00	na		602
06/29/99	Tingo Section	TG-14	176.00	na		603
06/29/99	Tingo Section	TG-15	182.00	na		604
06/29/99	Tingo Section	TG-16	200.00	na		605
06/29/99	Tingo Section	TG-17	205.00	na		606
06/29/99	Tingo Section	TG-18	210.00	na		607
06/29/99	Tingo Section	TG-19	217.00	na		608
06/29/99	Tingo Section	TG-20	239.00	na		609
06/29/99	Tingo Section	TG-21	245.00	na		610
06/29/99	Tingo Section	TG-22	248.00	na		611
06/29/99	Tingo Section	TG-23	253.00	na		612
06/29/99	Tingo Section	TG-24	280.00	na		613
06/29/99	Tingo Section	TG-25	290.00	na		614
06/29/99	Tingo Section	TG-26	298.00	na		615
06/29/99	Tingo Section	TG-27	307.00	na		616
06/29/99	Tingo Section	MT-1	na	na	Mitu redbed at base of tingo section (maranon river)	617
06/29/99	Tingo Section	MT-2	na	na	Mitu redbed at base of tingo section (maranon river)	618
06/29/99	Tingo Section	MT-3	na	na	Mitu redbed at base of tingo section (maranon river)	619
06/29/99	Tingo Section	MT-4	na	na	Mitu redbed at base of tingo section (maranon river)	620
					31 total smpls	
Tesoro Section						
6/7/99	Tesoro Section	TS-01	4.50	na		621
6/7/99	Tesoro Section	TS-02	4.90	na		622
6/7/99	Tesoro Section	TS-03	9.00	na		623
6/7/99	Tesoro Section	TS-04	22.50	na		624
6/7/99	Tesoro Section	TS-05	31.00	na		625
6/7/99	Tesoro Section	TS-06	40.50	na		626
6/7/99	Tesoro Section	TS-07	44.00	na		627
6/7/99	Tesoro Section	TS-08	56.00	na		628
6/7/99	Tesoro Section	TS-09	76.00	na		629
6/7/99	Tesoro Section	TS-10	89.50	na		630
6/7/99	Tesoro Section	TS-11	91.00	na		631
6/7/99	Tesoro Section	TS-12	103.00	na		632
6/7/99	Tesoro Section	TS-13	107.50	na		633
6/7/99	Tesoro Section	TS-14	118.00	na		634
6/7/99	Tesoro Section	TS-15	123.00	na		635
6/7/99	Tesoro Section	TS-16	136.00	na		636
6/7/99	Tesoro Section	TS-17	141.00	na		637
7/7/99	Tesoro Section	TS-18	148.00	na		638
7/7/99	Tesoro Section	TS-19	154.00	na		639
7/7/99	Tesoro Section	TS-20	171.50	na		640
7/7/99	Tesoro Section	TS-21	173.00	na		641
7/7/99	Tesoro Section	TS-22	176.00	na		642

7/7/99	Tesoro Section	TS-23	200.00	na		643
7/7/99	Tesoro Section	TS-24	217.50	na		644
7/7/99	Tesoro Section	TS-25	234.00	na		645
7/7/99	Tesoro Section	TS-26	244.00	na		646
7/7/99	Tesoro Section	TS-27	241.00	na		647
7/7/99	Tesoro Section	TS-28	253.00	na		648
7/7/99	Tesoro Section	TS-29	265.00	na		649
7/7/99	Tesoro Section	TS-30	275.50	na		650
7/7/99	Tesoro Section	TS-31	283.00	na		651
7/7/99	Tesoro Section	TS-32	293.50	na		652
7/7/99	Tesoro Section	TS-33	295.00	na		653
7/7/99	Tesoro Section	TS-34	302.00	na		654
7/7/99	Tesoro Section	TS-35	325.00	na		655
7/7/99	Tesoro Section	TS-36	334.00	na		656
7/7/99	Tesoro Section	TS-37	343.00	na		657
8/7/99	Tesoro Section	TS-38	356.00	na		658
8/8/99	Tesoro Section	TS-39	370.00	na		659
8/9/99	Tesoro Section	TS-40	374.50	na		660
8/10/99	Tesoro Section	TS-41	383.00	na		661
8/11/99	Tesoro Section	TS-42	385.50	na		662
8/12/99	Tesoro Section	TS-43	400.00	na		663
8/13/99	Tesoro Section	TS-44	424.00	na		664
8/14/99	Tesoro Section	TS-45	433.00	na		665
8/15/99	Tesoro Section	TS-46	458.00	na		666
8/16/99	Tesoro Section	TS-47	476.00	na		667
8/17/99	Tesoro Section	TS-48	491.00	na		668
8/18/99	Tesoro Section	TS-49	512.00	na		669
8/19/99	Tesoro Section	TS-50	544.00	na		670
8/20/99	Tesoro Section	TS-51	570.00	na		671
8/21/99	Tesoro Section	TS-52	600.00	na		672
8/22/99	Tesoro Section	Tesoro showing #1			tesoro showing - sulphide	
8/23/99	Tesoro Section	Tesoro showing #2			tesoro showing - sulphide	
8/24/99	Tesoro Section	Tesoro showing #3			tesoro showing - oxide	
					52 total smpl	
NARANJTOS SECTION						
7/12/99	Naranjitos Section	07/12/99 - 1	na	na		673
7/12/99	Naranjitos Section	Carm - 1	na	na		674
7/12/99	Naranjitos Section	Carm - 2	na	na		675
7/12/99	Naranjitos Section	Carm - 3	na	na		676
7/12/99	Naranjitos Section	Carm - 4	na	na		677
7/12/99	Naranjitos Section	Carm - 5	na	na		678
7/12/99	Naranjitos Section	Carm - 6	na	na		679
7/12/99	Naranjitos Section	Carm - 7	na	na		680
7/12/99	Naranjitos Section	Carm - 8	na	na		681
7/12/99	Naranjitos Section	Carm - 9	na	na		682
7/12/99	Naranjitos Section	Carm - 10	na	na		683
7/12/99	Naranjitos Section	Carm - 11	na	na		684
7/13/99	Naranjitos Section	Nar - 1	0.25	na		685
7/13/99	Naranjitos Section	Nar - 2	6.50	na		686
7/13/99	Naranjitos Section	Nar - 3	13.50	na		687
7/13/99	Naranjitos Section	Nar - 4	26.40	na		688
7/13/99	Naranjitos Section	Nar - 5	35.20	na		689
7/13/99	Naranjitos Section	Nar - 6	1.00	na	due to unmeasurable terrain - reset loggin at 0m.	690
7/13/99	Naranjitos Section	Nar - 7	14.00	na		691
7/13/99	Naranjitos Section	Nar - 8	18.50	na		692
7/13/99	Naranjitos Section	Nar - 9	41.00	na		693

7/13/99	Naranjitos Section	Nar - 10	52.00	na		694
7/13/99	Naranjitos Section	Nar - 11	61.00	na		695
7/13/99	Naranjitos Section	Nar - 12	75.00	na		696
7/13/99	Naranjitos Section	Nar - 13	96.00	na		697
7/13/99	Naranjitos Section	Nar - 14	125.00	na		698
7/13/99	Naranjitos Section	Nar - 15	135.00	na		699
7/13/99	Naranjitos Section	Nar - 16	154.00	na		700
					27 total smpl	

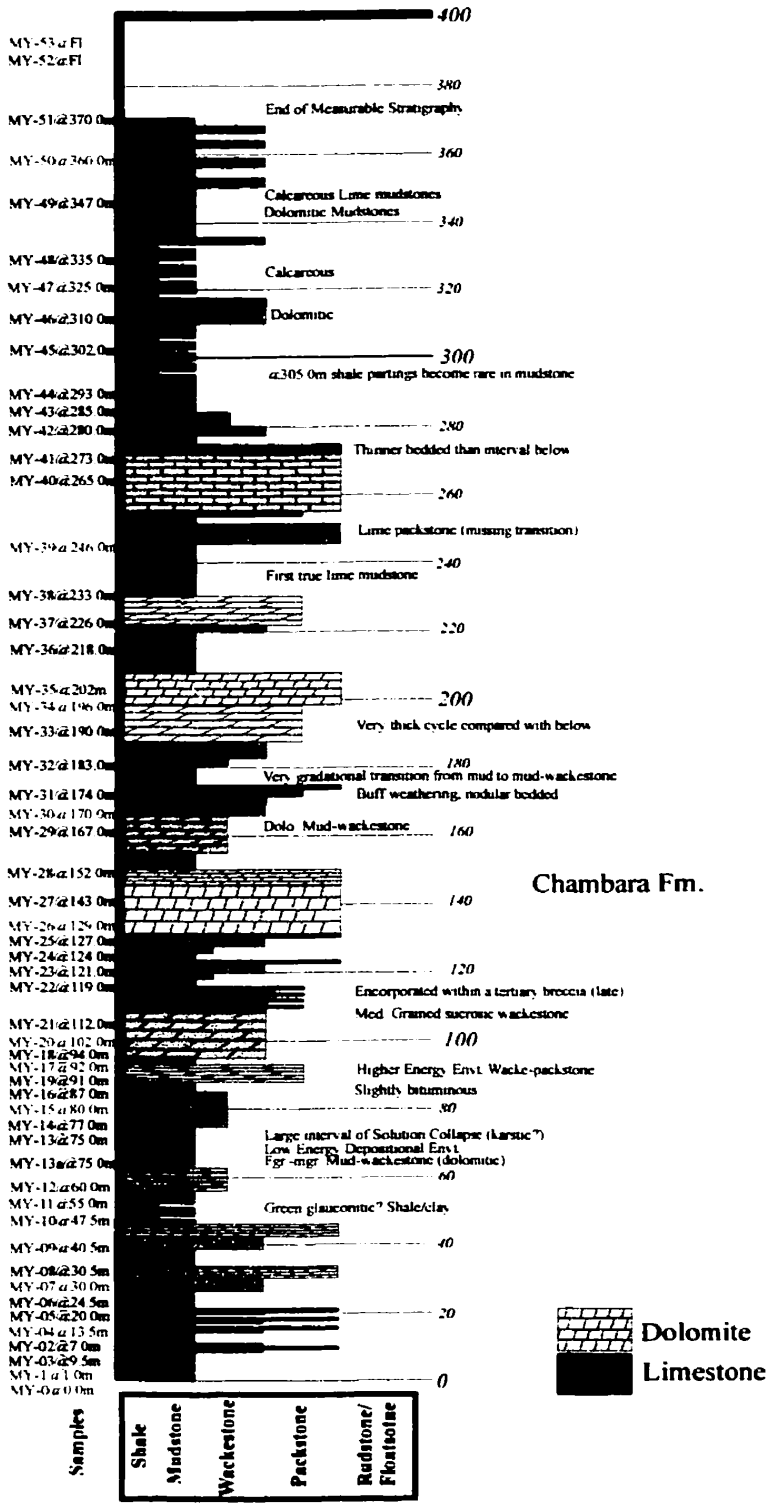

Appendix 2 - Maino Section

Maino Section

Meterage: To:	From:	Description:
0	10	Fine grained dolomitic mudstone. bedded on a dm scale. late large cm vugs filled by coarse crystalline calcite. pink to buff colour.. towards 7 m. becomes slightly thinner bedded with calcareous surface partings - thin shale partings @ 7.5 meters never more than 5 cm thick..
10	11.75	Well defined linternal laminations. possible algal laminae in a fine dolomudstone. Thin laminations with no grading identified. light reddish to purple colour. fine to med. grained. large open vugs infilled by late coarse calcite crystals.
	11.75	Black clay marker? black clay shale bed (5 cm) thins and swells with undulous bedding.
11.85	13.5	Thin-med. Beeded dolomudstone-wackestone. faint internal laminations. undulous. weathering to a buff colour on fresh surface. mm scale vuggy porosity. locally diagenetic alteration is very fine grained. appears early when compared texturally with late coarse hydrothermal dolomite observed further up section. locally very thin packstones (? may just be coarse recrystallization)
13.5	15	Development of open fenestral vuggy porosity (cyclic) fenestral may be a result of fossil casts that have developed cyclicly (20-50 cm cycles)
15	21.5	30 cm scale cycles continue but thicken to a metric scale. still a dolomitic mudstone. fenestral porosity is confined to wackestone and packstones within interval - fenestral cycles contain up to 25 % porosity infilled by late very coarse grained calcite. dolomite rims infilled by late calcite.
21.5	45.5	Nodular horizon over 20 cm and alligned parallel with bedding - structure remains extremely consistent. possible stylolites lined by ankerite. large fracture coating mm dendrites along bedding surfaces. each remains essentially the same.
45.5	50	Bioturbated dolo mudstone upto 45.5 @ 10 cm thin scaley well laminated dolo. mud horizons with low porosity Green glauconitic shale clay.
50	55	At 50 m starts to get thicker bedded another green clay @ 52.5 m. 15 cm thick. (@ 55
55	57	Above description
57	62	Fine to med grained dolomitic mud-wackestone. bedded on a decimentric scale. fine disseminations oif Fe oxide. late porosity fill.
63	76	Large scale beautiful solution collapse feature. fragments are dm scale. planar laminated by late dolo frags are angular and rotated.
76	80	Thinnly to very thinnly undulous bedded on a cm scale. becomes calcareous and slightly bituminous conforms to general bedding
80	85	Thicker bedded (15-50cm) buff coloured. dolomudstones and matrix is fine grained dolomite with a late hydrothermal character. Haloes around vug openings later filled by coarse calcite still remains mud-wackestone with late hydrothermal alteration.
85	87	Dolomitic mudstone remains fairly concictent. patchy dolospar. slightly coarser grained than last unit. past 86. fine grained buff monoteneous dolomitic mudstone.
87	93	Definently a different facies. changes more to a yellow brown colour with well developed vuggy-fenestral porosity. almost aligning itself parrallel with bedding. seems coarse grained (wackestone) no fossil content. hydrothermal dolomite lining fenetral porosity.
93	95	Dolomitic mudstone marking well developed cycle.
95	109	Late tertiary breccia frags are more or less in place.
109	115	Dolomitic wackestone with late clacite vug filling and rare hydrothermal dolomite. possible crinoids associated with a high energy facies. still in alteration of late breccia. I believe that cyclic high /low e facies below is just contiunuing on a slightly thicker scale.

115	130	Late tertiary breccia for 2 m. then into a higher energy facies dolomitic pseudobreccia and beaurtiful zebra textured rocks. Beautiful ground preparation conforms to high energy facies as porosity after fossil including gastropods. crinoid ossiclcles and bivalves. thin muddly beds show beautiful perserved internallaminations between 115-130. High E on top. higher E facies shows hydrothermal altaration. low E facies bedded-laminated mudstoens and wackestones @ 125 start to get into thin-med. Bedded consistently dolo-mudston-wackestone startaigaraphy topped by higher E facies ranging from .5n to 2 meter (odd facies) - at 128 thick. higher energy enviornment showing fantastic psuedobrecciated hydrothermal replacement 05/08/99 R% #23/24/25/26 @ 138 - note: not sure if high energy system continues through section. intense late hydrothermal alteration masks litho on fresh surface (may help determine true protolith)
130	143	Coarse dolo packstone appears to be host to stratabound alteration filled by late calcite looks like approx. 45% coarse calcite srystals - another vuggy horizon between...
144	150	with significant 20% + hydrothermal dolomite alteration
150	170	At 150 end of cycle - fine bedded resistnat dolomudstones for 4.0 m At 153 still buff dolo mudstone to wackestone but bedding becomes very undulous and in places appears almost nodular - so far it looks like we have gone through 2 or possiblv 3 cvcles of the TCh 1/2.
170	176	At 170 thin bedded buff brown to pale grey dolomite mud-wackestone. undulous to slightly nodular appearance in bedding. Coarser dolomitic wacke-packstone. dolomitic. but finer grained than lower in stratigraphy (different phase?). grades into a high energy crinodial packstone and becomes thicklv bedded on a m-dm scale
176	182	Med to thck bedded (0.5-1m) dolomudstones. rather pristine without much alteration except surfical calcite. at 182 grades into a thick bedded undulous lightly nodular dolomudstone-wackestone
182	208	bedding becomes slightly thicker. bedded upto metric scale
208	220	Thin bedded dolomudstones. fairly nlodular and locally undulous. At 220 return into a thick bedded. possibly recrystallized wacke-packstone (dolo). At 232 very distinctive med. Bedded nodular -lime mudstone. first preserved calcareous horizon - possibly dedolomitized. concoidla fractue. very thin bedded.
220	245	At 245 contrast into a beautifully perserved crinoidal/oncoidal packstone. thick to med bedded on a meter scale remains fairly continous
245	251	Limestone (no dolo altn.). high e fossil packstone.
251	255	Low E enviornment. Undulous lime mudstone over 3 meter interval grading back into a med. Bedded wack-packstone higher e facies @ 255.
255	272	Thin bedded nodular packstone. Higher E env. perserved lime packstone (biota comp. 15%)
272	280	Same lithology just thinner bedded Lime wacke-packstone at 274 cycle ends into well bedded (med-thin) lime-dolomudstone and wackestone possibly transistion into U TCh2/TCh3. bedding is undulous and locallv nodular. well perserved monotis. Perserved monotis in wacke.
280	338	Limestone. med bedded. grey mud-wackestone. Remains extremely consistent low E package of black lime mudstones thin to med. Bedded.

Appendix 2 - Maino Log

Bivalves commonly perserved along bedding planes between mudstones and shales. bedding remains extremely consistent at 15-20 cm. at 305m. shale partings become rare. beds become slightlv thinner and more undulous in character.

At 315 dolomite again. appears it increases with grain size perhaps we are moving back into another larger cycle of TCH2 equivvalent.
At 318 back into a thin bedded mudstone with shale partings and undulous bedding - lime mudstone-
Remains extremely consistent. shale beds thin and swell with undulous bedding. Becomes slightly coarser grained at 335

338 370 At 338 remains very similar but starts to get very thin bedded ona 5-10 cm scale s

Dolomitic mudstones @ 350 break into coarser more altered dolostones (almost sucrosice) wackeston - same package just coarse alteration
Samples are all now very calcareous and beautifull clean limemudstones starting @345 (no shaley horizons) - 05/08/99 R5 33/34 consistent package what changes is the amount and intensity of dolomite - note*undulous bedding has remained constant for this entire section
At 370 measureable outcrop stops - we are ina up TCH@ equivalent ?? Great dolomitic psuedo breccias can be observed 300 meters up the path.

370 Cretaceous sandstones

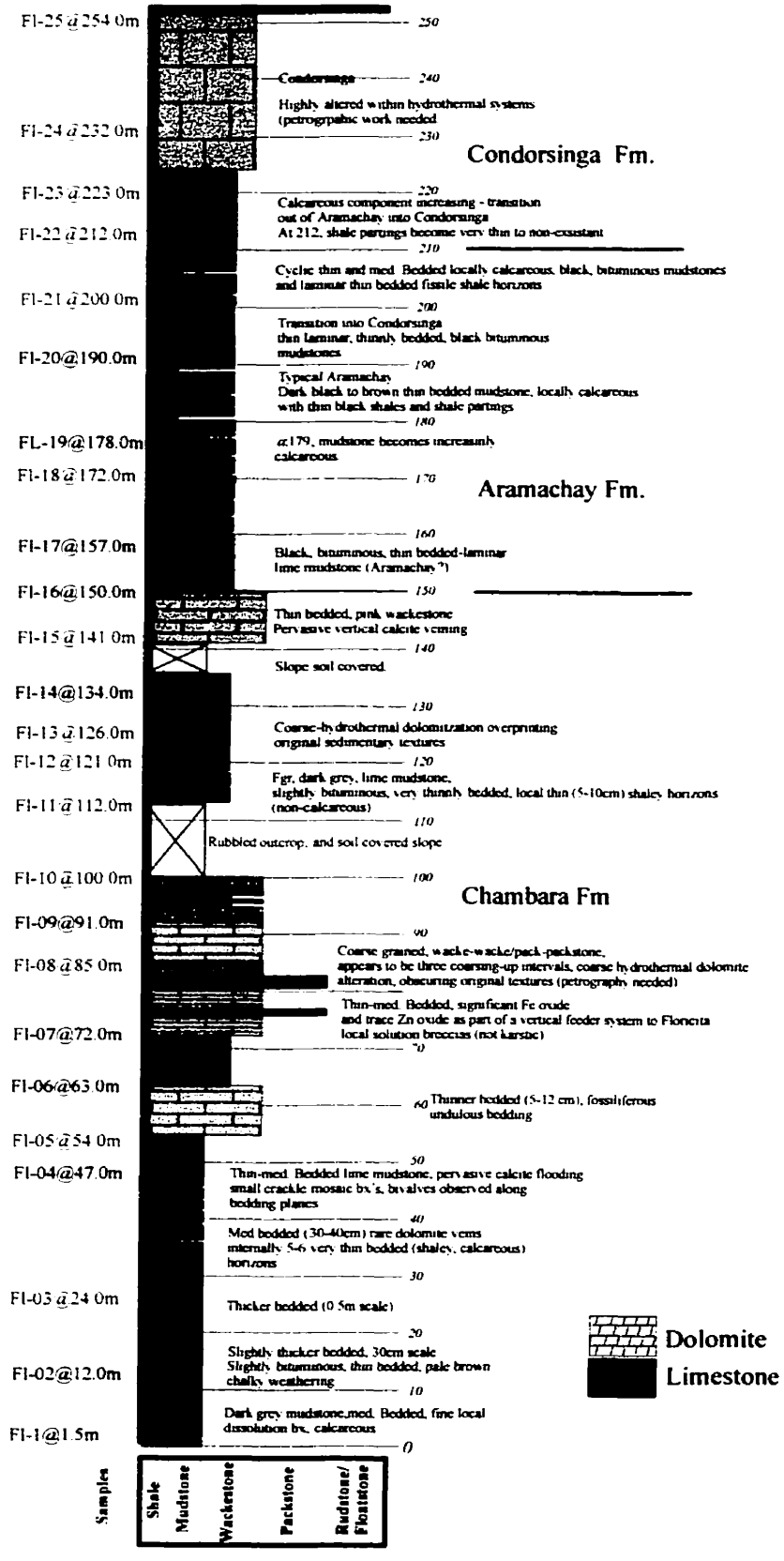

Appendix 2 - Floricita Section

Floricita
Section:

Meterage To:	From:	Description:
0	6	Very fine grained grey to dark grey mudstone, med bedded on a 10-40 cm scale, fairly homogeneous with a local fine dissolution breccia, looks like a solution collapse but frags are rounded to oval and small (less than 2 cm), limestone, thin subvertical calcite veins
12	18	Slightly thicker bedded, calcite veining increases, lime mudstones, bedding is flat and consistent
18	24	Slightly thicker bedded to a 0.5 meter scale.
24	47	ASA in med bedded (40-50cm) bedded section, rare dolomite veins and alteration along vein boundary, 5-6 thin bedded intervals section
47	54	Thin-med bedded mudstone with pervasive calcite flooding as thin veins locally causing small crackle mosaic breccias. Litho remnains the same, bivalves observed @ 54 meters parralel along bedding planes
54	63	Bedding becomes thinner ranging from 5-20 cm, same lithology, slightly more of a wackestone, fossiliferous, slightly undulous bedding.
63	72	Thin, med. bedded limestone with significant Fe oxide and Trace Zn oxide as part of vertical feeder system to Floricita, causes local solution collapse breccia features, oxide forms small poddy character. (R12 1/2 1. Oxide zone, 2) road and river along section).
		very coarse calcite flooding likely and alteration event first observed white hydrothermal ?? Dolomite coarse nature makes me think that perhaps protolith was likely a wacke-packstone (petrography needed). Bedded mudstone and wackestones.
72	85	Coarse crystalline wackestone and rare packstone preserved, predominantly wackestone
85	93	Thin coarse hydrothermal dolo veins and gashes through coarse wacke limestone @91 m.
93	100	Altered wackestone, med bedded consistent structure, dolo forms small metric scale solution zones, 2 thin (1-2 m cycles of w-mudstone, limestone , thinnly bedded. Med. bedded, slightly undulous dark grey, fine grained lime mudstone, as @ base of section
		note* nature of hydrothermal system moving in and out of section (vertical), Fl-10 has coarse calcite and baroque dolomite veining while matrix remains relatively unaltered.
100	112	No outcrop, rubbeled and soil covered
112	123	TCh3 - fine grained, dark grey lime mudstone with thin calcite veining, slightly bituminous, appears to be fairly thin bedded, local thin shaley horizons, may be approaching Aramachay contact, slightly thinner bedded, darker colours increased, more bituminous, undulous bedding upto 20 cm, local thin calcite veins parrallel with bedding, all lime mudstone.
123	128	Oxide zone along section 5-8 meters wide of Fe oxide, py + smithosiste and galena plus rare sphalerite, surrounded by flooding of dolomite and and calcite veins, convergent structural conduit original rock must have been fine grained mudstone due proximity with Aramachay contact, dolomite veining forms a mosiac and crackle breccia locally with small scale solution collapse features and cross cutting veings
		Oxide zone described above, some parts of the showing total sulphide, sample of dolomite alteration and coarse recrysta, asscoiated with hydrothermal event - surrounding rocks are all lime mudstone , local poddy confined vertical conduit.
		Above oxide, thin (5-15cm) bedded dark grey botuminous mudstone. TCh3 continuation of transistion into Aramachay due to trail and accesibility am moving slightly out of verticlal Floricita feeder system to south before I cut back.
128	136	TCh3 as last page described
136	141	no outcrop
141	150	Small outcrop pinkish wackestone, fairly thin bedded, med. grained limestone likely a thin wackestone unit in mud package may be local recrystallization due to proximal calcite veining.

Appendix 2 - Floricita Log

150	153	Aramachay? Fine grained thin internal laminations, black bituminous limestone, may represent a transition zone, not a lot of outcrop, following structural trend...
153		Aramachay with local solution , frags are monolithic, various in size, angular, total grey and black limestone, bedded, no fossils identified.
		Aramachay, typical thin bedded lmst very bituminous, appears to be a fine associated organic component
160	169	Black, very fine grained thin bedded, non calcareous mudstone with slightly finer shale partings.
		Aramachay - typical late clear white subvertical calcite veining.
		Beautiful exposure thin cliff face of thin bedded to laminar black-dark grey very bituminous, locally undulous and locally well perserved large coarse nodules in places up to 0.5 m long found conformably orientated with stratigraphy, locally fissile black shale partings - very finely laminated.
183	195	Nodules and undulous bedding in Aramachay
195	200	Transition into Condorsinga thin laminar bedded black bituminous mudstones.
		Cyclic thin and medium bedded locally calcareous black bituminous mudstones and laminar thin bedded fissile shale horizons, starts to get brown towards 210 more
180	210	calcareou transition into Condorsinga approx. 230/240, bedding in Upper Aramachay/Condorsinga very undulous, between 0.5-1m between each med. bedded 20-40 cm bed.
		At 206 contiunation of thin shaley beds and thicker 20 cm black bituminous fine grained calcareous mudstone - large cyclic interval
212		Beds become thicker +/- 40 cm and shaley partings considerably thinner to almost non exsistent inot a fairly monotenous med. Bedded package
		Condorsinga , coarse recrystallized (?) dolomite due o proximity of Floricita deposit (not recrystallized) - significant amount of hydrothermal dolomite alteration (ground preparation).
232		Lowest adit - predominantly coarse grained dolomite and hydrothermal dolomite and sphalerite.
		Condorsinga forms a bedding parallel vein system with local dissolution along bedding planes. excellent samples for fluid work as well, dissolution collapse can be on a metric scale.
		Though pervasively altered and oxidized beds remain very consistent, similar to typicla condorsinga through 236
		Solution collapse , all avaliable stratigraphy until across collapse structure and head up the other side or trail to camp. I can visibly see the Goya cutting down through the stratigraphy.

Floricita Samples	**Description**
cjr25/06/99-1	From lower zone of Floricita @ upper adit, very coarse sphalerite and py + dol and calcite (3 pieces - representative - Condorsinga
cjr25/06/99-2	Show beautiful frags (pyrite/marcasite) and classic mvt/sphalerite/dol cement, beautiful sample - same location upper adit Condorsinga.
cjr25/06/99-3	Fine-med. Grained dolomitic mudstone of Condorsinga Fm (from upper adit)
cjr25/06/99-4	Fine grained dolomite of condorsinga immediately out of system
cjr25/06/99-5	60 m from adit along trail p 14/15, no sphalerite, Fe and dolo show frags different alteration style
cjr25/06/99-6	From 12 m above adit plus 60 m north
cjr25/06/99-7	Lg. massive sample from tunnel Condorsinga
cjr25/06/99-8	Lg. sphalerite from tunnel
cjr25/06/99-9	Vein of dolo and sphal in rather fine unaltered dol above main showing below Goya contact excellent vertical feeder example
cjr25/06/99-10	From 25 m above adit coarse sphalerite and dolomite alteration and mineralization
cjr25/06/99-11	Zebra below goya, 20 m above adit (467364 (old cominco smpl site)
cjr25/06/99-12	Odd fe oxide + pyrite and dolomite and gerrisite + hematite alteration nyear goya
cjr25/06/99-13	Coarse sphalerite and dolomite with Fe style alteration near goya contact (pic 23/24 and odd Fe cement. Some quartz grains (collapse from goya)

Appendix 2 - Floricita Log

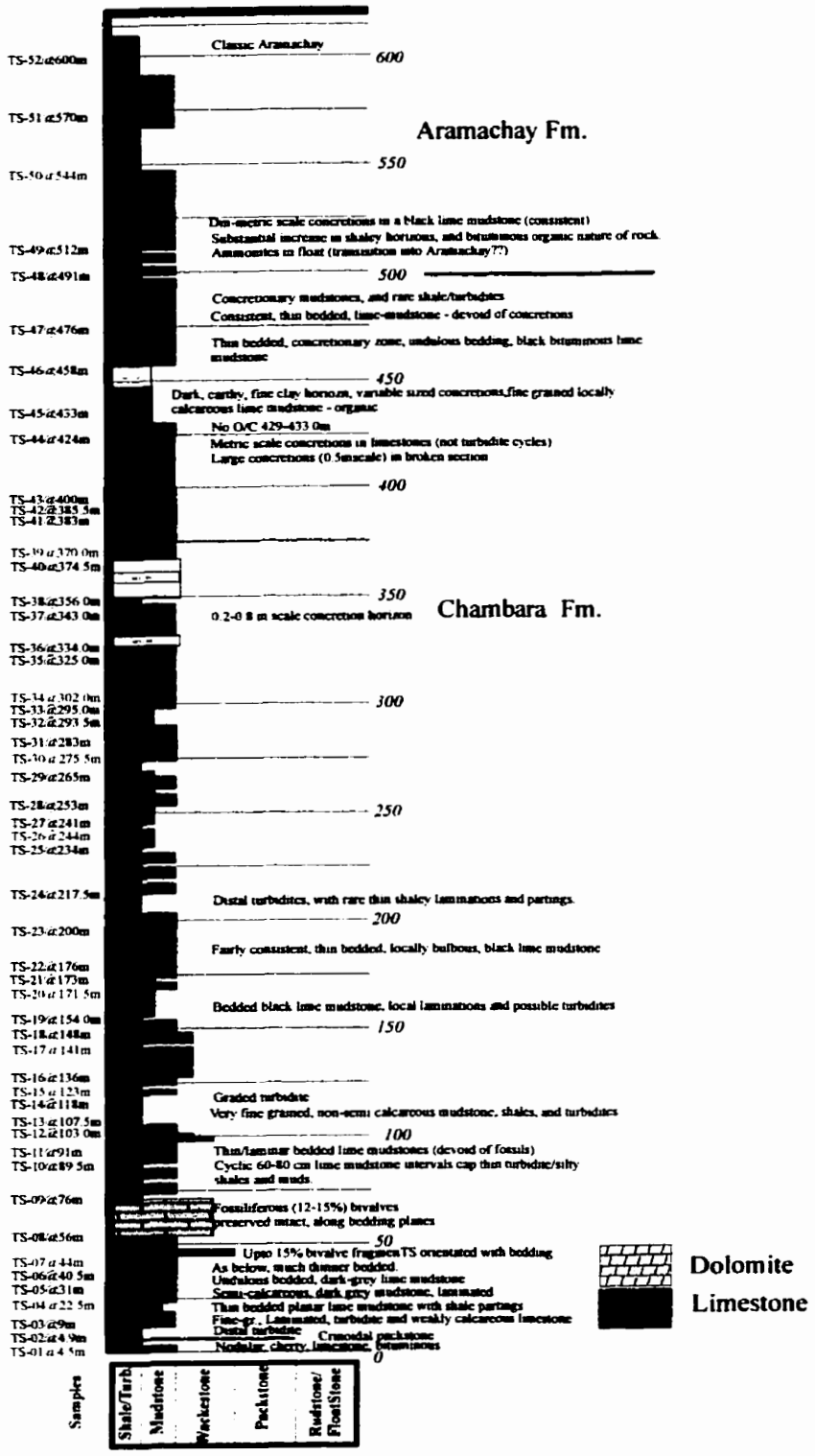

Appendix 2 - Tesoro Section

Tesoro Section Log

Meterage To:	From:	Description:
0.0	2.2	Very fine grained, grey weathering, black organic-bituminous, chert nodular, lime mudstone, fine bedding (8-10cm), lg. Resistive weathered blocks (2-3m), weathers to an undulous - seminodular character. Chert nodules are black and irregular in shape (2-10cm).
2.2	4.5	Thin undulous (nodular0 bedded black bituminous locally laminated on a cm-mm scale (distal turbidite).
4.5	4.9	Med bedded (30cm) crinoidal packstone, with rare bivale fragments, med-coarse grained limestone, rare calcite veining.
4.9	9.0	Fine grained, black-brown-grey, thin-med. bedded with thin internal laminations (distal turbidites), very black-d.grey fresh surface, bedded on a 5-10 cm scale, with internal lams remaining fairly planar.
9.0	18.0	Thin bedded (8-10 cm), black, semi bituminous, planar lime mudstone, bedded with thin (2-3 cm0 black shaley horizons (2-3/m).
18.0	21.0	Thin-med bedded, fine grained black-dark grey, bedding (5-15cm), local rare internal lams - calcite veins (vertical-subvertical over 0.5m) (2-3 cm wide look extensional with rare internal tension gashes).
21.0	27.0	Similar med-thin bedded black to dark brown slightly bituminous lime mudstone with thin cm-mm scale internal lams and rare calcite veins, locally lams and veins weather out resitavely. (likely distal turbidites).
27.0	31.5	As above but thin shaley-silty layers, parralel with bedding every 15-20 cm, slightly undulous towards the top (nodular).
31.5	36.0	Thin-med consistently planar dark grey-black lime mudstones, slightly undulous (nodular) @ 34.0 m 20 cm cherty horizon, @34.8-35.0 waterfall, zone continues up.
36.0	43.0	Slightly thinner bedded and undulous-nodular, dark-brown, light-med. Grey lime mudstones, rare internal laminations in undoulous horinzons, coarse calcite veining.
43.0	46.0	No OC @44.0m fine grained, dark grey, lime mudstone packed full of larege intacet 5 cm bivalves.
46.0	53.0	Med-thin bedded (5-30 cm) dark grey-black fairly non descript lime mudstone, weathered surface is fairly brown, thin-thick sub-vertical calcite veins forming locally a distinct mosiac-crackle pattern - prominent fracture pattern can easily be confused for bedding.
53.0	72.0	Med. Grained, medium bedded dark gry to brown weathering slightly nodular lime mudstone with abundant fossils observed along bedding planes (intact up to 4-6 cm), bedding can once again be easily confused with subvertical fracture system.
72.0	88.0	Same as above but devoid of bivalve debris, bedding has remained fairly consistent, thin to local med. (5-20 cm scale) remains very dark grey lime mudstone, thin bedded units usually cap 60-80 cm cycles with rare underlying thin laminar zones representing possible distal turbidites, rare fossil debris (intact bivalve monotis through 88).
88.0	94.0	Black to brown very fine grained, med-thin bedded (cyclic) (15-40 cm) with local networks of coarse calcite veining gennerally subvertical small poddy local areas of coarser recrytallization.
94.0	100.0	Slightly coarser grained wackestone, rare nodular horizons, rare large intact bivalves perserved along bedding plane@ 97.0 m (complete intact bed). Black weathering with grey fresh surface to brownish/buff, thin finer grained limestone beds through upper half of this zone.
100.0	103.0	Slightly thinner bedded, locally nodular with undulous bedding, slightly more orgainc and bituminous with rare larger blebs of pyrite - large bivalves still observed intact.
103.0	107.5	Brown weathering, dark grey fresh surface, med-thin bedded (10-20cm) slightly undulous with thin shaley horizons defining slightly thicker beds, locally nodular in more compotent rocks, sub vertical calcite veining throughout (rare lg. Intact bivalves @107.5 bedding has really shallowed.)
107.5	118.0	No oc, however creek boulder fill (angular) suggests that the same horizon is present @111.5 boulders are observed as rare angular blocks that exhibit fine internal laminations likely representing distal turbidites, and in one case a thin (5cm0 samdy grade turbidite was observed).
118.0	121.0	Dark grey-black, thin bedded locally bituminous, rare laminations, local Fe oxide (limonite) alteration.
121.0	123.0	Thin graded turbiditic horizon with dark grey laminar very fine grained to local cm scale sandy beds, very calcareous.

123.0	127.0	Med. Bedded. limemudstone, dark gry with intact bivalves along bedding planes and pervasive subvertical clacite veins withing extensional fracture systems. Slightly undulous to nodular. local coarse recrystallization due to calcite flooding.
127.0	148.0	Thin bedded. nodular. rare thin lams in more compotent units. lime mudstones-wst within thin pyritic horizon - huge (8-10cm) intact bivalves perserved along bedding planes. bivalve zone becomes med bedded but remains consistently fossiliferous through 136m. local calcite veining with pyrite observed within samll local dissolution zones observed at cross cutting vein boundaries.
148.0	154.0	Similar with slightly more nodular black to dark grey organic beds. Top of unit can likely be subdivided due to identification of local thin laminations suggesting distal turbidites (no graded or sandy horizons identified).
154.0	167.5	Thin-med. Bedded black lime mudstone. local laminations and possible turbidites, weathering is pale brown and implaces a slightly bulbous, fairly pervasive calcite veining (non fossiliferous) increase in fine laminations of the rock.
167.5	171.5	Very laminar in 0.5 m thick bedded cycles - dark grey-black. brown to grey weathering. @168.5 - 0.4m nodular horiozon black calcareous lime mudstone. @169 coarse clacite veining forming a local solution collapse and intersecting vein systems. frags all very angular and sub rounded.
171.5	173.0	Med. Bedded on a 0.5 meter scale, slightly undulous bedding, fairly large vugs and pods of coarse calcite, rare thin internal laminations (dubious turbidites)
173.0	200.0	27 m of strat exposed but unable to study due to very steep waterfall and vertical rounded water shoot, you can see the rock has become slightly thinner bedded and does show some internal laminations that are being resitively weathered, black todark grey weathering and locally slightly bublous - structure reamians very consistent.
200.0	205.0	Black, very fine grained, semi-bitumionous, med-thin bedded. lime mudstone, locallylaminar, thin bedded lenses and zones of pyrite , local bulbous weathering, laminar interbeds of limemud and siltstone with thin to med bed.
205.0	211.0	Thin bedded turbidites with thin shaley partings, possible more proximal coarse grained turbidites over 20 cm.
211.0	234.0	Thin bedded. black-dark grey, bituminous mudstones showing differential palnar weathering marks a continuation to this zone - bedding got farily steep @ upper waterfall. Main character of rock remains a black semi bituminous thin bedded lime mudstone with local turbidites, zone continues as described - laminar nature, black fresh surface. very fine grained. brown weathered surface.
234.0	253.0	Local very fine grained, laminar, black semi-organic, semi bituminous, lime mudstone, structure through 238 slightly undulous, local nodular texture, samples show fine grained black organic matrix with very thin laminations of pyrite and slightly coarser calcite with possible very thin - fine graded bedding, sample is an excellent of what this unit looks like @241 boulder of fe oxide plus collaformal pyrite all rocks in this unit are very laminar, exhibiting differential weathering, sandy-fine turbiditic laminations observed.
253.0	265.0	Slightly more med bedded, but very sonsistent, rare internal laminations (possible distal turbidites), difficult section due to another waterfall.
265.0	272.0	Beautiful bedded turbiditic horizon, shows fine lamination, locally grading down to a basal sandy horizon. very dark grey-black, fine grained, slightly bituminous, fine bedded to laminar.
272.0	283.0	Appears fairly thin bedded with knotty bulbous to undulous (nodular?) weathering. Black, to d. grey lime mudstone, strucutre remains fairly consistent, local boulders show well developed fine laminations (distal turbidites?) fairly common brownish weathering associated with a pitch balck fresh surface.
283.0	293.5	Beautiful laminar, dark brown lime mudstone bedded on a 10-15 com scale, thin-very thin istal turbidites observed sporatically throughout unit. local rare slightly undoulous bedding - v. fgr.
293.5	302.0	Same zone. very black, finely laminated +/- pyrite, late poddy and veining calcite has very local poddy coarse grained pyrite - perhaps as a remobilization or as a result of a later system, locally beeded on a slightly thicker scale but still showing fine internal laminations, only slightly calcareous slightly silty with the rare fine shaley bed - blebby to poddy brassy coloured pyrite observed (blebs 2-4 cm)
302.0	314.0	(Cominco reference point - p.161 MT) fine grained, pitch blakc, med. bedded limestones with fine sphalerite blebs (2 cmx4cm very coarse grained red sphalerite) taking the same form as pyrite has in the system (replasive) orientated parrelle with bedding (seddexy) planar bedded thin (5-8cm) and thin internal laminations throughout.

314.0	318.0	Dark grey to borwn, bedded with 1-2 thicker beds (upto 25 cm) per 2 m of stratigraphy. Still slightly laminated except with no grading observed.
318.0	323.5	Difficult oc - weathered surfaces showing bulbous nodular weathered surfaces, med. Bedded, slightly bituminous, d. grey fresh surface lime mudstone - fairly monoteneous.
323.5	326.0	Very fine grained black laminar very calcareous lime mudstone with lams on a cm-mm scale commonly slightly coarser grained with silty lams, fine bedding parrallel pyrite, in river blocks containing decimentric to metric scale concretions obsereved.
326.0	334.0	No OC - quaternary debris and gravels, with smal angular blocks of lime mudstones.
334.0	340.0	Fine bedded, laminar , pyritic, fairly consistent calcite veining, beds are slightly thinner and becoming more undulous, havent observed anv well preseved concretions since lower horizon
340.0	343.0	Fine bedded, laminar , pyritic, fairly consistent calcite veining, beds are slightly thinner and becoming more undulous, havent observed any well preseved concretions since lower horizon, some coarse filled extensional calcite veins with rare glauconite and ankerite (Fe carbonate)
343.0	349.0	Fine grained, black-dark grey with brownish weathered surface, fine internal laminations (distal turbidites) however no graidng or sandv beds observed.
349.0	366.0	No O/C - good structural correlation
366.0	370.0	Very thin bedded to laminar dark grey-black weathered grey fresh surface, calcareous lime mudstone, laminar to platev (thin shalev horizons begin to develop (2-3 cm)
370.0	374.5	Fine grained, with locally coarser wst limestone, thin-med bedded with no fine laminations or pyrite observed, local platev shalev thin horizons still observed.
374.5	383.0	Fne grained, black - dark grey, laminar lime mudstone, fine disseminated pyrite, o?c's show very consistent thin bedding with local thin organic layers and local brown weathering, observed turbidites in creek boulders.
383.0	397.0	very laminar to fine bedded brown weathering, undulous bedded, very faint wavelength (amplitude), locally no clacerous, fissile with thin shaley partings interbedded on a 20-30 com of fairly massive fine-locally recrvstallized limestone, local laminated.
397.0	400.0	Black, organic, brown weathering, slightly undulous (locally concretionary) with fine disseminated pyrite. Concretions varv in size from 5-25 cm, and are orientated parrellel with bedding.
400.0	408.0	Black, -dark grey , very fine grained, thin to laminar bedding, concretions as above interbedded, med-slightly thicker beds (30-40 cm) rare.
408.0	424.0	No O/C, NOTE: very large concretions (upto 1m) preserved in subcrop in creek.
424.0	429.0	black, very organic, thinnly laminar (distal turbidite) lime mudstone, very black with fine disseminated pyrite and large concretions observed @ 429 large metric cscale concretions
429.0	433.0	No O/C
433.0	442.0	Dark earthy almost limonitic weathering with fine clay horizons interbedded, *very reminisent of transition @ Buenos Aires -variably sized concretions still observed - horizon can definently be described as concretionary in a verv fine grained lime mudstone, locallv organic lime matrix.
442.0	458.0	O/C sparse @445 concretions observed
458.0	470.0	Thin-med. Bedded, concretionary zone, with associated undulous apperance to bedding, black bituminous limestone.
470.0	476.0	Incredible section of med. bedded bituminous lime mudstones with cm-metric scale concretions, small waterfall beautifully cut through stratigraphy so I got an excellent cross section (through a thin shaley organic concretionarv package and then into a med. bedded concretionarv package.
476.0	486.0	Slightly thinner bedded, more bituminous and derease or lack of any concretions, bedding planar.
486.0	491.0	Thin-med. bedded (5-15/20 cm) concretionary as above in fine organic dark grey-black organic matrix. Thicker beds defined bv (5-10 cm) thin shalev fissile non-calcareous horizons (locallv silty).
491.0	512.0	Substantial increase in shaley horizons and bituminous/organic nature of the rock **ammonites in float - no O/C vet, thin-med. Bedded (8-15) calcareous grev-black fresh surface - brown weathering.
512.0	521.0	Lg. Metric-dm scale concretions in very black fgr. Calcareous organic lime mudstone, thin 3-5 cm shale horizons marking limestone beds.
521.0	545.0	Thin- locally med. Bedded, undulous-planar very reminiscent of last 20 m - rare concretions however a dramatic decrease in overall total content.
545.0	562.0	Fine-very fine grained, black-d. grey, bituminous to organic, locally non clacareous with 30% shale horizons, and local siltv lavers (lenses). Verv rare cm-dm scale concretions.

Appendix 2 - Tesoro Log

562.0	585.0	No O/C, black bituminous fine grained. locally calcareous, brown weathering, shaley limey mudstone (rubble).
585.0	618.0	Excellent Aramachay - black to very dark grey, grey weathering, locally clacareous mudstones, fine-thin bedded with thin (5-15 cm) lime mudstones horizons every 2-3 meters, extrememly organic and bituminous, rare dm scale concretions in certains more organic horizons, no fossils identified vet.
618.0		END SECTION - teraine to steep and Aramachay stratigraphy becomes overgrown by jungel. Getting very high up in the canyon now...

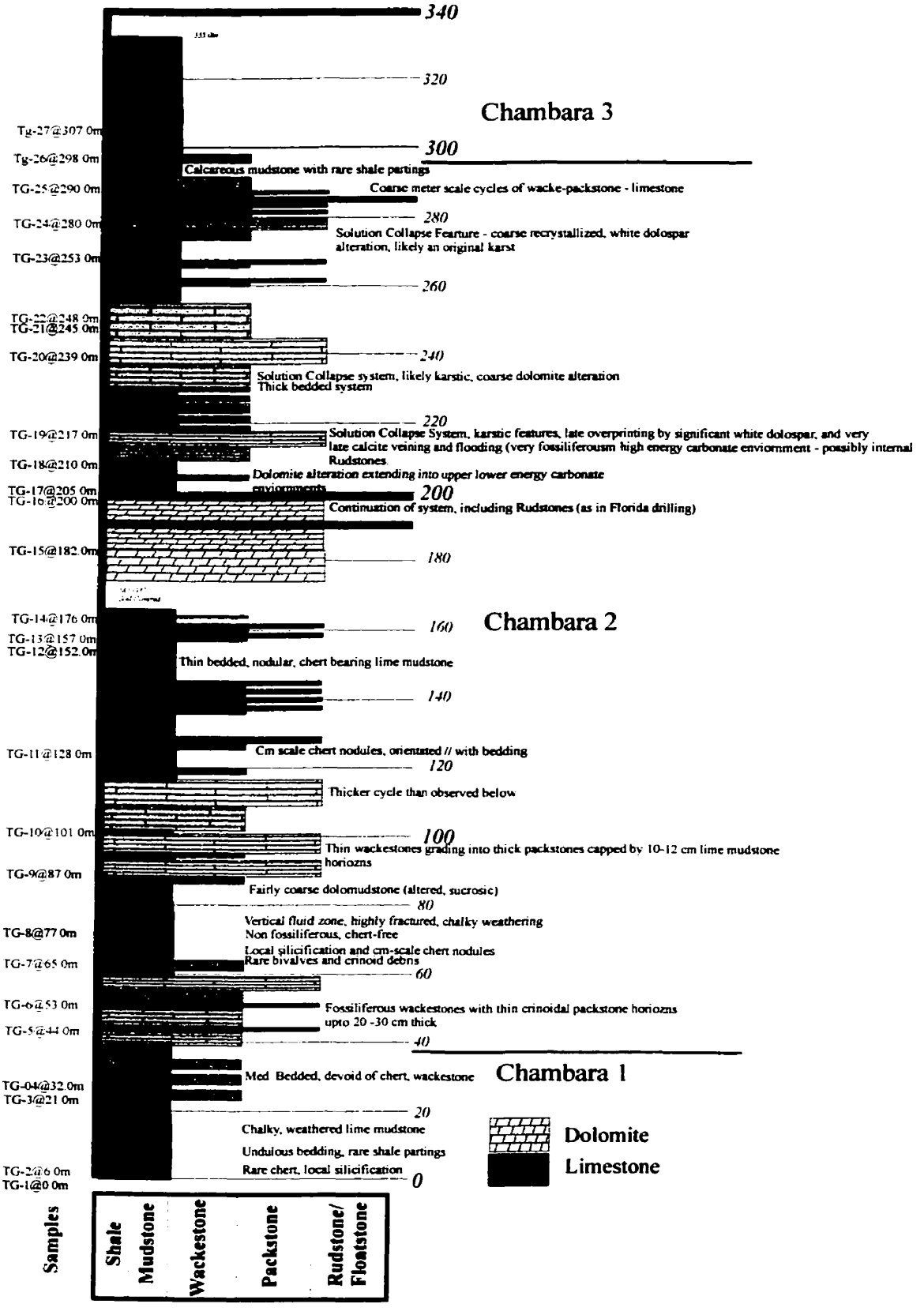

Appendix 2 - Tingo Section

Tingo Section

Meterage To:	From:	Description:
0	9	Fine grained dark grey-black, beige weathered, thin bedded (10-15 cm), slightly bituminous lime mudstone, (cm) scale chert nodules aligned parallel with bedding.
		At 6 meters bedding remains the same but undulous defined by weathering, appears thinner, slightly shaley thin calcareous mud horizons, rare chert nodules, local silicification.
9	15	Chalky altered, fault zone, rubble, predominately a lime mudstone, no original sedimentary textures preserved.
15	18	Same unit, thin, undulous bedding, lime mudstone as at start
18	23	White chalky alteration, focused along fractures, predominately a mudstone horizon - nor original textures observed due to alteration
23	33	At 23 meters bedding becomes med. (20-30 cm scale), highly fractured with calcite veins, black-to dark grey, very fine grained, not bituminous lime mudstone.R13-#4, med. Bedded 15-20 cm dark grey to black lime mudstone, rare large blebs of calcite, thin late calcite veining, consistent structure, locally undulous, beige to grey weathered, locally recrystallized to a wackestone texture (check with petrography) - devoid of chert.
33	39	Med. bedded (15-20cm), very undulous limestone defined by thinner lime mudstones along bedding contacts R13#5/6
39	53	Similar undulous med. bedded but wackestone, rotted weathering, locally fossiliferous packstone
53	59	Fossiliferous wackestone-packstone, intact bivalves and crinoids plus other unidentifiable debris, high energy environment.
59	65	Med. to thin undulous bedded lime mudstone, thin bedded 95-10cm), rare bivalves preserved with partial crinoid osicles (wacke).
65	71	Nodular undulous chert lime mudstone, no fossils identified.
		Chert zone, rare late calcite veining, vertical mosaic developed and nodules of non chert similar to TCH3.
71	78	No chert, med. Bedded, undulous dark grey chert lime mudstone, fairly consistent, no fossils, no chert locally silicified.
78	81	Local fault zone, local fault gauge. Angular fragments, chalky, no structure observed.
81	86	Small poddy local zones of dolomite and dolomite veins following vertical calcite network observed below., dark grey to black lime mudstones, no fossils, chert med. Bedded to undulous - similar calcite veining, structure remains very consistent to level.
86	101	Chert nodular (5-8 cm) undulous bedded (thin wackestone wand packstones marked by thin 15 cm mudstone intervals.
101	116	Transitional thick wackestone to packstone marked by a slightly thicker 20 cm mudstone bed.
116	119	Lime croinoidal Wackestone, med. grained, thin to med. Bedded, locally undulous bedding .
119	125	Undulous chert - med.-thin bedded 10-20 cm pervasive

Appendix 2 - Tingo Log

125	128	Wackestone-packstone - med. Thick bedded
128	135	Thick bedded , locally undulous limemudstone, no calcite alteration observed,
135	146	Wackestone, lime, calcareous, crinoidal, med. to locally coarse grained, internal packstones over cm scale intervals of coarse shelly high-energy debris.
146	155	Thin bedded, nodular chert bearing lime mudstone.
155	161	Crinoidal wackestone-packstone as per typical Florida TCH2.
161	166	Black dolomite-lime mudstone, med. Bedded, thin cm scale wackestone interbeds (0..5 m scale) recrystallized dolomite locally giving a sucrosic look.
166	173	No outcrop poor slope soil cover
173	182	Solution collapse system, fragments are generally med. Coarse grained with significant fossil debris (high environment, locally the protolith was a very porous packstone. Pervasive dolomite alteration (hydrothermal? Coarse white baroque dolomite.) Highly altered but possible internal sediments identified. Dolomitic wackestone coarse crystalline recrystallization of matrix, brown to beige weathered surface with late coarse calcite veins.
182	191	
191	200	Total recrystallization of system by coarse calcite, must represent replacement into a higher energy packstone or rudstone (some dolomite - overprinted by calcite.).
200	210	System extending through 206 meters fragments are predominantly high energy wackestones and rare thin black bituminous mudstones (calcareous). Dolomite altered local solution collapse system. Outcrops are rounded and weathered and devoid of all structure alteration and breccia/fault matrix is a very yellow-white chalky carbonate matrix dolomite appears to be confined to the lower parts.
210	217	Coarse recrystallized lime packstone, very coarse recrystallized dolomite and calcite, thick bedding on a 0.5 m scale, beige to white Fe oxide stains along fractures likely upper part of collapse system below.
217	233	Thin bedded undulous lime wackestone with thin mudstone intervals
233	245	Coarse recrystallized lime wackeston and packstone, thick bedded unit, very altered, solution collapse system, likely y overprinting of a early karst system (possible thin internal sediment).
245	253	Coarse- med. grained lime wackeston, white to pink weathering, very coarse calcite may be packstone of reefal facies.
253	274	Thin-med. bedded undulous lime mudstone.
274	280	Solution collapse feature, fragments are round, predominantly wackestones, with rare packstone clasts, fine grained dolomite matrix
280	287	Large intact bivalve wackestone-packestone cycle, coarse crystalline calcite and limestone, fragments are predominately high energy shell debris Thick bedded to 0.5 m scale and yellow weathering, local @ 283 reefal floatstone for 4 meter thickness

287	290	Med. grained wackestone, rare crinoids
290	294	Thin bedded lime mudstone, thin black shaley partings, undulous laminar bedding, is bivalve observed along bedding planes.
294	298	Fossilifeorus wackestone, thin-med. bedded with rare bivalves intact locally undulous
290	315	Black thin bedded laminar, local lime mudstone
315	335	Planar thin bedded local undulous lime mudstone

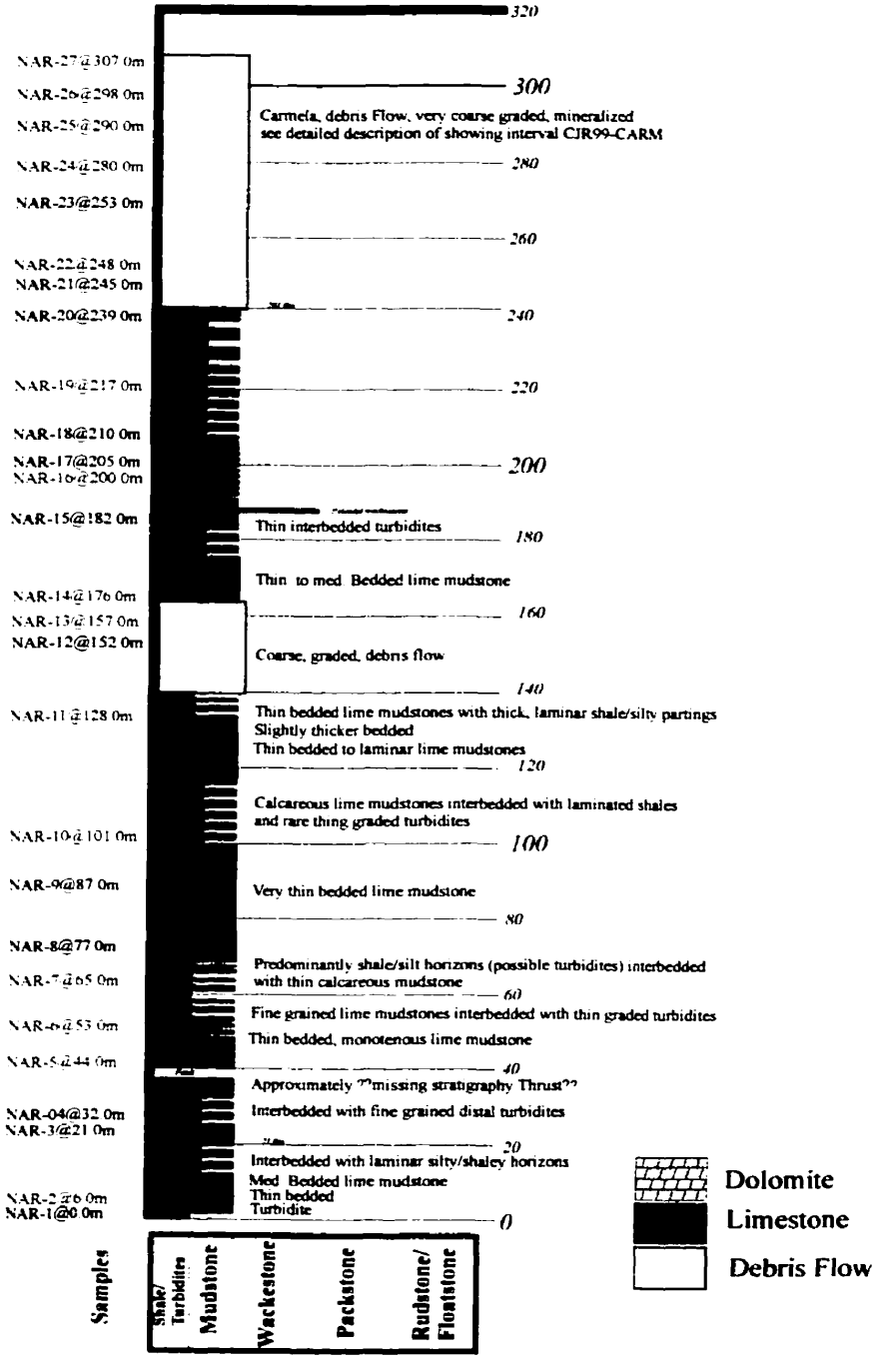

Appendix 2 - Naranjitos Section

Naranjitos Section

Meterage From:	To:	Description:
		note: mitu contact approximately 100 m (strat) down section).
0	0.5	Med. bedded, 30-40 cm, brown weathered, planar bedded, defined by calcareous silty lamination. Beds no more than 10 cm thick, representing interbedded graded turbidites, fine grained black lime mudstone.
0.5	5.5	Same lithology slightly thinner bedded and back to non turbiditic intervals (10-30 cm)
5.5	12.5	Black semi-bituminous very fine grained med. Bedded (20-40 cm) planar lime mudstone without any bedding silty units (possible thin interval @ 6.5 m of graded distal turbidite (sample) o/c devoid of any alteration
12.5	21	Same med. Bedded unit with renewal of thin laminar silty calcareous horizons over 5 cm thick, rare thinner beds (8-15cm) interbedded planar
21	26	Loose o/c but structure remains very consistent, beds are subvertical.
26	32	Same unit except consistently med. To locally thick bedded, still defined by these shaley, probably finely graded distal turbidites.
32	35	10-15 cm thin bedded non-bituminous lime mudstones, dark black to dark grey 34 m - med.-thick bedded, dark brown -dark grey lime, non-bituminous lime mudstone without the shaley-silty calcareous laminar sections, seams very homogeneous and structure is consistent, likely very deep stable basinal conditions 35 m -1, 40 cm thick bed shows very fine black semi-undulous laminations singled bed weathers to a much paler brown, buff colour though slightly coarser grained no graded bedding is observed 39m - on wet surface weathered surface varies from planar laminations, size grading observed, turbiditic horizon R15 3/4/5/6/ (differential weathering) Entire zone shows grading between a buff brown for thicker beds (less bituminous dark grey brown) lime mudstone with fine possible organic wisps and dark grey slightly more bituminous slightly coarser lime mud-wackestones
0	9	**Thrust Sheet** Fairly thick section of predominantly thin bedded lime mudstones, light -med. Brown weathers with a dark-grey locally black, non bituminous fresh surface, bed is planar 10-15 cm.
9	15	Fine to locally coarser grained lime mudstone with fine very well defined turbidites on a dm scale over interval in total each thin-med. bed is marked by either a bedding // or planar resistively weathered silty zone or an interval semi undulous well defined graded turbidite, sample 7 exhibits local soft sediment deformation
15	31	Thin bedded (8-12) cm) marked by 2-5 cm thin black resistively weathered semi-calcareous silty - shaley beds within thin bedded buff weathering dark grey non bituminous lime mudstone beds, either very fine distal turbidites of possible thin algal laminae's. R15 9/10 - silty/shaley lams

Appendix 2 -Naranjitos Log

31	38	Units becomes more of planar thin bedded dark grey weathered monotonous lime mudstone local thin poddy wackestone beds, showing local diagenetic recrystallization to a slightly sucrosic texture, rare calcite veining that really shows no significant alteration, veins run sub-horizontally in a vein-web network.
38	51	Becomes very black weathered thin to laminar bedded-dark black fresh surface very bituminous no apparent alteration very fine grained lime mudstone, though laminar, no where can say this has any turbiditic characteristics, commonly fine grained blebs to fine disseminated pyrite is observed, blebs tend to be// with bedding and look like tiny concretions no greater than 5 cm in scale.
51	60	Slightly thicker bedded black lime mudstone (15-25 cm scale bedding) planar - laminar turbiditic unit with fine disseminated py and blebby py - more laminar than other overlying intervals - good samples
60	75	61 meters -same unit but turbidites and bituminous mudstone units become thicker up to 30-40 cm - again alternating zones are becoming very well defined based upon differential weathering as observed earlier in section south of thrust.
75	87	Fine bedded, very bituminous laminar to finely bedded lime mudstone with thinner possible turbidites, but a much more limey mudstone, thin bedded, unaltered section
87	94	Same but much more black and bituminous thin laminar semi-calcareous lime mudstones
94	99	Out of laminar zone and back into very thin bedded black weathered dark-grey fresh surfaced limestones with thin silty parting// and planar to bedding, local areas of slightly coarser grain size as a result of coarse calcite veining and associated poddy recrystallization
99	123	Debris flow, conglomerate large boulder fragments med. (5cm) fragments in a breccia fashion appears all polymictic with rare siliciclastic quartz and sandstones (predominately mudstones, look like Mitu picked up in slope debris...
123		Appear to be a thinly bedded lime mudstone exhibiting differentiated weathering, slightly coarser grained lime mudstone-wackeston first visible o/c
135		Fine grained, thin bedded, laminar turbidic limemudstone Very black and very bituminous
135	149	Planar non turbiditic lime mudstone, rare calcite veining, thin wackestone intervals (oolitic)?? Petrography needed, non turbiditic.
149	201	Dark to med. Grey weathered, fine (thin) med. Bedded, thin laminar colour features defined by differentiated weathering - 1 m zone of friable non calcareous black very bituminous siltstone-shale, thin laminations show very fine grain size variation and possible grading suggesting possible thin turbidites - o/c is right in a waterfall and hence in a very eroded, bulbous and difficult to sample - very black with fine grained disseminated pyrite coarse calcite veining forming a subvertical network through stratigraphy - possible soft sediment deformation shows laminar displacement along beds - slump not total detachment.
	201	End Section - loss of measurable outcrop

Appendix 2 -Naranjitos Log

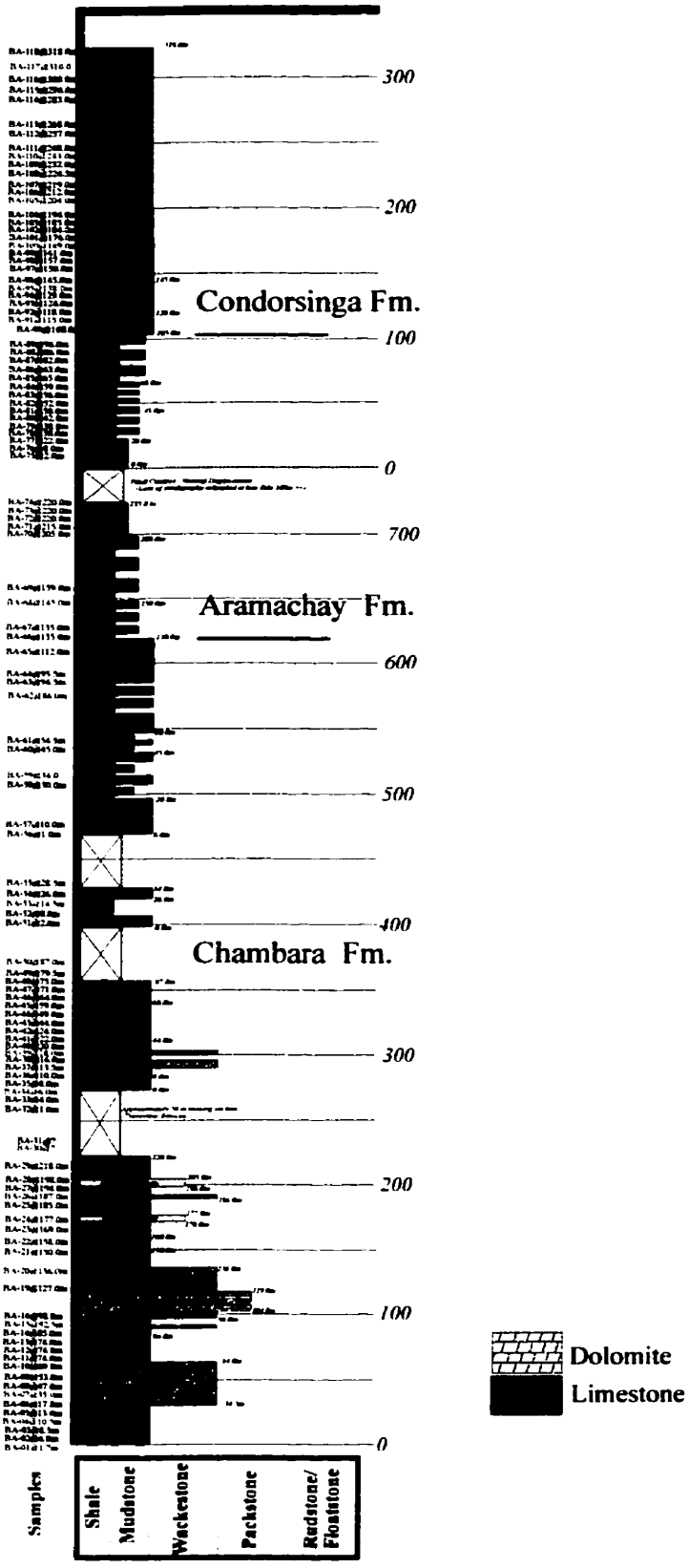

Appendix 2 - Buenos Aires Section

Buenos Aires Section:

Meterage To:	From:	Description:
0	5	Black to dark grey fresh surface. fine grained, lime mudstone, very calcareous, cut by thin fine calcite veins orientated parallel with bedding. Med.bedding thickness between 15 and 20 cm, slightly bituminous, thin darker oragnic wisps. Gets slightly thinner bedded towards 5.0 m, possible pelloids.
5	34.5	Rock remains medium to thinnly bedded, dark brown, fine grained , crystalline limestone, locally very late dissolution breccia, frags are up to 15 cm, angular and of above mentioned protolith cemented by late crystalline calcite in places forming beautiful vug lined crystal growths (travertine).
34.5	64	Possible fine grained pelloidal content . Dark brown/gey to black, very fine to fine grained with local med. Grained beds(?), Medium parralel bedded (20-40 cm scale), rock remains consistent except it appears to pick-up pelloidal-oolitic fragments in groundmass. changing character to a more lime wackestone.
64	84	Solution breccia/fracture travertine, matrix of rock remains consistent, looks like a very late travertine as described above. It appears that the travertine or late breccia has reworked approx. 20 meters of the stratigraphy so I am going to assume that the bedding remains consistent and will sample through this section. parts of the alteration cement may be ferroan calcite , very coarse grained and openly vuggy, likely related to fault structure, Frags exhibit fine scaled bedding on a cm scale , and is still a lime mudstone with possible wacke intervals.
84	96	Very thinnly bedded, pale grey mudstone, locally with thin wackestone horizons, bedding is very thin on a 5-10 cm scale, as where below 64m it was a 20-40 cm scale (all very well defined), late calcite veining and alteration away from vein core.
96	104	Medium to thick bedded interval up to 50 cm, dark grey to locally black, very fine grained lime Wackestone, very homogeneous, possible pelletal content.
104	119	Back into thin bedded, buff weathering grey to dark brown fine grained lime stone, with possible psuedomorphs plus pellets(?), possible bivalve frags replaced by late calcite, very thin bedded on a 5 cm scale.
119	136	Travertine, late calcite /Fe calcite, possible a previous sbx due to visible features in talus fall. Bx frags to compare with original litho, likely slightly coarser wackestone or packstone lithofacies.No true high energy features, likely a wackestone. Thin bedded, dark grey lime mudstone-wackestone., medium bedded, dark grey limestone, no visible particles or frags, monotenous, calcareous, lightly fractured very difficult to estimate bedding in outcrop.
136	150	Medium to thick bedded (30-60 cm scale), lime mudstone, dark grey to brown, with rare calcite nodules (possible psuedomorphs?
150	160	Thin to rare medium bedded (5-25+/- cm scale) lime mudstones, local late travertine breccias and calcite veining, trace pyrite and rare oxidation of pyrite in grains of calcite Dark grey to brown, monotenous lime mudstone. Cyclic thin bedded monotenous lime mudstone, remains consistently thin bedded, no visible pelloids <<very difficult to see due to rain>>, late calcite veining , no evident fossiliferous content.
160	170	fine grained, dark brown, mudstone
170	177	Fine to very fine grained, black, bituminous, organic lime mudstone. Thin to very thinnly bedded (5-10 cm scale). Homogeneous and fairly consistent, no fossils observed. Possible slight pelloidal content(?), gives a wacke appearance in places.
177	186	As above, black fine grained bituminous lime mudstone to locally wackestone, however with well preserved full bivalve fossils in parralesim with bedding planes, very well bedded (thinnly 5-12 cm scale). Beautifully preserved bivalve (monotis) in a black semi-bituminous, fine grained lime mudstone matrix .
186	196	First lithofacie above bivalve unit (above)., med grained, highly recrystallized, sucrosic wacke (?). In places it looks like a packstone, but this is likely due to the coarse recrystalliztion, no true enviornmental indicators observed., finely bedded (5-12 cm scale). Alteration consists of a fine calcite veining and vug filling, possible with ferroan calcite . First lithofacie above bivalve unit (above)., med grained, highly recrystallized, sucrosic wacke (?). In places it looks like a packstone, but this is likely due to the coarse recrystalliztion, no true enviornmental indicators observed., finely bedded (5-12 cm scale). Alteration consists of a fine calcite veining and vug filling, possible with ferroan calcite. Black, fine grained, bituminous, organic, lime mudstone.
196	205	Dark grey, to brown and black, thin bedded (5-10 cm scale) , calcareous lime mudstone/wackestone (thin beds), slightly less bituminous, coarser pelletal content (?), may be diagenetic, worth subdiving from above and below calcareous/bituminous unit. Slightly more wacke than above, similar features, possible late diagentic recrystalliztion or pelloetal compositon.

205	220	Black, to dark brown, fine grained, bituminous, organic, calcareous, thinnly bedded (5-8 cm scale), rare fine calcite veining and sucrosic crystallization bordering veins, rather homogeneous and monotentous, still very calcareous, @220m enter into approx. 50 m (triangulation) of stratigraphy caught up in a late travertine breccia as described above in interval 64-84m. Samples BA-30 and 31 taken from within travertine (TBx) interval. Will start measuring strat at 0m. again
0	9	Very fine grained dark brown, well bedded (5-15 cm scale), nodular (first apperance - corresponds with silica as well??), cut by late calcite veins, weathers to a buff brown, very monotenous, 5-10% chert identifed in this interval. Mudstone, locally calcareous, could be defined as a lime mudstone
9	44	Same rock facies, mudstone, calcareous, slightly massive (resistant westhering), chert nodules upto 15-20%, inplaces, they seam to be forming/replacing in slightly more wackeish intervals. Possible thin wackestone beds, no visible pellets, however recrystallization to slightly coarser grain size gives apperance . Shows well developed late alteration fabrics, and a secondary porosity (diagenetic). Much higher chert concentration than above interval. Much thicker bedded upto 1 meter scale. siliceous/chert bearing mudstones show larger vugs filled by a late ferroan(?) oxide/calcite (?), fairly consistent over interval at 1-2%, rare bivalve fossil frags
		Fe OX/Chert and vug filling calcite .
49	63	Missing stratigraphy. Slope suggests that massive bedding observed below continues, rare fossil frags.
63	68	Consistent thin bedded section (+/-5 cm), lime mudstone, homogeneous, monotentous, fine grained, rare calcite veining, @ 68 meters 20 cm's of faint silicification.
68	87	Thickly bedded, dark brown mudstone, bedded on a 1-0.5 meter scale, local chert nodules and partially perserved bivalve fragments - orientated parallel with bedding planes., late calcite veining cross cutting bedding, massive TCh3 equivalent.
	87	Same rock type, med. Bedded, nodular, undulous bedding, dm to 5 cm scale. preserved bivalve (monotis?) fragments, late Fe oxide after pyrite?
		estimated 40 m of missing section (fault?) - start measuring at 0m
0	26	Very fine bedded (2-5 cm scale), beds almost upright providing for easy measurement, fine grained, black to dark brown lime mudstone over first two meters grading into interbeds of very thin shaley horizons. Alteration appears limited to late calcite flooding and veining with rare silicifcation. Very black, at time bituminous past 12.0 meters bedding gets slightly thicker 10-15 cm.
26	34	Med. Bedded (20-40 cm), section ends at 34 m. Either upper TCh3/L. Aramachay - some small fragments were perserved near base (chert) - good bedding to this small section.
0	20	Very thin bedded, black bituminous mudstone, well defined cm scale thin bedding.
20	45	Interbedded-, shale and mudstone, preferential horizons weathered to a bright brown, brick red colour?
45	60	Med. to fine bedded, predominantly non clacareous mudstones with thin black bituminous shaley horizons, rare thin strataformal horizons of mm. scale bedded pyrite, very common as well as thin late white calcite veining
60	130	Black thin bedded, locally bituminous, non - silicified mudstone with rare shale partings.
130		Slightly thicker bedded limemudstone with interbedded thin bedded black bituminous shales, either this is a section of the Aramachay or I just went threw a thick sucessioj of non-calcareous mudstones in the Tch3 equivalents
130	150	Rythmic thin and thick beds. Thin beds are gennerally shaleier. Thick beds are black, bituminous and fine grained, most coated by late calcareous partings.
200	235	Pitch black, fissile, bituminous, thin bedded mudstone - section continues to 235m. *across fault contact with Aramachay and Condorsinga, appears to be a slight fold so I have projected the section to start at the lowest most stratigraphy exposed, appears to be consistently thin to med. Bedded and in this section of road as incredibly well exposed for about 400 meters. - start at 0 again.*
0	24	Fine to med. Bedded (cm-dm) black bituminous mudstones and limestones (part of Aramachay) based upon preservation of three good ammonite samples 8-15 m bedding remains very consistent. Condorsinga black mudstones and shales, lose carbonate component and become very well bedded. Poorly consolidated Aramachay sequence, black organic mudstones (more of a mud) becomes more choclate brown with thin bedding of white to yellow clays (not calcareous - volcanic?).
24	45	Thinnly bedded black non calcareous mudstones and semi-consolidated mud and siltstones, bedding remains extremely consistent as earlier
45	52	Units become more consistent though they remain thinnly bedded 5-10/15 cm and slightlky calcareous.
56	68	Remains as above with three 1 meter sections of bedded 5-15 cm intervals
68	105	Thick bedded, slightly calcareous, fine-med. grained (locally) brown mudstone
105	120	Non calcareous brown to dark mudstone (grey to black) calcareous monotenous mudstone, med-thickly bedded (50cm-1.5 m)
120	145	Consistent thin bedded lime mudstone - at 161.0 meters becomes interbedded thin and thick beds, brown lime mudstones
		Total measured stratigraphy 1390 meters.

Appendix 3 - XRD Mineral Identification					
		Mineral Species Identification			
Sample #	Lab #	(a - abundant, m - moderate, l - minor, vl - very minor, ? - questionable)			
		(a,m,l,vl - relative mineral abundance)			*** - not applicable
		1st	2nd	3rd	4th
CR03-1	14463	calcite (a)	quartz (vl)	sphalerite (?)	smectite (?)
CR1-2	14464	dolomite (a)	calcite (vl/?)	***	***
CR1-3	14465	dolomite (a)	quartz (l)	calcite (l)	smectite (?)
CR2-1A	14466	dolomite (a)	calcite (m)	smectite (?)	***
CR2-1B	14467	calcite (a)	dolomite (m)	quartz (vl)	smectite (?)
MN-10	14468	dolomite (a)	quartz (l)	calcite (vl)	smectite (?)
FC69-1A	14469	dolomite (a)	quartz (l)	smithsonite (?)	***
FC69-1B	14470	dolomite (a)	smithsonite (m)	sphalerite (m)	sphalerite (m), gypsum (vl), calcite (?), smectite (?)
FC64-1	14471	dolomite (a)	quartz (l)	calcite(?)	smectite (?)
FC37-2A	14472	dolomite (a)	quartz (vl)	***	***
FC37-2B	14473	dolomite (a)	smectite (?)	***	***
FC23A-1	14474	dolomite (a)	calcite (?)	smectite (?)	***
FC23A-2	14475	dolomite (a)	sphalerite (l)	galena (l)	quartz (vl), cerussite (vl)
FC14-1	14476	dolomite (a)	calcite (vl)	sphalerite (vl)	smectite (?)
FC14-2	14477	calcite (a)	quartz (l)	dolomite (l)	smectite (?)
Milagros Show	14478	dolomite (a)	calcite (vl)	sphalerite (vl)	smectite (?)
Naranjitos Show	14479	calcite (a)	dolomite (l)	pyrite (l)	quartz (vl), smectite (?)
Carmela Show	14480	dolomite (a)	quartz (l)	calcite (vl)	smectite (?)
Anita Show A	14481	dolomite (a)	quartz (vl)	calcite (vl)	smectite (?)
Anita Show B	14482	dolomite (a)	calcite (vl)	smectite (?)	***
Yolanda Show	14483	cerussite (a)	goethite (l)	quartz (vl)	calcite (vl), smectite (?), mica (?)
Nancy Show	14484	dolomite (a)	sphalerite (a)	***	***
Charito Show #2	14485	calcite (m)	sphalerite (m)	quartz (l)	plagioclase (l), mica (vl), pyrite (vl)
Raquel A	14486	dolomite (a)	sphalerite (vl)	clacite (vl/?)	galena (?), Quartz (vl/?), smectite (?)
Raquel B	14487	dolomite (a)	quartz (vl)	sphalerite (vl)	calcite (vl/?), smectite (?)
Raquel C	14488	quartz (a)	dolomite (vl)	sphalerite (vl)	sphalerite (?)
Sonche	14489	dolomite (a)	calcite (?)	***	***
Isabel 1	14490	dolomite (a)	calcite (?)	smectite (?)	***
Isabel 2	14491	dolomite (a)	calcite (?)	sphalerite (vl)	***
My-23	14492	dolomite (a)	calcite (l)	quartz (vl)	***
My-11A	14493	dolomite (a)	quartz (vl)	smectite (?)	***
My-11B	14494	dolomite (a)	quartz (vl)	calcite (vl)	smectite (?)
My-3A	14495	dolomite (a)	calcite (vl)	quartz (vl)	***
My-3B	14496	dolomite (a)	quartz (l)	calcite (vl/?)	***
My-53A	14497	dolomite (a)	calcite (m)	***	***
My-53B	14498	dolomite (a)	calcite (vl)	quartz (?)	smectite (?)
FC4-15	14527	dolomite (a)	calcite (vl)	quartz (vl)	smectite (?)
FC4-21	14528	dolomite (a)	calcite (m0	quartz (vl)	***
FC4-16	14529	dolomite (a)	calcite (l)	sphalerite (l)	quartz (vl)
FC4-03A	14530	dolomite (a)	calcite (vl/?)	***	***
FC4-03B	14531	dolomite (a)	quartz (vl)	***	***
FC21-9	14532	quartz (a)	calcite (m)	***	***
FC21-47	14533	calcite (a)	quartz (l)	dolomite (vl)	***
FC21-36	14534	dolomite (a)	calcite (vl/?)	quartz (vl)	smectite (?)
FC29-32A	14535	calcite (a)	dolomite (m)	quartz (vl)	smectite (?)

FC29-32B	14536	dolomite (a)	fluorapatite (l)	quartz (vl)	calcite (vl)
FC36-40	14537	dolomite (a)	calcite (vl)	smectite (?)	***
FC36-35	14538	dolomite (a)	quartz (l)	sphalerite (l)	calcite (vl/?)
FC39-45	14539	dolomite (a)	calcite (l)	smectite (?)	***
FC39-43A	14540	dolomite (a)	calcite (l)	***	***
FC39-43B	14541	dolomite (a)	calcite (m)	***	***
FC26-09A	14542	dolomite (a)	calcite (vl/?)	smectite (?)	***
FC26-09B	14543	dolomite (a)	quartz (l)	pyrite (vl)	***
FC26-11	14544	dolomite (a)	quartz (l)	pyrite (vl)	***
FC26-17A	14545	dolomite (a)	***	***	***
FC26-17B	14546	dolomite (a)	quartz (l)	pyrite (vl)	***
FC26-24	14547	dolomite (a)	quartz (l)	calcite (l)	***
TG-14	14548	calcite (a)	quartz (l)	***	***
TG-24	14549	dolomite (a)	calcite (vl)	***	***
CJR25/06/99#2A	14550	dolomite (a)	pyrite (l)	gypsum (l)	***
CJR25/06/99#2B	14551	sphalerite (a)	dolomite (m)	gypsum (l)	smithsonite (vl)
CJR25/06/99#6A	14552	dolomite (a)	calcite (l)	pyrite (l)	quartz (vl), gypsum (?)
CJR25/06/99#6B	14553	sphalerite (a)	calcite (m)	dolomite (m)	gypsum (l), quartz (vl)
CJR25/06/99#15	14554	sphalerite (a)	dolomite (m)	gypsum (m)	pyrite (l), baryte (vl/?)
Tingo S - A	14555	calcite (a)	***	***	***
Tingo S - B	14556	dolomite (a)	calcite (l)	smectite (?)	***
Tingo S - C	14557	dolomite (a)	calcite (a)	quartz (vl)	smectite (?)
TS22 A	14558	calcite (a)	quartz (l)	dolomite (vl/?)	***
TS22 B	14559	calcite (a)	quartz (l)	***	***
BA-26	14560	calcite (a)	quartz (l)	dolomite (vl/?)	***
BA-39	14561	calcite (a)	dolomite (a)	quartz (vl)	***
BA-30	14562	dolomite (a)	calcite (l)	***	***
NRS-18	14563	quartz (a)	calcite (a)	plagioclase (l)	dolomite (vl), mica (l)

Appendix 4 - Stable Carbonate Isotope Data

Sample #	Paragenetic Stage	$\delta^{13}C$	$\delta^{13}C$ repeat	$\delta^{18}O$	SMOW	$\delta^{18}O$ repeat	SMOW
BA-39	C1	-2.13	-1.57	-6.32	24.3946488	-6.4	24.312176
CR03-1	C1	-9.92	-9.79	-7.34	23.3431206	-6.76	23.9410484
CR2-1A	C1	-0.35		-7.07	23.6214663		
CR2-1B	C1	-4.17	-4.1	-7.59	23.0853931	-7.43	23.2503387
FC29-32A	C1	-9.89		-12.13	18.4050617		
FC29-32B	C1	-5.78		-13.53	16.9617877		
FC39-43B	C1	-3.74	-3.34	-8.89	21.7452101	-8.74	21.8998466
FC69-1A	C1	1.38		-11.31	19.2504079		
Naranjitos Show	C1	-2.25	-2.07	-6.43	24.2812487	-6.26	24.4565034
NRS-18	C1	0.06	0.26	-6.63	24.0750667	-6.59	24.1163031
Tingo S - A	C1	-4.6	-4.52	-9.89	20.7143001	-10.16	20.4359544
TS22 A	C1	1.03		-6.7	24.002903	-6.84	23.8585756
TS22 B	C1	-0.29	-0.08	-7.07	23.6214663	-7.09	23.6008481
Anita Show B	D1	0.67	0.93	-10.51	20.0751359	-10.17	20.4256453
CJR25/06/99#2A	D1	1.17	1.51	-12.49	18.0339341	-12.57	17.9514613
FC26-09B	D1	0.54	0.63	-11.66	18.8895894	-11.69	18.8586621
FC26-11	D1	1.48		-11.07	19.4978263		
FC26-17B	D1	1.35	1.41	-11.76	18.7864984	-11.75	18.7968075
FC26-24	D1	1.18	1.15	-12.67	17.8483703	-12.79	17.7246611
FC4-03B	D1	1.06	1.03	-10.55	20.0338995	-11.07	19.4978263
Isabel I	D1	-0.25	-0.48	-11.7	18.848353	-11.66	18.8895894
MN-10	D1	-0.66	-0.28	-8.79	21.8483011	-8.46	22.1885014
My-11A	D1	-1.8	-1.71	-7.66	23.0132294	-7.31	23.3740479
My-3A	D1	1.85	1.66	-2.94	27.8791246	-3.39	27.4152151
My-3B	D1	1.39	1.37	-3.58	27.2193422	-3.73	27.0647057
Raquel B	D1	1.42		-11.38	19.1782442		
Raquel C	D1	1.07	1.18	-11.47	19.0854623	-11.51	19.0442259
Tingo S - C	D1	-3.19	-2.84	-8.64	22.0029376	-8.54	22.1060286
BA-30	D2	0.92	1.02	-8.49	22.1575741	-8.62	22.0235558
Charito Show #2	D2	-1.15	-0.93	-9.65	20.9617185	-9.69	20.9204821
CJR25/06/99#15	D2	0.54	0.17	-10.73	19.8483357	-10.56	20.0235904
CJR25/06/99#2B	D2	0.59	0.24	-10.36	20.2297724	-10.6	19.982354
CJR25/06/99#6A	D2	0.15	0.15	-9.48	21.1369732	-9.27	21.3534643
CJR25/06/99#6B	D2	-1.67	-1.7	-11.37	19.1885533	-11.87	18.6730983
CR1-2	D2	0.744	1.02	-10.6	19.982354	-10.86	19.7143174
CR1-3	D2	1.17	0.88	-10.62	19.9617358	-10.22	20.3740998
FC14-1	D2	0.03	0.16	-10.95	19.6215355	-11.04	19.5287536
FC21-36	D2	1.08		-11.45	19.1060805		
FC26-09A	D2	-0.4	-0.49	-10.86	19.7143174	-11.13	19.4359717
FC26-17A	D2	1.21	1.17	-11.48	19.0751532	-11.43	19.1266987
FC36-35	D2	1.02	1.21	-11.82	18.7246438	-11.91	18.6318619
FC36-40	D2	1.2	1.38	-11.87	18.6730983	-11.26	19.3019534
FC39-43A	D2	0.89	0.95	-10.52	20.0648268	-10.66	19.9204994
FC39-45	D2	0.93	0.96	-10.23	20.3637907	-10.13	20.4668817
FC4-03A	D2	0.91	1.12	-11.15	19.4153535	-11.31	19.2504079
FC4-15	D2	1.26		-11.6	18.951444		
FC4-16	D2	0.06		-11.13	19.4359717		

FC4-21	D2	0.2	-0.09	-10.44	20.1472996	-10.55	20.0338995
FC64-1	D2	1.07	0.88	-11.18	19.3844262	-12.06	18.4772254
FC69-1B	D2	1	1.35	-10.38	20.2091542	-10.28	20.3122452
Isabel 2	D2	0.65		-11.42	19.1370078		
My-11B	D2	-1.77	-1.98	-7.98	22.6833382	-7.59	23.0853931
My-23	D2	-1.06	-1.29	-7.59	23.0853931	-7.69	22.9823021
My-53A	D2	-0.08	-0.16	-7.66	23.0132294	-7.58	23.0957022
My-53B	D2	1.38	1.39	-7.15	23.5389935	-6.7	24.002903
Nancy Show	D2	0.6	0.74	-12.25	18.2813525	-12.47	18.0545523
Raquel A	D2	0.26	0.37	-10.05	20.5493545	-10.57	20.0132813
Sonche	D2	0.53	0.77	-9.06	21.5699554	-8.81	21.8276829
TG-24	D2	0.87	0.7	-9.57	21.0441913	-10.07	20.5287363
Tingo S - B	D2	0.71	0.85	-8	22.66272	-7.98	22.6833382
BA-26	H	2.17	2.44	-5.96	24.7657764	-6.11	24.6111399
FC14-2	H	1.51	1.56	-9.79	20.8173911	-9.72	20.8895548
FC21-47	H	1.66	1.51	-10.15	20.4462635	-10.2	20.394718
FC21-9	H	1.64	1.5	-7.07	23.6214663	-7.27	23.4152843
TG-14	H	3.37	3.32	-8.04	22.6214836	-7.9	22.765811